Imperial College London

Faculty of Medicine

National Heart & Lung Institute

The iron regulatory axis of pulmonary artery vascular cells; disruption and implications for PAH subtypes

A thesis submitted to Imperial College London for the degree of Doctor of Philosophy

Quezia Keller Toe

March, 2022

This work has been fully funded by the British Heart Foundation (BHF)

British Heart Foundation

i. Abstract

Introduction: Pulmonary artery hypertension (PAH) is a devastating and rare disease characterised by restricted flow through the pulmonary arterial circulation resulting in increased pulmonary vascular resistance; which ultimately results in right heart failure and death. Vascular remodelling is hypothesised to be caused by chronic inflammation, disrupted metabolism and dysregulated growth factors leading to endothelial and smooth muscle cell proliferation. Iron deficiency is prevalent in PAH and has been associated with reduced exercise capacity and increase mortality that makes iron deficiency clinically relevant and a potential therapeutic target for PAH. Systematically iron is regulated by the hepcidin/ferroportin axis, hepcidin, described as the global iron regulator, binds to ferroportin, an iron exporter, causing internalisation, thus preventing iron export. Hepcidin has been described to be elevated in patients with idiopathic PAH, therefore the present of this axis has been investigated in human pulmonary endothelial cells (hPAECs) and the manipulation of this axis will lead to iron retention by these cells with consequences that could influence responses locally of other surrounding cells.

Methodology: hPAECs were grown and treated with either hepcidin, IL-6 or haemoglobin. Gene expression was examined by real-time PCR and protein expression by western blot or flow cytometry. hPAECs mediators release was determined by ELISA and proliferation by BrdU and MTS assays. hPAECs and

human smooth muscle cells (hPASMC) mitochondrial function were examined by the Seahorse assay.

Conclusions: this study present findings that demonstrated the presence of the hepcidin/ferroportin in hPAECs that allows for local iron homeostatic control and modulation of this axis in these cells presents a PAH like phenotype that could contribute to vascular remodelling. Furthermore, IL-6 and hepcidin caused aberrant-BMPR2 signalling, in which BMPR2 protein is downregulated, however downstream signalling of BMPR2 remains active. The results present here here also supports the hypothesis that subclinical haemolysis may have a role in PAH pathophysiology.

ii. Declaration of Originality

I, Quezia Keller Toe, hereby declare that I wrote this thesis and experiments describe herein were performed by myself. Any information or data was derived from other sources or was done in collaboration has been clearly and appropriately acknowledged and cited.

iii. Copyright declaration

iv. Dedication

"But who am I, and who are my people, that we should be able to give as generously as this? Everything comes from you, and we have given you only what comes from your hand." (I Ch 29:14)

This thesis is especially dedicated to my great-grandmother Isaura Keller, although she is no longer physically in my life, her advice and support for my studies was never forgotten. She was not allowed to have an education, but throughout her life she encouraged me to pursue the education she couldn't have. I also dedicate this thesis to my parents, Daniel and Liliane Toe, for their unwavering support, love and encouragement. Their good example has taught me to work hard and fight for the things I want to achieve.

v. Acknowledgments

I will begin by thanking the Almighty God for all His blessing upon my life and without it this study would not be possible.

First and foremost, I want to acknowledge my supervisor Dr Gregory Quinlan for his support, patient, guidance and trust. His insight, scientific knowledge was invaluable throughout my PhD. In the difficult moments, Dr Quinlan always provided encouragement and insight, more importantly kindness that steered me back on track. Finally, I have always enjoyed our morning coffee, pub lunches and many long conversations that had nothing to do with this PhD.

I would like to acknowledge Dr John Wort for his key role in encouraging and supporting me during the course of this PhD.

I would like to thank my studentship sponsor the British Heart Foundation (BHF) for their generous support, without it this study would not be possible.

I would also like to thank the lab members for their support and great working atmosphere. In particular I want to thank fellow PhD student Abdul Mohamed and Mr Theo Issitt for their support throughout this study.

A special thanks to my AD Belem church community for their support, prayers and love throughout my studies. Mostly I am very grateful for the constant encouragement and advice from my Pastor Francis Brito. Finally, I thank my amazing family and friends for all their love and support throughout this study.

vi. Publications

Papers

Ramakrishnan, L., Pedersen, S. L., Toe, Q. K., Quinlan, G. J. & Wort, S. J. 2018a. Pulmonary Arterial Hypertension: Iron Matters. *Frontiers in Physiology,* 9, 641.

Ramakrishnan, L., Pedersen, S. L., Toe, Q. K., West, L. E., Mumby, S., Casbolt, H., Issitt, T., Garfield, B., Lawrie, A., Wort, S. J. & Quinlan, G. J. 2018b. The Hepcidin/Ferroportin axis modulates proliferation of pulmonary artery smooth muscle cells. *Scientific Reports,* 8, 12972.

Conference Abstracts

A S Mahomed, A Burke-Gaffney, Q Toe, J Naser, G J Quinlan, S J Wort, Effects of varying shear stress profiles on the regulation of pulmonary artery endothelial cell gene expression: a focus on selected mediators of vascular tone, inflammation and angiogenesis, *European Heart Journal*, Volume 42, Issue Supplement_1, October 2021, ehab724.1892.

Panselinas I, Toe Q, Clementson K*, et al*. S92 Hepcidin and interleukin-6 downregulate BMPR2 and dysregulate BMPR2 downstream pathways; implications for pulmonary artery hypertension *Thorax* 2021;**76:**A56

Ioannis Panselinas, Quezia K Toe, Katie Clementson, Maziah M Ghazaly, S John Wort, Gregory J Quinlan. Pulmonary artery endothelial cell exposure to

hepcidin affects BMP-signalling; relevance to vascular remodelling in PAH. European Respiratory Journal Sep 2020, 56 (suppl 64) 1491;

Issitt, T., Toe, Q., Mohd Ghazaly, M., Quinlan, G. J. & Wort, S. J. 2019. Pulmonary vascular cell mitochondrial dysfunction in response to hepcidin. *European Respiratory Journal,* 54**,** PA1415.

Toe Q, Ying H, Issitt T*, et al*. S99 Hepcidin down regulates BMPRII in pulmonary artery endothelial cells mimicking pulmonary artery hypertension phenotypes. *Thorax* 2019;**74:**A61-A62.

Toe, Q., Mohd Ghazaly, M., Issit, T. J., Wort, S. J. & Quinlan, G. J. 2019. Cell free haemoglobin and pulmonary artery endothelial cell dysfunction. *European Respiratory Journal,* 54**,** PA5042.

Bukhari M, Mohd-Ghazaly M, Toe Q*, et al* S97 Haemoglobin challenge induces dysfunction in human pulmonary artery endothelial cells: potential relevance to pulmonary artery hypertension. *Thorax* 2019;**74:**A60-A61.

Pedersen, S., Toe, Q., John Wort, S., Quinlan, G. & Ramakrishnan, L. 2018. *Stabilised ferroportin activity affects pulmonary vascular cells responses: implications for pulmonary hypertension*.

Issitt, T. & Toe, Q. 2018. *Hepcidin treatment of human pulmonary artery smooth muscle cells and mitochondrial dysfunction*.

vii. Table of contents

1. Chapter 1 - Introduction 36

1.1 Pulmonary Arterial Hypertension (PAH) 37

1.1.1 Definition 37

1.1.2 Classification of PAH 37

1.1.3 Pathophysiology of PAH 38

1.1.4 Role of TGF-β signalling in PAH 47

1.1.5 Genetics of PAH 51

1.1.6 The role of Hypoxia in PAH 52

1.2 Iron Homeostasis 55

1.2.1 Introduction 55

1.2.2 Systematic iron regulation and transport 57

1.2.3 Cellular Iron regulation 58

1.2.4 Mitochondrial iron regulation 60

1.2.5 The ferroportin/hepcidin axis 61

1.3 Iron Deficiency and PAH 71

1.3.1 Iron deficiency and Eisenmenger syndrome 72

1.3.2 Haemolysis and PAH 73

1.4 Summary 77

1.5 Hypothesis 78

2. Chapter 2 - Methods 79

2.1 Materials and reagents 80

2.1.1 General Reagents 80

2.1.2 ELISA kits and reagents 80

2.1.3 Antibodies 81

2.1.4 Primers 83

2.2 Cell Culture 83

2.2.1 Human pulmonary artery endothelial cells 83

2.2.2 Human pulmonary smooth muscle cells 84

2.2.3 Cell cryopreservation and defrosting 88

2.2.4 General cell counting 89

2.2.5 Cell treatments 90

2.2.6 Cell viability 91

2.2.7 Cell gene knockdown by RNA interference 93

2.3 Microscopy 95

2.3.1 Wide-field Microscopy 95

2.3.2 Fluorescence Microscopy 96

2.4 Cell proliferation assay 100

2.4.1 MTS assay 100

2.4.2 BrdU 101

2.5 Polymerase Chain Reaction - PCR 102

2.5.1 Basic principles 102

2.5.2 RNA preparation 103

2.5.3 cDNA synthesis 104

2.5.4 Real Time PCR 106

2.6 Western Blot 108

2.6.1 Basic principles 108

2.6.2 Protein quantification - Bradford assay 109

2.6.3 Gel Electrophoresis, blotting and protein detection 110

2.7 Enzyme-linked immunosorbent assay (ELISA) 113

2.7.1 Basic principles 113

2.7.2 Detection of cytokines 114

2.8 Seahorse Assay 115

2.8.1 Mito Stress test 116

2.9 Flow Cytometry 119

2.9.1 Basic Principles 119

2.9.2 Cell cycle analysis 120

2.9.3 ROS detection 121

2.9.4 TMRM (tetramethylrhodamine methyl ester) assay 123

2.9.5 Cell Antigens Staining 125

2.10 Statistics 128

3. Chapter 3 – The ferroportin/hepcidin axis is present on pulmonary arterial endothelial cells 130

3.1 Rationale 131

Aims 132

3.2 The iron regulatory Ferroportin/hepcidin axis is expressed and modulate in hPAECs 133

3.2.1 Ferroportin and Hepcidin are expressed in hPAECs 133

3.2.2 The ferroportin/hepcidin axis is modulated in hPAECs 133

3.2.3 Hepcidin stimulates the release of IL-6 and hepcidin in hPAECs 137

3.2.4 IL-6 causes hPAECs to proliferate 140

3.2.5 Hepcidin does not affect hPAECs proliferation 141

3.2.6 IL-6 and Hepcidin increases the release of IL-8 and MCP-1 142

3.2.7 IL-6 and hepcidin does not affect mitochondria function in hPAECs 144

3.3 Summary and limitations 148

3.3.1 Summary 148

3.3.2 Limitations 149

4. Chapter 4 – Potential effects on BMPR2 protein expression by IL-6 or hepcidin treatment. 150

4.1 Rationale 151

4.1.1 Aims 152

4.2 Both IL-6 and hepcidin causes reduction of BMPR2 expression in hPAECs 152

4.2.1 IL-6 and hepcidin cause downregulation of BMPR2 mRNA in hPAECs 152

4.2.2 IL-6 and hepcidin cause reduction in BMPR2 protein 153

4.2.3 Signalling downstream of BMPR2 is active despite reduction of proteins expression 155

4.3 Summary and Limitations 164

4.3.1 Summary 164

4.3.2 Limitations 164

5. Chapter 5 – The effect of hPAEC conditioned media on hPASMC mitochondria 166

5.1 Rationale 167

5.1.1 Aims: 168

5.2 Hepcidin causes dysregulation of mitochondrial function on hPASMCs 168

5.3 hPAECs conditioned media from hepcidin treated cells promotes an increased mitochondrial metabolism 171

5.4 Summary and Limitations 172

5.4.1 Summary 172

5.4.2 Limitations 173

6. Chapter 6 - Haemoglobin effect on hPAECs and the implications to PAH 174

6.1 Rationale 175

6.1.1 Free haemoglobin exposure as contributor to the development of PAH 175

6.1.2 Haemoglobin handling: a role for haptoglobin and CD163 177

6.1.3 Aims 178

6.2 Results 179

6.2.1 Human Pulmonary Artery endothelial cells express the haemoglobin scavenger receptor CD163 179

6.2.2 Haemoglobin elevates inflammatory cytokines 182

6.2.3 Haemoglobin causes the activation of hPAECs 185

6.2.4 Free-haemoglobin elevates the production of Reactive oxygen Species 186

6.2.5 hPAECs proliferation is increased by haemoglobin in a time-dependent manner 189

6.2.6 Free-haemoglobin treatments does not affect hPAECs viability . 191

6.3 Summary and Limitations 192

6.3.1 Summary 192

6.3.2 Limitations 193

7. Chapter 7 - General Discussion 195

7.1 The biological context of the iron regulatory ferroportin/hepcidin axis 196

7.2 The ferroportin/hepcidin axis is expressed in hPAECs 197

7.2.1 The effects of IL-6 and hepcidin in hPAECs proliferation 200

7.3 Hepcidin and IL-6 both downregulates the expression of BMPR2 in hPAECs, mimicking pulmonary arterial hypertension phenotype 203

7.4 A role for haemolysis in PAH 207

7.5 Conclusion 211

7.6 Limitations of this study 213

7.7 Future Works 214

7.7.1 Hypoxia studies 215

7.7.2 Quantification of labile iron pool and total iron 215

7.7.3 Ferroportin knockdown experiments 215

7.7.4 Perform studies with blood outgrowth endothelial cells (BOECs) and tissues samples derived from patients with PAH 216

8. References 217

viii. List of Figures

Figure 1-1 Subcategories of PAH according to the 6th World Symposium on pulmonary hypertension *(Condon et al., 2019).* *38*

Figure 1-2 Representation of vascular remodelling in pulmonary arterial hypertension. *Cross-section of a normal pulmonary arteriole (left) and an arteriole affected by pulmonary hypertension (right). Adapted from Gordeuk et al. (2016). Image created in BioRender.* *39*

Figure 1-3 Proposed mechanisms for pulmonary vascular remodelling in PAH. *Increase in inflammation, hypoxia and blood flow via sheer stress coupled with altered BMPR2 signalling causes changes in endothelial cells to acquire a mesenchymal phenotype with a gene profile similar of smooth muscle cells. BMPR2, bone morphogenetic protein receptor; PAECs, pulmonary artery endothelial cells; ROS, reactive oxygen species; IL-6, interleukin-6; IRF-1, interferon regulatory factor-1; TGF-β, transforming growth factor beta; IL1-β, interleukin 1 beta; NFKβ, nuclear factor kappa beta; STAT3, signal transducer and activator of transcription 3. Adapted from Thenappan et al. (2018). Designed on BioRender.* *42*

Figure 1-4 Current PAH therapy strategy. *There are three main pathways that targeted for the treatment of PAH: the endothelin pathway; nitric oxide pathway; and prostacyclin pathway. These pathways are involve in vasodilation/vasoconstriction of blood vessel. Adapted from Boutet et al. (2008) and Fuso et al. (2011). Figure created in BioRender.* *47*

Figure 1-5 TGF-β and BMP signalling. *The TGF-β family members are subdivide in two groups. One group is formed by TGF-β signalling pathways and group two is formed of the BMP signalling pathway. Figure adapted from RoI et al. (2018). Image created in BioRender.* *48*

Figure 1-6 TGF-β and BMP signalling. *Signalling start by a "type 1" and "type 2" receptors forming a heterotetrametric complex, upon ligand biding the "type 2" receptor phosphorylate the "type 1" that will then phosphorylates signal transduction targets, usually R-SMADs that will form a complex with a co-SMAD that will enter the nucleus and bind BMP response element DNA sequence (Andruska and Spiekerkoetter, 2018). Image created in Biorender.* *49*

Figure 1-7 Simplified hypoxia signalling. *In normal oxygen conditions HIF-α subunits are inactivated by proly-4-hydroxilases (PHDs), which cause their degradation by triggering ubiquitination reaction via E3 ubiquitin Von Hipple-Lindau protein (pVHL). In hypoxic conditions hydroxylation of PHDs is inhibited, which allows HIF-α to translocate to the nucleus and dimierize to HIF-β that in turn will bind to the hypoxia-responsive elements. Figure created in BioRender.* *53*

Figure 1-8 Cellular iron homeostasis. *Diferric transferrin (TF) binds to to the transferrin receptor 1 (TRF1) on the plasma membrane and the complex is internalised in endosomes, and moved across the endosomal membrane by the divalent metal-ion transporter 1 (DMT1). Surplus iron that is not need by the cell can be exported to the extracellular space by ferroportin (FPN1). Some cell types can also import iron through other mechanisms, such as iron contained within ferritin, or within haemoglobin through the CD163 receptor. Iron storage and*

intake are regulated by the iron-responsive element and iron regulatory protein (IRP) system. Low iron concentration leads to the synthesis of TFR1 and suppression of ferritin, whereas in high cellular iron the opposite occurs, ferritin expression is increased and TFR1 decreased. Figure adapted from Wu et al. (2004). *59*

Figure 1-9 NMR structure of hepcidin. *Positively-charged residues are in blue, negatively-charged residues in red, disulphides in yellow. Image taken from Ganz (2005).* *63*

Figure 1-10 Simplified hepcidin Regulatory pathways. *Iron status extracellularly induces hepcidin transcription via the BMP-SMAD pathway, and in an extent through transferrin receptor 1 and 2, however this is not fully understood. Hepcidin expression is also regulated by inflammation through the JAK-STAT3 pathway, when IL-6 receptor is activated by the inflammatory cytokine IL-6. BMP6, bone morphogenetic protein 6; BMPR1, bone morphogenetic protein receptor 1; BMPR2, bone morphogenetic protein receptor 2; HJV, hemojuvelin; IL-6, interleukin 6; IL-6R, interleukin 6 receptor; JAK, janus kinase; STAT3, signal transducer and activator of transcription 3; SMAD1//5/8, sma and mothers against decapentaplegic homologue 1/5/8 complex; SMAD 4, sma and mothers against decapentaplegic homologue 4; TFR1, transferrin receptor 1; TFR2, transferrin receptor 2; HFE, hemochromatosis protein. Adapted from Rishi et al. (2015). Figure created with BioRender.* *65*

Figure 1-11 Structure of human haemoglobin. *Haemoglobin quaternary structure, alpha chains in grey and beta chains in tan. Figure taken form (Ahmed et al., 2020)* *75*

Figure 2-1 Image of hPAECs in culture. *Left panel cells at 90% confluence and right panels cells at 60 % confluence. Images were taken by an Olympus CX40 microscope.* *84*

Figure 2-2 hPASMCs cells in culture*. These cells show the typical long and narrow spindle shape morphological characteristics. Images were taken by an Olympus CX40 microscope.* *85*

Figure 2-3 . Confocal images of hPASMCs from three donors*, (A) donor-A, (B) donor-B, and (C) donor-C; grown in smooth muscle cell growth medium 2 (Promocell, Germany) or DMEM 15% FBS medium. Top 3 panels of each figure were immuno-stained with rabbit anti-SM22 alpha (red) and mouse anti- SMA (Smooth muscle actin). Bottom 3 panels were immuno-stained with rabbit anti-SM22 alpha (red) and anti-mouse MHC (smooth muscle myosin heavy chain; green). Scale bar = 10 μM* *87*

Figure 2-4 Fast-Read®102 counting chambers and a representation of the scoring inside each chamber. *89*

Figure 2-5 Graph representing the different readings of the alamar blue assay. *The alamar blue reagent will react with metabolites in active cells to release a reduced form of a compound that absorbs at 570nm. The oxidised form which is associated with non-viable cells absorbs at 600nm* *92*

Figure 2-6 Basic principle of a laser scanning microscope. *Laser light is focused on the sample, the laser excites fluorescence throughout the sample and it is focused onto the image plane. The pinhole only allows light from the confocal plane to reach the PMT. Figure taken from Sanderson et al. (2014).* *98*

Figure 2-7 RNA extraction protocol. *104*

Figure 2-8 cDNA synthesis protocol. *..... 105*

Figure 2-9 Real time PCR protocol. *..... 107*

Figure 2-10 Bradford assay protocol. *..... 110*

Figure 2-11 Western Blot protocol. *..... 113*

Figure 2-12 General sandiwich ELISA protocol. *..... 115*

Figure 2-13 - Seahorse XF cell mito stress test protocol. *..... 119*

Figure 2-14 Simple schematic of a flow cytometer*. Cells are pulled thorough a nozzle together with sheath fluid a laser bin is aimed at each cell as they pass through. Forward and side scatter light together with fluorescence are detected form stained. Picture taken from https://www.abcam.com/protocols/introduction-to-flow-cytometry. 120*

Figure 3-1 IL-6 (A) and hepcidin (B) treatments do not affect hPAECs viability*. Cell viability was determined by the Alamar Blue assay and the assay was performed as described in section 2.2.6. Data is shown as mean ±SEM, n=3. ..... 136*

Figure 3-2 The iron exporter ferroportin is expressed in hPAECs*. **(A, B)** ferroportin mRNA transcription after IL-6 and hepcidin treatment for 2 hours. Real-time PCR analysis was performed as described in section 2.4. Data shown are mean ±SEM n=6. Unpaired t-test was performed. *p<0.05; **p<0.01. **(C)** Western blot analysis of ferroportin protein expression after IL-6 and Hepcidin treatments for 24 hours. Western blot assay was performed as described in section 2.5. **(D)** Immune fluorescence image showing the expression of ferroportin on hPAECs. Top panel cells treated with media alone; middle panel*

cells treated with 10 ng/mL IL-6; bottom panel cells treated with 1 µg/mL hepcidin. Immune-fluorescence was performed as described in 2.3.2.3. 135

Figure 3-3 The iron hormone hepcidin is expressed in hPAECs. *(A) Hepcidin mRNA transcription in hPAECs after IL-6 stimulation for 2 hours. Real-time PCR analysis was performed as described in section 2.4. Data shown are mean ±SEM n=6. Unpaired t-test was performed. *p<0.05; **p<0.01. (B) Hepcidin release into hPAEC supernatants after 24 hours stimulation with IL-6. hPAECs supernatant s were analysed by ELISA as described in section 2.6. Data shown are mean ±SEM n=12. . Kruskal-Wallis test followed by Dunn's post hoc test were performed *p>0.05..... 137*

Figure 3-4 hPAECs release IL-6 after hepcidin treatment. *(A) IL-6 mRNA transcription in hPAECs after hepcidin stimulation for 5 hours. Real-time PCR analysis was performed as described in section 2.4. Data shown are mean ±SEM n=6. (B) IL-6 release into hPAECs supernatants after 24 hours stimulation with hepcidin (0.1, 1 µg/mL). hPAECs supernatant s were analysed by ELISA as described in section 2.6. Data shown are mean ±SEM n=12.Kruskal-Wallis test followed by Dunn's post hoc test were performed *p>0.01; ****p>0.0001. ..... 137*

Figure 3-5 Hepcidin stimulates the release of IL-6 and hepcidin in hPAECs. ***(A, B)*** *hepcidin mRNA transcription from hPAECs after treatment with hepcidin for 1 (A) and 24 (B) hours. Real-time PCR analysis was performed as described in section 2.4. Data shown are mean ±SEM n=6. Unpaired t-test was performed **p<0.01.* ***(C)*** *Hepcidin release into the supernatants of hPAECs after 24 hours treatment with hepcidin. hPAECs supernatants were analysed by ELISA as described in section 2.6. Data shown are mean ±SEM n=12. Kruskal-Wallis test*

*followed by Dunn's post hoc test were performed *p>0.05.* ***(D)*** *Hepcidin release is decreased by its knockdown. Hepcidin knockdown was performed as described in section 2.2.7. hPAECs supernatants were analysed by ELISA as described in section 2.6. Data shown are mean ±SEM n=3. Kruskal-Wallis test followed by Dunn's post hoc test were performed *p>0.05..... 139*

Figure 3-6 IL-6 induces hPAEC proliferation after 24 hours stimulation. (A, B) *hPAEC proliferation measured by BrdU assay and MTS assay (B) after 24 hours treatment with IL-6. Assays were performed as described in section 2.3. Data shown are mean ±SEM n=6. Kruskal-Wallis test followed by Dunn's post hoc test were performed *p<0.05; **p<0.01. ..... 141*

Figure 3-7 Hepcidin does not affect hPAEC proliferation. (A, B) *hPAEC proliferation measured by BrdU assay and MTS assay (B) after 24 hours treatment with hepcidin. Assays were performed as described in section 2.3. Data shown are mean ±SEM n=6. ..... 142*

Figure 3-8 IL-6 and hepcidin increases the release of IL-8 and MCP-1 after 24 hours stimulations. *(A, B) MCP-1 release in hPAECs supernatants after 24 hours stimulation with IL-6 (A) and hepcidin (B). IL-8 release in hPAECs supernatants after 24 hours stimulation with IL-6 (C) and hepcidin (D).ELISA analysis was performed as described in section 2.6. Data shown are mean ±SEM n=12. Kruskal-Wallis test followed by Dunn's post hoc test were performed *p<0.05; **p<0.01; ****p<0.0001. ..... 143*

Figure 3-9 IL-6 (A) and Hepcidn (B) does not affect hPAEC mitochodria membrane potential. *Mitochondrial membrane potential was determine by the TMRM assay as described in section 2.8.4. Data are shown ±SEM n= 5. ..... 145*

Figure 3-10 IL-6 effect on hPAEC mitochondria metabolism. *Oxygen consumption rate (OCR) was determined by the sehorse XF analyser mito stress assay as descrbed in section 2.7. Data are shown ±SEM n= 6. One-way ANOVA test followed by Dunnett's post hoc test were performed * p<0.05; ***p<0.001. ..... 146*

Figure 3-11 Hepcidin effect on hPAEC mitochondria metabolism. *Oxygen consumption rate (OCR) was determined by the sehorse XF analyser Mito stress assay as descrbed in section 2.7. Data are shown ±SEM n= 6..... 147*

Figure 4-1 hPAECs BMPR2 mRNA transcription after 24h treatment with IL-6 (A) and hepcidin (B). *Real-time PCR analysis was performed as described in section 2.4. Data shown are mean ±SEM n=6. Unpaired t-test was performed **p<0.01;****p<0.0001..... 153*

Figure 4-2. Both IL-6 and hepcidin causes reduction of BMPR2. *(A) Western blot image of BMPR2 expression on hPAECs treated with hepcidin and IL-6. BMPR2 western blot bands relative density of hPAECs treated with hepcidin (B) and IL-6 (C) compared to untreated control. Data shown are mean ±SEM n=4. Kruskal-Wallis test followed by Dunn's post hoc test were performed *p>0.01; *p>0.05..... 154*

Figure 4-3 SMAD1/5 is phosphorylated after hepcidin treatment*. Western blot image and densitometry analysis of pSMAD1/5 phosphorylation and SMAD5 expression time course after treatment with 1 µg/mL hepcidin. Data shown are mean ±SEM n=6. Kruskal-Wallis test followed by Dunn's post hoc test were performed **p>0.01. ..... 156*

Figure 4-4 mRNA transcription of the BMPR2 downstream targets *ID1(A), ID2 (C), ID3 (C) and ID4 (D) after hepcidin treatment. Real-time PCR analysis was performed as described in section 2.4. Data shown are mean ±SEM n=6. Unpaired t-test was performed *p<0.05..... 158*

Figure 4-5 mRNA transcription of the BMPR2 downstream targets *ID1(A), ID2 (C), ID3 (C) and ID4 (D) after IL-6 treatment. Real-time PCR analysis was performed as described in section 2.4. Data shown are mean ±SEM n=6. Unpaired t-test was performed *p<0.05..... 159*

Figure 4-6 hPAECs ID1 protein expression is increased by IL-6 and hepcidin after 24 hours stimulation. *(A) Western blot image demonstrating that both IL-6 and hepcidin increase ID1protein expression. (B, C) Densitometry analysis of the western blot bands showed significant ID1 protein increase after 24h treatment with IL-6 (1 and 10 ng/mL) and hepcidin (0.1 and 1 µg/mL) compared to untreated controls. Data shown are mean ±SEM n=6. Kruskal-Wallis test followed by Dunn's post hoc test were performed ***p>0.001..... 160*

Figure 4-7 hPAEC BMPR2 knockdown time-course. *BMPR2 mRNA transcription analysis after 24 (A) and 48 (B) hours of knockdown. . Real-time PCR analysis was performed as described in section 2.4. Data shown are mean ±SEM n=6. Unpaired t-test was performed **p<0.01; ***p<0.001. (C) Western blot image of hPAECs protein lysates over time. Bands on the left were incubated with a control siRNA and bands on the right were incubated with a BMPR2 siRNA for 6 hours. Lysates were them collected at 24, 48, 72, and 96 hours. Western blot analysis was performed as described in section 2.5..... 162*

Figure 4-8 Knockdown of BMPR2 leads to upregulation of downstream BMPR2 targets*: SMAD 1 and 5, ID1, 2, 3 and 4. Real-time PCR assay was performed as described in section 2.4. Data shown are mean ±SEM n=6. Unpaired t-test was performed *p<0.05..... 163*

Figure 5-1 Hepcidin treatments causes mitochondrial changes in hPAECs *(A) and hPASMCs (B). hPAECs and hPASMCs were stained with Mitotracker (green) and DAPI (blue) following treatment with or without hepcidin. Orange boxes show magnified regions, scale bars, 20 µm. Images taken by Theo Issitt. 167*

Figure 5-2 Hepcidin treatments changes hPASMCs mitochondrial metabolism. Mito *stress test were performed following treatment with or without hepcidin for 24 hours. The assay was performed as described in section 2.7. Data are shown ±SEM n= 6. One-way ANOVA test followed by Dunnett's post hoc test were performed * p<0.05..... 169*

Figure 5-3 – hPAECs conditioned media with hepcidin increased the energy demand of hPASMCs. *Mito stress test were performed following treatment of hPASMCs with hPAECs conditioned media either with hepcidin or media alone. The assay was performed as described in section 2.7. Data are shown ±SEM n= 6. One-way ANOVA test followed by Dunnett's post hoc test were performed * p<0.05. ..... 172*

Figure 6-1 hPAEC CD163 mRNA transcription is upregulated by free-haemoglobin. *hPAECs cells were seeded in a 12-well plate at 75,000 cells per well and incubated overnight for cell attachment. The cells were then serum starved overnight and treated with free-haemoglobin for 3 hours. RNA extraction,*

*cDNA synthesis and Real-time PCR were performed as described in section 2.4). Data is shown as mean ±SEM, n=8. One-way ANOVA test followed by Dunnett's post hoc test were performed ** p<0.01. ..... 180*

Figure 6-2 CD163 protein is expressed in hPAECs. *hPAECs were seeded into a 6-well plate at 250,000 cells per well. The cells were incubated overnight for attachment. Cells were then treated with haemoglobin for 24 hours at 1, 3 and 10 µM concentrations. Western blot were performed as described in section 2.5. ..... 181*

Figure 6-3 CD163 is expressed on hPAECs membrane. *Cells were seed in T25 flasks until they were 70% confluent. Cells were then treated with haemoglobin for 24 hours at 1, 3 and 10 µM concentrations. Flow cytometry assay was performed as described in section 2.8. Data is shown as mean ±SEM, n=4. One-way ANOVA test followed by Dunnett's post hoc test were performed ** p<0.01. ..... 181*

Figure 6-4 IL-6 (A), IL-8 (B) and MCP-1 (C) mRNA transcription is increased by haemoglobin. *hPAECs cells were seeded in a 12-well plate at 75,000 cells per well and incubated overnight for cell attachment. The cells were then serum starved overnight and treated with haemoglobin for 3 hours. RNA extraction, cDNA synthesis and Real-time PCR were performed as described in section 2.4). Data is shown as mean ±SEM, n=8. One-way ANOVA test followed by Dunnett's post hoc test were performed *p<0.05..... 182*

Figure 6-5 Haemoglobin increases the release of the cytokines IL-6 (A), IL-8 (B) and MCP-1 (C) in hPAECs supernatants. *hPAECs supernatant s were analysed by ELISA as described in section 2.6. Data is shown as mean ±SEM,*

*n=12. Kruskal-Wallis test followed by Dunn's post hoc test were performed *p>0.05; ** p<0.01; ***p>0.001; ****p>0.0001. ..... 183*

Figure 6-6 - Free-haemoglobin increases the release of the hormone hepcidin. *(A) hPAEC mRNA transcription after 2 hours treatment with haemoglobin. Data is shown as mean ±SEM, n=8. One-way ANOVA test followed by Dunnett's post hoc test were performed * p<0.05. (B) Hepcidin release in hPAEC supernatants 24 hours after haemoglobin treatments. Data is shown as mean ±SEM, n=12. Kruskal-Wallis test followed by Dunn's post hoc test were performed *p>0.05; ** p<0.01; ***p>0.001; ****p>0.0001. ..... 185*

Figure 6-7 The expression of ICAM-1 and VCAM-1, markers of endothelial cell activation, are increased by haemoglobin treatments (24 hours). *ICAM-1 and VCAM-1 expression was determined by flow cytometry as described in section 2.8. Data is shown as mean ±SEM, n=4. One-way ANOVA test followed by Dunnett's post hoc test were performed ** p<0.01. ..... 186*

Figure 6-8 Free-haemoglobin elevates the production of Reactive oxygen Species (ROS). *ROS release was measured by flow cytometry as described in section 2.8. Data is shown as mean ±SEM, n=4. Kruskal-Wallis test followed by Dunn's post hoc test were performed *p>0.05; ****p>0.0001. ..... 187*

Figure 6-9 NOX2 expression in hPAECs is increased by haemoglobin exposure. (A) *NOX2 mRNA transcription after 2 hours stimulation with haemoglobin. Data is shown as mean ±SEM, n=8. One-way ANOVA test followed by Dunnett's post hoc test were performed * p<0.05; **p<0.01.* ***(B)*** *Expression of gp91phox a subunit of NOX2 in hPAECs after 24 hours treatment with*

haemoglobin at 3 different concentrations. Western blot was performed as described in section 2.5..... 188

Figure 6-10 hPAECs proliferation is increased by free-haemoglobin in a time-dependent manner. *hPAECs proliferation was determined by the MTS assay as described in section 2.3.1. Data is shown as mean ±SEM, n=6. Statistical test were performed separately by each time point against each correspondentl controls. One-way ANOVA test followed by Dunnett's post hoc test were performed * p<0.05..... 190*

Figure 6-11 hPAECs proliferation is increased by free-haemoglobin in a time-dependent manner. (A) *Graph representing the increased proliferation of hPAECs through time. Data is shown as mean ±SEM, n=6.* ***(B)*** *Graph showing the proliferation of hPAECs without any treatment through time. Data is shown as mean ±SEM, n=6..... 191*

Figure 6-12 Free-haemoglobin treatments does not affect hPAECs viability*. Cell viability was determined by the Alamar Blue assay and the assay was performed as described in section 2.2.6. Data is shown as mean ±SEM, n=3. ..... 192*

Figure 7-1 Diagram showing the effect of hepcidin in hPAECs that could contribute to the development of PAH*. Elevated levels of serum hepcidin has been identified in PAH patients. Hepcidin downregulated BMPR2, however SMAD1/5 phosphorylation was increase, which increased expression of Id 1,2,3,4 proteins and hepcidin. This signalling may occur by activation of other TGF-β receptors to compensate for the loss of BMPR2. Upregulation of hepcidin cause degradation and internalisation of ferroportin that could lead to iron*

accumulation. Increased iron retention has been linked to activation of transcription factors that will cause the release of inflammatory markers, in this case IL-6, IL-8 and MCP-1. IL-6 is an agonist of hepcidin, which would lead to more hepcidin synthesis. Figure created in BioRender. 212

Figure 7-2 Summary of haemoglobin effects in hPAECs. *Haemoglobin treatment of hPAECs caused an increase of cell proliferation, endothelial activation, oxidative stress and inflammation markers. CD163 was found to be expressed in hPAECs that provides a route for haemoglobin uptake and increase in intracellular iron. Elevated levels of intracellular iron in turn could lead to the activation of transcription factors for the expression of the inflammatory markers IL-6, IL-8 and MCP-1 also for the adhesion molecules ICAM-1 and VCAM-1. Haemoglobin also caused and increase in reactive oxygen species (ROS), which in turn can cause DNA damage and activation of TLR signalling, which will activate transcription of inflammatory markers. It is also possible that haemoglobin itself could activate TLR signalling. Hepcidin synthesis was also increased by haemoglobin, which would lead to internalisation of ferroportin causing iron retention. 213*

ix. List of Tables

Table 2-1 Primary antibodies utilised in this project. *..... 81*

Table 2-2 – Secondary antibodies used in this project. *..... 82*

Table 2-3 Primers used for real-time PCR experiments. *These were purchased from Sigma, UK..... 83*

Table 5-1 – Mito stress test assay parameters definitions. Adapted from (Divakaruni et al., 2014). *..... 170*

x. Abbreviations

- 6MWD - 6-minute walk distance
- AD - Alzheimer's disease
- ATP - adenosine triphosphate
- BCEC - Brain capillary endothelial cells
- BMP - bone morphogenetic proteins
- BMP6 - bone morphogenetic protein 6
- BMPR2 - bone morphogenetic protein receptor type 2
- BRE - BMP response element DNA sequence
- BSA – bovine serum albumin
- CCCP - 2-[2-(3-Chlorophenyl)hydrazinylyidene]propanedinitrile
- cDNA - complementary DNA
- CFH - cell free haemoglobin
- CM - conditioned media
- CTD - connective tissue disease
- CTEPH - chronic thromboembolic pulmonary hypertension
- CXCL4 - CXC-chemokine ligand 4
- DHE - Dihydroethidium
- DMEM - Dulbecco's Modified Eagles' Medium
- DMSO - dimethyl sulfoxide
- DMT1 - divalent metal-ion transporter 1
- DNA
- DNA - deoxyribonucleic acid

- dNTP - deoxynucleoside triphosphate
- dsRNA - double-stranded RNA
- ECM - extracellular matrix
- EGM2 - endothelial cell growth medium 2
- ELISA - enzyme-linked immunosorbent assay
- EndoMT - endothelial-to-mesenchymal transition
- ES - Eisenmenger syndrome
- ETC - electron transport chain
- FACS - fluorescence-activated single cell sorting
- FBLX5 - F-Box and leucine rich repeat protein 5
- FCCP - phenylhydazone
- FPN1 - ferroportin
- GM-CFS - granulocyte/macrophage colony stimulant factor
- HAMP - hepcidin gene
- HBSMC - human bronchial smooth muscle cells
- HBSS – Hanks' Balanced Salt Solution
- HFE2 – hemochromatosis
- HIF - hypoxia inducible factor
- HJV - haemojuvelin
- HO-1- haem oxygenase 1
- HPAH - heritable pulmonary hypertension
- HRP - horseradish peroxide
- HASMC - human airway smooth muscle cells
- ICAM-1 - intercellular adhesion molecule-1

- ID - Iron deficiency
- ID1/2/3/4 - inhibitor of DNA binding 1/2/3/4
- IFN- γ - interferon γ
- IL-1β - interleukin 1 beta
- IL-6 - interleukin 6
- IL-6R - interleukin 6 receptor
- IPAH - idiopathic pulmonary artery hypertension
- IRE - iron responsive element
- IRP - iron regulatory protein
- JAK - janus kinase
- LEAP-1 - liver-expressed antimicrobial peptide
- LED - light-emitting diodes
- LPS - lipopolysaccharide
- LSCM - lase-scanning confocal microscopy
- MAPK - mitogen activated protein kinase
- MCP-1 - onocyte chemoattractant protein 1
- mPAP - mean pulmonary artery pressure
- mRNA - messenger RNA
- MTS - 3-(4,5-dimethylthiazol-2-yl)-5-(3-carboxymethoxyphenyl)-2-(4-sulfophenyl)-2H-tetrazolium
- NADH - nicotinamide adenine dinucleotide plus hydrogen
- NADPH - nicotinamide dinucleotide phosphate
- NMR - nuclear magnetic resonance
- OCR - oxygen consumption rate
- PAC - pulmonary arterial compliance

- PAEC - pulmonary artery endothelial cell
- PAH - Pulmonary arterial hypertension
- PASMC - pulmonary artery smooth muscle cell
- PBS – phosphate buffered saline
- PCR - polymerase chain reaction
- PCWP - pulmonary capillary wedge pressure
- PDGF - platelet-derived growth factor
- PES - phenazine ethosulfate
- PH - pulmonary hypertension
- PI - propidium iodide
- PMT - photomultiplier tube
- PVH - pulmonary venous hypertension
- PVR - pulmonary vascular resistance
- r&bVECs - retinal and brain retinal and brain vascular endothelial cells
- RCF - relative centrifugal force
- RISC - RNA-induced silencing complex
- RNA - ribonucleic acid
- RNAi - RNA interference
- ROS - reactive oxygen species
- SM-22 alpha
- SMA - alpha smooth muscle actin
- SMAD - sma and mothers against decapentaplegic homologue
- SMC - smooth muscle cell
- SM-MHC - smooth muscle myosin heavy chain

- STAT1 - signal transducer and activator of transcription 1
- STAT3 - signal transducer and activator of transcription 3
- Tf- transferrin
- TfR1 - transferrin receptor 1
- TGF - transforming growth factor
- TMRM - tetramethylrhodamine methyl ester
- UMC - unaffected mutation carrier
- UTR - untranslated region
- VCAM-1 - vascular cell adhesion molecule-1
- VEC - vascular endothelial cell
- VEGF - vascular endothelial growth factor

1. Chapter 1 - Introduction

1.1 Pulmonary Arterial Hypertension (PAH)

1.1.1 Definition

Pulmonary arterial hypertension (PAH) is a rare and progressive disease defined by elevated pulmonary vascular resistance (PVR), if left untreated will lead to right ventricular failure and death. PAH is a type of pulmonary hypertension (PH) that affects mostly the pulmonary vasculature. PAH is defined by a resting mean pulmonary artery pressure (mPAP) of 20 mmHg (as defined by the 6th World PH symposium) or above, pulmonary capillary wedge pressure (PCWP) below equal to 15 mmHg and PVR above or equal 3 Wood units (Condon et al., 2019).

1.1.2 Classification of PAH

Pulmonary hypertension has been divided into five clinical groups: group 1 – pulmonary hypertension due to pulmonary vascular disease; group 2 – PH due to left heart disease; group 3 – PH due to to long disease or hypoxia, group 4 – PH due to chronic thromboembolic disease; and group 5 – a miscellaneous collection of PH caused by a variety of disorders.

PAH falls within the group 1 causes of pulmonary hypertension, which is then further stratified into subcategories (figure 1-1). Patients within each of these groups share pathophysiology, prognosis and therapeutic responses.

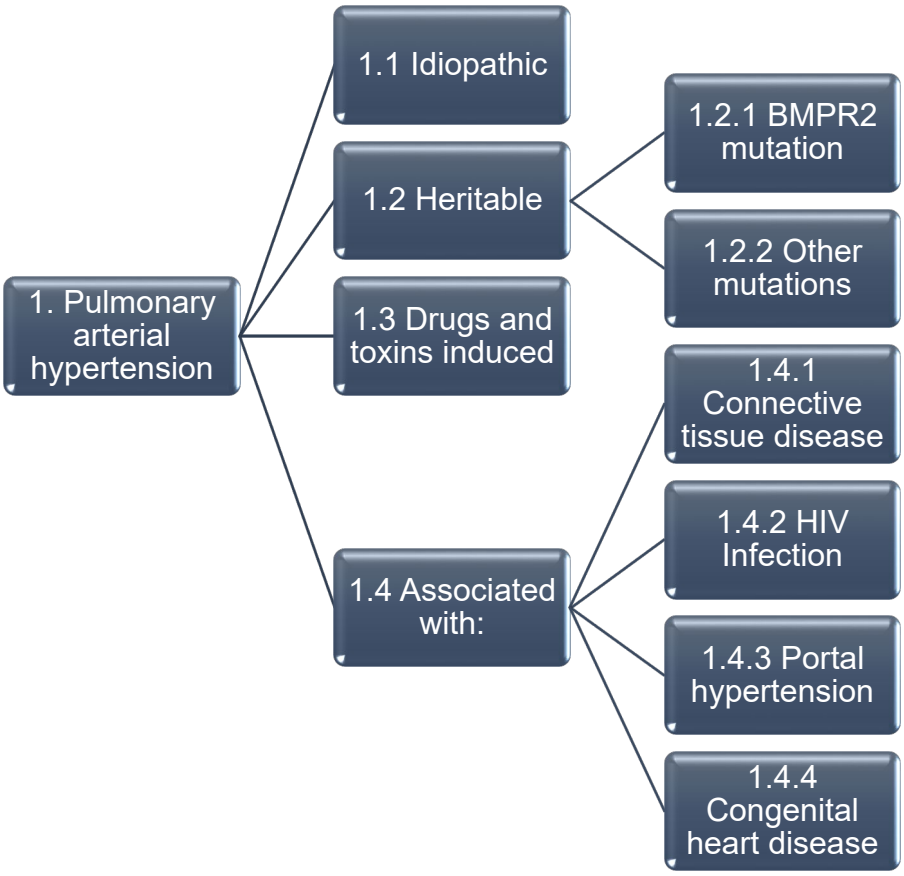

Figure 1-1 Subcategories of PAH according to the 6th World Symposium on pulmonary hypertension *(Condon et al., 2019).*

1.1.3 Pathophysiology of PAH

The pathophysiology of PAH is complex and multifactorial, even though the subcategories differ in relation to underlying causes, however all these groups have similar characteristics such as excessive pulmonary vasoconstriction, and abnormal vascular remodelling that affects all vessel layers (intima, media, and adventitia) (figure 1-2). This remodelling leads to severe loss of cross-sectional area and increasing right ventricular afterload, which is caused by elongated right ventricular systole that results in an abnormal reversal of the left-to-right pressure

gradient altering cardiac performance (Schermuly et al., 2011a, Coons et al., 2019, Cecconi et al., 2006).

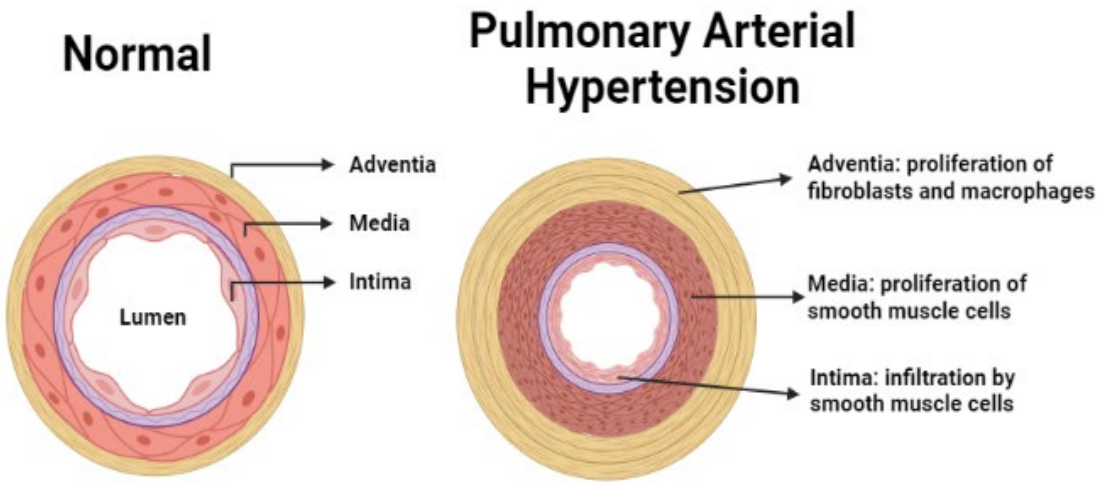

Figure 1-2 ***Representation of vascular remodelling in pulmonary arterial hypertension.*** *Cross-section of a normal pulmonary arteriole (left) and an arteriole affected by pulmonary hypertension (right). Adapted from Gordeuk et al. (2016). Image created in BioRender.*

Changes the intimal layer include endothelial injury, endothelial cell proliferation, myofibroblast like cells invasion of the intima layer, increased matrix deposition with intimal fibrosis and occlusion of the vascular lumen by plexiform lesions. Another important feature of PAH is smooth muscle cell proliferation. All these changes suggest a change from a quiescent state to a proliferative, apoptosis-resistant cellular phenotype. The main causes of these changes are mostly unknown, however it is hypothesised the instead of a single cause there are specific risk factors and/or types of vascular injury that may lead to vascular remodelling. These factors can be a genetic predisposition or exposition of an environment factor or have a dysfunctional immune system or it can be a mixture of those where a patient can accumulate enough of these “hits” to the pulmonary

vasculature, leading to endothelial cell dysfunction and smooth muscle cell proliferation (Tuder et al., 2009, Coons et al., 2019, Tuder et al., 2007).

1.1.3.1 Vascular Cell dysfunction in PAH

Blood vessels are formed of three distinct layers: the tunica intima, tunica media and tunica adventitia (figure 1-2). The intima layer consists of a monolayer of endothelial cells, a basal lamina composed of type IV collagen and the adhesion molecules fibronectin and laminin. The medial layer (prominent on small to large vessels) consists primarily of smooth muscle cells embedded in a plexus of elastin, different types of collagen and proteoglycans. The adventitia layer (present only on large vessels) consists mostly of fibroblasts, type I collagen, and an amalgamate of elastic fibres, nerves, and its own vasculature. Dysfunction of the layers that form blood vessels are hallmark characteristics of PAH (Gordeuk et al., 2016).

A healthy pulmonary circulation is a low pressure, high compliance system, however in PAH due to remodelling of the extracellular matrix (ECM) there is an increase in vascular stiffness and reduced pulmonary arterial compliance (PAC) (Thenappan et al., 2018). The most common characteristic across all forms of PAH remodelling is the muscularisation of distal peripheral arteries within the respiratory acinus, which is defined as the region of lung supplied by a first-order bronchiole that includes the respiratory bronchioles, alveolar ducts and alveolar sacs distal to a single terminal, also defined as the largest lung unit in which all airways participate in gas exchange (Humbert et al., 2008, Lumb, 2017). This remodelling occurs within all three layers of the blood vessel, where there is

proliferation of smooth muscle and endothelial cells, leading to plexiform lesion and pulmonary smooth muscle cell hypertrophy and hyperplasia. The expansion of ECM will cause stiffness and reduction of compliance, while the lesions caused by the proliferation of endothelial and smooth muscle cells reduce the vessels luminal area (or even its obliteration) and increase vascular resistance, which eventually can lead to right ventricular failure (Thenappan et al., 2018).

The exact mechanisms that drive these changes in are still poorly understood, however several mechanisms have been proposed (figure 1-3). Changes in the structure and function of endothelial cells has been proposed as the initial event. Pulmonary endothelial cells injury can be caused by several factors including increased flow, sheer stress, pulsatility, in addition inflammation can also cause dysfunction and cell damage; all of which results in loss of barrier function and increased permeability. This loss of endothelium integrity allows circulating factors to infiltrate the vessel wall and stimulate smooth muscle cells to secrete serine elastases, which in turn can cause the degradation of the ECM releasing active growth factors that are stored therein. These growth factors then can lead to increased deposition collagen, elastin, and fibronectin by via smooth muscle cell and fibroblasts stimulation all of which ultimately leads to remodelling of blood vessels (Thenappan et al., 2018, Thompson and Rabinovitch, 1996).

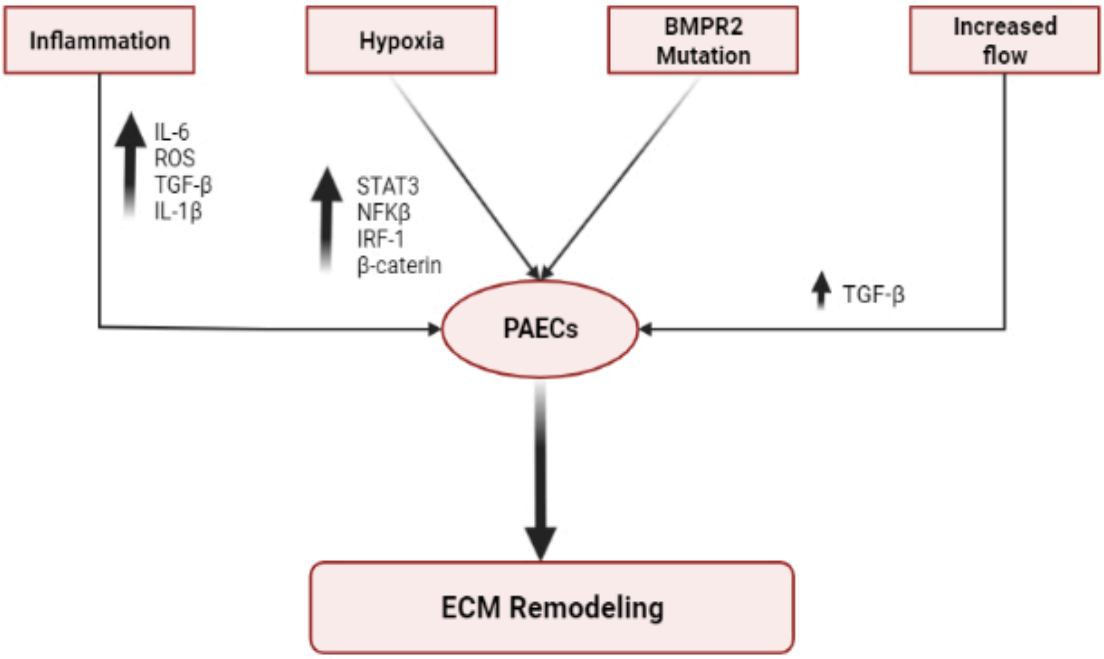

Figure 1-3 Proposed mechanisms for pulmonary vascular remodelling in PAH. *Increase in inflammation, hypoxia and blood flow via sheer stress coupled with altered BMPR2 signalling causes changes in endothelial cells to acquire a mesenchymal phenotype with a gene profile similar of smooth muscle cells. BMPR2, bone morphogenetic protein receptor; PAECs, pulmonary artery endothelial cells; ROS, reactive oxygen species; IL-6, interleukin-6; IRF-1, interferon regulatory factor-1; TGF-β, transforming growth factor beta; IL1-β, interleukin 1 beta; NFKβ, nuclear factor kappa beta; STAT3, signal transducer and activator of transcription 3. Adapted from Thenappan et al. (2018). Designed on BioRender.*

In addition, vessel remodelling has also been linked to endothelial-to-mesenchymal transition (EndoMT), where endothelial cells gain a mesenchymal phenotype with genetic profile of smooth muscle cells. This transition occurs when endothelial cells dissociate from the surrounding cells, which allows them to migrate from the cell monolayer. Loss of endothelial markers in these cells leads to the loss of cell-to-cell adhesion and increased migration (Arciniegas et al., 2007, Stenmark et al., 2016).

1.1.3.1.1 Inflammation in PAH

Established studies have described altered immunity and inflammation as recognised core features in PAH. Firstly, there was a recognition that some inflammatory conditions also had a high incidence of PAH (Hu et al., 2020). Secondly, lung biopsies from PAH patients detected the presence of inflammatory cells (macrophages, T and B lymphocytes and dendritic cells), all of which indicates the involvement of cytokines, chemokines and growth factors in this disease process and potentially as promoters of hyperproliferation of PAECs and PASMCs. Increased levels of IL-1 and IL-6 have been reported in the serum and lung tissue of severe PAH patients, and this was further confirmed in PAH animal models (Humbert et al., 1995, Kherbeck et al., 2013). Moreover, the extent of inflammation correlates with clinical outcomes, vascular remodelling and haemodynamics. Such observations have led to many clinical trials focused on treatments targeting inflammation, auto-immunity, metabolism, and immunotherapies. Large-scale human trials of immunological therapies are ongoing, such as inhibition of neutrophil elastase by elafin, and the IL-1β antagonist anakinra (Goldenberg et al., 2019). Even though there is increasing evidence that inflammation and immunity are involved in the pathobiology of PAH, such role in relation to disease causation remains to be demonstrated; in short are these events a promoter, or just a downstream consequence of the disease (Hu et al., 2020).

1.1.3.1.1.1 Inflammatory Mediators

Interleukin 6 is a pleiotropic pro-inflammatory cytokine that mediates many different physiological functions, which includes cell proliferation, cell survival and easing of apoptotic signals. IL-6 is also involved in bone formation, metabolism, endocrine functions and it can affect many cells of different organs and systems (Hodge et al., 2005). IL-6 acts through classic protein kinases such as MAPK (mitogen activated protein kinase). IL-6 directly activates the transcription factors STAT1 and STAT3 via the JAK tyrosine kinase (Hodge et al., 2005).

Patients with PAH have showed increased levels of IL-6 in their serum and lungs, which also correlates with prognosis (Soon et al., 2010). Moreover, overexpression of IL-6 in transgenic mice was able to induce mild PAH and the combination of IL-6 overexpression with hypoxia treatment resulted in vascular remodelling similar to severe PAH (Steiner et al., 2009, Golembeski et al., 2005). Similarly mice exposed to human recombinant IL-6 also exhibited similar response, whereas IL-6 knockout protected mice from developing hypoxia induced PAH (Golembeski et al., 2005, Savale et al., 2009). These mice also demonstrated elevated IL-6 mRNA levels in their PASMCs and increased cellular migration when exposed to IL-6. Moreover, examination of PASMCs from PAH patients showed upregulation of membrane bound IL-6R (IL-6 receptor), and overexpression of the IL-6R in these cells was shown to increase the expression of anti-apoptotic proteins (Tamura et al., 2018). Given the compelling nature of all these studies a clinical trial (NCT02676947) for tocilizumab, a monoclonal antibody against the IL-6 receptor currently used for the treatment of rheumatoid

arthritis, was undertaken from 2016 onwards to assess the drug response in group 1 PAH patients. The trial was completed; however no results have been posted as yet.

1.1.3.2 Current PAH treatment strategies

PAH is a multifactorial and heterogonous disease with multiple and different pathogenic alterations. Therefore the underlying mechanism of PAH development have still to be completely elucidated, which makes the treatment of PAH difficult. Current treatments includes supportive therapy such as diuretics, supervised rehabilitation, and oxygen supplementation if needed (Sommer et al., 2021, Ulrich et al., 2019).

The current pharmacological therapies available for PAH treatment targets three pathways (figure 1-4) that regulate endothelial factors with vasoconstrictive/vasodilatory and proliferative properties. Calcium channel blockers are indicated for patients that exhibit vasoreactivity, and inhaled nitric oxide is used in most clinical centres. Another strategy is the use of endothelin receptors antagonists (ERAs) to counter the overexpression of the vasoconstrictor endothelin-1 in PAH. Bosentan is an ERA that targets both ET_A and ET_B receptors and ambrisentan and macitentan (also active for ET_B, however is 100-fold more selective for ET_A) which selectively targets ET_A. Phosphodiesterase-5 (PDE5) inhibitors are used to inhibit cyclic guanosine monophosphate (cGMP) breakdown. cGMP contributes to smooth muscle cell vasodilation by increasing NO, a potent vasodilator. There are two PDE5 inhibitors available: tadalafil and sildenafil; and also riociguat a soluble GC

stimulator. The use of prostanoids (prostacyclin analogues) is also a therapeutic strategy for PAH. Prostacyclin induces vasodilation and its synthesis is decreased in PAH patients (Galiè et al., 2003). Prostanoids available to treat PAH are epoprostenol, treprostinil, and iloprost; there is also the orally available IP (prostaglandin I2) receptor agonist selexipag. Furthermore, improvement in the outcome of patients with PAH have been possible by the use of combination therapy that targets multiple pathways (Fuso et al., 2011, Sommer et al., 2021, Humbert et al., 2019).

It is important to consider that these treatments target vasodilatory pathways and does not treat the underlying pulmonary remodelling, therefore it is important to investigate and elucidate remodelling mechanisms to improve therapy strategies.

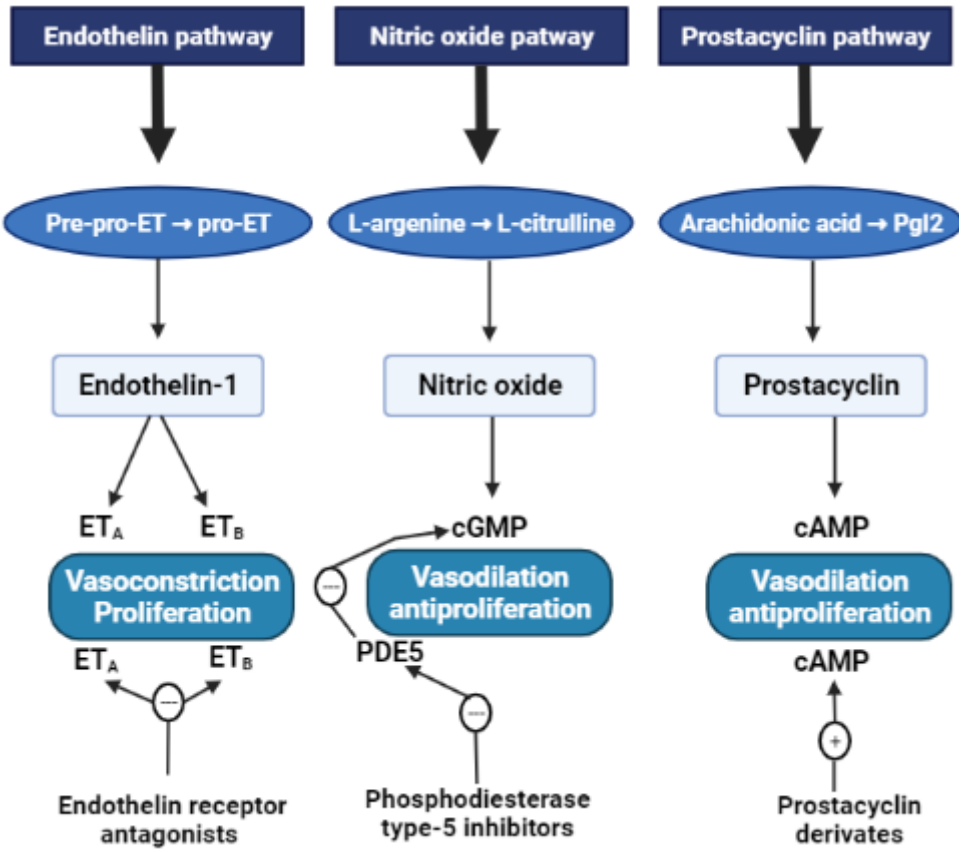

Figure 1-4 Current PAH therapy strategy. *There are three main pathways that targeted for the treatment of PAH: the endothelin pathway; nitric oxide pathway; and prostacyclin pathway. These pathways are involve in vasodilation/vasoconstriction of blood vessel. Adapted from Boutet et al. (2008) and Fuso et al. (2011). Figure created in BioRender.*

1.1.4 Role of TGF-β signalling in PAH

1.1.4.1 TGF-β signalling

The transforming growth factor-β (TGF-β) is an evolutionary conserved family of growth factors that control a plethora of cellular responses that are mostly involved in cell differentiation, morphogenesis, tissue homeostasis and regeneration. Therefore many diseases have been linked to malfunction of TGF-β signalling (Massagué, 2012, Tzavlaki and Moustakas, 2020).

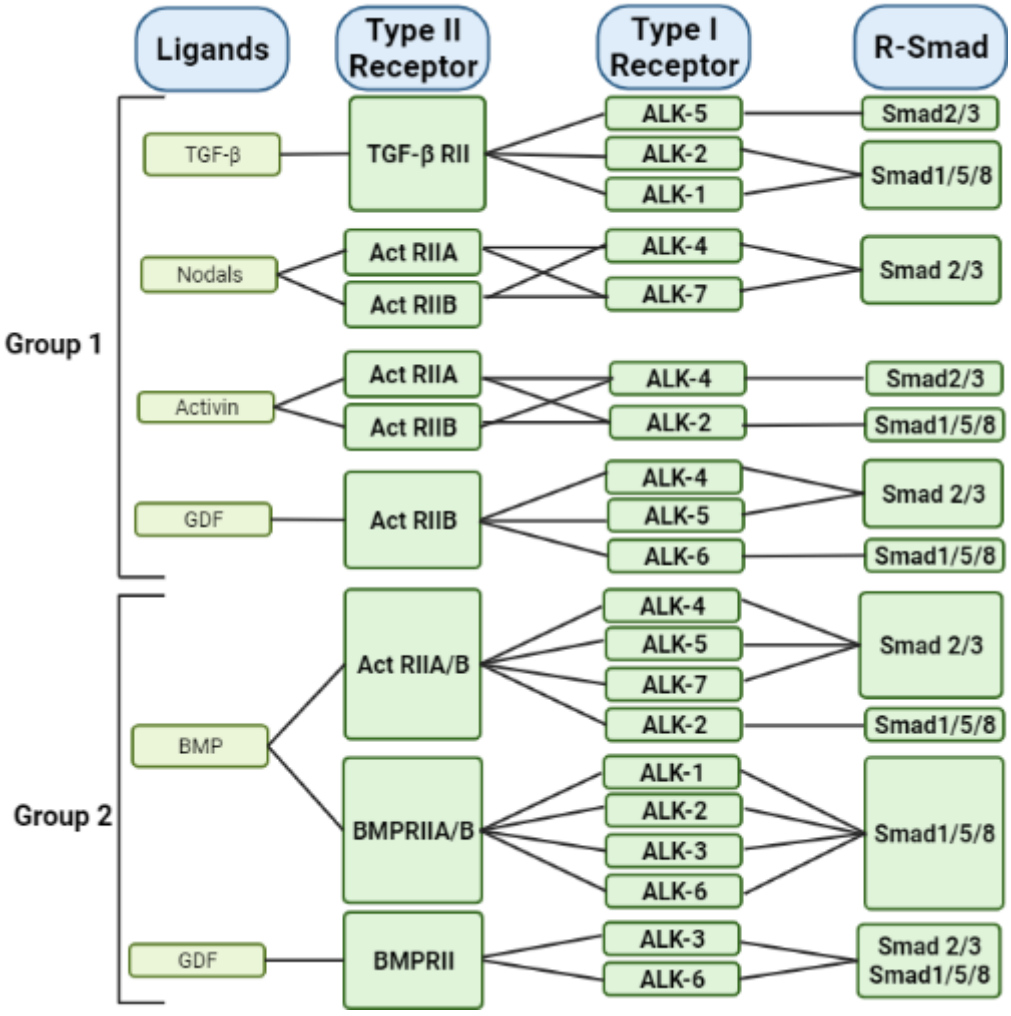

Figure 1-5 TGF-β and BMP signalling. *The TGF-β family members are subdivide in two groups. One group is formed by TGF-β signalling pathways and group two is formed of the BMP signalling pathway. Figure adapted from Rol et al. (2018). Image created in BioRender.*

There are two functional groups of the TGF-β family members (figure 1-5), the TGF-β group that comprises mostly of the three TGF-β isoforms (TGF-β1, TGF-β2 and TGF-β3) which are collectively referred as TGF-β, and the BMP group that include all BMPs and most growth and differentiation factors (GDFs). TGF-β signals by forming dimers and binding to a heterotetrameric complex of type I and type II serine/threonine kinase transmembrane receptors, mostly as a result of

TβRII forming a complex with TβRI (or ALK5). BMPs signal through the BMP type II receptor (BMPR2), ActRIIA or ActRIIB in combination with a type I receptor (ALK1, ALK2, ALK3 or ALK6) (Oh et al., 2000, Rol et al., 2018). Once these receptors complexes are activated they will transduce the signal from the membrane to nucleus through phosphorylation of the SMAD transcription factors (figure 1-6).

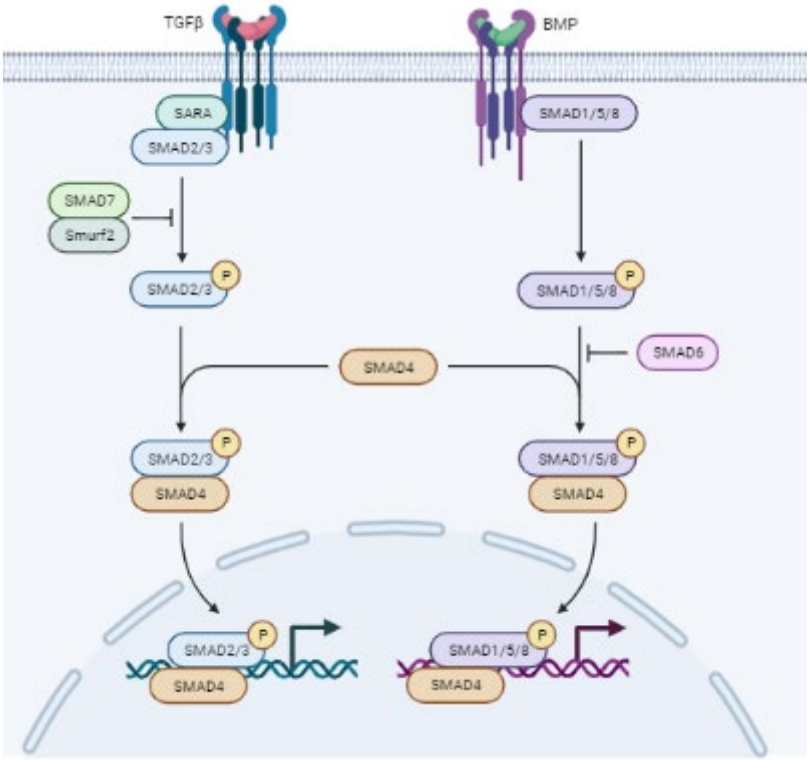

Figure 1-6 TGF-ß and BMP signalling. *Signalling start by a "type 1" and "type 2" receptors forming a heterotetrametric complex, upon ligand biding the "type 2" receptor phosphorylate the "type 1" that will then phosphorylates signal transduction targets, usually R-SMADs that will form a complex with a co-SMAD that will enter the nucleus and bind BMP response element DNA sequence (Andruska and Spiekerkoetter, 2018). Image created in Biorender.*

1.1.4.2 TGF-β signalling in PAH

The TGF-β family is thought to play a major role in the development of PAH. Mutations in the BMPR2 receptor were the first identified genetic link to PAH, and since then the identification of other BMPR2 genetic mutations; new genetic mutations have been identified in other members of the TGF-β family (Tzavlaki and Moustakas, 2020) . Other studies have demonstrated that TGF-β ligands are increased in endothelial cells an in plexiform lesions (Ma et al., 2011, Jonigk et al., 2011). A study by Yang et al. (2011) showed that endothelial cells transfected with a truncated BMPR2 protein increased their susceptibility to apoptosis. More interestingly these transfected cells released higher levels of TGF-β1 and PASMCs proliferation was increased by conditioned media from PAECs that expressed mutated BMPR2. Increased levels of TGF-β and increased expression of ALK1 and ENG receptors have been found in iPAH patients compared to normal controls (Gore et al., 2014). Balanced signalling between TGF-β and BMP is vital for tissue homeostasis and a study by Hiepen et al. (2019) showed that BMPR2 may serve as a gatekeeper of this balance. They demonstrated that BMPR2 deficiency did not abolish SMAD1/5 signalling, instead signalling was maintained by the formation of mixed TGF-β and BMP receptor complexes increasing the expression of extracellular matrix proteins. This imbalance has been used as the basis of the development of new treatment, for example, Sotatercept, which binds to activins and GDFs to restore balance (Humbert et al., 2021).

1.1.5 Genetics of PAH

In the year 2000 the first genetic link of PAH was identified, heterozygous mutations in BMPR2 these mutations were then also identified in IPAH patients (Deng et al., 2000, Lane et al., 2000). Since then it has been stablished that 70-80% of familial PAH and 10-20% of IPAH cases are caused by mutations in BMPR2 (Evans et al., 2016). Even though it has been confirmed that mutations in the BMPR2 protein is pathogenic the penetrance of the disease phenotype is incomplete. It is estimated that penetrance in males is around 14% and in females is around 42% (Larkin et al., 2012), which makes the female sex a critical factor for the penetrance of BMPR2. Other factors that may influence BMPR2 penetrance are genetic (other genes), epigenetics and/or environmental factors.

Since BMPR2 was identified, gene sequencing of BMP-SMAD signalling intermediaries identified sequence variants in SMAD1, SMAD4 and SMAD9 that have a role in PAH. A study of a 3-generation family with a several affected members with PAH but with no mutations in BMPR2 or TGF-β, identified a mutation in caveolin-1 (CAV1), which functions to physically colocalise BMP receptors (Austin et al., 2012). Exome sequencing also identified mutations in KCNK3 (potassium channel subfamily K member 3) in familial cases of PAH and also in unrelated patients with IPAH (Ma et al., 2013). Whole exome sequencing (WES) of paediatric patients and adult-onset patients with HPAH and IPAH, identified a deleterious variant in the TBX4 gene in paediatric patients compared to adult onset patients (Zhu et al., 2018). Whole genome sequencing of 1048 patients with PAH identified mutations in GDF2 (the gene for BMP9) and

recognised ATP13A3, AQP1 and SOX17 (Gräf et al., 2018, Condon et al., 2019, Morrell et al., 2019).

There are 16 genetic risk factors that have been identified for PAH, and the majority of these variants are associated with the BMP-SMAD signalling pathway, which includes *BMPR2*, *ACVRL1* (activin receptor-like1; also known as ALK1), *ENG* (endoglin), *SMAD4*, *SMAD9* and *CAV1*. Therefore, dysregulation of BMP signalling remains the principal risk factor for the development of PAH (Southgate et al., 2020).

1.1.6 The role of Hypoxia in PAH

1.1.6.1 Hypoxia signalling pathway

Hypoxia is controlled by hypoxia-inducible factor (HIF) stabilisation. HIF is a family of transcription factors formed as a heterodimer of a constitutively expressed subunit, HIF-β and an oxygen controlled subunit, HIF-α (Semenza, 2007, Corrado and Fontana, 2020). HIF regulation is dependent on the activity of proly-4-hydroxilases (PHDs) that regulate the activity of the alpha subunit post-translationally. In normoxic conditions HIF-α subunits (HIF1-α, HIF2-α or HIF3-α) are kept inactive by hydroxylation of specific residues by PHDs, triggering an ubiquitination reaction by E3 ubiquitin Von Hippel-Lindau protein (pVHL) causing degradation of HIF. By contrast, under low oxygen levels, HIF-α hydroxylation is inhibited allowing HIF-α to be translocated to the nucleus and to dimerize with the HIF-β, which in turn will then bind to the hypoxia-responsive elements (HREs)

of specific target genes (Slemc and Kunej, 2016, Corrado and Fontana, 2020, Lee et al., 2019). A summary of hypoxia signalling can be found in figure 1-7.

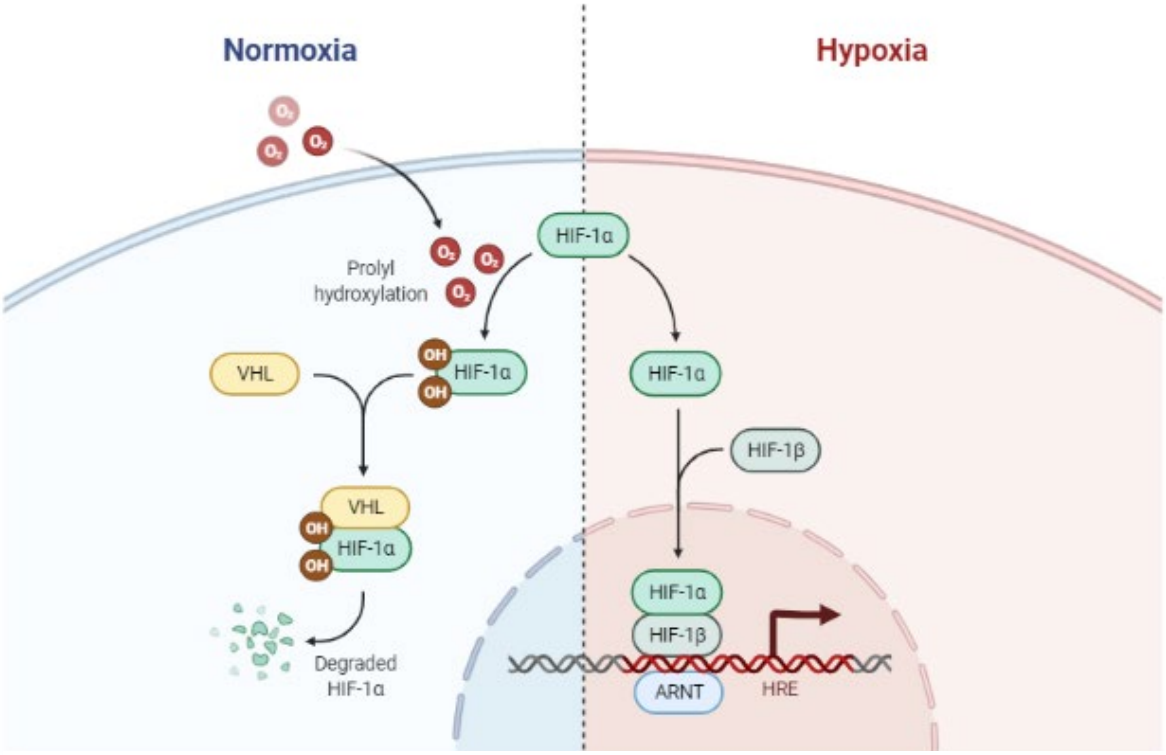

Figure 1-7 Simplified hypoxia signalling. *In normal oxygen conditions HIF-α subunits are inactivated by proly-4-hydroxilases (PHDs), which cause their degradation by triggering ubiquitination reaction via E3 ubiquitin Von Hipple-Lindau protein (pVHL). In hypoxic conditions hydroxylation of PHDs is inhibited, which allows HIF-α to translocate to the nucleus and dimierize to HIF-β that in turn will bind to the hypoxia-responsive elements. Figure created in BioRender.*

1.1.6.2 PAH and hypoxia

The main evidence that hypoxia is a major factor in the development of pulmonary hypertension is demonstrated by observations that native sea-level dwellers who move to high altitude/low oxygen environments develop increases in pulmonary vascular resistance and pulmonary arterial pressure, without the presence of pre-existent lung disease (Rowan et al., 2016, Pak et al., 2007, Young et al., 2019).

Hypoxia has been recognised as a factor involved in the proliferation/remodelling pulmonary vascular cells. A study by Howell et al. (2003) demonstrated that the

volume and length of blood vessels was increased in the pulmonary circulation of hypoxic Sprague-Dawley rats as compared to normoxic controls. Furthermore hypoxic rat lungs showed an increased capillary surface area and increased numbers of vascular cells compared to the lungs of animals maintained in normal oxygen levels. In vitro studies have demonstrated that hypoxia can cause proliferation of pulmonary cell fibroblasts, however systemic fibroblasts remained unaffected under the same conditions (Welsh et al., 2006). Moreover, hypoxia has been shown to inhibit anti-proliferative factors, such as prostacyclin, and to increase the release of pro-proliferative and inflammatory factors, such as IL-6, IL-8, MCP-1 and VEGF from smooth muscle cells, endothelial cells and fibroblasts; so increasing proliferation vascular cells (Kourembanas et al., 1991, Mukhopadhyay et al., 1995, Pak et al., 2007).

Specific studies of HIF isoforms have shown the involvement of HIF in the regulation of vascular cell function. Deletion of HIF1-α in PASMCs reduced vascular remodelling and right ventricular systolic pressure in hypoxic mice (Ball et al., 2013). Another study by Sheikh et al. (2018) demonstrated a dependence on HIF1-α for cell migration and expansion of PASMC progenitors. Furthermore, they demonstrated that hypoxic endothelial cells secrete factors that modulate distal arteriole muscularisation. Deletion of prolyl-4-hydrolase 2 (PHD2) in the endothelial cells of mice induced vascular remodelling and severe pulmonary artery hypertension in these animals (Kapitsinou et al., 2016, Dai et al., 2016).

Hypoxaemia is a characteristic of PAH, thus it is of potential importance as hypoxia inducible factor (HIF) is regulated by both oxygen and iron and the

interplay between these species will impact on HIF activity with consequences for cellular iron uptake, cell growth and also inflammatory responses (Price et al., 2012, Ramakrishnan et al., 2018a). An increasing number of genes involved in iron homeostasis have been shown to possess IREs as well as hypoxic responsive elements (HREs) within their promoter and/or regulatory regions, Thus expression of these proteins can be regulated not only by IRPs but also by HIF. Furthermore, HIF is controlled by the enzymatic activity of the iron and oxygen sensing prolyl hydroxylases, and exhaustion of either iron or oxygen can lead to HIF activation and an array of transcriptional responses (Ramakrishnan et al., 2018a, Simpson and McKie, 2015). Therefore, iron deficiency could potentially lead to HIF activity under normoxic conditions.

1.2 Iron Homeostasis

1.2.1 Introduction

Iron is essential for oxygen utilisation in the human body, the importance of iron lies in its ability to mediate electron transfer. Oxygen is a stable chemical element (two unpaired electrons with parallel spin), therefore, a relatively unreactive molecule. Iron as a transition metal can subsist in different states of valence, thus it can donate or accept electrons singly, enabling it to convert oxygen to a metabolically reactive state. As a result, body iron requirements are mostly involved with oxygen utilisation, such as respiration, molecular transport, molecular storage, antioxidant protection and biosynthesis (Ramakrishnan et al., 2018a, Andrews and Schmidt, 2007).

Iron is essential for life and it is utilised in many aspects of cell function, it is involved in ATP (adenosine triphosphate) production, and is an absolute requirement for ribonuclease reductase activity, an enzyme which has a critical role in DNA synthesis. Furthermore, iron is also required in the brain for myelogenesis and myelin maintenance, amongst many other requirements. Therefore, a readily supply of iron is vital for all organs in the body (Gao et al., 2019). However, iron can also be toxic to the body by catalysing the formation of damaging reactive oxygen species (ROS) that can damage bio-molecules, cells and tissues; in addition, there are impacts on redox signalling processes, all of which indicates why tight control of body iron resources is necessary. Iron homeostasis is regulated at systemic and cellular levels. Systemic iron is regulated by controlled absorption of dietary ferrous Fe^{2+} or haem by enterocytes present in the proximal small intestine (Ghio, 2009, Andrews and Schmidt, 2007) and through reprocessing and recycling of iron resources, these are multifactor processes that are chiefly regulated by the liver (Ramakrishnan et al., 2018a)

Iron absorption is controlled by a variety of factors such as inflammation; oxygen and haemoglobin concentration; erythropoiesis levels; and total iron stores. Iron uptake from diet provides 1 – 2 mg of iron on a daily basis, which is largely balanced, by similar iron losses. As such, there are no specific iron excretory mechanisms, rather iron losses occur through sweating, shedding of intestinal epithelial and skin cells, and blood loss. Although iron loss is compensated by iron uptake from the gut, this is not enough to fulfil the daily requirement of 20 mg (adult male). Therefore, such iron requirements are met by recycling endogenous iron and stores (Ramakrishnan et al., 2018a).

Iron absorption mainly occurs in the small intestine facilitated by mature enterocytes, to move from the lumen of the intestine to the blood stream iron must cross the apical and basolateral membranes of enterocytes and this occurs via DMT1 (divalent metal-ion transporter 1). Once iron enters the cell and it is not required immediately it becomes sequestered within the cell to the iron storage protein ferritin. If the iron is then required it can be exported by the iron exporter ferroportin (Anderson and Frazer, 2017).

1.2.2 Systematic iron regulation and transport

Freshly absorbed or iron released from storage as Fe^{3+} is bound to plasma transferrin (Tf), which is the main protein to transport iron in the the body, and sent to sites where iron is needed. Transferrin delivers iron into cells by binding to transferrin receptor 1 (TfR1) present in the cellular membrane that initiates a receptor-mediated endocytotic process where the Tf-TfR1 is internalised, upon release of iron within the endosome the Tf-TfR1 complex is recycled (figure 1-4) (Anderson and Frazer, 2017, Gao et al., 2019).

At the systemic level iron demands and variations thereof are communicated to the liver which then modulate the expression and release of the peptide hormone hepcidin. Hepcidin regulates cellular iron needs by binding to ferroportin, an iron exporter, causing it to be internalised and degraded, thus reducing cellular iron efflux (Gao et al., 2019). This will covered in more detail below.

1.2.3 Cellular Iron regulation

Cellular iron (figure 1-4) is regulated by two cytoplasmic proteins with mRNA-binding properties, iron regulatory proteins 1 and 2 (IRP1 and IRP2), when active these proteins bind to regulatory motifs termed iron responsive elements (IRE) either located at the 5' or 3' ends of target mRNA, present in several iron related proteins. IRP binding to IREs is depended on cellular iron availability, even though IRPs do not sense iron levels directly.

When cells are iron-replete and oxygenated IRPs are ubiquitinated and degraded, this occurs by IRPs interacting with the FBLX5 (F-Box and leucine rich repeat protein 5) that recruits an E3 ligase complex and promotes the ubiquitination and degradation of IRPs. The iron sensing ability of FBXL5 is within the iron-binding N-terminal haemerythrin-like (Hr) domain of FBXL5. When not bound to iron the Hr domains changes conformation leading to polyubiquitination and degradation of FBLX5 causing the accumulation of IRP2 (Muckenthaler et al., 2017, Thompson et al., 2012).

IRP binding to IRE is promoted when iron concentration is low by binding to the 5' untranslated region (UTR) of the target mRNA supressing protein translation, in the other hand, translation is enhanced when the IRE binds to the 3' UTR. Thus, cells low in iron can reduce synthesis of ferritin (5' UTR) at same time increase synthesis of transferrin receptor (3'UTR), which allows the cell to increase iron uptake from plasma. When cellular iron increases IRPs dissociate from the IRE, reversing the process, stopping iron uptake and encouraging iron storage in ferritin (Lal, 2020). Other iron regulatory proteins also have IREs, such

as DMT1, ferroportin and hypoxia induced factor 2α making it possible to regulate these important iron regulatory proteins according to cellular needs (Kuhn, 2015).

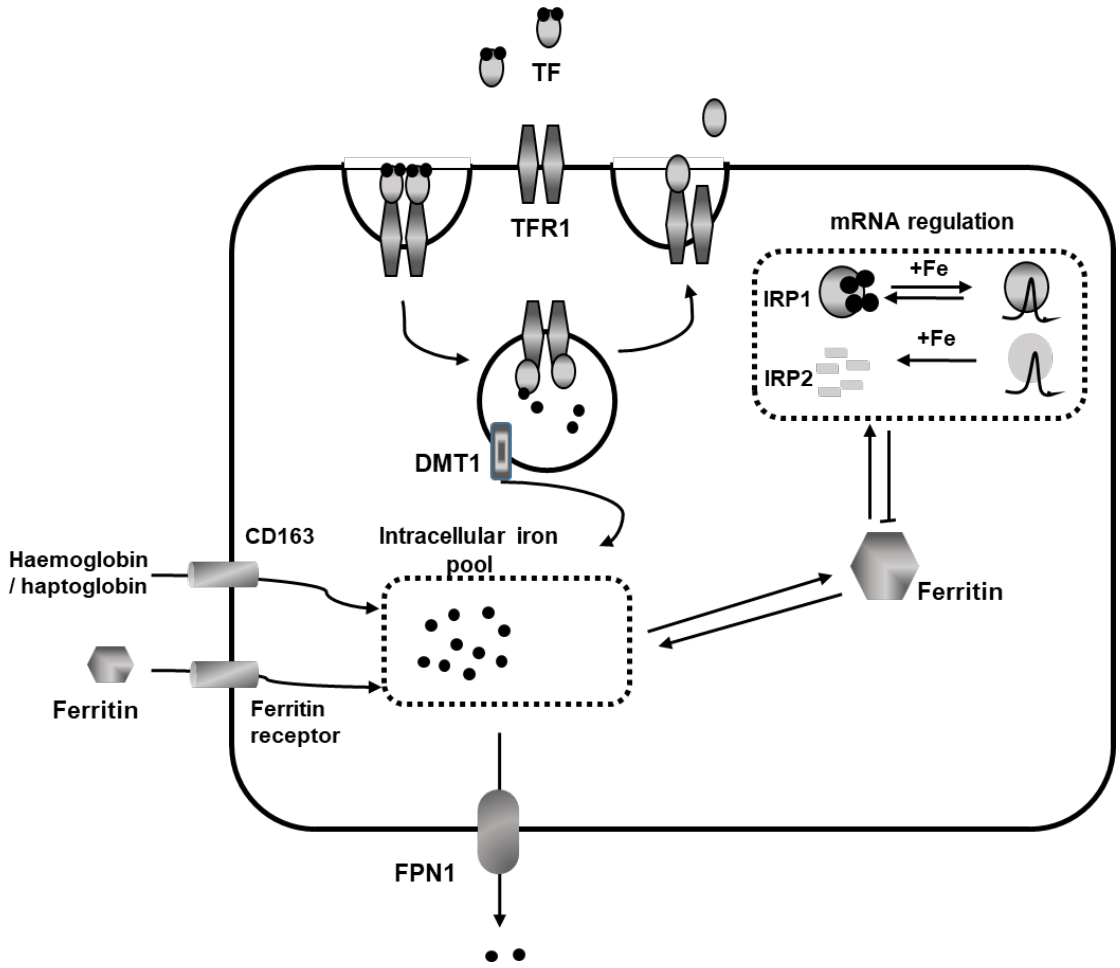

Figure 1-8 Cellular iron homeostasis. *Diferric transferrin (TF) binds to to the transferrin receptor 1 (TRF1) on the plasma membrane and the complex is internalised in endosomes, and moved across the endosomal membrane by the divalent metal-ion transporter 1 (DMT1). Surplus iron that is not need by the cell can be exported to the extracellular space by ferroportin (FPN1). Some cell types can also import iron through other mechanisms, such as iron contained within ferritin, or within haemoglobin through the CD163 receptor. Iron storage and intake are regulated by the iron-responsive element and iron regulatory protein (IRP) system. Low iron concentration leads to the synthesis of TFR1 and suppression of ferritin, whereas in high cellular iron the opposite occurs, ferritin expression is increased and TFR1 decreased. Figure adapted from Wu et al. (2004).*

1.2.4 Mitochondrial iron regulation

Mitochondria are critical for the survival of eukaryotic cells as they are necessary for energy metabolism. Mitochondria is also essential for the generation of metabolites and the regulation of trace elements such as iron, copper, manganese, and zinc (Kashiv et al., 2016, Cheng et al., 2022). Thus, appropriated mitochondrial regulation of these elements are vital for mitochondrial function.

Iron is utilised by the mitochondria in three major pathways: haem synthesis, iron-sulphur (Fe-S) cluster biogenesis and iron storage in mitochondria specific ferritin. Fe-S clusters are co-factors in proteins that are involved in vital functions, i.e. electron transport, redox reactions and many other functions (Lill et al., 2006). Haem synthesis it is exclusive to the mitochondria, occurring in eight phases four of which take place within the mitochondria while the remaining steps take place in the cytoplasm (Ponka, 1997, Richardson et al., 2010). Another important role for mitochondria is iron storage, as mitochondria require a regular influx of iron to maintain the synthesis of Fe-S clusters and haem. Therefore in order to satisfy this constant requirement mitochondria are able to store iron in a protein complex akin to ferritin but specific to this organelle and named mitochondrial ferritin. Iron has to be stored in this manner to minimise the potential toxic effects of iron. Mitochondrial ferritin oxidises Fe^{2+} to the less redox-active Fe^{3+} and then stores this resource safely within the protein matrix (Richardson et al., 2010, Cheng et al., 2022). In addition to iron storage and utilisation mechanisms, mitochondria must also regularly iron export, as failure to do so can cause severe mitochondrial iron overload which results dysfunction and potential disease presentation, such

as neurodegenerative disease (Huang et al., 2009, Mena et al., 2015) and cardiomyopathies (Cardenas-Rodriguez et al., 2018).

Indeed, the consequences of dysregulation of mitochondrial iron homeostasis has been linked with many diseases and cause organ dysfunctions, of the nervous system, heart and muscle (Gao et al., 2021). Haem synthesis has been shown to be increased in lung cancer cells (Hooda et al., 2013), studies of other cancer types has shown that mitochondria in these cancerous cells utilises iron to synthesise cofactors to meet the needs of a rapid proliferating cell (Tan et al., 2015, Vyas et al., 2016). More importantly, mitochondria dysfunction has emerged as critical factor in PAH. Studies have shown that PAH PASMC mitochondria have impaired mitochondrial metabolism, where there is a shift in metabolism from glucose oxidation in the mitochondria to the less energy efficient process of glycolysis in the cytosol (Hagan et al., 2011). In PAH mitochondria gain changes in redox signalling, they have impaired fusion and increased fission causing fragmentation of mitochondrial networks in PASMC (Ryan et al., 2015). The importance of iron regulation in mitochondria in any disease where impaired iron homeostasis has been identified and should therefore be considered as potentially of relevance for any disease presentation.

1.2.5 The ferroportin/hepcidin axis

1.2.5.1 Hepcidin peptide

Hepcidin is a small peptide hormone that functions as an iron homeostasis regulator and also as mediator of host defence and inflammation. Hepcidin was first isolated from urine and plasma ultrafiltrate and was initially named LEAP-1

(liver-expressed antimicrobial peptide), however it was subsequently named hepcidin due to its hepatic (liver) origin and antimicrobial effect (Park et al., 2001, Krause et al., 2000). The involvement of hepcidin in iron regulation was first described in a hepcidin knockout mouse model, where iron accumulation was observed in the liver, pancreas and to lesser extent in the heart of these mice (Nicolas et al., 2001).

1.2.5.2 Forms and Structure

Human hepcidin is a 25 amino acid peptide, in addition to the 25 amino acid form there is also two minor forms composed of either 20- or 22 amino acids that are truncated at the N-terminus. The N-terminus of hepcidin is essential for activity, therefore deactivation of hepcidin occurs by cleavage of the N-terminus (Nemeth et al., 2006). All three hepcidin isoforms are detected in urine, however only hepcidin – 25 and hepcidin-20 are detected in serum, which supports the idea that hepcidin-22 is just a degradation product of hepcidin-25 (Erwin et al., 2008). The hepcidin gene (*HAMP*; OMIM 606464) located on chromosome 19q13.1 has 3 exons that encode an 84- amino-acid preprohepcidin that undergoes enzymatic cleavage resulting in mature bioactive hepcidin 25 amino acid form. NMR analysis of human hepcidin showed it contains 8 cysteine that forms hairpin shaped molecule with a distorted β-sheet stabilised by four disulphide bridges. One of these bridges is located close to the hairpin loop, which suggests it could be a crucial domain for molecule activity (figure 1-5) (Erwin et al., 2008, Ganz, 2005, Hunter et al., 2002).

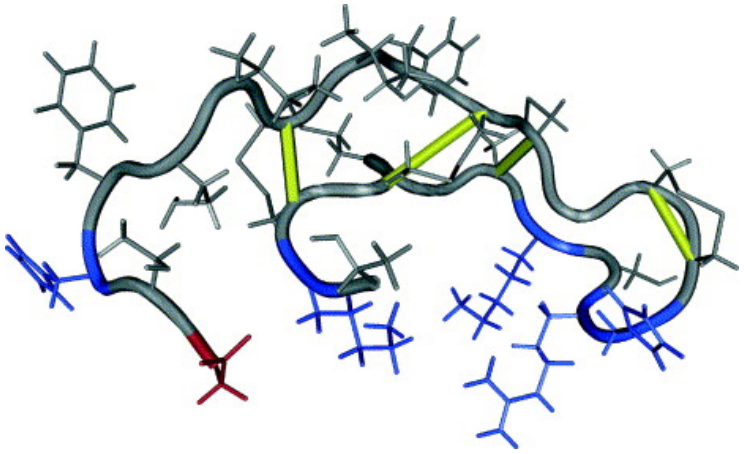

Figure 1-9 NMR structure of hepcidin. *Positively-charged residues are in blue, negatively-charged residues in red, disulphides in yellow. Image taken from Ganz (2005).*

1.2.5.3 Hepcidin synthesis regulation

Hepcidin synthesis has been extensively studied, however many aspects of it are poorly understood. Hepcidin main function is to negatively regulate iron absorption and hepcidin expression is upregulated by elevated iron levels and inflammation. Studies following hepcidin discovery observed that iron levels, erythropoiesis and inflammation regulates hepcidin expression, however the exact mechanisms of this regulation are still unknown. The two main pathways involved in hepcidin expression are the bone morphogenetic proteins (BMPs) and the JAK2-STAT3 pathway through the IL-6 receptor (Vyoral and Jiri, 2017).

Hepcidin expression is inhibited in iron deficiency, hypoxia and erythropoietic expansion (Camaschella and Pagani, 2018). Human studies showed that levels of circulating hepcidin during hypobaric hypoxia is downregulated (Piperno et al., 2011, Talbot et al., 2012), however the underlying mechanism for hepcidin downregulation in hypoxia are lacking. This reduction of hepcidin expression during hypoxia is hypothesised to arise by reduction of iron availability. However,

Talbot et al. (2012) demonstrated that the suppression of hepcidin during hypoxia is too fast to be caused by a decreased in iron availability, suggesting that erythropoiesis and/or hypoxia induction factors (HIF) could be responsible for this setting. Sonnweber et al. (2014) showed that the platelet-derived growth factor-BB (PDGF-BB) produced during hypoxia by several cell types significantly decreased serum levels of plasma hepcidin in healthy volunteers. However, hepcidin has been shown to be significantly elevated in IPAH patients (Rhodes et al., 2011a).

1.2.5.3.1 Bone morphogenetic proteins and regulation of hepcidin

Bone morphogenetic proteins are part of the transforming growth factor (TGF)β family that play an role in many aspects on embryonal development, bone development, tissue haemostasis and regeneration (Nickel and Mueller, 2019). The work by Meynard et al. (2009) showed that the deletion of the bone morphogenetic protein 6 (BMP6) on animal models caused a great increase in iron overload and more importantly hepcidin was not detected in the blood serum of these animals. This work and subsequent studies established that hepcidin expression and regulation by iron occurs via the BMP-SMAD pathway. Increased levels of iron in the liver leads to increased expression of BMP6. BMP6 binds to the receptors BMPR-1/BMPR-2 causing the phosphorylation of SMADs proteins (SMAD 1,5,8) which forms a complex with SMAD 4 that are translocated into the cell nucleus activating hepcidin transcription (Figure 1-10). The BMPR co-receptor haemojuvelin (HJV) it is essential for hepcidin expression, mutations in

its gene (HFE2) are known to be responsible for the iron overload condition known as juvenile haemochromatosis (Malyszko, 2009).

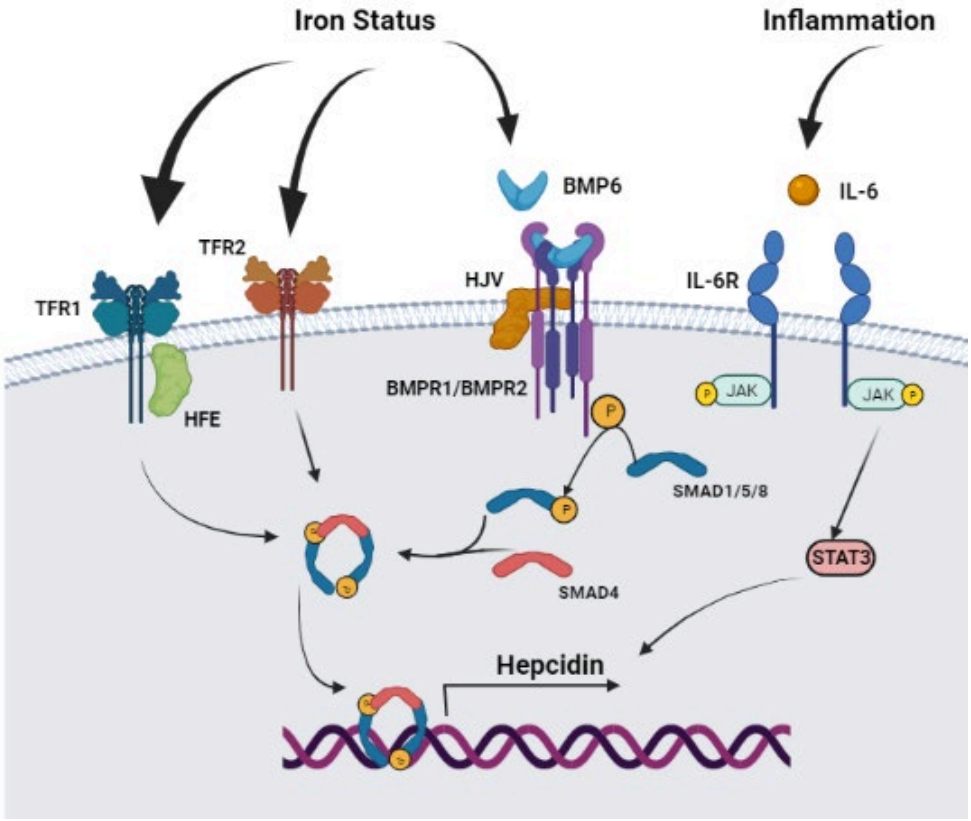

Figure 1-10 Simplified hepcidin Regulatory pathways. *Iron status extracellularly induces hepcidin transcription via the BMP-SMAD pathway, and in an extent through transferrin receptor 1 and 2, however this is not fully understood. Hepcidin expression is also regulated by inflammation through the JAK-STAT3 pathway, when IL-6 receptor is activated by the inflammatory cytokine IL-6. BMP6, bone morphogenetic protein 6; BMPR1, bone morphogenetic protein receptor 1; BMPR2, bone morphogenetic protein receptor 2; HJV, hemojuvelin; IL-6, interleukin 6; IL-6R, interleukin 6 receptor; JAK, janus kinase; STAT3, signal transducer and activator of transcription 3; SMAD1//5/8, sma and mothers against decapentaplegic homologue 1/5/8 complex; SMAD 4, sma and mothers against decapentaplegic homologue 4; TFR1, transferrin receptor 1; TFR2, transferrin receptor 2; HFE, hemochromatosis protein. Adapted from Rishi et al. (2015). Figure created with BioRender.*

1.2.5.3.2 Hepcidin Regulation by inflammation

Inflammation regulates hepcidin expression induced predominantly by interleukin (IL)-6 (but also IL-1β and IL-22). IL-6 binds to its receptor (IL-6R) followed by Janus kinase (JAK)/signal transducer activation/phosphorylation of the transcription factor (STAT)-3 and biding to the hepcidin promoter (figure 1-10) (Lee et al., 2006). IL-6 infusion in humans increased hepcidin production and decreased serum iron and transferrin saturation (Nemeth et al., 2004). Furthermore, studies have shown that hepcidin induction in hepatocyte cells and mice by microbial molecules are dependent on IL-6, and induction was reversed by IL-6 inhibition with neutralising antibodies and also in mice lacking IL-6 (Sangkhae and Nemeth, 2017).

Studies have suggested that the BMP-SMAD and JAK/STAT pathways may interact to to induce hepcidin. Inhibition of SMAD1/5/8 in animal models of anaemia of inflammation blunted hepcidin production. Moreover knockout of SMAD4 in mice decreased hepcidin expression by a 100-fold in liver (Wang et al., 2005, Theurl et al., 2011). Another study that used knockout mice models of BMP type I receptors (Alk3 and Alk2) showed that induction of hepcidin expression is dependent on the presence of BMP type I receptor Alk3. Therefore, the BMP signalling mechanisms required for IL-6 induction of hepcidin expression (Alk-3 dependent) diverge from the ones required for iron sensing (dependent on Alk2 and Alk3) (Mayeur et al., 2014b).

1.2.5.4 The Iron Exporter Ferroportin

The bioactive form of hepcidin inhibits the release of iron from the cell cytoplasm into the circulation by regulating the only known iron exporter ferroportin (FPN1) present on the membrane of cells. Ferroportin is the product of the *FPN1* (*SLC40A1*) gene, which is highly expressed in the liver and spleen macrophages. Ferroportin is part of the major facilitator superfamily of transporters of small molecules, it is a 12-transmembrane domain protein and both the N and C terminals are located within the cytoplasm (Drakesmith et al., 2015).

Ferroportin is regulated by a several factors, including haem, iron regulatory proteins (IRPs) and post translationally by hepcidin. Hepcidin regulates ferroportin by binding to the extracellular loop causing the intracellular lysine residues to be ubiquitinylated leading FPN1 internalisation and degradation in lysosomes (Pietrangelo, 2017). Increased levels of intracellular iron disrupts the interaction between IRPs and IRE within *FPN1* mRNA increasing ferroportin in the cell membrane for accelerated iron export. In the other hand, at low intracellular iron levels IRPs bind to IRE inhibiting translation of ferroportin thus interrupting iron efflux (Yang et al., 2020).

Very little is known about how ferroportin transports iron, however recent studies have suggested that calcium (Ca^{2+}) is a required co-factor for iron efflux raising the possibility that calcium has a regulatory role and ferroportin activity could be limited in conditions where calcium availability is reduced (Deshpande et al., 2018). Furthermore, a study by Billesbølle et al. (2020) that hepcidin binding to

ferroportin is potentiated by iron rather than targeting exporters which are not active.

1.2.5.5 Ferroportin/hepcidin axis and iron disorders

As iron homeostasis requires very tight control, it is not surprising that dysregulation of iron metabolism leads to a number of disorders. As the main regulatory mechanism of iron homeostasis is the ferroportin/hepcidin axis this section will address a number of disease processes caused by disruption of this axis.

1.2.5.5.1 Ferroportin Disease

Ferroportin disease is the most common causes of genetic hyperferritinemia (high levels of ferritin), it is an autosomal dominant hereditary disorder associated with mutations within the ferroportin gene. The general pathophysiological basis of the disease is impairment of iron storage/recycling towards the blood stream, this is particularly important in macrophages (Pietrangelo, 2017).

1.2.5.5.2 Haemochromatosis

Haemochromatosis is a genetic disorder, which causes systematic iron overload due to deficiency of hepcidin either because of decreased production or decreased activity of hepcidin-ferroportin binding. The most common cause of haemochromatosis is homozygous mutations in hereditary haemochromatosis protein (HFE, which has a role in hepcidin regulation) specifically the p.Cys282Tyr (C282Y) this mutation is mostly found in white individuals. Mutations in other genes, including *HAMP* (hepcidin), *HJV* (haemojuvelin, also known as

HFE2) and *TFR2* (transferrin receptor protein 2). Individuals with haemochromatosis can be asymptomatic for years, with symptoms developing around 30-40 years of age, mostly affecting several organ systems (Brissot et al., 2018).

1.2.5.5.3 Anaemia of inflammation

As discussed above, pro-inflammatory cytokines IL-6 and IL-1β can induced hepcidin expression, therefore when these cytokines are produced in chronic infections, autoimmunity, cancer, renal failure and other chronic diseases it can lead to increased levels of hepcidin leading to low serum iron despite adequate iron stores and mild to moderate anaemia. Anaemia of inflammation can regress by treating the underlying disease. However, treatments are often unsatisfactory, thus targeting the hepcidin pathway has been proposed as a novel therapeutic opportunity (Camaschella et al., 2020, Nemeth and Ganz, 2014).

1.2.5.6 The role of ferroportin/hepcidin axis in local tissue iron haemostasis

In addition to its role as the sole cellular iron exporter in cells and tissues that are involved in systematic iron control (duodenum, iron recycling macrophages, hepatocytes) there is now an increasing evidence base that ferroportin is expressed and involved in local iron regulation in other cells and tissues that are not normally associated with iron homeostasis. Baumann et al. (2019) showed that ferroportin has a role in localised iron regulation in retinal and brain vascular endothelial cells (r&bVECs). Deletion of ferroportin from VECs in a mouse model lead to iron accumulation in the retina and brain VECs, demonstrating localised

iron regulation and further insight into neurodegenerative diseases involving iron accumulation.

This function of ferroportin was also demonstrated in cardiomyocytes. Deletion of ferroportin in cardiomyocyte specific mouse model showed that these animals had severe impaired cardiac function. Furthermore, these mice were compared to a haemochromatosis ubiquitous hepcidin knockout mice model, which showed a milder phenotype even though having greater iron loading in the heart. The cardiomyocyte specific knockout iron loading was only within cardiomyocytes compared to hepcidin knockout where iron accumulation was predominately in other cell types. This demonstrate that ferroportin is essential for iron regulation in cardiomyocytes, moreover it also shows that severity of cardiac function is dependent on which cell type/site the iron accumulation occurs (Lakhal-Littleton et al., 2015).

Previous work (Latha Ramakrishnan, 2018, Ramakrishnan et al., 2018b) by this group demonstrated that ferooportin and hepcidin is expressed in human pulmonary arterial smooth muscle cells (hPASMC). Hepcidin treatment of hPASMC caused iron retention and stimulated proliferation of these cells, processes that were reversed by a ferroportin monoclonal antibody LY2928057 (this antibody stabilises ferroportin and maintains activity despite hepcidin availability/interaction). Furthermore, IL-6 treatment of hPASMCs increased hepcidin mRNA expression and hepcidin released.

1.3 Iron Deficiency and PAH

Iron deficiency (ID) and anaemia has a high frequency in pulmonary hypertension, with a prevalence of 63% to 27% across different forms of pulmonary hypertension (HP). Iron deficiency has been associated with reduce exercise capacity and increased mortality, which makes iron deficiency clinical relevant and a potential therapeutic target for pulmonary hypertension (Ruiter et al., 2011, Rhodes et al., 2011b, Ghio et al., 2021).

In cases of IPAH and HPAH iron deficiency is prevalent without apparent anaemia and which could suggest an important prognosticator (Naito et al., 2013), moreover there is no significant difference in functional capacity between anaemic and no-anaemic iron deficient patients suggesting that the issues are caused by systematic low iron than aneamia (Ghio et al., 2021). IPAH patients that were iron deficient had a significantly lower 6-minute walk distance (6MWD) than those with normal iron levels, furthermore when these patients were split into aneamic and non-aneamic groups there was no significant difference in the 6MWD (Ruiter et al., 2014).

Rats that were fed an iron-defient diet for 4 weeks exibited vascular remodelling with notable muscularisation, medial hypertrophy, inflammatory cell infiltration and raised pulmonary arterial presure. These changes were reversed by iron supplementation, suggesting that iron may have a important role in pulmonary vascular homeostasis (Cotroneo et al., 2015).

Oral administration of iron are not effecive in reversing iron deficiencies, suggesting that dietary uptake may be compromised in IPAH, which is partially

explained by high levels of hepcidin despite low circulating iron (Rhodes et al., 2011a). Moreover, PAH patients had increased levels of circulating soluble transferrin receptor, high red cell distribuition widths and elevated zinc-protoporphryn (Zn-pp) levels (Decker et al., 2011, Mathew et al., 2016). In normal iron condtions, protoporphyn would form haem, so raised Zn-pp is an indication of iron deficiency. All of these three markers of iron deficiency are associated with disease severity and poor outcome (Mathew et al., 2016, Rhodes et al., 2011a). Therefore, these studies suggest that dysregulated iron homeostasis may play a central role in PAH.

1.3.1 Iron deficiency and Eisenmenger syndrome

Eisenmenger Syndrome (ES) represents the severest manifestation of congenital heart disease (CHD) affecting between 3-10% of this patient group and it represents the most advanced form of pulmonary arterial hypertension (PAH) (Elshafay et al., 2018, Ereminiene et al., 2017). PAH in ES is caused by a left-to-right shunt that is eventually reversed into a cyanotic right-to-left shunt. Therefore, ES is characterised by pulmonary hypertension, reversal of the central shunt's flow and cyanosis secondary to CHD associated with a non-repaired intra- or extra-cardiac shunt (de Campos and Benvenuti, 2017). ES presents clinically with multiple organ involvement with a progressive deterioration of function over time that includes central cyanosis, dyspnoea, fatigue, dizziness, haemoptysis, syncope, and reduced quality and expectancy of life (Ereminiene et al., 2017).

Iron deficiency in has been identified in Eisenmenger syndrome patients for a much longer than other forms of PAH, this is thought be caused by increased

secondary erythrocytosis due to chronic cyanosis. However, the underlying mechanism still needs to be elucidated (Ramakrishnan et al., 2018a). Van De Bruaene et al. (2011) demonstrated that iron deficiency was associated with a higher risk of adverse outcome in ES patients. The available data for iron homeostasis disruption markers are limited in ES patients, however a small study carried out by our group (Mumby et al., 2016) shows significant increases in an array of plasma markers such as soluble transferrin receptor, free haem, iron saturation of transferrin, IL-6 and hepcidin (Ramakrishnan et al., 2018a). These results clearly suggest that dysregulated iron homeostasis may play a key role in ES pathophysiology.

1.3.2 Haemolysis and PAH

Haemolysis has been touted as a potential cause of pulmonary arterial hypertension for the past 20 years. PAH has been reported in almost all chronic haemolytic diseases that include sickle cell anaemia, thalassemia and also diseases that affects red blood cell membranes such as spherocytosis and stomatocytosis. PAH is the leading cause of morbidity and mortality in patients with haemolytic disorders (Barrington et al., 2016).

1.3.2.1 Haemoglobin

Haemoglobin is a protein found in erythrocytes (red blood cells), and haemoglobin primary function is the transport oxygen from the lungs to tissues and carbon dioxide (CO_2) from tissues to the lungs, however it is also involved in other functions such as pH regulation and redox balance (Ahmed et al., 2020).

Human haemoglobin (figure 1-11) is a tetramer protein consisting of two α-subunits and two β-subunits, these four polypeptides have a large central hydrophobic pocket where a haem group (an iron-protoporphyrin IX molecule) is bound. The iron atoms present in haemoglobin is primarily in the physiological ferrous (FeII) state. The α-subunits gene locus is found on chromosome 16 and β-subunits gen locus is located on chromosome 11. Haemoglobin can also bind other ligands such as nitrite ion (NO^{2-}), carbon monoxide (CO), cyanide (CN^{-}), sulphur monoxide (SO), sulphide (S^{2-}). These ligands can act as competitive inhibitors for oxygen binding making some of them highly toxic to humans, for example CO affinity to haemoglobin is 240 times greater than oxygen (Ahmed et al., 2020).

There are over a thousand naturally occurring haemoglobin variants and a number of these have been associated to pathologies that can range from mild to severe. The most well-known variant is the single mutation (βGlu6Val) in the β-globin chain of normal haemoglobin to give rise to sickle cell anaemia (Kato et al., 2018). Thalassemia is another disorder caused by mutations in either the α-globin or β-globin, therefore mutations in the α-globin results in α-thalassemia and mutations in the β-globin leads β-thalassemia (Kim et al., 2017).

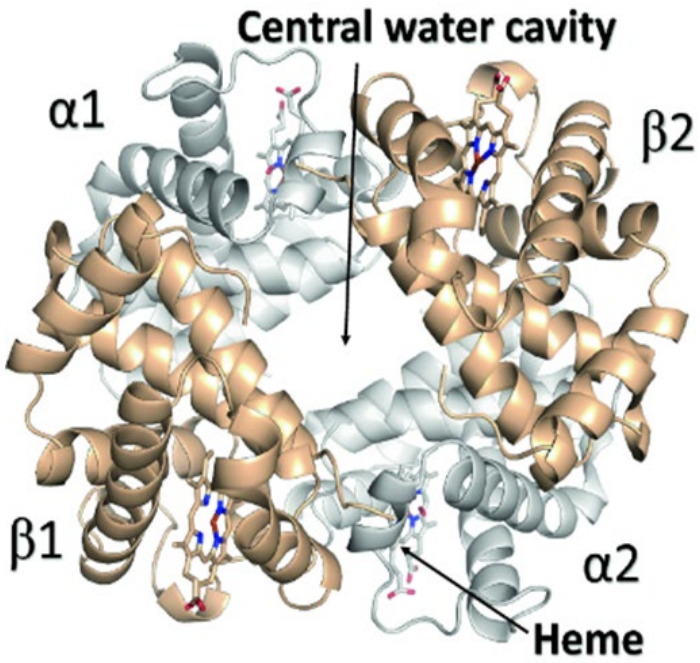

Figure 1-11 Structure of human haemoglobin. *Haemoglobin quaternary structure, alpha chains in grey and beta chains in tan. Figure taken form Ahmed et al. (2020).*

1.3.2.2 Cell free haemoglobin clearance mechanism

Cell-free haemoglobin CFH is normally cleared in healthy humans via the binding of haemoglobin to haptoglobin, which in turn binds to CD163, a scavenger receptor seen in certain cell types, the haemoglobin/haptoglobin complex is then uptaken by subsets of macrophages which present with CD163 where haemoglobin is metabolised to biliverdin by haem oxygenase-1 (HO-1) and to bilirubin biliverdin reductase, followed by secretion from the liver. Any haem released from haemoglobin is cleared by haemopexin binding of haem and macrophage processing by a similar mechanisms to CFH (Schaer and Buehler, 2013). These process protect against four major mechanisms for CFH-mediated organ injury, which are, nitric oxide sequestration by haemoglobin, endothelial

damage, inflammation and oxidative stress (Janz and Ware, 2015). Moreover, disruption of these clearance mechanisms has also been associated with organ dysfunction (Ware et al., 2011, Janz et al., 2013a). And in it has been shown that in patients with sepsis and ARDS, disease processes associated with haemolysis, decreased levels of haptoglobin, haemopexin and HO-1 that have been shown to be significantly associated with poor outcomes (Janz et al., 2013b).

1.3.2.3 Decomparmentalisation of haemoglobin, a role for haemolysis in PAH

Destruction of red blood cells causes haemoglobin to be released to the vasculature and once in plasma haemoglobin disassociates to dimeric forms, is subject to release free haem and is also likely to shed iron that if not bound by transferrin (when saturated), will be available to catalyse damaging hydroxyl radical formation and also other damaging oxidants. Hydroxyl radicals are highly toxic causing peroxidation of membrane polyunsaturated fatty acids, damaging protein and DNA (Fishbane et al., 2014, Kell, 2009). Therefore, there are potentially numerous iron containing breakdown products released/formed as consequence of haemolysis, which may have implications for the pathogenesis of diseases including PAH. Camus et al. (2015) has demonstrated that red blood cell micro particles ladened with haemoglobin/haem accompany haemolytic events. These particles have known effects on the endothelium with resultant vascular occlusion in sickle cell disease, such a haemolytic complications that may also be relevant to PAH.

Moreover, associations between disease processes that involve a haemolytic component and the development of PAH are also well established (Souza et al., 2009b). in this regard, studies in patients with IPAH and HPAH have shown red blood cell abnormalities; specifically increased levels of zinc-protoporphyrin (Decker et al., 2011), elevated creatine (Fox et al., 2012) and plasma free haemoglobin (Brittain et al., 2014), which all indicate iron deficiency and sub-clinical haemolysis. A study Buehler et al. (2012) demonstrated that intravenous infusion of low concentrations of haemoglobin induced PAH in a rat model. Increased levels of free haemoglobin in PAH patients have been associated with disease severity (Rafikova et al., 2018). More importantly, haemoglobin is known to interact with nitric oxide (NO), an important vasodilator, and act as scavenger of NO bioactivity (Su et al., 2020). This consumption of NO by haemoglobin has been associated with increased systematic vascular resistance and/or vasoconstriction, characteristics of pulmonary hypertension (Reiter et al., 2002, Minneci et al., 2005, Boretti et al., 2009).

1.4 Summary

PAH is a rare and devastating and incurable disease that affects people of all ages. PAH is characterised by excess proliferation and apoptosis resistant vascular cells, which leads to obliterative remodelling of pulmonary blood vessels. The mechanisms underlying these changes are still not well understood. Recently disruption in iron homeostasis has emerged to have potential a role in the development of PAH. Previous studies by this laboratory have demonstrated that manipulation of the hepcidin/ferroportin iron regulatory axis causes proliferation of hPASMCs, furthermore the haemoglobin scavenger receptor

CD163 was found to be expressed in PASMCs. Iron deficiency is prevalent in PAH and iron supplementation clinical trials have yielded disappointing results, with no relevant clinical improvements suggesting that other aspects of cellular iron regulation should be considered when investigating pathophysiology of PAH.

1.5 Hypothesis

The iron regulatory hepcidin/ferroportin axis is expressed in hPAECs and manipulation of this axis will lead to iron species uptake and retention by these cells with consequences for; cell fate, intracellular signalling, mediator release and influences on proliferative responses locally for PASMCs.

Main Aims

i. To determine the expression of hepcidin and ferroportin in hPAECs
ii. To investigate the role of hepcidin and IL-6, regulators of the hepcidin/ferroportin axis on hPAEC proliferation and BMPR2 signalling processes. To further investigate any role for mediator release from HPAECs as drivers for hPASMC proliferation. .
iii. To investigate if cell free haemoglobin can contribute to the development of PAH characteristics/ phenotype in hPAECs.

2. Chapter 2 - Methods

2.1 Materials and reagents

2.1.1 General Reagents

All reagents were purchased from Sigma, unless specified.

2.1.2 ELISA kits and reagents

All ELISA kits were purchased from R&D systems unless specified.

Human IL-6 DuoSet ELISA – DY206; Human IL-8/CXCL8 DuoSet ELISA – DY208; Human CCL2/MCP-1 DuoSet ELISA – DY279; Human Hepcidin DuoSet ELISA – DY8307-05.

2.1.3 Antibodies

2.1.3.1 Primary Antibodies

Table 2-1 Primary antibodies utilised in this project.

Primary Antibody	Specie	Dilution	Company	Used for	Cat. Number
VCAM-1	Mouse	1:200	SantaCruz	Flow cytometry	sc-13160
ICAM-1	Mouse	1:200	SantaCruz	Flow cytometry	Sc-8439
CD163	rabbit	1:500	SantaCruz	Western Blot	Sc-33559
CD163	Mouse	1:200	SantaCruz	Flow cytometry	Sc-20066
BMPR2	Mouse	1:500	BD biosciences	Western Blot	612292
GAPDH	Rabbit	1:1000	Cell Signalling	Western Blot	
Ferroportin	Rabbit	1:500	NovusBio	Western Blot	NBP1-21502
A-tubulin	Mouse	1:2000	Cell Signalling	Western Blot	
P-SMAD1/5	Rabbit	1:500	Cell Signalling	Western Blot	
Myosin heavy chain	Mouse	1:200	ABCAM	Fluorescence Microscopy	ab683
ACE2	Rabbit	1:1000	ABCAM	Western Blot	ab15348
α-SMA	Mouse	1:200	biotechne	Fluorescence Microscopy	MAB1420
SMAD5	Rabbit	1:500	Cell Signalling	Western Blot	12534

2.1.3.2 Secondary Antibodies

Table 2-2 – Secondary antibodies used in this project.

Secondary Antibody	Specie	Dilution	Company	Used for	Cat. Number
Anti-mouse HRP-linked	Horse	1:2000	Cell signalling	Western Blot	7076S
Anti-rabbit HRP-linked	Goat	1:2000	Cell signalling	Western Blot	7074S
Alexa Fluor 568 anti-rabbit	Goat	1:500	Invitrogen	Fluorescence Microscopy	A11011
Alexa Fluor 488 anti-rabbit	Goat	1:500	Invitrogen	Fluorescence Microscopy	A11001
Alexa Fluor 488 anti-mouse	Goat	1:500	Invitrogen	Fluorescence Microscopy	A11008
Alexa Fluor 700 anti-rabbit	Goat	1:500	Invitrogen	Fluorescence Microscopy	A21038

2.1.4 Primers

Primers on table 2-1 were purchased from Sigma, UK.

Table 2-3 Primers used for real-time PCR experiments. *These were purchased from Sigma, UK.*

Gene	Forward	Reverse
SMAD5	GATCTCACTATGTTGCTCAG	GTCCTGTAATCCCAGTTATTC
SMAD1	TCAACAGAGGAGATGTTCAG	AATTCCGGTTAACATTGGAG
BMPR2	AACAACAGCAATCCATGTTC	TATCTGTATACTGCTGCCATC
β-actin	GACGACATGGAGAAAATCTG	ATGATCTGGGTCATCTTCTC
ID1	CCGGTCTCATTTCTTCTCGT	TCGGTCTTGTTCTCCCTCAG
ID2	ATGAAAGCCTTCAGTCCCGT	TTCCATCTTGCTCACCTTCTT
ID3	TCATCTCCAACGACAAAAGG	ACCAGGTTTAGTCTCCAGGAA
ID4	TGAACAAGCAGGGCGACA	CGTGCAAAGAAAGAATGAAAG
HAMP	GTTTTCCCACAACAGACG	CTTTGATCGATGACAGCAG
NOX4	AATTTAGATACCCACCCTCC	TCTGTGGAAAATTAGCTTGG
NOX1	CCGGTCATTCTTTATATCTGTG	CAACCTTGGTAATCACAACC
GAPDH	ACAGTTGCCATGTAGACC	TTGAGCAGGGTACTTTA

2.2 Cell Culture

2.2.1 Human pulmonary artery endothelial cells

Human pulmonary artery endothelial cells (hPAECs; figure 2-1) were purchased fully characterised from Promocell (Germany) and ATCC (USA); cells were purchase from two suppliers to increase the number of donors. PAECs were maintained on endothelial cell growth medium 2 (EGM2; Promocell) supplemented with foetal calf serum (2%, FCS), epidermal growth factor (5 ng/mL), basic fibroblastic growth factor (10 ng/mL), insulin-like growth factor (20 ng/mL), vascular endothelial growth factor 165 (0.5 ng/mL), ascorbic acid (1 µg/mL), heparin (22.5 µg/mL) and hydrocortisone (0.2 µg/mL). hPAECs cells were passaged when 90% confluent was reached. Briefly, cell monolayer was briskly washed with phosphate buffered saline (PBS), incubated with trypsin

(0.05%, GIBCO) at 37°C for 3-5 minutes to detached cells followed by trypsin quenching with EGM2 medium. Cells were pelleted by centrifugation at 260 RCF for 5 minutes at room temperature. PAECs were then re-suspended in EGM2 medium and counted prior to seeding at different densities depending on number of cells required for each experiment. Further, the cells were cultured with fresh medium in T25 / T75 flasks at 10000 cells per cm^2, incubated at 37°C and 5% CO2. Only cells from passage 4-8 were used in the experiments.

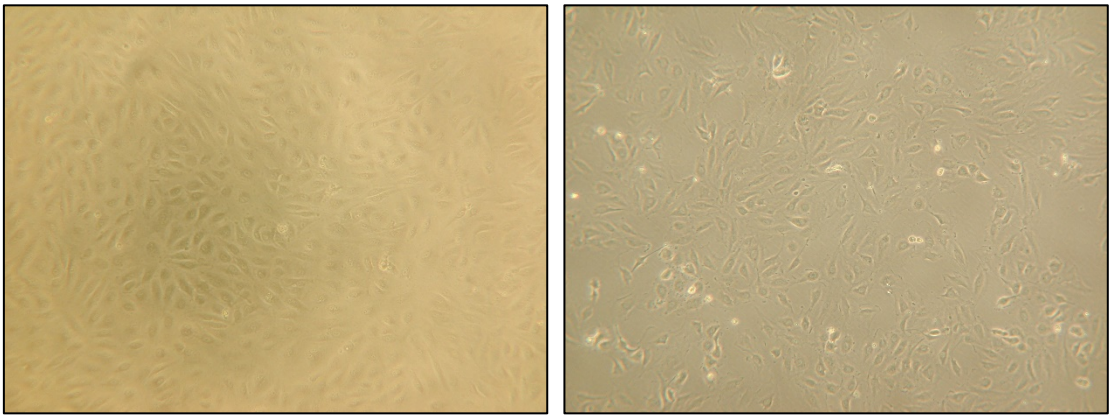

Figure 2-1 Image of hPAECs in culture. *Left panel cells at 90% confluence and right panels cells at 60 % confluence. Images were taken by an Olympus CX40 microscope.*

2.2.2 Human pulmonary smooth muscle cells

Human Pulmonary Artery Smooth Muscle Cells (hPASMC) were isolated from patients at the Royal Brompton Hospital (London, UK) that had lung lobectomy, these patient were smokers. Briefly, a sample from the pulmonary artery, the resection samples was taken from approximately the 4^{th} to 6^{th} branch, the adventia layer was removed and the resection sample was then cut into smaller pieces (1-2 mm), placed within a T25 culture flask 1 cm apart and followed by the addition of 2 mL of Dulbecco's Modified Eagles' Medium (DMEM; SIGMA, USA)

supplemented with 15% fetal bovine serum (FBS), 2 mM glutamine, 100 U/mL penicillin and 100 µg/mL streptomycin. The artery pieces were removed after 7 days and the cells were grown to confluency. hPASMCs were selected by culturing them over a period of time in high serum DMEM excluding other cell types and first characterising by morphological examination (figure 2-2).

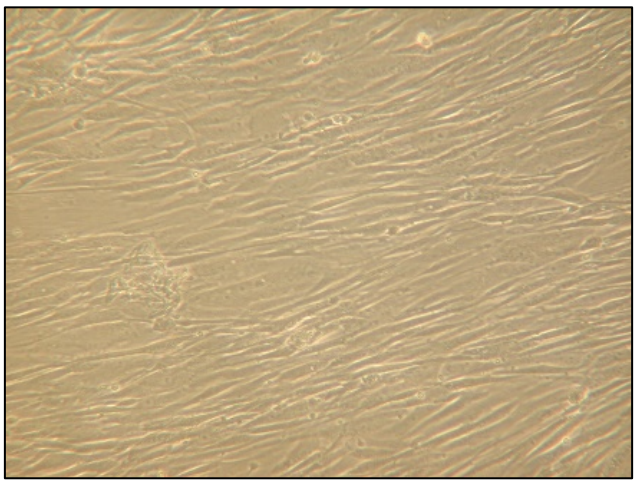

***Figure 2-2 hPASMCs cells in culture**. These cells show the typical long and narrow spindle shape morphological characteristics. Images were taken by an Olympus CX40 microscope.*

Only the cells that had a typical long and narrow spindle shape with mono nucleus in the centre were propagated further and stained for smooth muscle cell markers (figure 2-3) SMA alpha smooth muscle actin), SM-22 alpha and SM-MHC (smooth muscle myosin heavy chain). hPASMCs purchased from Promocell fully characterised were used as positive control. All characterised cells were culture and maintained in smooth muscle cell (SMC) growth medium 2 (Promocell) or DMEM media supplemented with 15% fetal bovine serum (FBS), 2 mM glutamine, 100 U/mL penicillin and 100 µg/mL streptomycin. hPASMCs were passaged when 90% confluent was reached. Briefly, cell monolayer was briskly washed with phosphate buffered saline (PBS), incubated with trypsin (0.05%,

GIBCO) at 37oC for 3-5 minutes to detached cells followed by quenching with DMEM medium. Cells were pelleted by centrifugation at 260 RCF for 5 minutes at room temperature. Cells were then re-suspended in DMEM medium and counted prior to seeding at different densities depending on the number of cell required for each experiment. Further, the cells were cultured with fresh medium in T25 / T75 flasks at 5000 cells per cm^2, incubated at 37^oC and 5% CO2. For experiments, only cells from passage 4-8 were used. The use of normal lung tissue has been approved by the Royal Brompton and Harefield NHS Trust Research Ethics Committee (ethics number GQJW1).

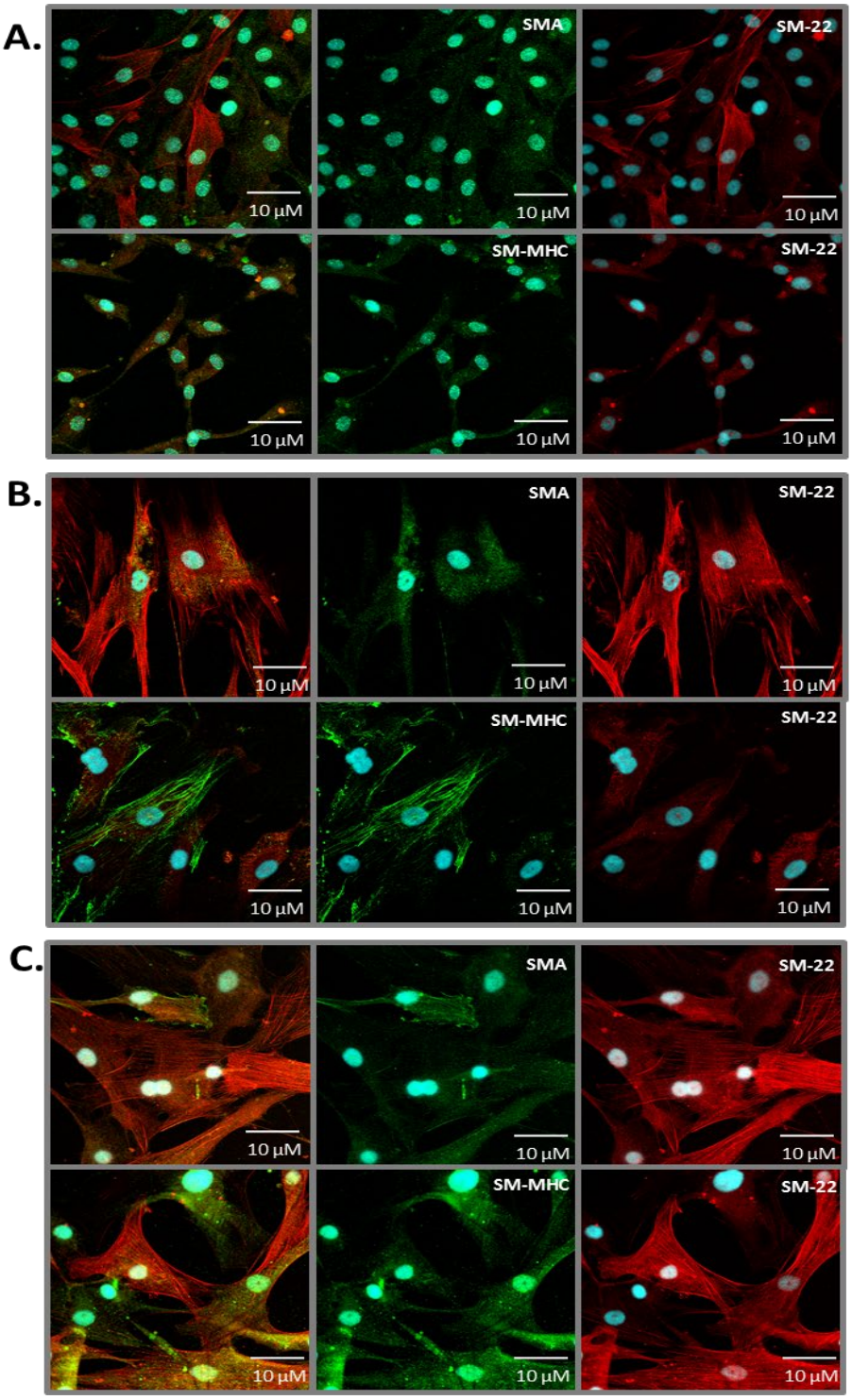

Figure 2-3 **. Confocal images of hPASMCs from three donors**, *(A) donor-A, (B) donor-B, and (C) donor-C; grown in smooth muscle cell growth medium 2 (Promocell, Germany) or DMEM 15% FBS medium. Top 3 panels of each figure were immuno-stained with rabbit anti-SM22 alpha (red) and mouse anti- SMA (Smooth muscle actin). Bottom 3 panels were immuno-stained with rabbit anti-SM22 alpha (red) and anti-mouse MHC (smooth muscle myosin heavy chain; green). Scale bar = 10 µM*

2.2.3 Cell cryopreservation and defrosting

PAECs were purchased (Promocell or ATCC) either cryopreserved or proliferating, upon arrival cryopreserved cells were transferred immediately to liquid nitrogen. The cells were expanded for two passages and prepared to for subsequent use. Following passage the cells were resuspended with freezing medium cryo-SFM (a protein-free, defined and animal component-free cryopreservation medium; Promocell, Heidelberg, Germany) and dispensed in 1mL aliquots into cryovials. The cryovials were then transferred to a freezing container ("Mr Frosty", Nalgene Labware) containing propan-2-ol to be cooled at a rate of -1^{o}C min^{-1} for 24h in a -80^{o}C freezer, after 24h the cryovials were transferred into liquid nitrogen. Proliferating cells were transferred into the incubator for a few hours to warm up, before replacing the transporting medium with complete medium. Once the cells reached 90% confluency, the cells were expanded for two passages and prepared (as described above) for subsequent use. Following isolation of hPASMCs the cells were either expanded for use or cryopreserved for later use as describe above.

When needed the cells were thawed in a 37^{o}C water bath for 1-2 minutes, which allowed the cells to quickly thaw, minimising any damages to the cell membranes. Once thawed the cells were decontaminated with chemgene spray. The contents were then transferred to a flask containing pre-warned complete medium, after 24h the medium was changed to remove any remaining DMSO (dimethyl sulfoxide).

2.2.4 General cell counting

Cells were counted under an inverted phase contrast microscope (CK40, Olympus, Southend, UK) using the Fast-Read®102 counting chambers (Kova International, CA, USA). The total number of cells in the ten squares (figure 2-4; 1x1 mm) were counted. Cells were included with they were entirely within the boundaries of squares. Total number of cells in suspension was determined by the following formula.

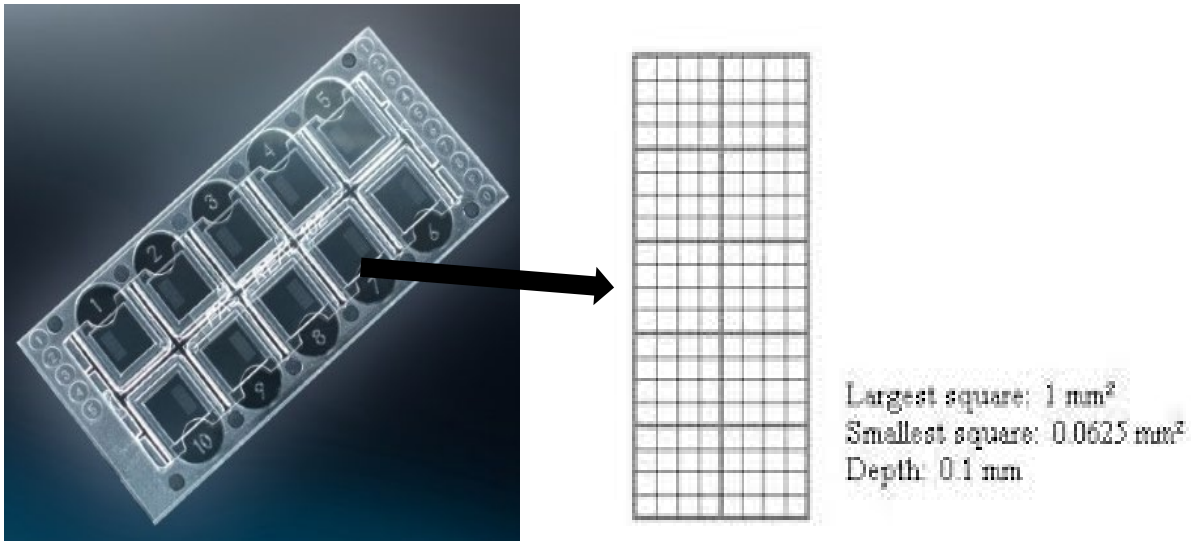

Figure 2-4 Fast-Read®102 counting chambers and a representation of the scoring inside each chamber.

$$total\ cell\ count = \frac{cell\ count\ of\ 10\ squares}{10}\ x10^4\ x\ dilution\ factor$$

2.2.5 Cell treatments

2.2.5.1 hPAECs

For hPAECs treatments heparin and hydrocortisone were omitted from the media. Heparin was excluded because it is a strong hepcidin inhibitor (Poli et al., 2011) and hydrocortisone was removed due to its anti-inflammatory properties.

Hepcidin peptide was purchased from Peptides International (now knowns as vivitide, Massachusetts, USA). The lyophilised peptide was re-suspended with double-distilled, sterile water to the stock concentration of 1 mg/mL. Stock aliquots were made and store at -80^{o}C for long term storage. Recombinant human interlukin-6 (IL-6) was purchased from GIBCO, USA, the carrier free lyophilised protein was reconstituted with 100 mM acetic acid to a concentration of 100 µg/mL. The reconstituted protein was apportioned into to working aliquots and stored at -20^{o}C. Haemoglobin (predominately methaemoglobin) was purchased from Sigma-Aldrich (Darmstadt, Germany). Haemoglobin was prepared to stock solution of 100 µM in EGM2 treatment medium. The solution was incubate at 37^{o}C for 30 minutes and then filtered (0.2 µm). For all the different treatments the stock solutions were further diluted to the desired concentrations with the media required for experimental protocols.

2.2.5.2 hPASMCs

hPASMCs treatments were prepared with Dulbecco's modified Eagle's medium (DMEM) medium supplemented with fetal bovine serum (FBS), 2 mM glutamine, 100 U/mL penicillin and 100 µg/mL streptomycin. Serum concentration was changed depending on experiments.

2.2.6 Cell viability

Cell viability and cytotoxicity the Alamar Blue assay was used. The active ingredient of Alamar Blue is reasazurin, which is water-soluble, non-toxic and permeable through cell membranes. The assay works by monitoring the reducing environment of living cells and the dye acts as an intermediate electron acceptor in the electron transfer chain, it does not interfere with normal transfer of electrons (Rampersad, 2012). As the dye accepts electrons, it changes from the oxidised blue state to the reduced pink state. This change from oxidised state to a reduced state (blue to pink) allows flexibility of detection, where measurements can be quantitative by spectrophotometric absorbance measurements at two wavelengths (570 and 600 nm), or qualitative as a visible change in colour indicate the presence or absence of viable cells (Rampersad, 2012).

To determine cell viability cells were seeded in a 96-well plate (2500 cells for PASMCs and 4000 cells for PAECs). Following 24h after cell seeding, the cells were treated for 24h. After treatment, alamar blue was added to media (1:10 dilution). The media present in the plates were removed and replaced by the prepared alamar blue solution and the plate was incubated for 4h at 37^{o}C and 5% CO2. The plate was read in a plate reader Synergy HT (Biotek) at the wavelengths 570 and 600 nm (figure 2-5).

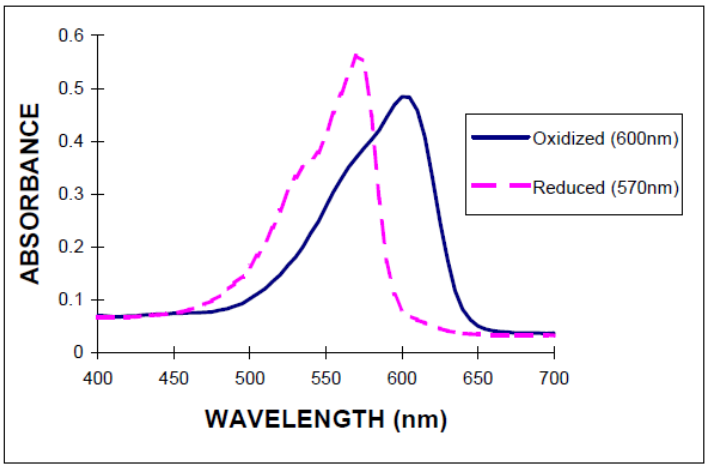

Figure 2-5 Graph representing the different readings of the alamar blue assay. *The alamar blue reagent will react with metabolites in active cells to release a reduced form of a compound that absorbs at 570nm. The oxidised form which is associated with non-viable cells absorbs at 600nm*

Viability was determine by calculating the difference between the reduce state (pink) that indicates viable cells and oxidised state, however this difference is not sufficient to calculate percentage of reduced (viable) cells as it will give rise to negative values, therefore a correction value must be calculated (equations below).

$$percentage\ difference\ in\ reduction$$

$$= \frac{A_{LW} - (A_{HW}\ x\ R_o)for\ test\ well}{A_{LW} - (A_{HW}\ x\ R_o)\ positive\ growth\ control}\ x\ 100$$

Top line of the equation:

ALW = absorbance at 570 of Sample

AHW = absorbance at 630nm of Sample

Ro = ALW (alamar blue working only) / AHW (alamar blue working only)

Bottom line of the equation:

ALW = absorbance at 570 of Control

AHW = absorbance at 630nm of Control

Ro = ALW (alamar blue working only) / AHW (alamar blue working only)

2.2.7 Cell gene knockdown by RNA interference

2.2.7.1 Basic Principles

Gene knockdown or gene silencing of a specific gene expression of cells in culture, has been a widely used technique to study the effects of loss-of-function of a specific gene. The most utilised method is the induction of such gene-specific mRNA degradation post-trans. This method uses RNA interference (RNAi), which is a small double-stranded RNA (dsRNA), when this dsRNA is introduced into cells it activates the RNA-induced silencing complex (RISC) directing it to the target RNA. RISC is a nuclease complex that is responsible to the complete degradation of a target RNA, thus silencing the gene targeted (Han, 2018).

2.2.7.2 Protocol

- Reagents
    - hPAECs cells
    - EGM2 growth medium
    - Opti-MEM I reduced serum medium (Gibco,)
    - DharmaFECT 1 transfection reagent (Horizon,)

- RNase free water (Gibco,)
- siRNAs – BMPR2, Ferroportin and non-targeting siRNA controls (Horizon,)

- Cell Preparation
  - Grow hPAECs as described in section 2.2.1. Once cells reached 90% confluence they were seeded into cell culture plates.
  - For protein extraction cells were seeded into 6-well plates at 300,000 cells seeding density.
  - For RNA analysis cells were seeded into 6-well plates at 100,000 cells seeding density.
  - After, cells were completely adhered to the bottom of the wells, confluence was check under the microscope. For knockdown experiment 70% confluence is ideal.
- Gene knockdown
  - Prepare a 20 μM siRNA stock by adding 250 μL of siRNA buffer. The buffer comes 5x concentred, thus it needs to be dilute to 1x with RNase free water.
  - Prepare solution A (transfection solution) – for each well of a 6-well plate, 200 μL of this solution will be needed. For each well add 2 μL of DharmaFECT 1 transfection reagent to 198 μL Opti-MEM I reduced serum media.
    - Example if preparing solution for 1 control well and 1 gene knockdown well, 400 μL will be needed.

- Prepare solution B (siRNA solution): for each well of 6-well plate prepare 200 µL of solution by adding 2 µL of siRNA to 198 µL of Opti-MEM I reduced serum media. Prepare solutions for the siRNA of interest and the control siRNA.
- Once solution A and B are prepared leave them incubating for 5 minutes. Add half of solution A to the siRNA control and half to the siRNA for the gene of interest and incubate these mixture for 20 minutes.
- While the siRNAs mixtures are incubating, wash the cells 3x with Opti-MEM I reduced serum media. After, the washes add 1.6 mL of Opti-MEM I reduced serum media.
- Following the 20 minute incubation, add 400 µL of siRNA solutions to the designated wells and incubate it for 6 hours.
- After the 6 hours incubation, remove the siRNA solution to regular growth medium.
- After, collect the samples at the require time points, or if running experiments treat cells as described in section 2.2.5.

2.3 Microscopy

2.3.1 Wide-field Microscopy

The conventional wide-field microscopy is one the most simple microscopy techniques. In this technique the entirety of a sample is lit by lamp light source from either below (an upright microscope) or above (an inverted microscope) the samples being examined. An upright microscope is mostly used to view samples that are mounted onto a microscope slide. Inverted microscopes are most often

used to view or image samples that are immersed in liquid or samples that cannot be mounted on slides, such as cells being culture or observing fruit flies under the microscope.

To image cells in culture the phase-contrast microscopy technique was used, this technique provides better contrast than bright-field by scattering light from the sample. This is done by illuminating the sample with a ring of light and having a second ring in front of the microscope viewfinder, as the light scatter differently on parts of the sample appears lighter or darker.

2.3.2 Fluorescence Microscopy

Fluorescence microscopy is based on the process of fluorescence, which involves the absorption of light energy (a photon) by an indicator followed by the emission of some of this light energy (another photon). In this process there is a loss of energy, therefore the emitted photon has less energy than the absorbed photon and this change is called the stoke shift. Thus the main objective of fluorescence microscopy it is to separate emitted light from excitation light (Sanderson et al., 2014). There are two common techniques used, wide-field fluorescence microscopy and confocal microscopy that will be described below.

2.3.2.1 Wide-field fluorescence microscopy

A fluorescence microscope is similar to a regular wide-field microscope, however this instrument in addition to the white light bulb it also has a light that it is able to excite a fluorophore(s) in a sample. This light is usually a mercury or xenon high-pressure bulb, however newer models are using a single-wavelength light-emitting diodes (LEDs) that have a longer life and provides a tighter wavelength

control. The emitted fluorescence of the sample can be viewed by eye or captured by a camera. However, because all parts of sample image can be viewed simultaneously, it causes the projection of out-of-focus light to be projected onto the single image that results in images of low contrast and poor resolution. Nevertheless, this is an advantage as it allows for faster imaging (Sanderson et al., 2014).

2.3.2.2 Confocal microscopy

To overcome the issue of out-of-focus light found in wide-field fluorescence microscopy lase-scanning confocal microscopy (LSCM) was developed. The same principles of fluorescence still applies to LSCM. The main differences are the excitation source (normally a laser), a sequential scanning method of the point source of of illumination and light detection by a photomultiplier tube (PMT) (Sanderson et al., 2014). Out-of-focus light is reject from the image by a pinhole aperture, which ensures that light hitting the detector only comes from the confocal point in the sample where the excitation light was focused (figure 2-6).

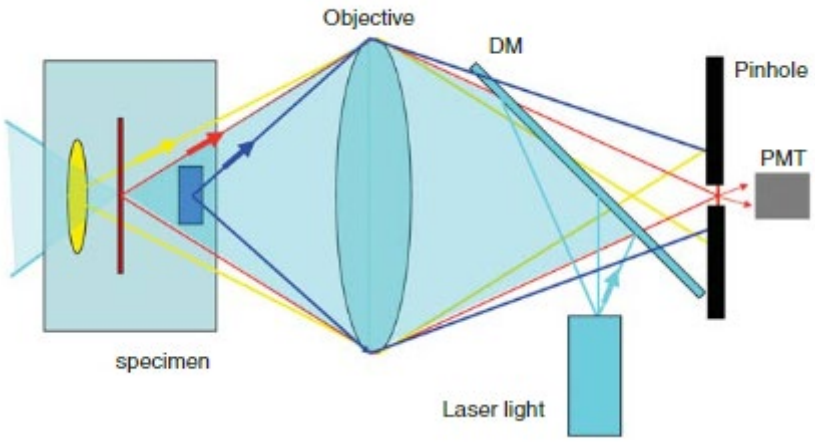

Figure 2-6 Basic principle of a laser scanning microscope. *Laser light is focused on the sample, the laser excites fluorescence throughout the sample and it is focused onto the image plane. The pinhole only allows light from the confocal plane to reach the PMT. Figure taken from Sanderson et al. (2014).*

2.3.2.3 Protocol

- Materials and reagents
    - 4% formaldehyde (PFA) solution. To make 4% solution add 10 mL of 16% solution in 30 mL of PBS.
    - 0.1% Triton X-100 solution. Add 100 µL of Triton X-100 to 10 mL of PBS.
    - Blocking buffer – add 2.5 g of BSA to 50 mL of PBS to have a 3% BSA solution.
    - 1x Phosphate buffered saline (PBS).
    - Primary and secondary antibodies that are listed in section 2.1.6.
    - Millicell® EZ slides 8-well glass sterile (Merck, UK).
    - Glass slide cover slips.
    - Nuclear stain DAPI (4, ‘6-diamidino-2-phenylindole).
    - VectaShield mounting medium.

- Clear nail varnish.

- Cell preparation
  - Culture hPAECs and hPASMCs as described in sections 2.2.1 and 2.2.2 respectively.
  - Seed hPAECs at 10,000 cells per well and hPAMCs at 5,000 cells per well of Millicell® EZ slides. Incubate cells overnight for complete adhesion to the slide. Remember to have a non-stain control well.
  - Treat cells as described in section 2.2.5, as required per experiment.
- Cell staining
  - Following treatments of cells, gently aspirate cell supernatant and wash the cells with 1x PBS.
  - Fix the cells with ice cold 4% PFA for 10 minutes.
  - Permeabilise the cells with the 0.1% Triton-X solution for 5 minutes and then blocked for 1 hour with blocking buffer.
  - Dilute primary antibodies with blocking buffer as indicated in the primary antibody section 2.1.6.1. Incubated cells with primary antibodies for at least 2 hours. Cells can also be incubated overnight at 4^0C.
  - Wash cells with 1xPBS four times and incubate with secondary antibody for 1 hour. Dilute secondary antibody with blocking buffer as indicated in section 2.1.6.2.

- After, incubation with secondary antibody, incubate cells with DAPI dilute 1:1000 with 1xPBS for 5 minutes. Wash cells 4x with 1xPBS.
- Remove the detachable wells, add 1 small drop of VectaShield mounting medium to each well and cover with glass cover slips. Use nail varnish around the borders to secure the cover slip.
- The slide is read to image or to be stored at 4^0C.
- Imagining was performed with a plan apochromat 40x oil objective on a SP8 inverted confocal microscope (Leica, UK).
- Images were analysed with ImageJ software.

2.4 Cell proliferation assay

2.4.1 MTS assay

Cell proliferation was analysed by the CellTiter 96 ® Aqueous One Solution Cell proliferation Assay (Promega, UK). In brief, MTS assays are based on the use of tetratozolium compounds that can be reduced by viable cells to generate formazan products that are soluble in cell culture medium. The assay contains a tetrazolium compound [3-(4,5-dimethylthiazol-2-yl)-5-(3-carboxymethoxyphenyl)-2-(4-sulfophenyl)-2H-tetrazolium, inner salt; MTS] and an electron coupling reagent (phenazine ethosulfate; PES). PES is an intermediate electron acceptor, that transfer electron from NADH (nicotinamide adenine dinucleotide plus hydrogen) in the cytoplasm to reduce MTS in the medium into formazan (Riss et al., 2004). Once, MTS is reduced into formazan it causes a colour change of the medium (yellow to brown) that can be measured by spectrophotometer at an absorbance wavelength of 490 nm. Following cell treatments after incubation period, the supernatant of each each (96-well plate) was removed and replace

with 100 µL of fresh complete medium and 20 µL of MTS assay was added to each well, 3 blank wells were also added, this well only contained media and MTS assay only. Cells were plated at 70% confluence, which means that the maximal cell proliferation expected is 30%. The plate was incubated for 4h at 37^{o}C and 5% CO2 and absorbance was then measure at 490 nm.

2.4.2 BrdU

2.4.2.1 Basic Principle

The colorimetric BrdU cell proliferation kit (Roche) was used to measure cell proliferation. This assay detect DNA synthesis by measuring the incorporation of the thymine analogue, bromodeoxyridine during the S phase of the cell cycle, making this nucleoside analogue it is and good marker of cell proliferation. The detection of this nucleoside is possible by the development of specific antibodies against it (Adan et al., 2016).

2.4.2.2 Protocol

hPAECs were plated on 96 well plate (2500 cells/well). . Cells were plated at 70% confluence, which means that the maximal cell proliferation expected is 30%. After initial adherence, the cells were serum starved (0.2% Serum) for 24h prior to treatment as described in section 2.2.5. Following treatment for 24h, BrdU was introduced (at the manufacturer recommended concentration) for an additional 24h incubation before harvesting the plates. Proliferation was quantified using anti-BrdU-POD antibody, according to the manufacturer's instructions. All treatments were undertaken in triplicate.

2.5 Polymerase Chain Reaction - PCR

2.5.1 Basic principles

Polymerase chain reaction is one the most used molecular biology techniques and it first described in 1985 (Saiki et al., 1985). PCR allows distinct DNA sequences to be amplified, moreover it only needs an infinitesimal amount of DNA to start and result in large amounts of copies for analysis. PCR has also been modified to ascertain the quantity of mRNA expressed in tissues or cells to give insight into genetic adaptation to cellular environment changes. Briefly, during PCR two primers (oligonucleotides sequences) complementary of a DNA target sequence. DNA polymerases then synthesises a complementary strand of DNA from the primer sequences, resulting in two new strands of DNA. As this cycle occurs the new synthesised is denatured and new copies are made resulting in multiples copies of the original target sequence (Clark et al., 2019). Each cycle consists of 3 steps:

Step 1 (denaturation): The samples are heated to 95^{o}C for 5 seconds. This allows for the disruption of the hydrogen bonds between the two strands of DNA causing their separation.

Step 2 (annealing): the samples are cooled down to 55-65^{o}C for 10 seconds, which will allows the primers in the sample to bind to the complementary DNA sequences.

Step 3 (extension): the samples are then heated up to 72^{o}C for 10 seconds, this is the optimal temperature for Taq polymerase to attached to the end of the

primers and start extending the DNA sequence by adding dNTPs that are complementary to the template strand.

2.5.2 RNA preparation

2.5.2.1 Total RNA extraction

Total RNA was extracted form cells using the RNAeasy Mini preparation Kit (Qiagen, UK). Full protocol on figure 2-7. Briefly, the cell culture medium were completely removed before the addition of the RLT lysis buffer (supplement with β-Mercaptoethanol). 70% ethanol was then added to the samples and vortex, and transferred to the RNAeasy columns membrane. The columns were then centrifuged, which allows the RNA to bind to the membrane. This membrane was washed through various steps to remove contaminants and remaining DNA was digested by the addition of DNase. RNA was then eluted by the addition of RNase free water.

Total RNA Extraction

Reagents

RNAeasy mini kit – containing RLT lysis buffer, RW1 wash buffer, RPE wash buffer, mini spin columns, collection tubes

70% ethanol, β-Mercaptoethanol

Buffers working solutions:

RLT – add 10 µL of β-Mercaptoethanol per 1 mL of RLT buffer

RPE buffer – add four volumes of 70% ethanol

Procedure

1. Aspirate completely the supernatant from the cells

2. Add 350 µL of RLT buffer to each well, pipette up and down to disrupt the cell membranes. Transfer the contents into a 1.5 mL tube.
3. Vortex sample and keep it on ice. From this point samples can also be stored at -80°C and continue extraction at a later time.
4. Add an equal volume (350 µL) of ice cold 70% ethanol to samples and mix it by pipetting up and down.
5. Transfer samples to a mini spin column placed in a 2 mL collection tubes. Centrifuge at ≥8000 RCF for 15 seconds at room temperature. Discard flow through
6. Add 700 µL of RW1 buffer to the column and centrifuge at ≥8000 RCF for 15 seconds at room temperature. Discard flow through.
7. Add 500 µL of RPE buffer to the column and centrifuge at ≥8000 RCF for 15 seconds at room temperature. Discard flow through.
8. Add 500 µL of RPE buffer to the column and centrifuge at ≥8000 RCF for 2 minutes at room temperature. Discard flow through.
9. Transfer the spin column into a new collection tube and centrifuge at ≥8000 RCF for 1 minutes at room temperature to dry out the membrane.
10. Transfer the spin column into a 1.5 mL collection tube and add 30 µL of RNase free water to the spin column. Be careful to not stab the column membrane. Centrifuge at ≥8000 RCF for 1 minutes at room temperature to elute RNA.
11. Store samples at -80°C.

Figure 2-7 RNA extraction protocol.

2.5.2.2 RNA concentration and purity determination

To determine the concentration and purity of RNA the nano-drop spectrophotometer was used. RNA quantification occurs by measuring light absorption at 260 and 280 nm. For high quality RNA the absorbance ratio of the 260 and 280 wavelengths have to be close to 2.

2.5.3 cDNA synthesis

Complementary DNA (cDNA) is a strand of DNA synthesised from a RNA template, this reaction is possible through enzymes called reverse transcriptases. These enzymes are used by certain types of viruses to replicate their genome by integrating the new double stranded cDNA into the hosts' genomes. In brief, oligo

DT primers hybridises to the polyA tail of the messenger RNAs and cDNA synthesis can start by the reverse transcriptase from the primer. The new synthesised cDNA can then be used for real time PCR. Full protocol see figure 2-8.

cDNA synthesis protocol

Reagents

- 5x Reverse transcriptase buffer
- 0.1 M Dithiothreitol (DTT)
- 10 mM dNTPs (deoxyribonucleotide triphosphate) – dATP, dCTP, dGTP, dTTP: for 200 µL of mix add 20 µL of each dNTP
- RiboLock RNase inhibitor (Thermofisher Scientific, USA)
- $OligoDT_{12-18}$
- RNase/DNase free water
- MMLV reverse transcriptase

Protocol

1. For each sample add the necessary volume to have 500ng of RNA, and complete with water to have 10 µL.
2. Add 1 µL of dNTPs and OligoDT to the sample and incubate at 65ºC for 10 minutes, followed by 5 minutes on ice.
3. Prepare RT mixture: 4 µL of RT buffer, 2 µL of DTT, 1 µL MMLV and 1 µL RiboLock RNase inhibitor.
4. Add 8 µL of the RT mixture to each sample.
5. Incubate samples at 37ºC for 50 minutes.
6. Incubate at 70ºC for 15 minutes.
7. Dilute cDNA 1:10 with RNase/DNase free water (add 180 µL of water).
8. Store samples at -20ºC.

Figure 2-8 cDNA synthesis protocol.

2.5.4 Real Time PCR

Real time PCR is a permutation of PCR that allows the determination of the relative quantity of target DNA, i.e. a gene, in a sample by monitoring in real time the amount of DNA being amplified in cycle of PCR, which then can be compared to another control sample, and report as fold change. This quantification is based upon fluorescent dyes, such as SYBR green, that can bind to double stranded DNA ad its fluorescence increases 20-100 fold when bound to double stranded DNA or an oligonucleotide probe that binds an internal segment of the target DNA, between the two PCR primers. The probe has a fluorescent dye bound to the 5' end and fluorescence quencher bound at the 3' end. When the probe is hydrolysed by the DNA polymerase the fluorescent dye is released way from the quencher and emit light that will be detected by the RT-PCR instrument. Each reaction is characterised by the PCR cycle where the fluorescence signals rises above the background fluorescence, this is called cycle threshold (Ct). The lower the Ct value is, more copies of target DNA is present in a sample. The correlation between fluorescence and amount of amplified product enables quantification of the targeted molecules. Full protocol on figure 2-9.

Real-Time PCR protocol

Reagents

- 2x SensiFast SYBR LoROX PCR mix
- RNase/DNase free water
- Primers
- cDNA samples
- 0.1 mL PCR strip tubes

Protocol

1. Defrost all reagents and samples on ice
2. Prepare the reaction master mix, according to the number of reactions needed

1x Reaction Master Mix	Volume (µL)
2x SensiFast SYBR LoROX mix	5
Primer	1
cDNA Template	2
RNase/DNase free water	2
Total Volume	10

3. Add 8 µL of master mix to each reaction tube
4. Add 2 µL of cDNA template or water control to its corresponded tubes
5. 3-step cycling

Cycles	Temperature	Time
1	95°C	2 minutes
40	95°C 60 °C 72 °C	5 seconds 10 seconds 10 seconds

Figure 2-9 Real time PCR protocol.

2.6 Western Blot

2.6.1 Basic principles

Western blotting or protein immunoblotting is a widely used technique to detect a protein of interest from complex mixtures, such as cell lysates. Protein mixtures found in cell lysates are separated by molecular weight through gel electrophoresis. The separated proteins are then transferred and fixed to a nitrocellulose membrane. The membrane is then incubated with specific antibodies to the protein of interest. Unbound antibodies are washed off by repeated washes, and secondary antibodies conjugated with horseradish peroxidase (HRP) is added which binds to the primary antibody bound to the protein of interest. The bound antibodies are detected by the addition of enhanced chemiluminescence solution (ECL reagent, Biorad), which contains luminol ($C_8H_7N_3O_2$) and hydrogen peroxide (H_2O_2). In the presence of luminol HRP oxidises luminol, which generates a light signal that are captured by a charge-coupled device (CDD) camera or by exposure to X-Ray film. The intensity of the signal can be measured by densitometry. Protein markers are loaded onto the gels at the same as protein mixtures to certify the correct protein is identify. Following Identification of the protein of interest, membranes are reprobed for a loading control, such as α-tubulin, GAPDH, to ensure equal amounts of proteins were loaded. Cell lysate preparation

After incubation with treatments, the cell monolayer was washed with phosphate buffered saline (PBS), incubated with trypsin (0.05%, GIBCO) at 37oC for 3-5 minutes to detached cells followed by trypsin quenching with EGM2 medium. Cells were pelleted in 15/50 mL falcon tube by centrifugation at 260 RCF for 5

minutes at room temperature. The cell pellet was then washed PBS and centrifuged again to pellet the cells. The cell pellet was then lysed with 1x RIPA buffer (SIGMA, UK) supplemented with protease and phosphatase inhibitors (ABCAM, UK). The lysate was transferred into 1.5 mL Eppendorf's tubes and were incubated on ice for 10 minutes, vortexed and then centrifuged at maximu rpm (~14000) for 10 minutes at 4^{o}C.

2.6.2 Protein quantification - Bradford assay

To quantify the amount of protein in solution the Bradford protein assay was used. This assay is widely used in research laboratories across the world. It is based on the binding of the dye Coomassie blue G250 to protein. The unbound form (cationic) of the dye has has a maximal absorbance of 470 nm. In contrast, the protein bound form (anionic) has an absorbance of 595 nm, therefore the amount of bound dye can be determined by measuring a sample of cell lysate mixed with the dye at 595 nm (Kruger).

A serial dilution of BSA (Bovine Serum Albumin) was prepared as a protein standard between 0 and 2000 µg/mL in distilled water. Standards or diluted samples were loaded in duplicates in a 96-well plate. Bradford reagent was then added to each well and absorbance was measured at 595 nm in a plate reader. Protein amount of samples were calculated by creating a standard linear curve from the absorbance measurements of the protein serial dilutions. See protocol in figure 2-10.

Bradford assay for total protein quantification

1. Thaw samples on ice.
2. Add the appropriate volume of deionised water to the labelled tubes, and perform a **BSA standards** according to **Table below**.

✓ **QUALITY CONTROL NOTE:** When adding BSA to each tube, mix well by pipetting up and down.

3. In a clear, flat bottom 96-well plate, pipette 5 µl of each BSA dilution, and 1 µl of each protein sample and complete it with 4 ul of deionised water into their respective wells.
4. Dilute the Bradford assay 1:5 dilution factor, prepare the total volume required by following the steps shown in the **example** below:

EXAMPLE: Calculate total number of wells (BSA dilutions + protein samples) = 200 * N. **N is the number of wells needed.**

5. Add 200 µl of diluted Bradford assay.
6. Measure the absorbance at 595 nm on a plate reader (spectrophotometer).

Tube	Deionised water	BSA	BSA concentration	Final volume (water + BSA)
A	No water	200 µl of BSA protein standard	2000 µg/ml	100 µl
B	100 µl	100 µl from tube A	1000 µg/ml	100 µl
C	100 µl	100 µl from tube B	500 µg/ml	100 µl
D	100 µl	100 µl from tube C	250 µg/ml	100 µl
E	100 µl	100 µl from tube D	125 µg/ml	100 µl
F	100 µl	100 µl from tube E	62.5 µg/ml	100 µl
G	100 µl	100 µl from tube F	31.25 µg/ml	**200 µl**
H	100 µl	No BSA	0 µg/ml	100 µl

Figure 2-10 Bradford assay protocol.

2.6.3 Gel Electrophoresis, blotting and protein detection

After protein quantification Laemmli sample buffer (Bio-rad) was added to the cell lysate, which was then incubated at 95^{o}C for 10 minutes. The samples were then cooled on ice and loaded into a precast SDS-polyacrylamide gels, a protein ladder was also added to monitor electrophoresis progression. Once the samples and protein maker run through the gel, the protein were transferred onto a

nitrocellulose membrane. The membrane was then blocked with 3% BSA solution for 1 hour. Antibody incubation (list of antibodies shown on table 2.1.6) occurred overnight on shaker at 4ºC. Membranes were then washed three times, incubated with secondary antibodies and imaged after incubation with ECL reagent. The complete protocol for western blotting is shown in figure 2.11.

Western Blot Protocol

Reagents

- 1x RIPA cell lysis buffer
- Protease inhibitor diluted at 1:200
- Phosphatase inhibitor diluted at 1:49
- Laemmli sample buffer, supplemented with β-mercaptoethanol (1:10 dilution)
- Dual Xtra protein ladder
- 10x TRIS/Glycine buffer solution
- iBlot™ 2 transfer stacks
- Phosphate buffered saline tablets
- Tween-20
- 4-15% Mini-PROTEAN® TGX™ precast gels
- BSA powder
- Distilled water

Buffers

- **1x Running buffer** – 100 mL of 10x TRIS/Glycine buffer solution in 900 mL of distilled water
- **PBST** – 5 phosphate buffered saline (PBS) tablets, 500 µL of tween-20 in 1 L of distilled water
- **BSA blocking solution** – PBST, 3% w/v BSA. (50 mL PBST and 1.5g of BSA).

Protocol

1. Add laemmli loading buffer supplemented with β-mercaptoethanol to cell lysates in 1:4 ratio. Boil the sample for 5 minutes at 95^{o}C.
2. Load 20-50 µg of protein sample and 7 µL of protein ladder onto a precast gel.
3. Run the gel at 130V for 1 hour or until the samples reach the end of the gel.
4. Transfer the separated protein to a nitrocellulose membrane, using the iBlot™ 2 transfer stacks.
5. Block the membrane with 3% BSA blocking solution for 1 hour.
6. Incubate the membrane with the appropriate antibody diluted in the 3% BSA blocking solution overnight at 4^{o}C on a shaker.
7. Following antibody incubation, wash the membrane 3 times in PBST (10 minutes per wash).

8. Incubate membrane with the appropriate HRP-conjugated secondary antibody diluted in the 3% BSA blocking solution at room temperature for 1 hour on a shaker.
9. Wash the membrane 3 times in PBST (10 minutes per wash).
10. Incubate the membrane with ECL reagent for 1 minute and image it using the Licor Odyssey FC imaging system. Where western blot calculations were performed.

Figure 2-11 Western Blot protocol.

2.7 Enzyme-linked immunosorbent assay (ELISA)

2.7.1 Basic principles

ELISA is a technique used to detect the presence of an antigen in biological samples, which relies on specifics antibodies to accurately identify and quantify the presence of antigens in a biological sample. There four main types of ELISA, direct ELISA, indirect ELISA, sandwich ELISA and competitive ELISA. The most commonly used type is the sandwich ELISA, which requires two antibodies specific for different epitopes of the antigen. One of these antibodies is used to coat the surface of a 96-well plate to capture and immobilize the antigen; the second antibody is conjugated with a detection agent.

In, brief the capture antibody is immobilised onto the surface of the wells of a 96-well plate by adsorption. The surplus antibody is then washed and non-specific binding sites are blocked by adding a blocking buffer containing high concentrations of bovine serum albumin (BSA). Samples are then added and any antigen present will bind to immobilised capture antibody. After washing, the secondary antibody, which is conjugated with biotin and aimed to a different epitope of the antigen is added. Following incubation and washes, streptavidin horseradish peroxidase (HRP), which binds to the biotin bound to the second antibody is added for detection. HRP is detected and quantified by the addition

of TMB substrate reagent (BD OptEIA; BD biosciences, UK) in the presence of hydrogen peroxide. The colour develops in proportion to the quantity of antigen bound, the reaction is the terminated by acidification.

2.7.2 Detection of cytokines

Human IL-6, IL-8 and MCP-1 levels in cell supernatants were quantified using commercially available sandwich ELISA kits according to manufactures' guidelines (R&D systems, UK). The protocol is outline in figure 2-11. In general, all incubations occurred at room temperature and results were taken as mean values of duplicates. Data was analysed by a standard curve by non-linear regression of log transformed data, using GraphPad Prism.

General sandwich ELISA protocol

Reagents

- Half-area 96 well plates
- Sandwich ELISA kits containing capture and detection antibodies, standards and streptavidin-HRP
- Wash buffer – PBS (5 tablets/1L), 0.05% tween20 (0.5mL/1L).
- Blocking/Reagent diluent buffer – PBS (1 tablet/200 mL), 1% BSA (1g/100 mL).
- TMB reagent set (BD, USA) – 1:1 mixture of solution A (hydrogen peroxide); and solution B (3,3', 5,5' tetramethylbenzidine).
- Stop Solution – 1M Dihydroxidosulfur (H_2SO_2)

Protocol

1. Coat the well of the half-area 96-well plates with 50 µL capture antibody. Seal the plate and incubate overnight at room temperature.
2. Remove the capture antibody and wash each 3x with wash buffer (200 µL). After the lst wash, remove any remaining wash buffer by blotting the plate against clean paper towels.
3. Block the plate by adding 150 µL of blocking/reagent diluent buffer to each well and incubate at room temperature for a minimum of 1 hour.

4. Repeat the aspiration/wash as in step 2.
5. Add 50 µL of sample or standards, cover and incubate for 2 hours at room temperature.
6. Repeat the aspiration/wash as in step 2.
7. Add 50 µL of the working dilution of streptavidin-HRP to each well. Cover the plate and incubate for 20 minutes at room temperature, protecting the plate from direct light.
8. Repeat the aspiration/wash as in step 2.
9. Add 50 µL of substrate solution to each well. Cover the plate and incubate for 20 minutes at room temperature, protecting the plate from direct light.
10. Add 25 µL of stop solution to each well.
11. Determine optical density of each well, using a microplate reader set to 450 nm. For wavelength correction also read at 570 nm.

Figure 2-12 General sandwich ELISA protocol.

2.8 Seahorse Assay

The seahorse assay measures key parameters of mitochondrial function. Mitochondria are known as the powerhouse of the as they function as the energy supplier for the body. Adenosine triphosphate is generated by the mitochondrial respiratory chain through a process called oxidative phosphorylation. Mitochondria are involved in regulating apoptosis, cell proliferation, cell signalling, and reactive oxygen species. Dysregulation of mitochondrial function has been implicated in many human diseases ranging from rare genetic disorders to common ones such as diabetes (Yépez et al., 2018). The most significant test for mitochondrial function is the quantification of cellular respiration, by directly measuring oxygen consumption rate (OCR). Generally OCR is measured in real time using the seahorse XF Analyser in a 96-well plates, with multiple steps under consecutive treatments in a process called mitochondrial stress test.

2.8.1 Mito Stress test

This assay uses the injection ports on XF sensor cartridges, to add modulators of respiration into each well to uncover key parameters of mitochondrial function. This assays uses the following modulators, olygomycin, carbonyl cyanide-4 (trifluoromethoxy) phenylhydazone (FCCP), rotenone and antimycin. The assay stars by measuring basal parameters, which is followed by the first injection of oligomycin, which inhibits ATP synthase. It decreases the electron flow through the electron transport chain (ETC) reducing mitochondrial respiration or OCR. The second injection is FCCP, an uncoupling agent that collapses the proton gradient and disturbs the mitochondrial membrane potential. This results in uninhibited flow through the ETC and oxygen consumption reaches the maximum. With this stimulus spare respiratory capacity, which is the cell ability to respond to increased energy demand, can be calculated. This is calculated by taking the difference between maximal respiration and basal respiration. The third injection is a mixture of rotenone and antimycin A. This mixture halts mitochondrial respiration and allows for the calculation of non-mitochondrial respiration driven by process outside the mitochondria. The detailed protocol can be found in figure 2-12.

Seahorse XF Cell Mito Stress Test Protocol

Reagents: Oligomycin; FCCP; Rot/AA; XF DMEM medium; XF 1 M glucose solution; XF 100 mM pyruvate solution; XF 200 mM glutamine solution; XF Calibrant; XF cell culture microplates and Sensor Cartridge.

Protocol:

Day Prior the assay

1. Turn on the Searhorse XFe/XF analyserand leave it to warm up overnight
2. Hydrate the sensor cartridge in seahorse XF calibrant at 37^{o}C in a non-CO_2 incubator overnight.
3. Treat the cells with the required stimuli/drugs.

Day of Assay

1. Prepare assay medium - Supplement the seahorse XF DMEM medium with 1 mM pyruvate, 2 mM glutamine and 10 mM glucose in a cell culture hood. Warn the ready assay medium to 37^{o}C in a water bath.
2. Prepare compound stock solutions and working solutions. Use the prepare compounds on the same day.

2.1 Remove the 3 tubes containing oligomycin (blue cap), FCCP (yellow cap), and rotenone/antimycin A (red cap) from the pouch. Gently pipette up and down to solubilise the compounds.

2.2 Resuspend content in each tube with the prepared assay medium as specified in the table below.

Compound	Volume of assay medium	Stock Concentration
Olygomycin	630 µL	100 µM
FCCP	720 µL	100 µM
Rot/AA	540 µL	50 µM

2.3 Use the compound stock solutions to prepare the working solutions to be added to the injections ports on the sensor cartridges as shown in the table below.

	Final Well (µM)	Stock Solution volume (µM)	Media Volume (µM)	Volume added to port (µM)
Port A Oligomycin	1.5	450	2550	20

Port B FCCP	2	600	2400	22
Port C Rot/AA	0.5	300	2700	25

2.4 If not using a whole 96-well plate, prepare the necessary amount for the number of wells needed. Always make 20% extra to have enough volume for reverse pipetting technique.

3. Prepare seahorse XF cell culture microplate for assay

3.1 Change the cell culture growth medium in the plate to warmed assay medium (180 µL) using a multichannel pipette, and place the plate in a 37°C non-CO_2 incubator for 45 minutes to 1 hour prior the assay.

4. Load solutions into the sensor cartridge ports

4.1 Remove the hydrated cartridge from the non-CO_2 incubator

4.2 Place the row labels A-H to the left, and the triangular notch will be in the bottom left-hand corner.

4.3 Place the the loading guide (use the one for the port been loaded) flat on top of assay cartridge. Use fingertips to hold the outside edges of the loading guide to stabilise it, so the pipette tips do not move it out of place.

4.4 Using a 10-100 µL multichannel pipette, aspirate the required compound using the reverse pipetting technique.

4.5 Position the pipette tips (containing the compound) into the desired column in the loading guide, and orient the tips straight. Insert the tips as far as they will go without any resistance into the holes and dispense the compounds.

4.6 Slowly dispense the appropriated compound volume into the ports according to plate/group layouts shown in the picture below. Only press the pipette plunger to the first stop to avoid introducing bubbles. Do not tap the cartridge in any way to attempt to remove bubbles.

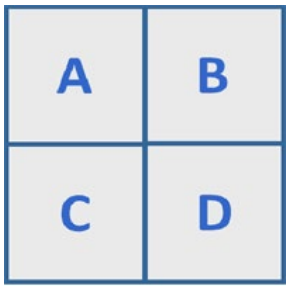

4.7 Visually inspect the injection ports for even loading.

5. Running the assay

5.1 Open the wave software and select the XF Cell Mito Stress test, and after designing the plate layout click start run.

5.2 When prompted, place the loaded cartridge with the calibrant plate into the seahorse instrument and follow the instructions (make sure that the lid of the cartridge is removed before loading). Calibration will be finished between 15 to 30 minutes.

5.3 Removed the cell plate from the non-CO_2 after calibration and equilibration and when prompted click I'm ready.

5.4 Load the cell plate (remove the plate lid before loading) and click I'm ready to run the assay.

Figure 2-13 - Seahorse XF cell mito stress test protocol.

2.9 Flow Cytometry

2.9.1 Basic Principles

A flow cytometer instrument is sophisticated, it can measure the optical a fluorescence characteristics of a single cell or any other particles that is prepared in a fluid stream when they pass through a light source (figure 2-12). These fluorescent features can be derived from either antibodies conjugated with dyes or direct dyes that can directly bind or fluoresce with any features of a cell (such as DNA). The fundamental principle of flow cytometry is scattering of light and fluorescence emission. Light scattering is related to structural and morphological properties of a cell, whereas fluorescence is related to emission from a fluorescence probe bound to a cell or cellular component (Adan et al., 2017). Flow cytometry can be used in many applications such as the detection of antigens on cell membranes, within the cytoplasm and nucleus; cell proliferation and cell cycle; cell membrane potential and reactive oxygen species (ROS) detection.

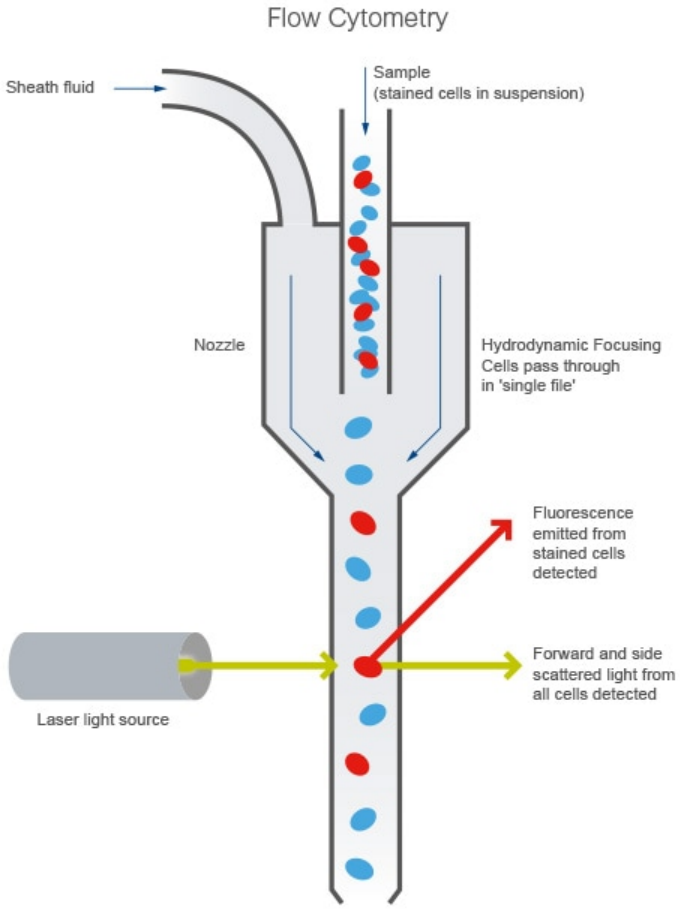

Figure 2-14 Simple schematic of a flow cytometer*. Cells are pulled thorough a nozzle together with sheath fluid a laser bin is aimed at each cell as they pass through. Forward and side scatter light together with fluorescence are detected form stained. Picture taken from https://www.abcam.com/protocols/introduction-to-flow-cytometry.*

2.9.2 Cell cycle analysis

Various methods to evaluate cell cycle progression has been developed. The most commonly used method is staining cells with propidium iodide (PI), this allows for univariate analysis of DNA content that reveals the distribution of cells in three major phases of cell cycle (G_1 vs S vs G_2/M). PI is a fluorochrome that requires a blue light as the excitation source. As PI also stains double strain RNA, RNase A is added to the staining solution. In brief, following treatments cells were trypsinized and pelleted by centrifugation. The cell pellet was then resuspended with 300 µL of PBS. Ice cold ethanol (100%) was then slowly added to the cell

suspension for fixation (at this point cells can be stored at -20ºC for a week). Spin cells down at 3400 rpm for 5 minutes to remove ethanol solution, wash cells with 1 mL PBS and repeat centrifugation step. During centrifugation prepare PI/RNase A solution in PSB. Final concentration of PI (Sigma, UK) at 50 µg/mL and RNase A (Invitrogen, UK) at 250 µg/mL. Suspended the cell pellet with 500 µL of PI/RNase solution and incubate at 37ºC in the dark for 45 minutes. Pellet the cells to remove PI/RNase A solution and wash the cells with 1 mL PBS. Spin down cells again, remove PBS and resuspended cells with 300 µL PBS. Use a cell strainer to remove any cell clumps before running the samples though the flow cytometer (BD Accuri C6).

2.9.3 ROS detection

2.9.3.1 Basic Principles

Reactive oxygen species (ROS) are molecules that by-products of anaerobic respiration. In normal conditions they mostly produced by mitochondria and nicotinamide dinucleotide phosphate (NADPH). Elevated levels of ROS can result in oxidative stress, which promotes the damage of proteins, lipids and DNA leading to cellular stress or death and pathological disease states (Shehat and Tigno-Aranjuez, 2019). Multiple assays have been utilised to measure ROS, this project used the commonly used dihydroethidium (DHE dye) to measeure overall ROS and MitoSOX red to measure mitochondrial ROS.

2.9.3.2 DHE and MitoSOX red

Dihydroethidium (DHE) is the reduced form of the DNA dye ethidium bromide. DHE has been widely used to detect de its high reactivity and facility to passively diffuse into cells. DHE is known to be the most specific fluorescence dye to detect cytosolic superoxide. DHE reacts with superoxide anions to form a red fluorescent product, 2-hydroxyethidium with excitation and emission peaks at 500 and 580 nm, respectively (Wojtala et al., 2014).

MitoSOX red is a dye used to measure superoxide production specifically produced by the mitochondria. MitoSOX red it is a cationic derivative of DHE, therefore its reaction is similar to that of DHE, however it does react more rapidly with superoxide than DHE and it is quickly targeted to the mitochondria, where it is oxidised to form 2-hydroxyethidium which excites and emits at 510 and 580 nm, respectively (Wojtala et al., 2014).

In brief, following treatments cells were trypsinised, pelleted and washed with PBS, cells were then ressuspended in 100 µL of PBS. The cell suspension were then split in two (one sample for DHE staining and one for mitoSOX), each 50 µL were diluted with 450 µL of PBS. To the samples set for mitoSOX staining 1 µL of mitoSOX red dye was added and the samples were analysed immediately in BD Accurri C6 flow cytometer. While the last sample of the mitoSOX stained samples are running, add 2 µL of DHE dye to each sample set out for DHE staining and run samples straight away.

2.9.4 TMRM (tetramethylrhodamine methyl ester) assay

2.9.4.1 Basic principles

Mitochondria maintains a negative potential across their inner membrane ($\Delta\psi$), which is vital for mitochondrial and cell function. Mitochondrial membrane potential is a key indicator of mitochondria heath and cell viability, therefore accurate determination of $\Delta\psi$ is important to answer many questions regarding cellular metabolism. Most assays to determine $\Delta\psi$ use lipophilic fluorescence cations that crosses the cellular and mitochondrial membranes freely, which accumulates in the mitochondrial matrix according to $\Delta\psi$ *(Distelmaier et al., 2008)*.

A number of different dyes has been used to determine $\Delta\psi$, such as JC-1 (5,5′,6,6′-tetrachloro-1,1′,3,3′-tetraethylbenzimidazolylcarbocyanine iodide) and $DiOC_6$ (3,3′-dihexyloxacarbocyanine iodide). These dyes do have limitations, JC-1 aggregation clusters within the mitochondria emits different spectra to its monomeric form, making its signal very concentration sensitive and $DiOC_6$ is very toxic to cells, which needs to be used at low concentrations making it hard to measure $\Delta\psi$ accurately. Therefore the tetramethylrhodamine methyl ester (TMRM) dye was chosen to measure $\Delta\psi$ due to its positive charge that enable it to accumulate within the mitochondria in an inverse proportion to $\Delta\psi$, most importantly this dye can be used at low concentrations to ensure mitochondrial function with no significant mitochondrial binding or electron transport chain inhibition (Distelmaier et al., 2008, Creed and McKenzie, 2019).

2.9.4.2 Protocol

hPAECs were seed into a 6-well plate with 300,000 cells per well. Cells were incubated overnight for attachment. Cells were then treated as necessary for each experiment performed. After the cells were treated for the required period of time they were incubated with the TMRM dye for 30 minutes as described below.

- TMRM stock solution was prepared by diluting the dye into DMSO to have a 100 μM solution.
- Working solutions were then freshly prepared by diluting the 100 μM into media to have a final concentration of 100 nM.
- CCCP (2-[2-(3-Chlorophenyl)hydrazinylyidene]propanedinitrile), a potent mitochondrial oxidative phosphorylation uncoupler was used as a positive control. A 50 μM solution was prepared with media and added to the positive control (no treatment) 10 minutes prior to the addition of the TMRM solution.
- Once all the treatment incubations, including the positive control, the media is removed and replaced with the TMRM solution prepared and incubated for another 30 minutes.
- Wash the cells with HBSS buffer and trypsinise cells and collect then into flow cytometry tubes to run the cells in a flow cytometer to detect changes of $\Delta\psi$.
- TMRM is detected at 561-nm excitation using emission filters appropriated for R-phycoerythrin.

2.9.5 Cell Antigens Staining

2.9.5.1 Basic Principles

Flow cytometry also enables the rapid detection of single antigens present within or the surface of cells, due to the ability of flow cytometry to measure these antigens in each cell it provides a robust method of quantification. Cellular samples labelled with a fluorescent conjugated antibody for a specific target will provide quantitative fluorescence intensity, the higher the fluorescence intensity, the greater the number of target molecules present in each cell (Hogg et al., 2015).

2.9.5.2 Protocol

- Buffers
    - FACS buffer: 1x PBS with 1% bovine serum albumin (BSA), sterile filter solution (0.2 µm). Store at 4ºC.
    - Cell fixing buffer: 4% formaldehyde in PBS (1x), store at room temperature.
    - Blocking buffer: 3% BSA in 1x PBS, store at 4ºC.
- Cell preparation
    - Grow hPAECs as the protocol and treat as required for each experiment. For flow cytometry use a T25 flask for each treatment condition.
    - Wash the cells once in sterile PBS, after add the required amount of 1x trypsin and incubate for maximum 3 minutes. Tap the flask, and transfer the cells to a 15 mL tube.

- Centrifuge the cells at 260 RCF for 5 minutes. Aspirate the supernatant and wash the cells with 1x sterile PBS and repeat the centrifugation step.
- To block cells to reduce unspecific binding, incubate the cells with blocking buffer for 1 hour.
- Centrifuge the cells at 260 RCF for 5 minutes. Aspirate the supernatant of samples.
- Wash the cells with 1x PBS by centrifuging it 260 RCF for 5 minutes.
- While cells are spinning prepare the required amount of antibody solutions.

- Antibody preparation
  - While washing the cells, prepare antibody solutions
  - Mix the primary antibody with ice-cold FACS buffer, to the desired antibody dilution. Prepare around 0.5 mL of antibody solution for each sample to be analysed.
  - Prepare the secondary antibody solutions, matching the species of primary antibody (if primary antibody was raised in mouse, choose an anti-mouse secondary fluorophore labelled antibody), and dilute 1:100.
- Cell Staining
  - Add 0.5 mL of primary antibody dilution to each of the appropriate samples and incubate with cells for 2 hours at room temperature in

the dark. DO NOT add the primary antibody to the cells that will be used as non-stained control or as secondary antibody only control.

- Pellet the cells by centrifugation (260 RCF for 5 minutes).
- Wash cells twice with 1x PBS by centrifugation (260 RCF for 5 minutes). Aspirate the supernatant from samples.
- Add the diluted fluorophore labelled secondary antibody to the samples stained with the primary antibody and the secondary antibody only control. Incubate for 1 hour at room temperature in the dark.
- Wash cells twice with 1x PBS by centrifugation (260 RCF for 5 minutes).
- If cells are to be analysed in the same day, resuspend cells in FACS buffer and keep in the dark at 4^{o}C for up to 2 hours. Alternatively, cells can be fixed with the fixing buffer and store at 4^{o}C for 2-3 days prior to analysis.
- Cells can now be analysed on the bench top BD Accuri C6 plus flow cytometer.

2.10 Statistics

Statistical analysis was performed using GraphPad V9, unless otherwise stated. Data are expressed as ± standard error of the mean (SEM) for n experiments. N is defined as samples from individual donors or as biological repeats in cell culture. For all experiments protocols were performed at least 3 times. Normally distributed data was analysed using parametric tests while non-normally distributed data were analysed by non-parametric test as detailed in individual figure legends. Statistical significance was assumed where $p>0.05$.

3. Chapter 3 – The ferroportin/hepcidin axis is present on pulmonary arterial endothelial cells

3.1 Rationale

The ferroportin/hepcidin axis is central for systematic regulation of iron homeostasis. Ferroportin is the only known iron exporter in mammalians. Binding of the iron regulatory hormone hepcidin to ferroportin leads to its internalisation and degradation stopping iron export to the extracellular space. Hepcidin is predominantly released by liver hepatocytes and ferroportin is primarily expressed in cells involved in systematic iron homeostasis such as macrophages, duodenal and hepatic cells. However, it also recently shown to be expressed in other cell types (Recalcati et al., 2017). Previous work from this laboratory has demonstrated that the ferroportin/hepcidin axis is expressed and functional in pulmonary artery smooth cells. Moreover, modulation of the axis was shown to cause proliferation of these cells, a known characteristic of PAH. Proliferation was attenuated by the monoclonal antibody (LY2928057), which targets ferroportin, maintaining activity despite the presence of hepcidin (Ramakrishnan et al., 2018b). Other studies have shown that ferroportin was present in and shown to regulate cellular iron locally in cardiomyocytes and further that specific knockdown of ferroportin in these cells resulted in severe impaired cardiac function as compared to ubiquitous hepcidin knockdown, demonstrating that the site of iron accumulation can determine disease severity (Lakhal-Littleton et al., 2015).

The expression of ferroportin in neurovascular cells types of rats has also been demonstrated, however the cellular content of ferroportin varied between cell types. Ferroportin expression in primary astrocytes and pericytes was very low;

in comparison, neurons had x27 and x3 greater expression of ferroportin respectively. Brain capillary endothelial cells (BCECs) had the highest expression of ferroportin, moreover ferroportin expression increased in BCECs when co-cultured with astrocytes (Helgudottir et al., 2020). Ferroportin and hepcidin expression were shown on staining of human brains; moreover, when control brains were compared to those of Alzheimer's disease (AD), the expression of hepcidin and ferroportin were both significantly reduced in diseased brains. Furthermore, hepcidin was expressed in abnormal neuritic process in surviving neurons within amyloid plaques (Raha et al., 2013), an interesting findings with implications for disease onset and progression.

The previous work from this laboratory from our lab and the examples described above demonstrated that the ferroportin/hepcidin has a role in regulating iron homeostasis locally, at least in the cell types highlighted. The main aims of the studies described in this chapter were therefore to explore the presence or otherwise of the hepcidin axis in human pulmonary artery endothelial cells (hPAECs), the modulation of the axis, and the subsequent downstream effects on cell metabolism and fate. The aim is to demonstrate that the ferroportin/hepcidin is expressed on hPAECs and that the axis can be modulated.

Aims

1. To demonstrate or otherwise the expression of hepcidin and ferroportin in hPAECs using qPCR, western blot and confocal imagining techniques.
2. To modulate the ferroportin expression by treating hPAECs with IL-6 (a known hepcidin inducer) and hepcidin itself.

3. To investigate whether both IL-6 and hepcidin treatment leads to hPAECs proliferation.
4. Evaluate the effect of IL-6 and hepcidin on mitochondria function.

3.2 The iron regulatory Ferroportin/hepcidin axis is expressed and modulate in hPAECs

3.2.1 Ferroportin and Hepcidin are expressed in hPAECs

Basal ferroportin and hepcidin mRNA and protein expression is detected in human pulmonary artery endothelial cells (figure 3-1 A and B). Western blot analysis (figure 3-1 C) of hPAECs cell lysates shows basal expression (control) of ferroportin, this was also confirmed by confocal microscopy (figure 3-1 D); ferroportin protein shown in red. ELISA assay analysis reveals hepcidin released from hPAECs (figure 3-2).

3.2.2 The ferroportin/hepcidin axis is modulated in hPAECs

Having established that ferroportin is expressed in hPAECs the next step was to investigate whether the axis could be modulated in hPAECs. In the first instance cells were treated with IL-6 (1 and 10 ng/mL) and hepcidin (0.1 and 1 µg/mL) in order to establish that treaments did not affect cell viability. Alarmar Blue assay (section 2.2.6) was used to this end (see methods section 2.2.6). Cell viability assays were performed by creating 2-fold serial dilution starting at the top concentration (10 ng/mL IL-6; 1 µg/mL hepcidin). The results showed that neither IL-6 (figure 3-3 A) nor hepcidin (figure 3-3 B) affected cell viability after 24 hour treatments.

Once it was determined that IL-6 and hepcidin did not affect cell viability, two concentrations of IL-6 (1 and 10 ng/mL) and hepcidin (0.1 and 1 µg/mL), were selected for further studies, being representative of the ranges of concentrations observed during disease processes (Baran et al., 2018, Taheri et al., 2015, Oustamanolakis et al., 2011).

Treatment of hPAECs with IL-6 (10 ng/mL) and hepcidin 1 µg/mL) for 3 hours significantly decreased ferroportin (gene SLC40A1) mRNA expression (figure 3-2 A and B), real-time analysis was performed as described in section 2.5. Furthermore, western blot analysis (figure 3-2) of hPAEC lysates showed reduced expression of ferroportin following treatment with IL-6 (10 ng/mL) and hepcidin (0.1 and 1 µg/mL). Western blot analysis is described in section 2.6. Immunofluorescence demonstrated cell surface localisation of ferroportin in unstimulated cells (figure 3-2 D upper panel); hepcidin treatment (1 µg/mL) caused a visual decrease of fluorescence intensity (figure 3.2 D bottom panel), however IL-6 did not show the same effect (figure 3-2 D middle panel).

To establish whether hPAECs also express hepcidin, cells were stimulated with IL-6 (1 and 10 ng/mL), a known positive regulator of hepcidin expression. Hepcidin mRNA transcription (*HAMP*) significantly increased by 6.9-fold after IL-6 (10 ng/mL) stimulation for 2 hours (figure 3-3 A). Hepcidin secretion into cell supernatants was also significantly increased after 24h treatments with IL-6 (1 and 10 ng/mL; figure 3-3 B). Methods described in section 2.7.

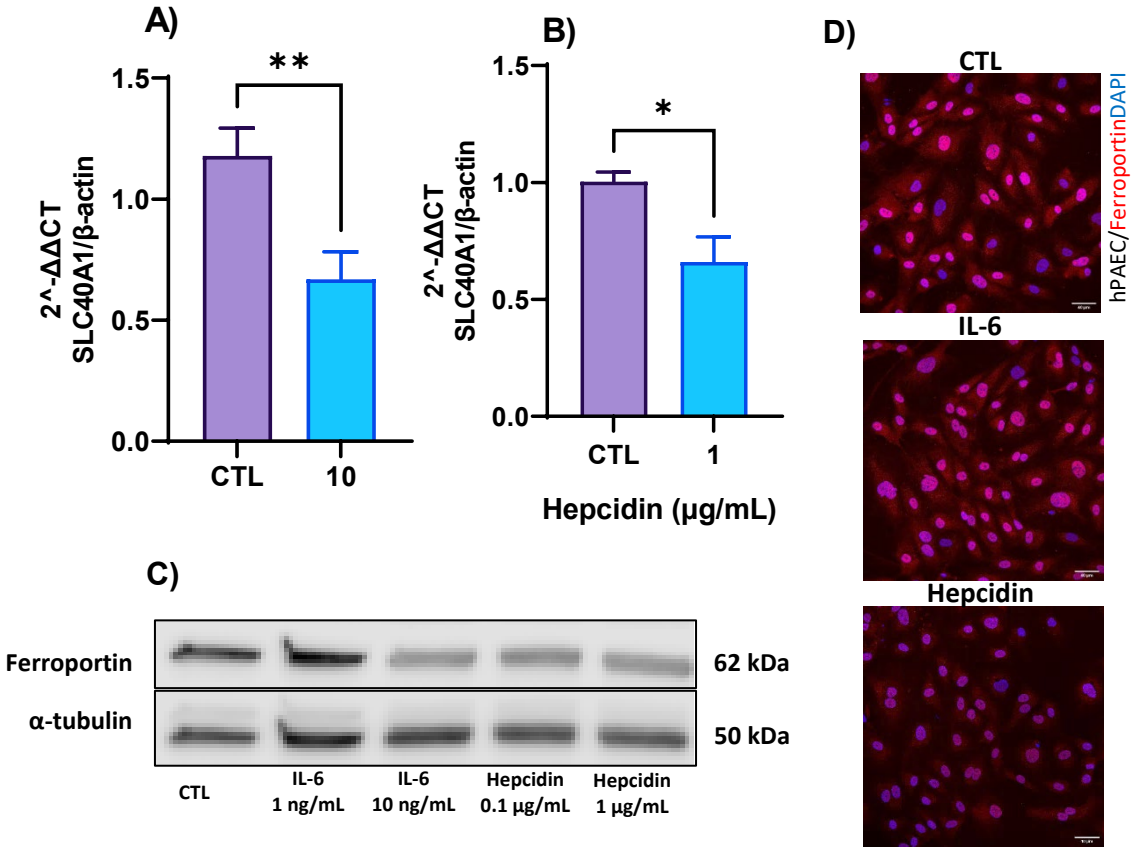

Figure 3-1 The iron exporter ferroportin is expressed in hPAECs. ***(A, B)*** *ferroportin mRNA transcription after IL-6 and hepcidin treatment for 2 hours. Real-time PCR analysis was performed as described in section 2.4. Data shown are mean ±SEM n=6. Unpaired t-test was performed. *p<0.05; **p<0.01.* ***(C)*** *Western blot analysis of ferroportin protein expression after IL-6 and Hepcidin treatments for 24 hours. Western blot assay was performed as described in section 2.5 (n=1).* ***(D)*** *Immune fluorescence image showing the expression of ferroportin on hPAECs. Top panel cells treated with media alone; middle panel cells treated with 10 ng/mL IL-6; bottom panel cells treated with 1 µg/mL hepcidin (n=1). Immune-fluorescence was performed as described in 2.3.2.3.*

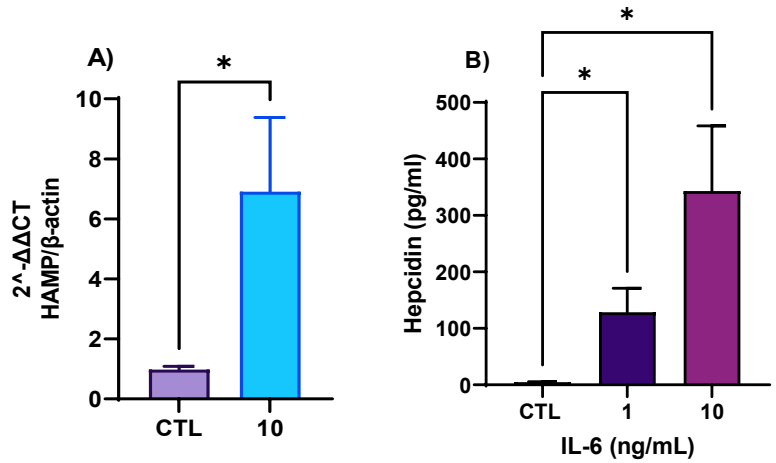

Figure 3-2 The iron hormone hepcidin is expressed in hPAECs. *(A) Hepcidin mRNA transcription in hPAECs after IL-6 stimulation for 2 hours. Real-time PCR analysis was performed as described in section 2.4. Data shown are mean ±SEM n=6. Unpaired t-test was performed. *p<0.05; **p<0.01. (B) Hepcidin release into hPAEC supernatants after 24 hours stimulation with IL-6. hPAECs supernatant s were analysed by ELISA as described in section 2.6. Data shown are mean ±SEM n=6. Kruskal-Wallis test followed by Dunn's post hoc test were performed *p<0.05.*

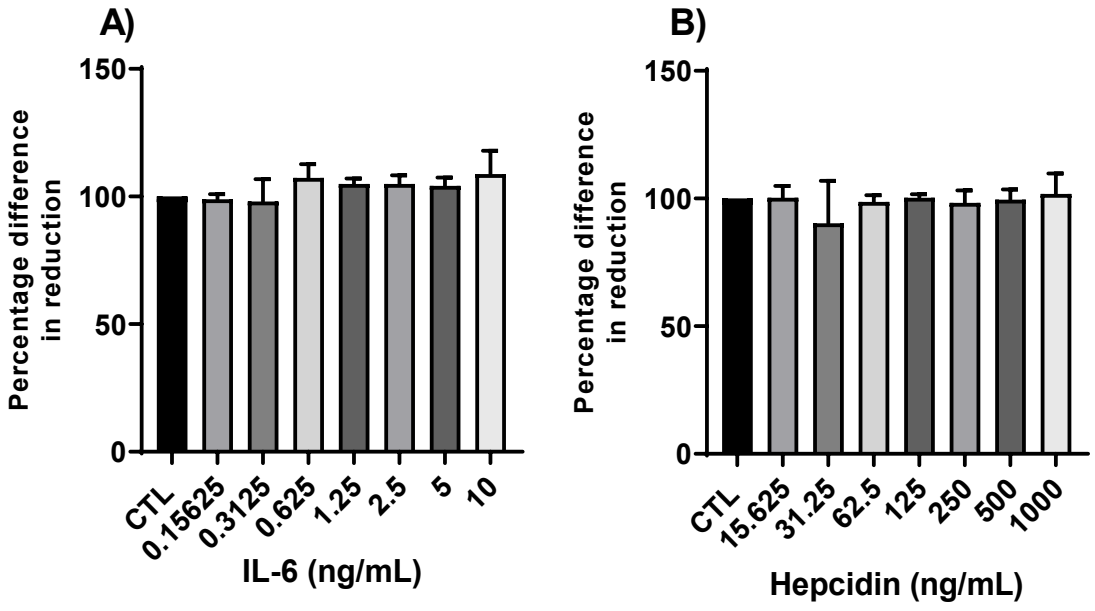

Figure 3-3 IL-6 (A) and hepcidin (B) treatments do not affect hPAECs viability*. Cell viability was determined by the Alamar Blue assay and the assay was performed as described in section 2.2.6. Data is shown as mean ±SEM, n=3.*

3.2.3 Hepcidin stimulates the release of IL-6 and hepcidin in hPAECs

Following hepcidin treatment, the potential for expression of the IL-6 cytokine was also investigated analysed. The results showed an increased in IL-6 mRNA transcription after 5h treatment with hepcidin (figure 3-4 A) (see methods section 2.5). Analysis of hPAECs supernatants by ELISA detected significantly increased levels of IL-6 release after 24h (figure 3-4B) (see methods section 2.7). Subsequently, hepcidin mRNA expression and released was analysed after hPAEC stimulation with hepcidin. Transcription of hepcidin mRNA was significantly increased after 1 hour and 24 hours treatments (figure 3-5 A and B). Hepcidin peptide release from hPAECs significantly increased after treatment with hepcidin (0.1 and 1 µg/mL; figure 3-5 C).

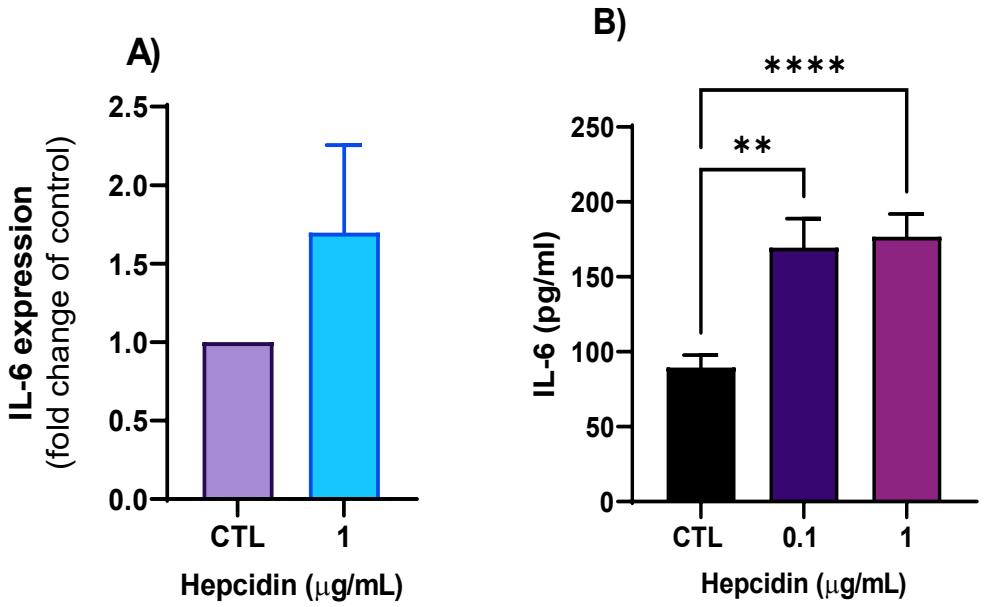

Figure 3-4 hPAECs release IL-6 after hepcidin treatment. *(A) IL-6 mRNA transcription in hPAECs after hepcidin stimulation for 5 hours. Real-time PCR analysis was performed as described in section 2.4. Data shown are mean ±SEM n=6. (B) IL-6 release into hPAECs supernatants after 24 hours stimulation with hepcidin (0.1, 1 µg/mL). hPAECs supernatant s were analysed by ELISA as described in section 2.6. Data shown are mean ±SEM n=12.Kruskal-Wallis test followed by Dunn's post hoc test were performed *p<0.01; ****p<0.0001.*

An additional control was incorporated in order to monitor hepcidin longevity under experimental conditions. Therefore, at the same time as the cells treatments were undertaken, additional wells containing only the media alone but and also including hepcidin with treatment without a cell interface were incubated for the same period of time as the cells were treated. ELISA results showed that in wells that contained the 0.1 µg/mL hepcidin concentration, after 24 hours incubation, hepcidin could not be detected. In addition, The wells containing media with 1 µg/mL hepcidin concentration showed a ~100 fold reduction in hepcidin detected by the ELISA assay (figure 3-5 C; no cells) (see methods section 2.7). Results indicate that hepcidin is not a long lived peptide under experimental conditions used for these studies.

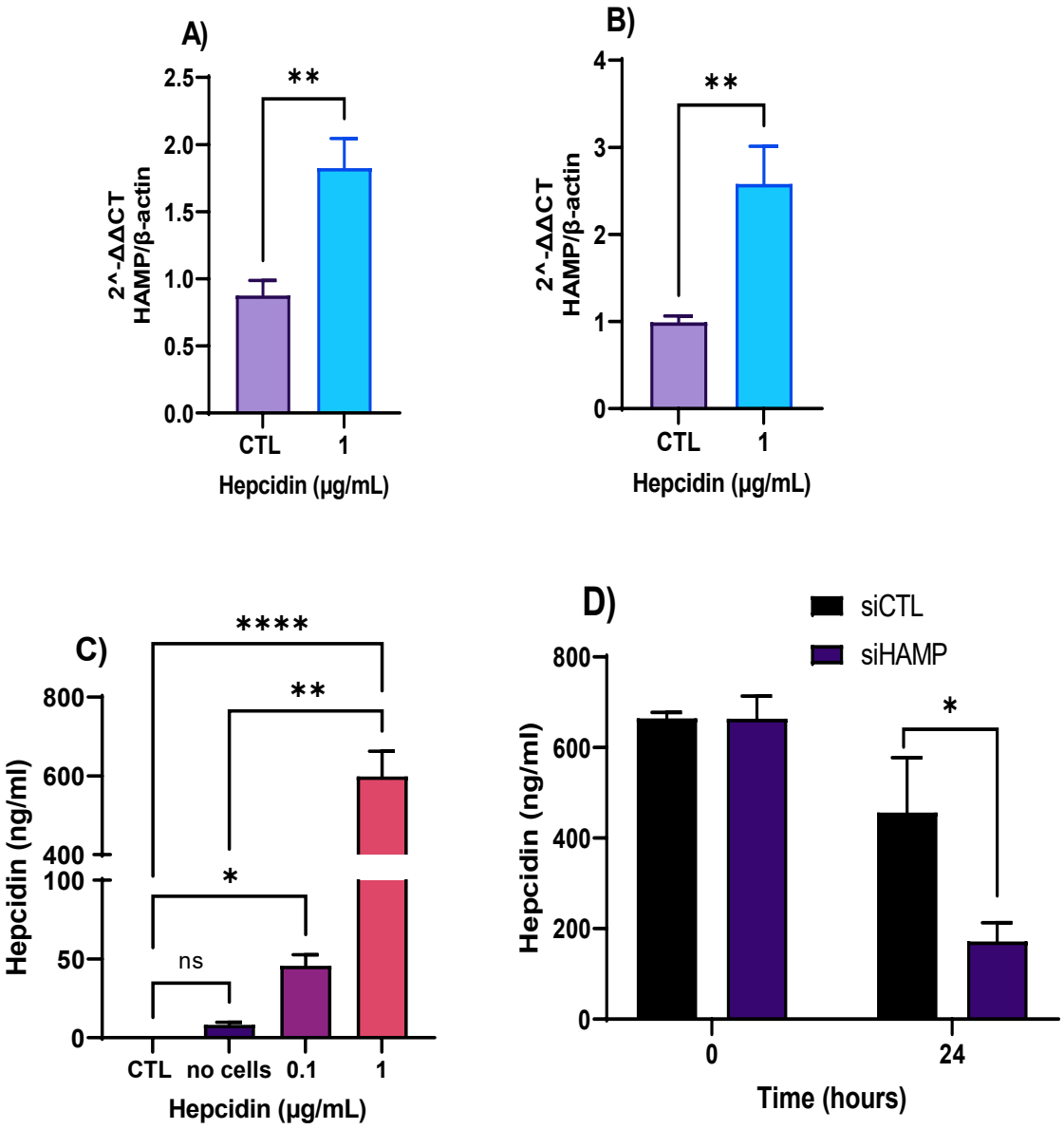

Figure 3-5 Hepcidin stimulates the release of IL-6 and hepcidin in hPAECs. (A, B) *hepcidin mRNA transcription from hPAECs after treatment with hepcidin for 1 (A) and 24 (B) hours. Real-time PCR analysis was performed as described in section 2.4. Data shown are mean ±SEM n=6. Unpaired t-test was performed **p<0.01.* ***(C)*** *Hepcidin release into the supernatants of hPAECs after 24 hours treatment with hepcidin. hPAECs supernatants were analysed by ELISA as described in section 2.6. Data shown are mean ±SEM n=12. Kruskal-Wallis test followed by Dunn's post hoc test were performed *p<0.05.* ***(D)*** *Hepcidin release is decreased by its knockdown. Hepcidin knockdown was performed as described in section 2.2.7. hPAECs supernatants were analysed by ELISA as described in section 2.6. Data shown are mean ±SEM n=3. Kruskal-Wallis test followed by Dunn's post hoc test were performed *p<0.05.*

To investigate further whether the hepcidin being detected is newly synthesised by hPAECs when stimulated by hepcidin, hepcidin gene (*HAMP*) knockdown was carried out (see methods in section 2.2.7). After 24h hours of knockdown, hPAECs were treated with 1 µg/mL hepcidin both on control and knockdown cells for 24 hours. Supernatants were then analysed by ELISA. The results demonstrated a significant decrease in hepcidin detected compared to siCTL, a 2.65-fold reduction (figure 3-5 D). There were no changes on the amount of hepcidin detected on both siCTL and knockdown. Along with the labile nature of hepcidin described above these studies further demonstrate that hepcidin detected in the cell supernatants are likely to be newly synthesised peptides, produced by hPAECs rather than residual hepcidin treatments.

3.2.4 IL-6 causes hPAECs to proliferate

Interleukin-6 (IL-6) is a pro-inflammatory cytokine that has a crucial role in the inflammatory response, immunological regulation and haemopoietic responses. IL-6 has also been shown to regulate cell proliferation, for example IL-6 augmented proliferation of human cerebral endothelial cells, blood outgrowth endothelial cells, peri-tumoral endothelial cells and human mesenchymal stromal cells (Dorronsoro et al., 2020, Fan et al., 2008, Yao et al., 2006).

To determine whether IL-6 stimulated hPAECs, BrdU and MTS assays were performed. hPAECs were plated in triplicate on a 96-well plate (see methodology in section 2.4.2). Cells were starved overnight and treated with two different concentrations of IL-6 for 24 hours. The results of both assays showed that IL-6 significantly induced proliferation of hPAECs of both assays shows that IL-6 significantly induced proliferation of hPAECs, BrdU incorporation increasing by 30% (figure 3-6 A). The proliferation increase shown by the MTS assay was modest increasing by 10% (figure 3-6 B).

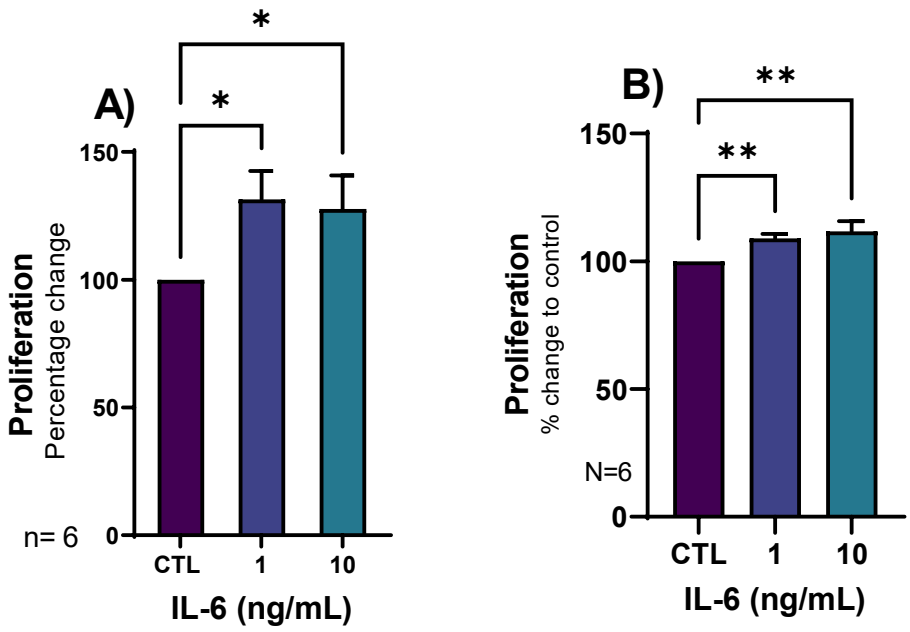

Figure 3-6 IL-6 induces hPAEC proliferation after 24 hours stimulation. (A, B) *hPAEC proliferation measured by BrdU assay and MTS assay (B) after 24 hours treatment with IL-6. Assays were performed as described in section 2.3. Data shown are mean ±SEM n=6. Kruskal-Wallis test followed by Dunn's post hoc test were performed *p<0.05; **p<0.01.*

3.2.5 Hepcidin does not affect hPAECs proliferation

Previous work by our group has demonstrated that hepcidin significantly increased hPASMCs proliferation (Ramakrishnan et al., 2018b). Therefore, the next step was to investigate whether hepcidin also caused hPAEC proliferation.

Experiments were carried out in the same manner as for IL-6; hPAECs were treated with two concentrations of hepcidin (0.1 and 1 µg/mL). Both BrdU and MTS assays showed that neither hepcidin concentrations used had any effect on hPAEC proliferation (Figure 3-7 A and B).

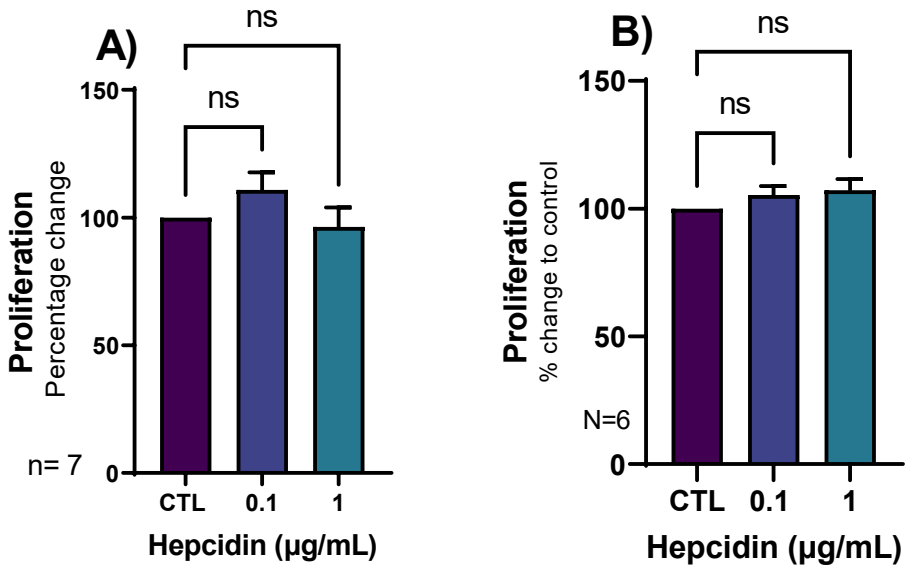

Figure 3-7 Hepcidin does not affect hPAEC proliferation. (A, B) *hPAEC proliferation measured by BrdU assay and MTS assay (B) after 24 hours treatment with hepcidin. Assays were performed as described in section 2.3. Data shown are mean ±SEM n=6.*

3.2.6 IL-6 and Hepcidin increases the release of IL-8 and MCP-1

Investigations were then undertaken to determine whether the cytokine interleukin-8 (IL-8) and the chemokine monocyte chemoattractant protein-1 (MCP-1) are released when hPAEC are treated with either IL-6 or hepcidin. These two molecules are known to stimulate cell proliferation and migration (Ning et al., 2011, Viedt et al., 2002). After 24 hours treatment with either IL-6 (1 and 10 ng/mL) or hepcidin (0.1 and 1 µg/mL), cell supernatants were then analysed by ELISA (see methods in section 2.7). Stimulation of hPAECs with IL-6 or hepcidin significantly increased MCP-1 release with both concentrations of each

of the treatments used (figure 3-8 A and B). IL-8 release in hPAECs increased in a dose-dependent manner for both IL-6 and hepcidin, reaching significance at the higher concentration of IL-6 (10 ng/mL) and hepcidin (1 µg/mL) (figure 3-8 C and D). Concentrations of IL-6 and hepcidin were selected to follow our previous published paper (Ramakrishnan et al., 2018b).

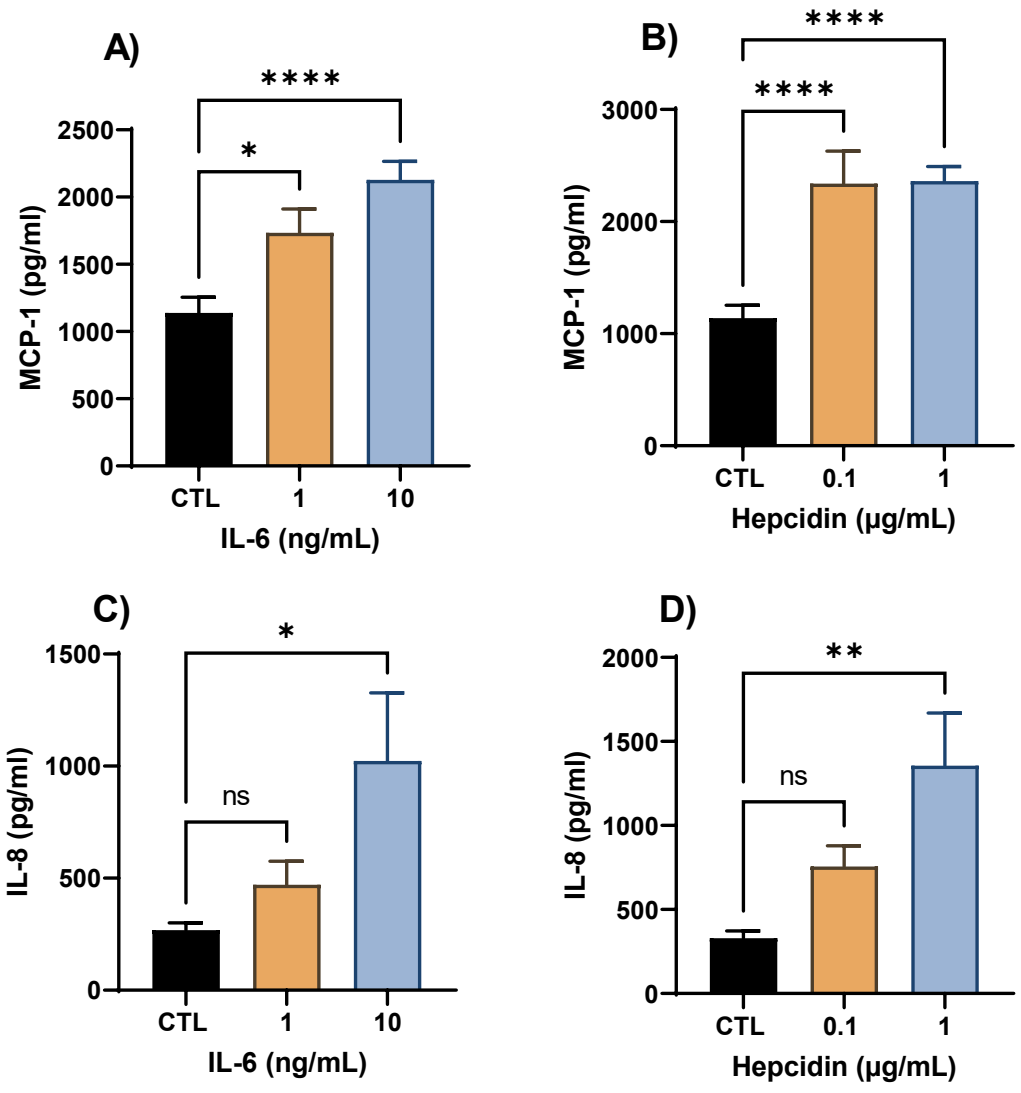

Figure 3.8 IL-6 and hepcidin increases the release of IL-8 and MCP-1 after 24 hours stimulations. *(A, B) MCP-1 release in hPAECs supernatants after 24 hours stimulation with IL-6 (A) and hepcidin (B). IL-8 release in hPAECs supernatants after 24 hours stimulation with IL-6 (C) and hepcidin (D).ELISA analysis was performed as described in section 2.6. Data shown are mean ±SEM n=12. Kruskal-Wallis test followed by Dunn's post hoc test were performed *p<0.05; **p<0.01; ****p<0.0001.*

3.2.7 IL-6 and hepcidin does not affect mitochondria function in hPAECs

Mitochondrial dysfunction has been suggested to contribute to the pathogenesis of PAH (Marshall et al., 2018). Previous work from this laboratory, demonstrated that IL-6 and hepcidin treatment of hPASMC caused mitochondria network fragmentation, reduction in mitochondrial volume and increased mitochondrial ROS production. By contrast, hPAEC only exhibited reduction in mitochondrial volume (Issitt and Toe, 2018). To further investigate whether IL-6 and hepcidin can impair mitochondrial function, analysis of mitochondrial membrane potential ($\Delta\psi$) using TMRM (tetramethylrhodamine methyl ester) assay was undertaken (method section 2.9.4). This assay detects changes in mitochondrial membrane potential, whereas in a healthy cell with active mitochondria TMRM is readily up taken emitting a red-orange signal, but when the mitochondrial membranes are depolarised the TMRM signal is reduced.

Following, 24 hours treatment with IL-6 (10 ng/mL) and hepcidin (0.1 and 1 µg/mL), hPAECs were incubated with TMRM dye for 30 minutes at 37^{o}C. Cells were then trypsinized and TMRM fluorescence was analysed by flow cytometry. Carbonyl cyanide chlorophenylhydrazone (CCCP) was used as positive control; CCCP it is known to induce mitochondria damage, therefore reducing membrane potential (methods in section 2.9.4). The experiments demonstrated that both IL-6 and hepcidin did not affect mitochondrial membrane potential (figure 3-9 A and B), further confirming previous results where it was established that neither IL-6 nor hepcidin caused mitochondrial dysfunction in hPAECs (Issitt et al., 2019).

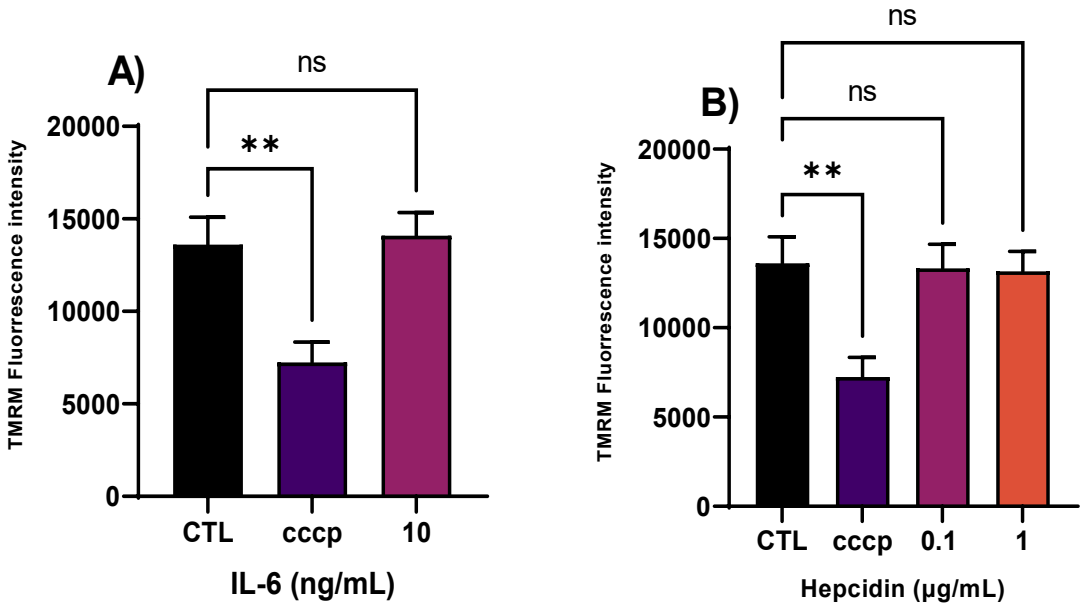

Figure 3-9 IL-6 (A) and Hepcidn (B) does not affect hPAEC mitochodria membrane potential. *Mitochondrial membrane potential was determine by the TMRM assay as described in section 2.8.4. Data are shown ±SEM n= 5. Kruskal-Wallis test followed by Dunn's post hoc test were performed; **p<0.01.*

In addition to TMRM, a more in-depth examination of mitochondrial function was undertaken by use of the seahorse assay. This assay is the gold standard for measuring mitochondrial function in cells. hPAECs were plated in triplicate wells in a 96-well plate, cells were then starved overnight and then treated with IL-6 (1 and 10 ng/mL) or hepcidin (0.1 and 1 µg/mL) for 24 hours. Analysis of results demonstrated that IL-6 treatments only had a modest effect on mitochondrial function. IL-6 significantly increased the spare respiratory capacity of hPAECs, and significantly decreased proton leak in these cells (figure 3-9) (methods in section 2.8).

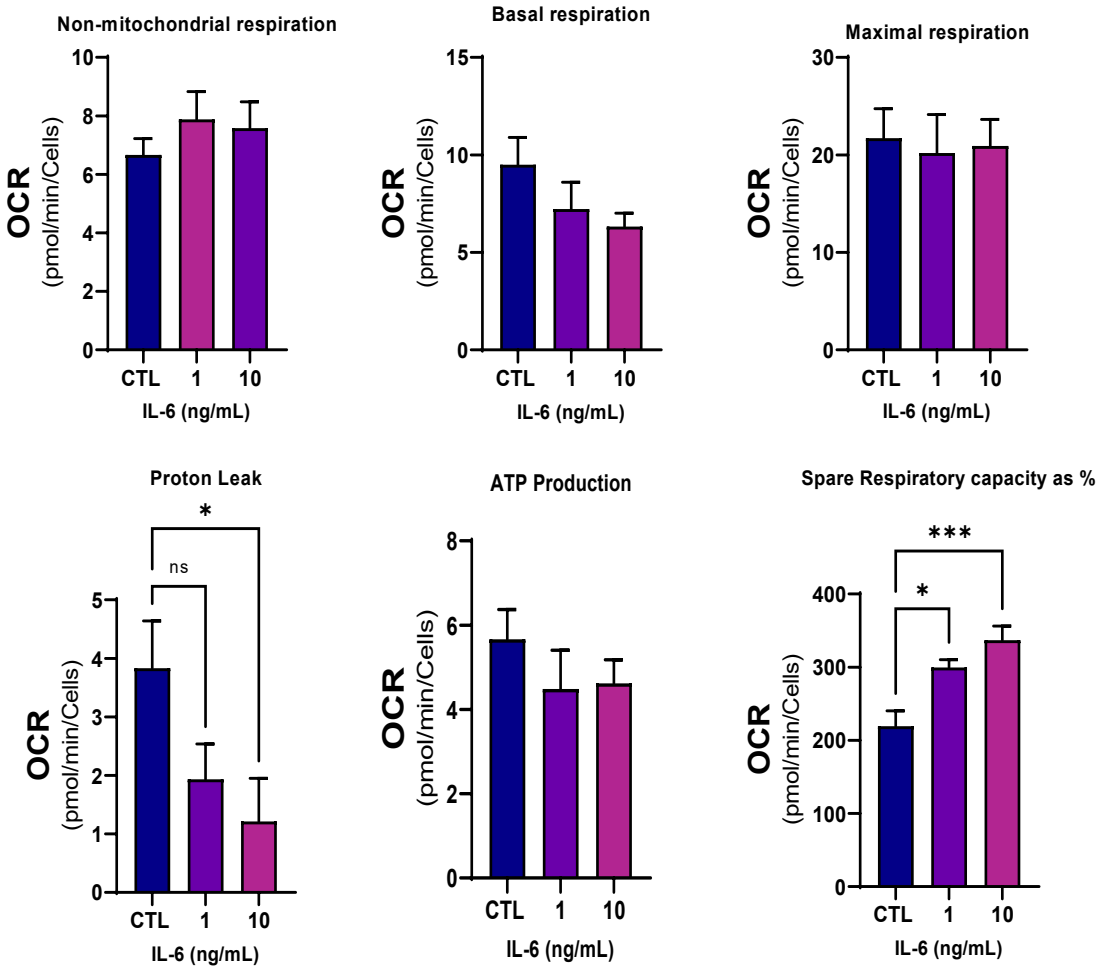

Figure 3-20 IL-6 effect on hPAEC mitochondria metabolism. *Oxygen consumption rate (OCR) was determined by the seahorse XF analyser mito stress assay as descrbed in section 2.7. Data are shown ±SEM n= 6. One-way ANOVA test followed by Dunnett's post hoc test were performed * p<0.05; ***p<0.001.*

Hepcidin similarly to IL-6 did not affect mitochondria function (figure 3-10). Even though not significant, there is a trend for increase in maximal respiration and ATP production (figure 3-11).

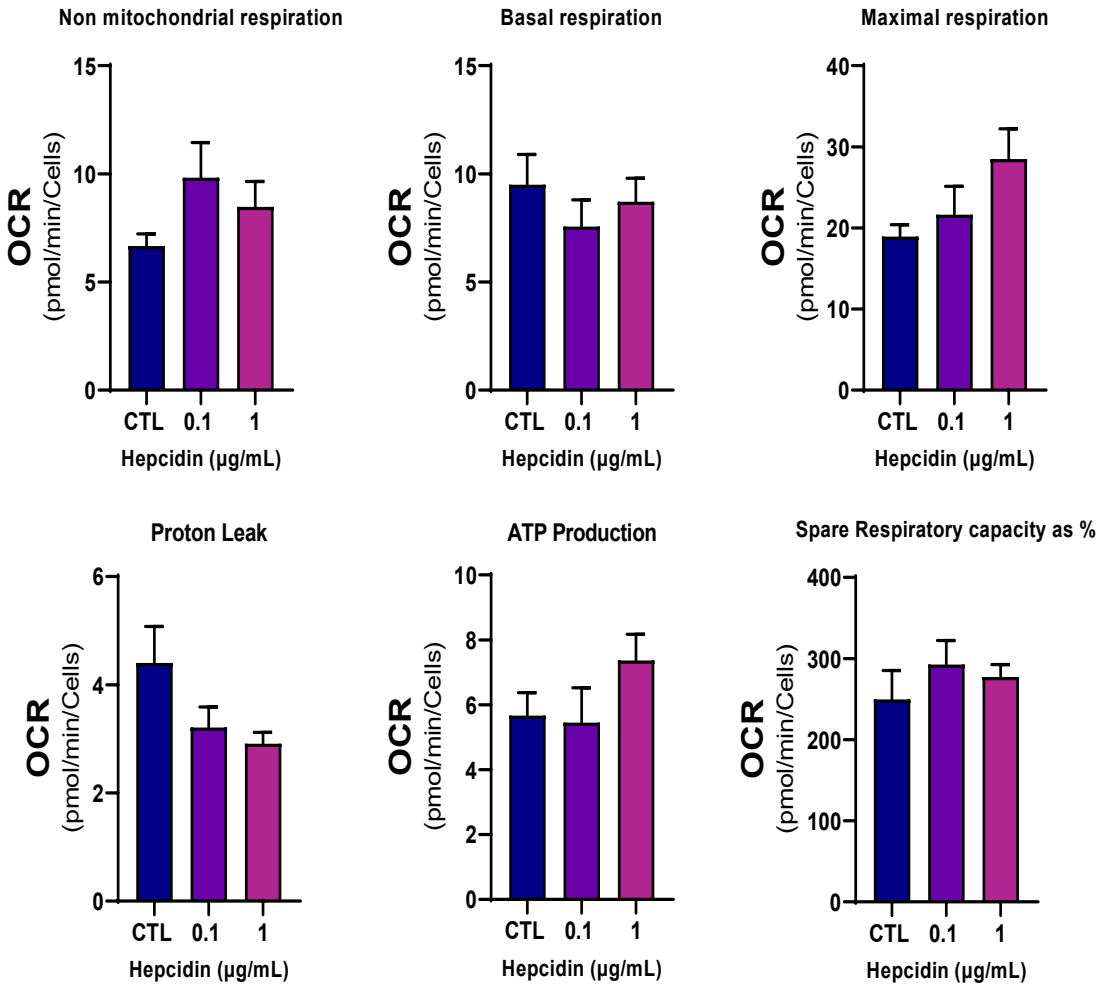

Figure 3-11 Hepcidin effect on hPAEC mitochondria metabolism. *Oxygen consumption rate (OCR) was determined by the seahorse XF analyser Mito stress assay as descrbed in section 2.7. Data are shown ±SEM n= 6.*

3.3 Summary and limitations

3.3.1 Summary

The main aim of this chapter was to demonstrate that the ferroportin/hepcidin axis is expressed and modulated in human pulmonary artery endothelial cells (hPAECs). The results described in this chapter show that in using varied experimental approaches, both ferroportin and hepcidin are expressed in these cells. Treatments with IL-6 (a known hepcidin agonist) and hepcidin caused ferroportin internalisation and degradation (figure 3-2). IL-6, as expected, increased the release of hepcidin in these cells (figure 3-3), demonstrating that the axis is modulated in hPAECs. Furthermore, hepcidin treatment resulted in increased IL-6 release (figure 3-4) and hepcidin release in an autocrine manner (figure 3-5). Manipulation of the axis by hepcidin elevated the release of the cytokines IL-8 and MCP-1 (figure 3-8). Hepcidin did not affect hPAECs proliferation, which contrasts with previous work by our group that showed hPASMCs proliferation after hepcidin treatments (Ramakrishnan et al., 2018b). Moreover, the results in this chapter show that hepcidin does not affect mitochondria function (figures 3-9B and 3-11), again contrasting with hPASMCs in which mitochondria function is vastly affected by hepcidin (Issitt and Toe, 2018). These results confirm that the ferroportin/hepcidin axis is present in hPAECs, furthermore manipulation of axis elicits a different response between cells that form the pulmonary artery wall (a more detailed discussion of the results of this chapter within the context of the entire thesis can be found in chapter 7).

3.3.2 Limitations

The results in this chapter are important, however there are limitations to be considered. Firstly, most of the studies were performed only for 24 hours which shows acute responses, however, it would be of value to examine a chronic response of hepcidin in these cells. Secondly, it was not possible to determine if there was iron retention within cells as none of the assays tested were sensitive enough measure iron retained within the cytoplasm, this is an important step to determine stronger evidence of disrupted iron homeostasis in the pulmonary vasculature. The mitochondria studies shown in this chapter were somewhat hampered due to the inadequate optimisation of cell number and drugs titration. This was mostly due to limited access to the seahorse analyser which only accommodated a 16-well format. Therefore, as it would have required excessive time to test all the parameters necessary for complete optimisation, a more selective approach was undertaken. Recently, a 96-well seahorse analyser has become available, and more detailed analyses are underway. Despite these shortfalls, the results obtained here correspond with previous work performed by this laboratory, which demonstrate that hPAECs mitochondria are not greatly affected by hepcidin, as compared with mitochondria in hPASMCs (Issitt and Toe, 2018).

4. Chapter 4 – Potential effects on BMPR2 protein expression by IL-6 or hepcidin treatment.

4.1 Rationale

The most common familial mutation related to heritable PAH is on the gene encoding the bone morphogenetic protein receptor type 2 (BMPR2). BMPR2 is part of the transforming growth factor-β (TGF-β) superfamily of signalling molecules. Following the identification of the familial link to BMPR2 mutations, subsequent studies on IPAH patients provided independent validation of the pathogenic variation in a subset of these patients, BMPR2 mutations account for 53-86% of familial PAH cases and 14-35% IPAH patients (Southgate et al., 2020). Interestingly, patients without mutations in BMPR2 have diminished downstream signalling (Dannewitz Prosseda et al., 2020). Moreover, many patients with BMPR2 mutation never develop disease due to incomplete penetrance (Larkin et al., 2012). Therefore, a better understanding of how BMPR2 functions in cells involved in the pathobiology of PAH is needed to unravel these confounding factors.

BMPR2 is a “type 2” member of the TGF-β superfamily of receptors, which requires a “type 1” co-receptor to for a heterotetrametric complex to transduce signals in response to ligand binding. There are four type 1 receptors: activating receptor like kinase 1(ALK1), BMPR-1A (ALK3), BMPR-1B (ALK6), and ActR-1A (ALK2). There are two “type 2“receptors: BMPR2 (ActRIIA) and ActRIIB. Once, the heterotetrametric complex is formed and a ligand binds to the complex, the “type 2” receptor phosphorylates the “type 1” receptor which then phosphorylates signal transduction targets. The canonical pathway R-SMAD protein is phosphorylated (typically SMAD 1/5/8), which then forms a complex with a co-SMAD (usually SMAD4), this complex then enters the nucleus and bind to a BMP

response element DNA sequence (BRE). Once the complex is bound to BRE it promotes the expression of transcription factors such as inhibitor of DNA binding 1, 2, 3 and 4 (ID1, ID2, ID3 and ID4). These transcription factors have effects on cell migration, proliferation, and apoptosis (Andruska and Spiekerkoetter, 2018).

4.1.1 Aims

To assess the potential of known regulators (IL-6 and hepcidin) of the hepcidin/ferroportin axis to influence changes of hPAEC BMPR2 expression.

1. To determine levels of BMPR2 mRNA and protein expression following treatments with IL-6 or hepcidin
2. To investigate changes in signalling downstream of BMPR2

4.2 Both IL-6 and hepcidin causes reduction of BMPR2 expression in hPAECs

4.2.1 IL-6 and hepcidin cause downregulation of BMPR2 mRNA in hPAECs

To determine whether IL-6 and hepcidin affects the mRNA expression in hPAECs, cells were treated with IL-6 (10 ng/mL) and hepcidin (1 µg/mL). As expected, IL-6 (Brock et al., 2009) caused downregulation of BMPR2 mRNA compared to untreated cells (figure 4.1 A). In a similar fashion, hepcidin treatment significantly decreased BMPR2 mRNA transcription (figure 4.1 B). Methodology used described in section 2.5.

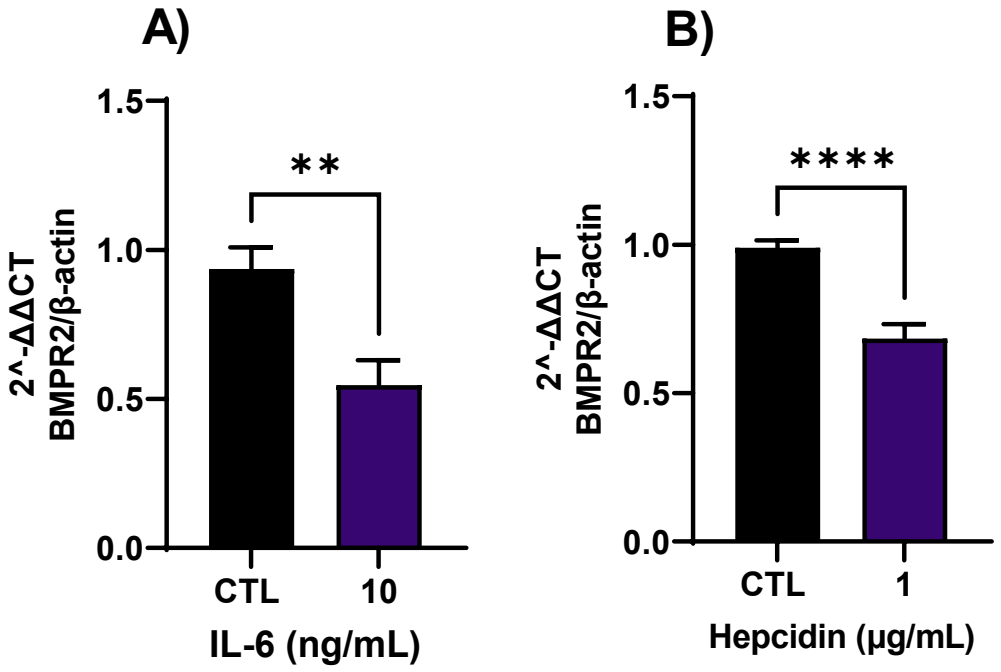

Figure 4-1 hPAECs BMPR2 mRNA transcription after 24h treatment with IL-6 (A) and hepcidin (B). *Real-time PCR analysis was performed as described in section 2.4. Data shown are mean ±SEM n=6. Unpaired t-test was performed **p<0.01;****p<0.0001.*

4.2.2 IL-6 and hepcidin cause reduction in BMPR2 protein

To investigate if the downregulation of BMPR2 messenger RNA is reflected in protein expression, cell lysates were analysed by western blot after 24h treatment with either IL-6 (1 and 10 ng/mL) or hepcidin (0.1 and 1 µg/mL). Western blot image analysis (figure 4.2 A) demonstrated that both IL-6 and hepcidin reduce BMPR2 protein expression. Densitometry analysis of the western blot bands showed significant BMPR2 protein reduction after 24h treatment with IL-6 (10 ng/mL) and hepcidin (1 µg/mL) compared to untreated controls (figure 4.2 B and C) (methodology used described in section 2.6)

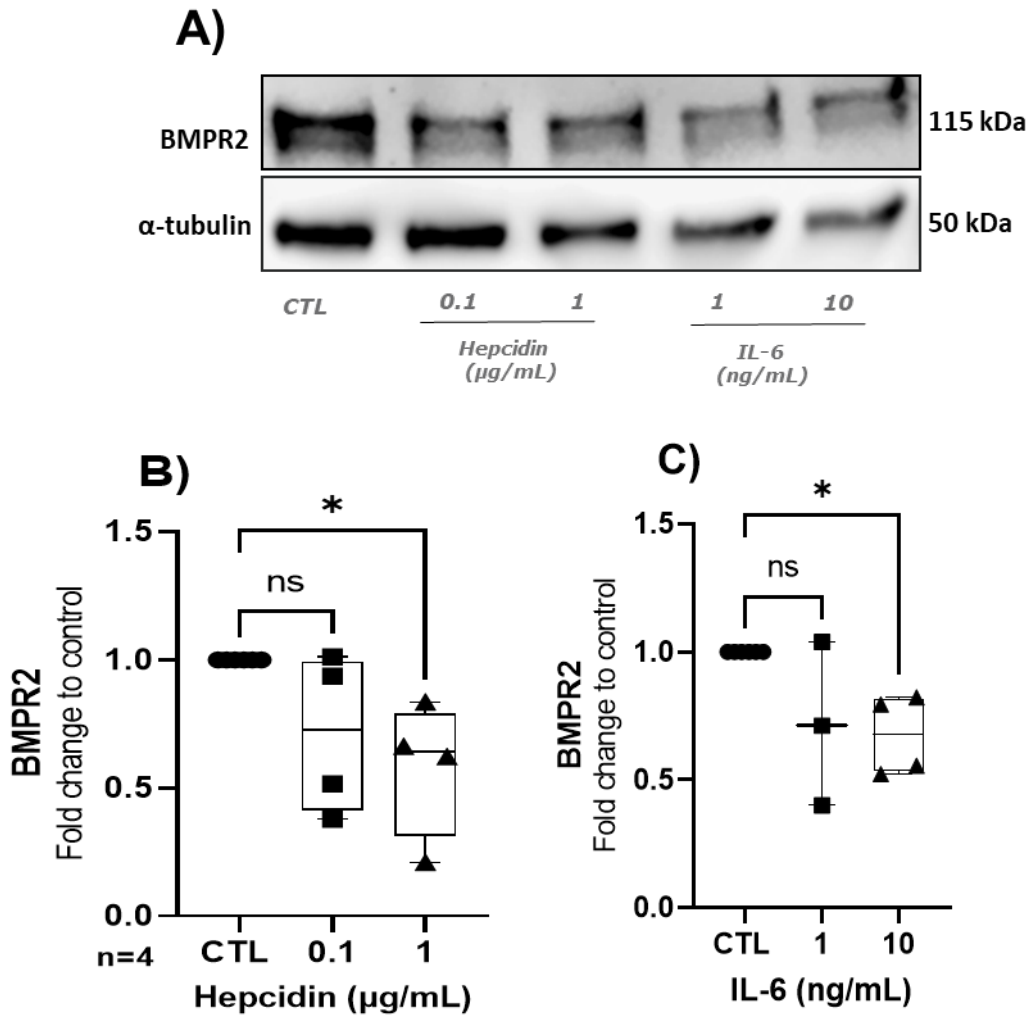

Figure 4-2. Both IL-6 and hepcidin causes reduction of BMPR2. *(A) Western blot image of BMPR2 expression on hPAECs treated with hepcidin and IL-6. BMPR2 western blot bands relative density of hPAECs treated with hepcidin (B) and IL-6 (C) compared to untreated control. Data shown are mean ±SEM n=4. Kruskal-Wallis test followed by Dunn's post hoc test were performed *p<0.01; *p<0.05.*

4.2.3 Signalling downstream of BMPR2 is active despite reduction of proteins expression

The R-SMAD proteins are the main signal transducers for the receptors of the TGF-β family of receptors. To determine if the reduction of BMPR2 protein caused by hepcidin also affected downstream signalling of BMPR2 via the R-SMAD proteins, an investigation of protein expression and phosphorylation (activation) of SMAD1 and SMAD5 was undertaken by western blot. hPAECs were serum starved overnight, cells were treated with hepcidin (1 μg/mL) at different time points, 30 minutes, 1 hour and 2 hours. Cell lysates were separated by SDS-page gel and transferred to a nitrocellulose membrane and incubated with phosphorylated anti-SMAD1/5 antibody. Results showed that SMAD1/5 phosphorylation significantly increased after 30 minutes (figure 4.3 A) and was subsequently significantly reduced by 1 hour and 2 hours after treatments (figure 4.3 A). SMAD1/5 phosphorylation was significantly increased after 24 hours treatment with IL-6 (10 ng/mL) and hepcidin (0.1 and 1 μg/mL). Methodology used described in section 2.6.

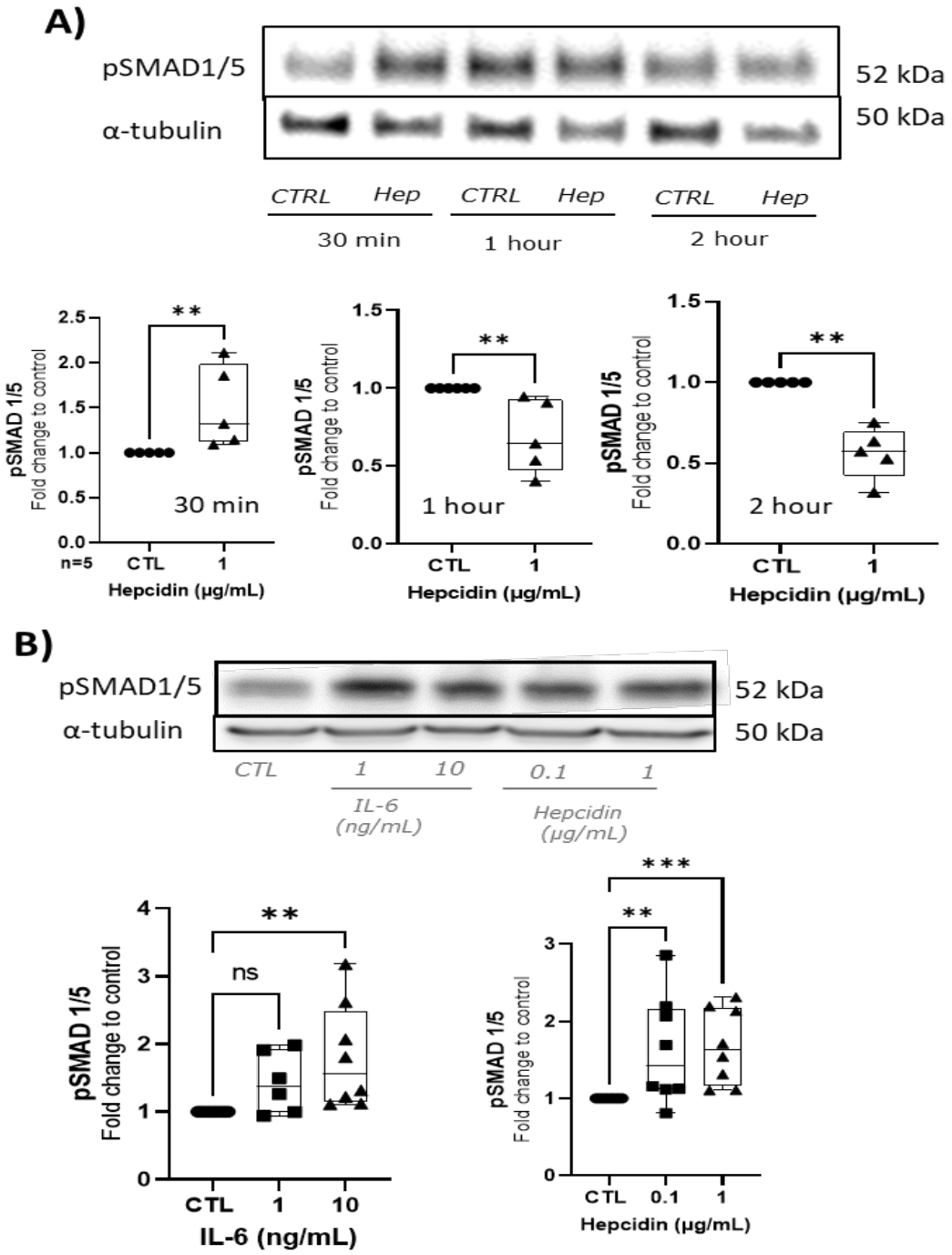

***Figure 4-3 SMAD1/5 is phosphorylated after hepcidin treatment**. **A)** Western blot image and densitometry analysis of pSMAD1/5 phosphorylation expression time course after treatment with 1 µg/mL hepcidin. Data shown are mean ±SEM n=5. Kruskal-Wallis test followed by Dunn's post hoc test were performed **p<0.01. **B)** Western blot image and densitometry analysis of pSMAD1/5 phosphorylation expression 24 hours after treatment with IL-6 (1 and 10 ng/mL) and hepcidin (0.1 and 1 µg/mL). Data shown are mean ±SEM n=5. Kruskal-Wallis test followed by Dunn's post hoc test were performed **p<0.01.*

The canonical signalling pathway of the heterotetrametric complex formed by a type 1 receptor and BMPR2, a type 2 receptor, leads to the expression of transcription factors ID1, ID2, ID3 and ID4. Therefore, an investigation of whether these downstream signalling events were influenced by either IL-6 or hepcidin treatment was undertaken. Results confirmed that downregulation of BMPR2 by IL-6 or hepcidin also caused an increase expression of these transcription factors. mRNA analysis by qPCR showed a significant increase of ID1 (1.97 fold) and ID3 (1.36 fold) transcription after 3 hours treatment with hepcidin (figure 4.4 A and C).

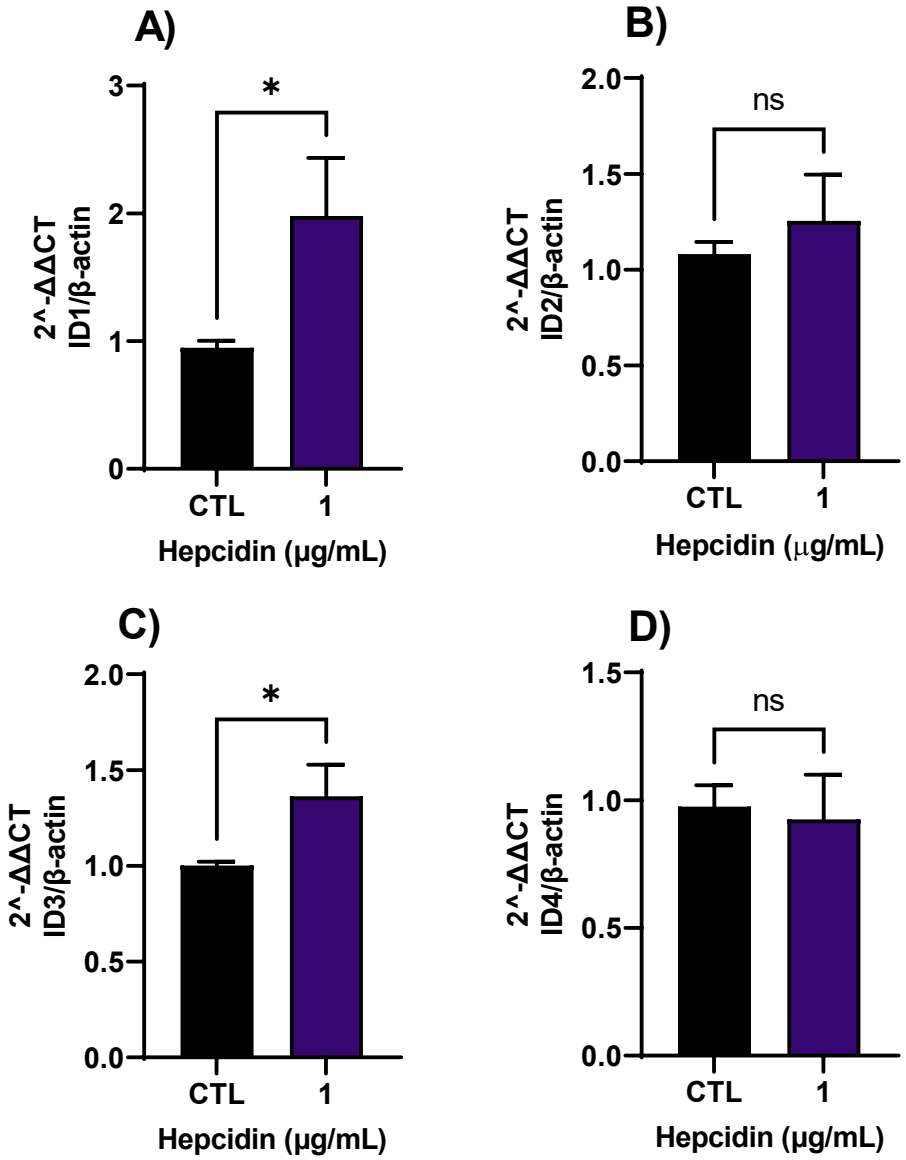

Figure 4-4 mRNA transcription of the BMPR2 downstream targets *ID1(A), ID2 (C), ID3 (C) and ID4 (D) after hepcidin treatment for 3 hours. Real-time PCR analysis was performed as described in section 2.4. Data shown are mean ±SEM n=6. Unpaired t-test was performed *p<0.05.*

Similarly, hPAECs treatment with IL-6 (10 ng/mL) caused a significant increase in mRNA transcription of ID1 (1.62 fold), ID2 (2.24 fold), ID3 (2.17 fold) and ID4 (2.08 fold) transcription factors (figure 4.5) after 3 hours treatments (methodology used described in section 2.5).

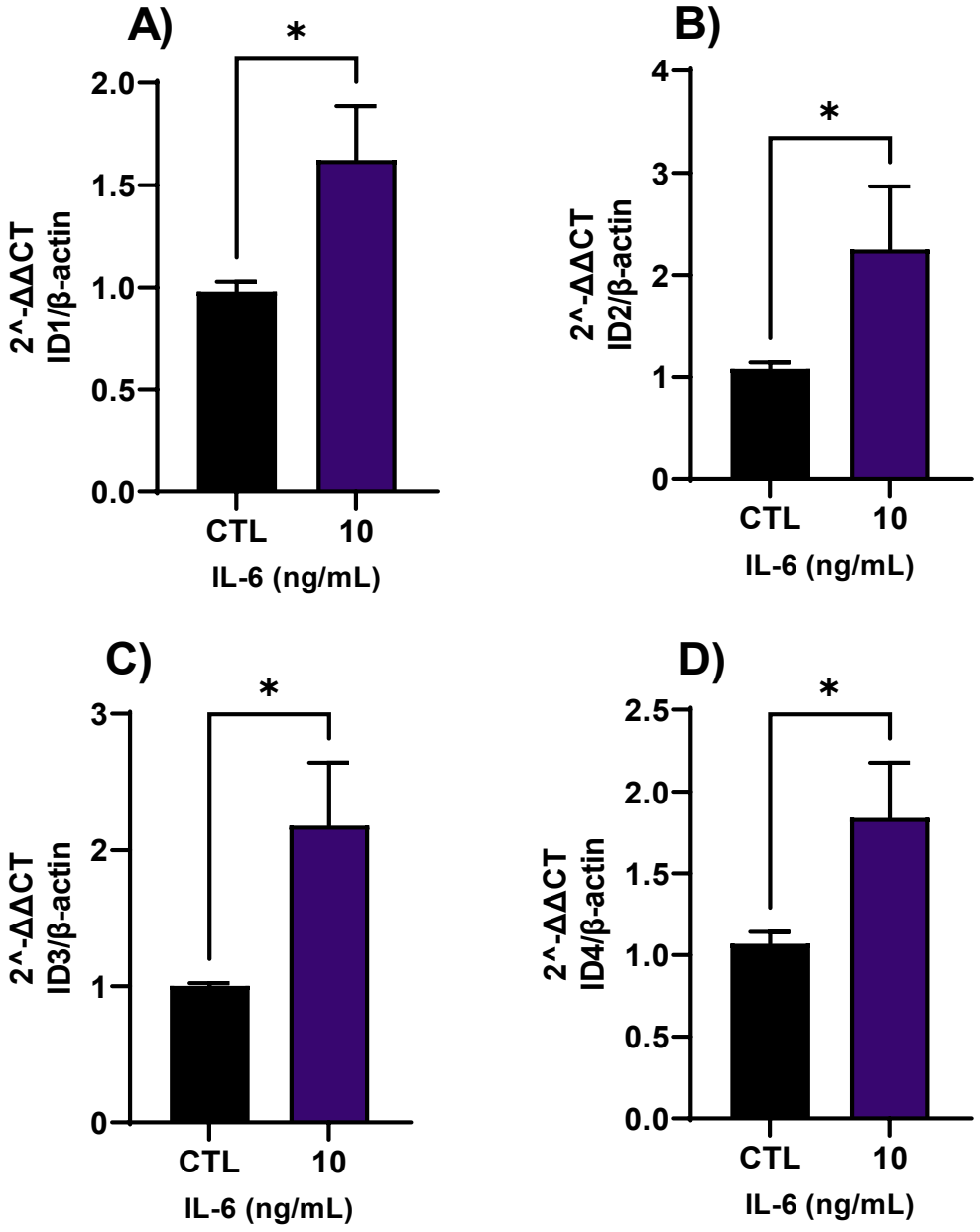

Figure 4-5 mRNA transcription of the BMPR2 downstream targets *ID1(A), ID2 (C), ID3 (C) and ID4 (D) after IL-6 treatment for 3 hours. Real-time PCR analysis was performed as described in section 2.4. Data shown are mean ±SEM n=6. Unpaired t-test was performed *p<0.05.*

To establish whether these changes in mRNA expression also lead to increase of ID1 protein changes, hPAECs lysates were analysed by western blot after treatment with IL-6 (1 and 10 ng/mL) and hepcidin (0.1 and 1 µg/mL) for 24 hours. Densitometry analysis of western blot bands (figure 4.6 A) showed a significant increase in ID1 protein after 24 hours treatments with both concentration of IL-6 or hepcidin (figure 4.6 B and C) (methodology used described in section 2.6).

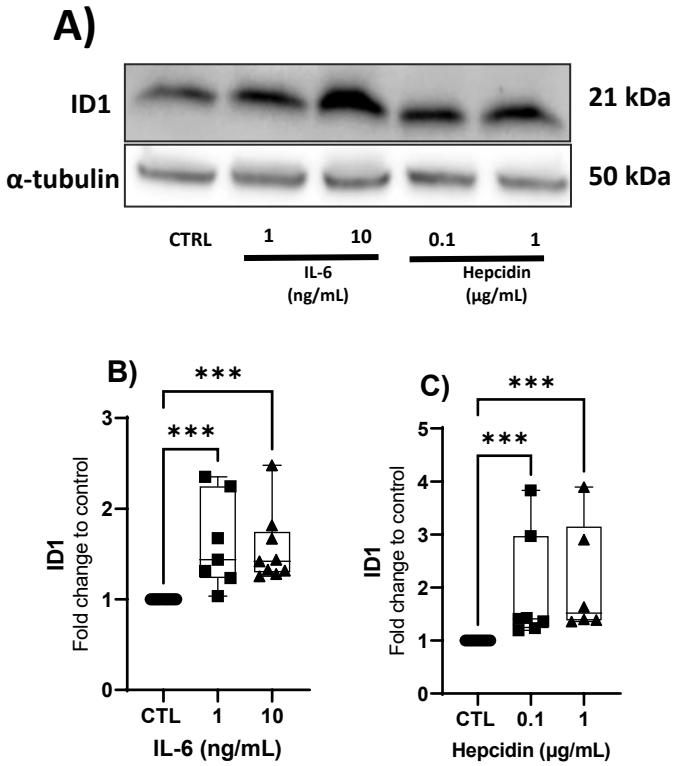

Figure 4-6 hPAECs ID1 protein expression is increased by IL-6 and hepcidin after 24 hours stimulation. *(A) Western blot image demonstrating that both IL-6 and hepcidin increase ID1protein expression. (B, C) Densitometry analysis of the western blot bands showed significant ID1 protein increase after 24h treatment with IL-6 (1 and 10 ng/mL) and hepcidin (0.1 and 1 µg/mL) compared to untreated controls. Data shown are mean ±SEM n=6. Kruskal-Wallis test followed by Dunn's post hoc test were performed ***p<0.001.*

4.2.4 Transcription of BMPR2 downstream targets are increased after BMPR2 knockdown

To investigate whether the increase in mRNA transcription of downstream targets of BMPR2 was caused by loss of BMPR2, a BMPR2 gene knockdown in hPAECs was performed using small interfering RNAs (siRNA). In brief, hPAECs cells seeded in a 6-well plate at 70% confluence. Once cells were completely attached, they were incubated with 20 nM of BMPR2 specific siRNA and 20 nM of non-targeting siRNA oligonucleotides (negative control) for 6 hours. After the incubation with siRNAs fresh media was added and cell lysates were collected at different time points for mRNA and protein analysis. Methodology used described in section 2.2.7.

Analysis of BMPR2 mRNA showed a 70% reduction of BMPR2 mRNA at the 24 and 48 hours' time points (figure 4.7 A and B). Furthermore, western blot analysis of hPAEC lysates displayed no discernible bands for BMPR2 protein (figure 4.7 C) up to 96 hours after knockdown. Relative quantification of the BMPR2 at the different time points showed significant reduction of protein at all time points, demonstrating that the knockdown was successful (Figure 4.7 D).

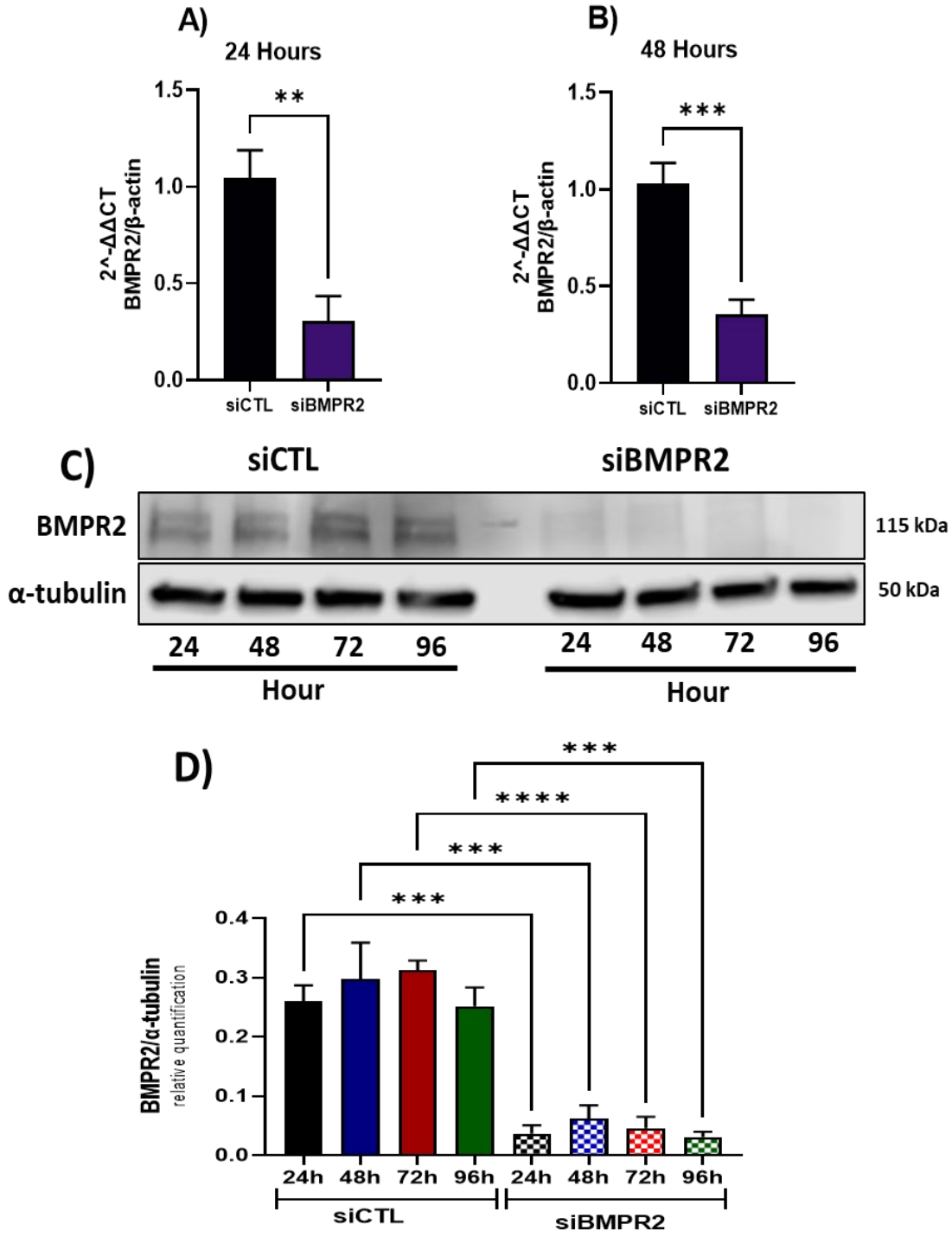

Figure 4-7 hPAEC BMPR2 knockdown time-course. *BMPR2 mRNA transcription analysis after 24 (A) and 48 (B) hours of knockdown. Real-time PCR analysis was performed as described in section 2.4. Data shown are mean ±SEM n=6. Unpaired t-test was performed **p<0.01; ***p<0.001. (C) Western blot image of hPAECs protein lysates over time. Bands on the left were incubated with a control siRNA and bands on the right were incubated with a BMPR2 siRNA for 6 hours. Lysates were them collected at 24, 48, 72, and 96 hours. Western blot analysis was performed as described in section 2.5. (D) Relative quantification of western blot using image J. Data shown are mean ±SEM n=3. One-way ANOVA test followed by Dunnett's post hoc test were performed; ***p<0.001, ****p<0.0001.*

After, the BMPR2 knockdown was established, an investigation of mRNA expression of the R-SMAD, SMAD1 and 5, and the ID proteins 1, 2, 3 and 4 was undertaken. Results showed a trend for increase with all the genes investigated, with ID1 and ID2 (figure 4.8 C and D) reaching significance after 24 hours of BMPR2 knockdown (figure 4.8).

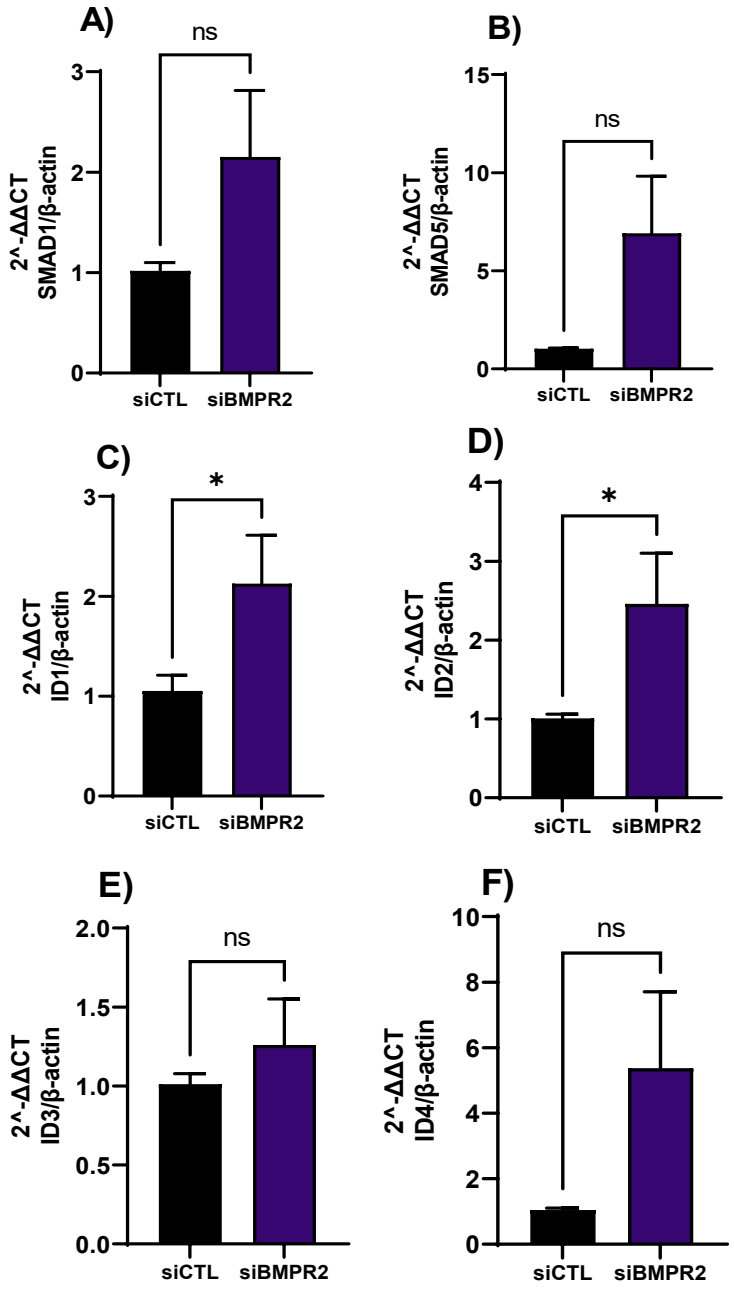

Figure 4-8 Knockdown of BMPR2 leads to upregulation of downstream BMPR2 targets*: SMAD 1 and 5, ID1, 2, 3 and 4. Real-time PCR assay was performed as described in section 2.4. Data shown are mean ±SEM n=6. Unpaired t-test was performed *p<0.05.*

4.3 Summary and Limitations

4.3.1 Summary

The main aim of this chapter was to establish the effect of IL-6 and hepcidin, both modulators of iron homeostasis, on BMPR2 expression. Mutations in the BMPR2 gene were the first identified genetic link to PAH, this study presented here demonstrate that hepcidin and or IL-6 significantly reduced BMPR2 expression in hPAECs at both the mRNA and protein level (figure 4-1 and 4-2). Paradoxically however, downstream signalling of BMPR2 is active despite reduction of in protein expression, this is demonstrated by increased SMAD1 and SMAD5 phosphorylation (figure 4-3). This increase occurred quite soon after treatment and it was reduced by two hours, however at 24 hours phosphorylation was increased again, which suggest a cyclical phosphorylation of these proteins, however a more extensive time course study is required. Hepcidin increased mRNA transcription of inhibitor of differentiation (ID) proteins 1, 2, 3 and 4. Western blot analysis also showed a significant increase of ID1 protein (figure 4-6) by both IL-6 and hepcidin. The increase of SMAD1/5 phosphorylation could explain the increase of the IDs proteins. hPAECs BMPR2 knockdown also showed an increase in SMAD1, SMAD5 and IDs proteins mRNA transcription (figure 4-8). A more detailed discussion of these results in the context of the entire thesis can be found in chapter 7.

4.3.2 Limitations

The main limitation of this chapter is the use of western blotting (WB) to quantify protein amounts as WB is traditionally a qualitative method. To have the best accuracy possible, reagents and experimental design were carefully optimised

and streamlined to ensure reproducible results. However, the BMPR2 antibody was a limiting factor due the inconsistency in performance; it would work perfectly well for some blots but not so for others. In addition this problem also arose with different batches (lots) of the antibody. Therefore, further experiments using a more quantitative assay, such as flow cytometry might be the best way to progress.

5. Chapter 5 – The effect of hPAEC conditioned media on hPASMC mitochondria

5.1 Rationale

Previous studies from this laboratory have demonstrated that hepcidin treatment increased hPASMC proliferation and this proliferation was abated by targeting ferroportin with a monoclonal antibody that stabilised ferroportin at the cell membrane, blocking the effect of hepcidin on ferroportin internalisation and degradation (Ramakrishnan et al., 2018b). Further studies also demonstrated that conditioned media from hPAECs treated with hepcidin and IL-6 caused an increase in hPASMC proliferation and migration (Pedersen et al., 2018, Shackshaft et al., 2017).

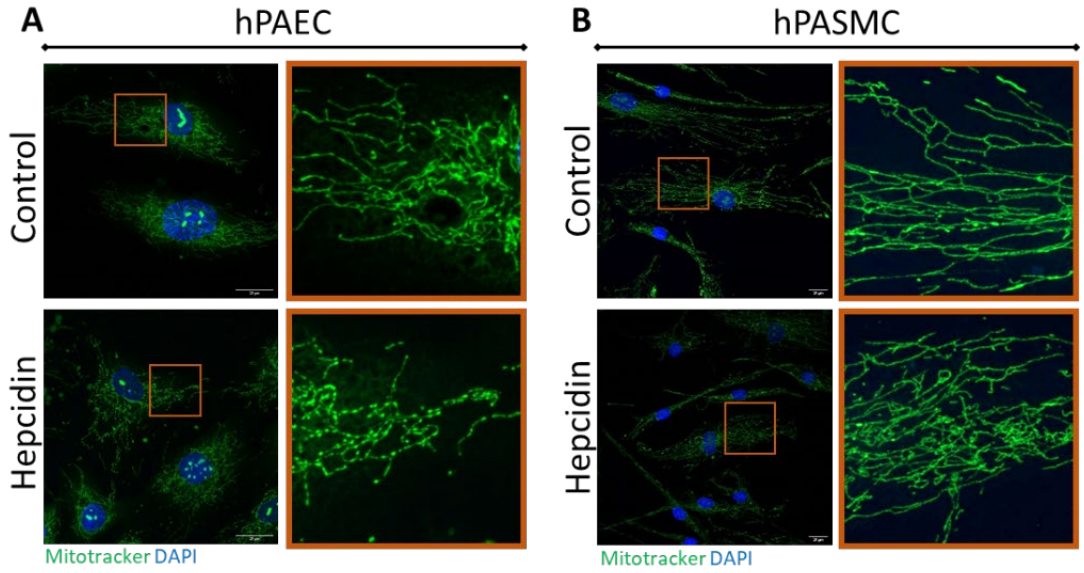

Figure 5-1 Hepcidin treatments causes mitochondrial changes in hPAECs *(A) and hPASMCs (B). hPAECs and hPASMCs were stained with Mitotracker (green) and DAPI (blue) following treatment with or without hepcidin. Orange boxes show magnified regions, scale bars, 20 µm. Unpublished data, experiments were run by me and Theo Issitt, confocal Images taken by Theo Issitt.*

To understand better, the effects of hepcidin on hPASMCs metabolism, studies were undertaken to investigate mitochondrial function of these cells after exposure to hepcidin. Dysfunction of mitochondrial metabolism is thought to be a

characteristic of vascular cells involved in PAH, where abnormalities found in mitochondrial metabolism promote a cancer like hyper-proliferative, apoptosis-resistant phenotype (Dasgupta et al., 2020). Confocal imaging showed profound disruption of hPASMC mitochondria networks after treatment with hepcidin, in contrast the mitochondria networks in hPAECs was slightly disrupted (unpublished data; figure 5.1).

5.1.1 Aims:

To investigate further the effects of hepcidin on hPASMCs mitochondria metabolism using seahorse assay that measure key parameters of mitochondrial function by measuring oxygen consumption rate (OCR).

1. To evaluate the effect of hepcidin treatments on hPASMCs
2. o compare the effects of conditioned media from 24 and 48 hour hepcidin treated PAECs with hPASMC on mitochondrial function.

5.2 Hepcidin causes dysregulation of mitochondrial function on hPASMCs

To investigate the effect of hepcidin on hPASMC mitochondrial function, cells from 3 different human donors were seeded ($2x10^5$ cells/well) into a 96-well seahorse assay plate in as triplicates. Once, the cells were attached they were starved overnight with 0.2% serum media. The cells were then treated with two concentrations of hepcidin, 0.1 and 1 µg/mL. The seahorse assay was performed as described in section 2.7. The assay measures different parameters, which are defined in the table 5-1 below. Hepcidin treatment caused a significant decrease in non-mitochondrial respiration; it also significantly increased basal respiration

and proton leak after 24 hours (figure 5.2). There were no changes in maximal respiration, ATP production and spare respiratory capacity (figure 5.2).

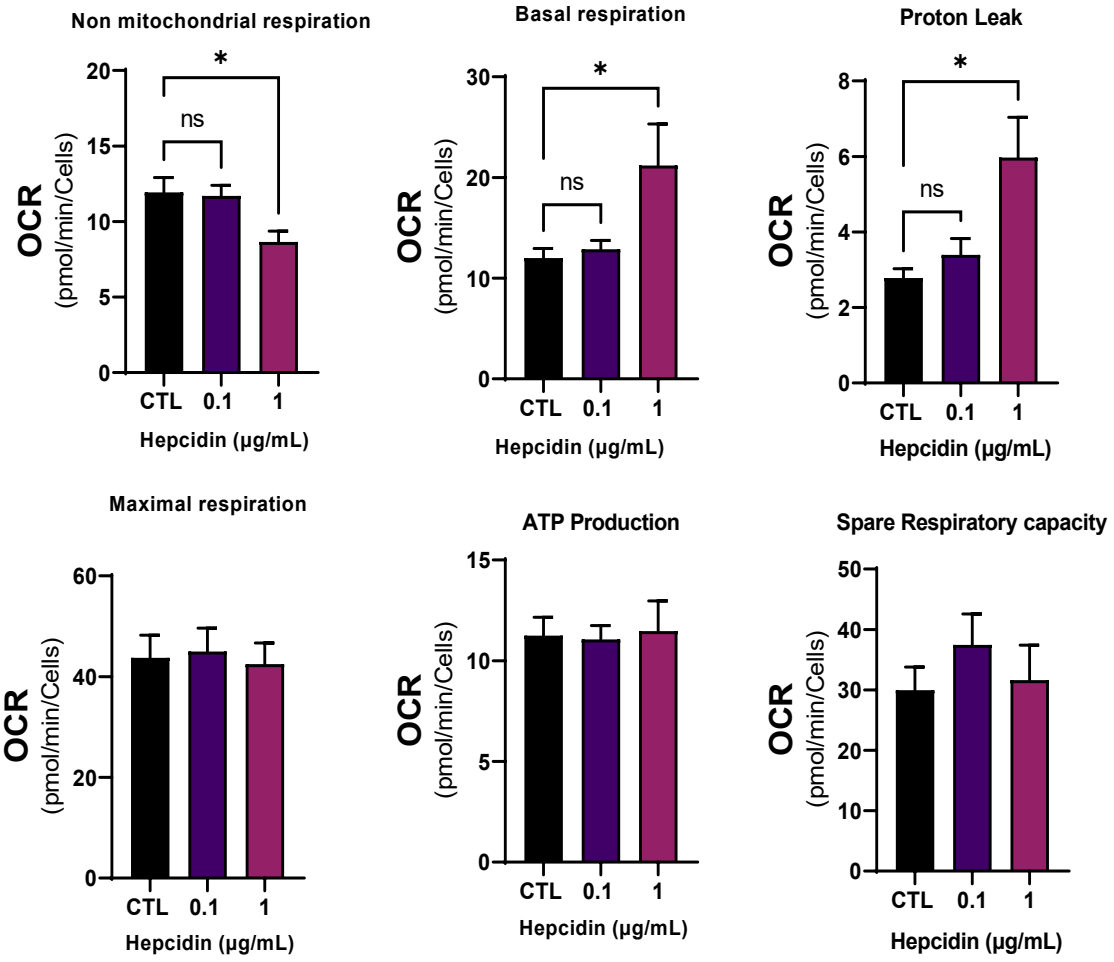

Figure 5-2 Hepcidin treatments changes hPASMCs mitochondrial metabolism. Mito *stress test were performed following treatment with or without hepcidin for 24 hours. The assay was performed as described in section 2.7. Data are shown ±SEM n= 6. One-way ANOVA test followed by Dunnett's post hoc test were performed * p<0.05.*

Table 5-1 – Mito stress test assay parameters definitions. Adapted from (Divakaruni et al., 2014).

Rate	Definition
Basal Respiration	Respiration used to meet the endogenous ATP demand of the cell and drive proton leak pathways.
ATP-linked respiration	Respiration that is sensitive to oligomycin can estimate the respiration that is used to drive mitochondrial ATP synthesis and the rate of ATP-linked respiration is mostly set by the ATP demand of the cell.
Proton leak	Oxidative phosphorylation is incompletely coupled, protons can leak across the inner membrane independently of ATP synthase. This leak can regulate several physiological processes. High leak can also indicate mitochondrial damage/injury or it can be used as a mechanism to regulate mitochondrial ATP production.
Maximal Respiration	A titrate amount of FCCP can estimate the maximum rate of respiration. In response to protonophore addition, substrate oxidation and respiratory chain activity increase in an attempt to maintain mitochondrial membrane potential. FCCP mimics a physiological “energy demand” by causing the respiratory chain to operate and maximal capacity. It shows the maximum rate of respiration a cell can achieve.
Spare-respiratory capacity	The spare respiratory capacity is the difference between the basal and maximal respiration, which indicates the ability of the cell to meet an increase in energy demand that can be an indicator of the cells fitness or flexibility.
Non-mitochondrial respiration	Oxygen consumption that persists after mitochondrial respiration is blocked upon addition of electron transport chain inhibitors such as rotenone and antimycin A. this is important to get an accurate measure of mitochondrial respiration.

5.3 hPAECs conditioned media from hepcidin treated cells promotes an increased mitochondrial metabolism

As mentioned above, previous work by this laboratory showed that conditioned media from hPAECs treated with hepcidin increased hPASMCs proliferation and migration. To investigate whether mitochondrial metabolism is affected by conditioned media from hepcidin treated hPAEC, hPAECs cells from 3 donors were seeded ($1x10^6$) in a 12-well plate. At the same time hPASMCs from 3 different donors were seeded into a 96-well seahorse assay plate in triplicates ($1x10^4$) and left incubating overnight for cell attachment. hPAECs were then treated with hepcidin (0.1 and 1 µg/mL) or media alone for 24 hours; hPASMCs were serum starved overnight. Conditioned media from hPAECs were then transferred into the hPASMCs for 24 hours. The seahorse assay was then run as described in section 2.7.

Seahorse assay results demonstrated that hPASMC exposed to hPAEC conditioned media for 24 hours caused mitochondrial metabolism to switch to a more energy demanding phenotype. Basal respiration was increased by hepcidin CM with both hepcidin concentrations, however it did not reach significance. ATP production, spare respiratory capacity and maximal respiration was elevated by hPAEC CM with 0.1 µg/mL hepcidin. CM with 1 µg/mL hepcidin also elevated ATP production and spare respiratory capacity, but did not reach statistical significance (figure 5.3). Proton leak was also increased by hPAEC CM with 0.1 and 1 µg/mL hepcidin, however significance was reached only with CM with 0.1 µg/mL (figure 5.3). The proton leak increase may indicate cell damage or more probably an increase in demand for ATP.

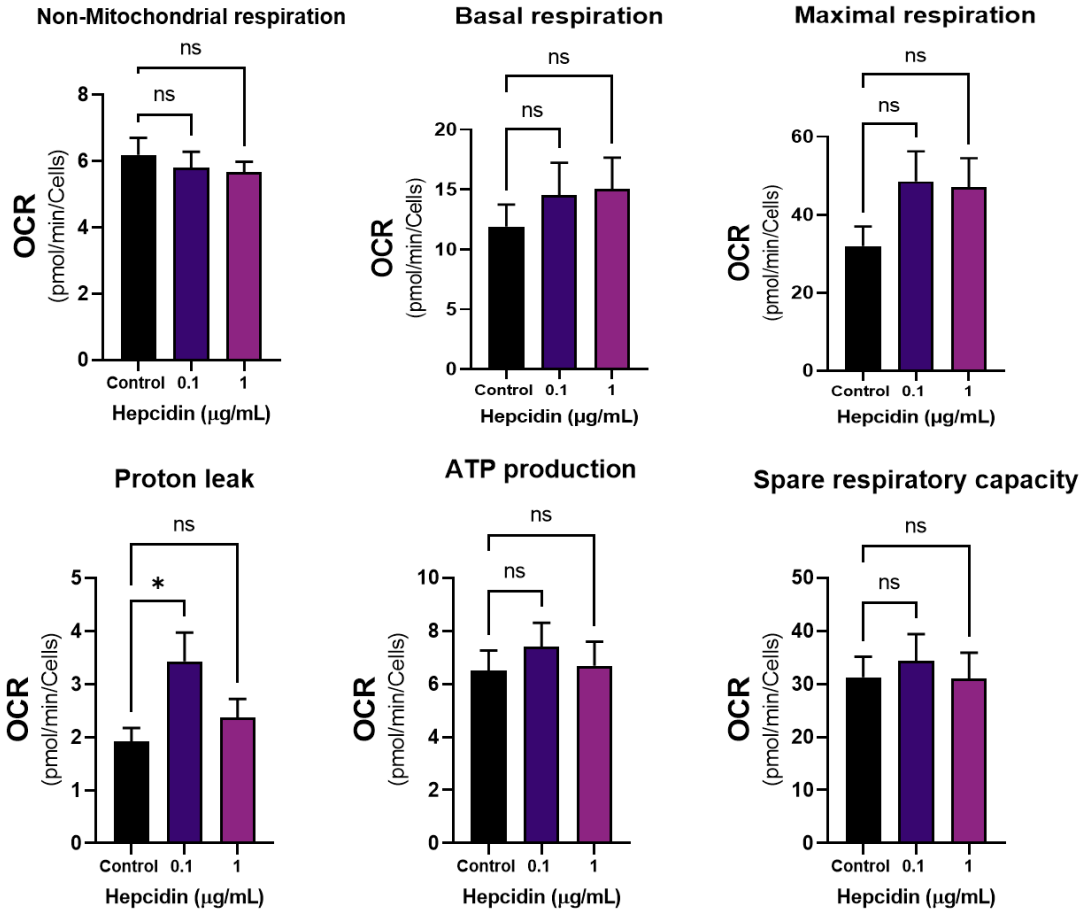

Figure 5-3 – hPAECs conditioned media with hepcidin increased the energy demand of hPASMCs. *Mito stress test were performed following treatment of hPASMCs with hPAECs conditioned media either with hepcidin or media alone. The assay was performed as described in section 2.7. Data are shown ±SEM n= 6. One-way ANOVA test followed by Dunnett's post hoc test were performed * p<0.05.*

5.4 Summary and Limitations

5.4.1 Summary

The results presented in this chapter strengthens and expands previous work performed in this laboratory, which showed that hepcidin caused mitochondrial dysfunction in hPASMCs (figure 5-1). Hepcidin treatment of hPASMCs resulted in increased proton leak, an indication of mitochondrial damage/injury, and basal respiration that indicates elevated levels of proton leak and demand for energy

(figure 5-2), which complements prior experiments where hepcidin treatment was shown to increase hPASMC proliferation (Ramakrishnan et al., 2018b). Further, the effects of hPAECs conditioned media after hepcidin treatments on hPASMC mitochondrial function were also examined; the results show that hPASMCs shifted to a more energy demand-based phenotype with elevated ATP production, spare respiration capacity and basal respiration (figure 5-3). A more in-depth discussion of these results in the context of thesis can be found in chapter 7.

5.4.2 Limitations

The results presented in this chapter is essentially a pilot data study of mitochondrial function in hPASMCs. Seahorse analysis is the standard assay for assessing mitochondria function, however it does have drawbacks. Due to its sensitivity, cell number and cell adherence in the wells were an issue. As these experiments used three different donors. However, one of the donor cells did not adhere properly to the well of the assay plate, leading to different responses even within the replicate wells, which is a common issue with these assays. With technical support from Agilent, issues were corrected. However, increasing the number of donors would strengthen these results and also help with issues such as low adherence from any particular donor. The COVID-19 pandemic lockdown also affected this work as I could not have access to donor tissue for PASMC isolation to run further experiments.

6. Chapter 6 - Haemoglobin effect on hPAECs and the implications to PAH

6.1 Rationale

6.1.1 Cell free haemoglobin exposure as contributor to the development of PAH

Pulmonary arterial hypertension is prevalent in patients with haemolytic anaemias such as thalassemia and sickle cell disease. Release of cell free haemoglobin (CFH, which will be referred as haemoglobin) and heam through haemolysis (which is the process red blood cell rupture), in the circulation is toxic deleterious to many organs and it has been associated with several numerous disease conditions including (acute lung injury, sepsis and, sickle cell disease). Elevated levels of CFH with promote an increased risk of kidney injury, myocardium infarction and death (Donadee et al., 2011, Janz et al., 2013, Natanson et al., 2008). The main potential mechanism for CFH association with the ability of CFH to cause vascular endothelium damage and vasoconstriction by scavenging nitric oxide (Reiter et al., 2002, Brittain et al., 2014). Vasoconstriction is a characteristic of PAH, and targeting the nitric oxide pathway is one of the major therapeutic approaches for the treatment of PAH.

A study by Brittain et al. (2014) of PAH patients of 200 PAH patients (85 IPAH; 25 HPAH; 63 connective tissue disease-associate - PAH; 21 congenital heart disease; and 6 portopulmonary PAH) compared to 19 healthy subjects, 29 with pulmonary venous hypertension (PVH) and 16 unaffected mutation carriers (UMC) showed that CFH was significantly elevated in PAH patients compared to controls. Interestingly, a retrospective study of 15 of these patients' blood smears did not show any evidence of haemolysis. Moreover, CFH elevation remained stable overtime (4-12 months). Elevated levels of CFH was associated with

increased mPAP (mean pulmonary artery pressure) and PVR (pulmonary vascular resistance).

Intravenous infusion of low plasma haemoglobin concentrations (range 3 -10 μM) into Sprague-Dawley rats induced pulmonary vascular disease by an increase in pulmonary arterial pressure, right ventricular hypertrophy, and a time-dependent increase in vascular remodelling. These effects were exacerbated by hypoxia; chronic exposure to haemoglobin also elevated the expression of pulmonary HO-1 (haem oxygenase 1, an enzyme that leads to haem degradation and that is also inducible by haem) and ICAM-1. HO-1 has an important role in reducing oxidative stress caused by exposure to haem and ICAM-1 is a marker of an activated endothelium and induces a pro-inflammatory effect. Therefore, these results suggest that in this model, oxidative stress and inflammation induced by chronic exposure to haemoglobin has a critical role in PAH development (Buehler et al., 2012).

Another study by Rafikova et al. (2018) using a sugen PH rat model demonstrated an increase of plasma free haemoglobin after 2 and 5 weeks of PH induction, depletion of haptoglobin and an increase in infiltration of inflammatory cells. This study also showed that PAH patients had increased levels of free haemoglobin and that this increase was associated with an increase in severity of PAH disease. Interestingly, they also demonstrated that despite the increase in haemolysis there was no change in the levels of haemoglobin suggesting an increase in erythropoiesis as a compensation mechanism (Karamanian et al., 2014).

6.1.2 Haemoglobin handling: a role for haptoglobin and CD163

Haemoglobin dimers formed by haemoglobin decompartmentalisation and release into the plasma are rapidly bound to the serum protein haptoglobin. Haptoglobin-haemoglobin complexes are recognised and endocytosed by the haemoglobin-haptoglobin scavenger receptor molecule, CD163, highly expressed on the surfaces of monocytes and macrophages, which leads to the degradation of the complex and recycling of iron resources within these specific cell types. In this process however, haptoglobin is not recycled but is instead consumed by the cell (Schaer et al., 2014, Thomsen et al., 2013). In haemolytic events, the rapid formation of haptoglobin-haemoglobin complexes leads to precipitous depletion of haptoglobin resources; therefore in diseases where haemolysis is prominent haptoglobin is typically undetectable (Rother et al., 2005, Thomsen et al., 2013). Nakamura et al. (2017) recently showed that serum haptoglobin levels were significantly decreased in PAH patients, which may indicate microangiopathy and subsequent subclinical haemolysis in the pulmonary arterioles. Another marker of haemolysis, serum lactate dehydrogenase (Barcellini and Fattizzo, 2015), was also elevated in their PAH (11 patients with IPAH and 24 with connective tissue disease (CTD) PAH) patient group. Other haemolytic markers such as bilirubin, were also elevated in chronic thromboembolic pulmonary hypertension (CTEPH) and pulmonary hypertension (PH) patients (Voelkel et al., 2000, Gong et al., 2015).

CD163 is a 130 kDa transmembrane protein and the mature protein consists of an extracellular region composed of nine scavenger receptor cysteine rich (SRCR) domains and a short cytoplasmic tail. CD163 mRNA are expressed in

several different variants that arise from alternative splicing of a single CD163 gene (Ritter et al., 1999, Nielsen et al., 2006). CD163 expression is regulated by several endogenous and exogenous molecules. IL-6, IL-10 and gloucocorticoids strongly upregulate CD163; by contrast IL-4, interferon γ (IFN- γ), lipopolysaccharide (LPS), CXC-chemokine ligand 4 (CXCL4) and granulocyte/macrophage colony stimulant factor (GM-CFS) downregulate CD163 expression. Therefore, the overall pattern is that CD163 expression is upregulated by anti-inflammatory mediators and downregulated by pro-inflammatory mediators (Thomsen et al., 2013). Human CD163 expression is reported to be exclusive to the monocytic-macrophage linage of cells (Etzerodt and Moestrup, 2013). However, this laboratory has shown that CD163 is expressed in hPASMC (Ramakrishnan et al., 2018b).

6.1.3 Aims

The studies described above suggest that free haemoglobin released by haemolysis of red blood cells could have an important role in the pathobiology of PAH. The studies undertaken here therefore aim to investigate aspects of haemoglobin interaction with hPAECs and the potential for induction of inflammatory responses and a PAH phenotype:

1. To Determine or otherwise the expression of the haemoglobin receptor CD163 in hPAECs Investigate haemoglobin effect on hPAECs
2. To investigate the effects of haemoglobin exposure to hPAECs on endothelial cell dysfunction including:
    - Inflammatory cytokine release and reactive oxygen species production

- Markers of endothelial cell activation, specifically ICAM-1 and VCAM-1 proteins.

6.2 Results

6.2.1 Human Pulmonary Artery endothelial cells express the haemoglobin scavenger receptor CD163

6.2.1.1 hPAEC CD163 mRNA transcription is upregulated by haemoglobin treatments

To investigate whether hPAEC express the CD163 mRNA transcription was determined by real time PCR as described in section 2.4.4. In brief, hPAECs cells were treated with haemoglobin at 1, 3 and 10 μM for 3 hours (detailed method in section 2.2.5.1). After treatment cells lysates were collected and real time PCR was performed as detailed in section 2.4.

Results showed that hPAECs expressed CD163 mRNA basally, moreover haemoglobin treatments increased CD163 mRNA expression in a dose response manner, reaching statistical significance at 10 μM haemoglobin (figure 6.1).

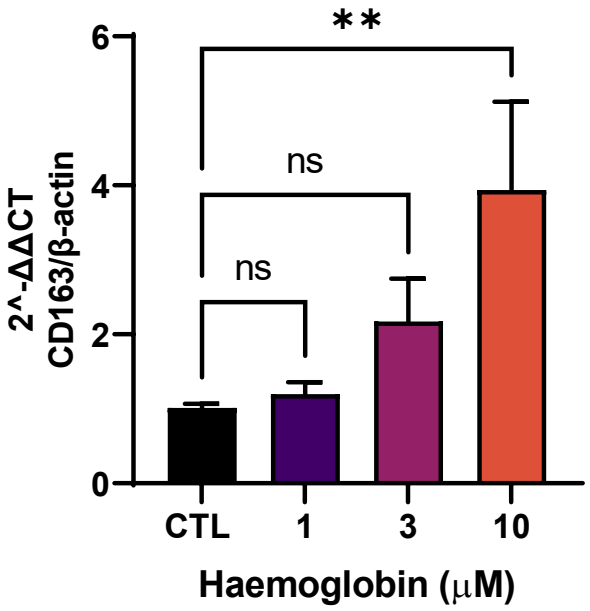

Figure 6-1 hPAEC CD163 mRNA transcription is upregulated by haemoglobin. *hPAECs cells were seeded in a 12-well plate at 75,000 cells per well and incubated overnight for cell attachment. The cells were then serum starved overnight and treated with haemoglobin for 3 hours. RNA extraction, cDNA synthesis and Real-time PCR were performed as described in section 2.4). Data is shown as mean ±SEM, n=8. One-way ANOVA test followed by Dunnett's post hoc test were performed ** p<0.01.*

6.2.1.2 CD163 protein is expressed in hPAECs.

Western blot analysis as described in section 2.5, showed CD163 protein is present in hPAECs basally after 24 hours treatment with haemoglobin, visual inspection of the proteins bands shows an increase in band intensity as haemoglobin concentration also increases (figure 6.2).

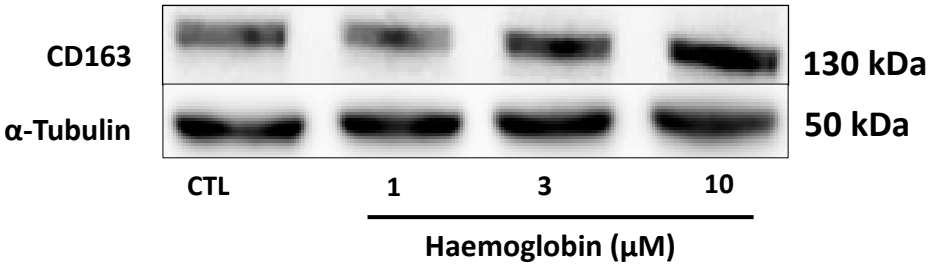

Figure 6-2 CD163 protein is expressed in hPAECs. *hPAECs were seeded into a 6-well plate at 250,000 cells per well. The cells were incubated overnight for attachment. Cells were then treated with haemoglobin for 24 hours at 1, 3 and 10 μM concentrations. Western blot were performed as described in section 2.5 n=1.*

To determine if haemoglobin caused an increase in protein expression in the same manner as mRNA transcription, CD163 protein presence on hPAEC cell membrane was measured by by flow cytometry as described in section 2.8.5. CD163 protein was significantly increased in hPAECs by 10 μM haemoglobin after 24 hours treatment (figure 6-3). The 1 and 3 μM haemoglobin concentrations did not cause changes in CD163 protein expression (figure 6-3).

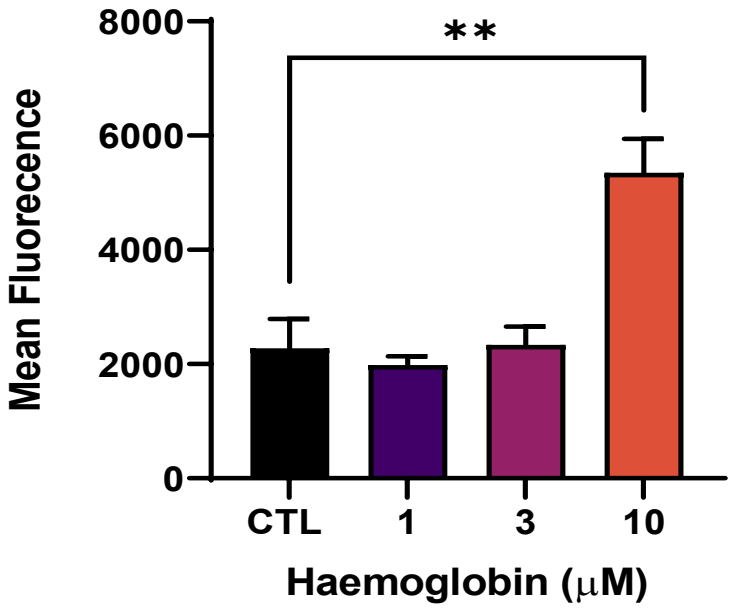

Figure 6-3 CD163 is expressed on hPAECs membrane. *Cells were seed in T25 flasks until they were 70% confluent. Cells were then treated with haemoglobin for 24 hours at 1, 3 and 10 μM concentrations. Flow cytometry assay was performed as described in section 2.8. Data is shown as mean ±SEM, n=4. One-way ANOVA test followed by Dunnett's post hoc test were performed ** p<0.01.*

6.2.2 Haemoglobin elevates inflammatory cytokines

6.2.2.1 IL-6, IL-8 and MCP-1 mRNA transcription is increased by haemoglobin

Increased inflammation is a key marker of PAH. To determine if haemoglobin causes the release of the inflammatory markers, IL-6, IL-8 and MCP-1, real –time of haemoglobin treatment for 2 hours showed a trend increased of mRNA transcription of IL-6 and IL-8 (figure 6-4 A and B) even though significance was

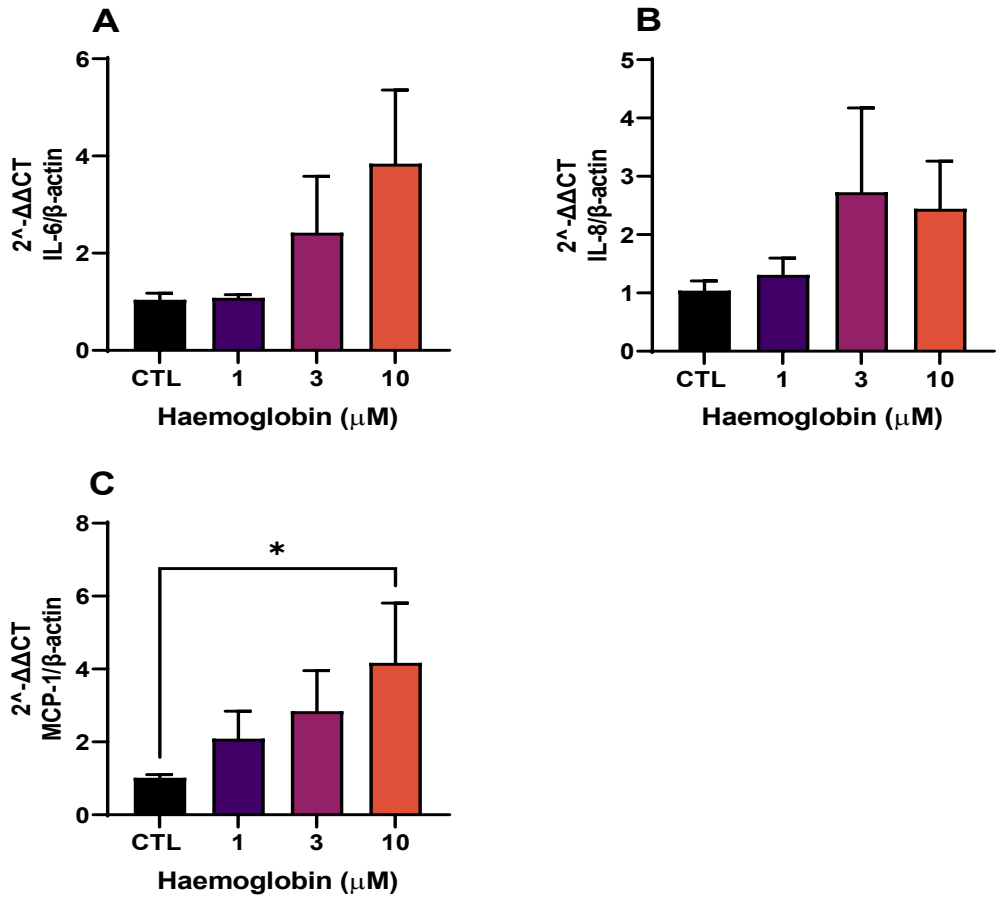

Figure 6-4 IL-6 (A), IL-8 (B) and MCP-1 (C) mRNA transcription is increased by haemoglobin. *hPAECs cells were seeded in a 12-well plate at 75,000 cells per well and incubated overnight for cell attachment. The cells were then serum starved overnight and treated with haemoglobin for 3 hours. RNA extraction, cDNA synthesis and Real-time PCR were performed as described in section 2.4). Data is shown as mean ±SEM, n=8. One-way ANOVA test followed by Dunnett's post hoc test were performed *p<0.05.*

not reached. MCP-1 mRNA transcription did also increase in a dose response manner reaching significance at 10 µM haemoglobin (figure 6-4 C).

6.2.2.2 Haemoglobin increases the release of the cytokines IL-6, IL-8 and MCP-1 in hPAECs supernatants

Next, to ascertain if the increase in mRNA transcription translated into an increase in protein expression in hPAECs supernatants, the levels of IL-6, IL-8

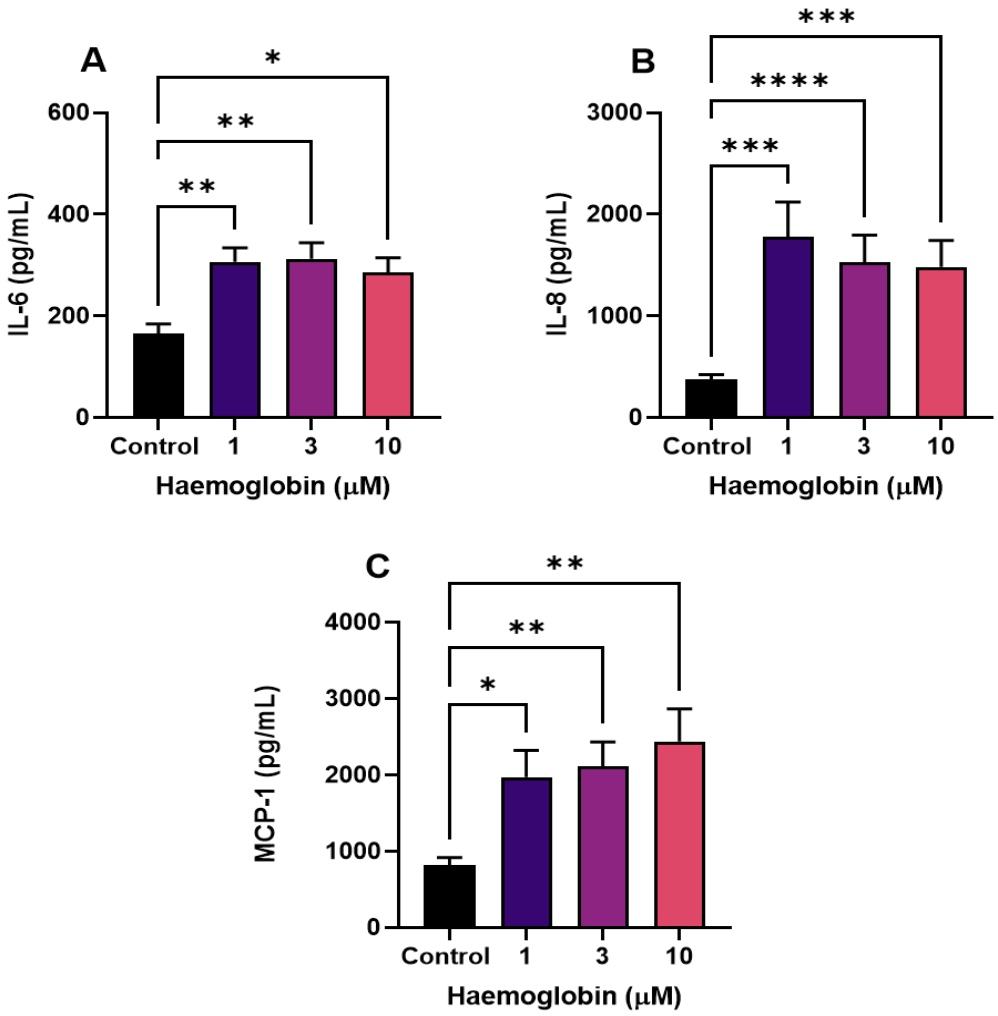

Figure 6-5 Haemoglobin increases the release of the cytokines IL-6 (A), IL-8 (B) and MCP-1 (C) in hPAECs supernatants. *hPAECs supernatant s were analysed by ELISA as described in section 2.6. Data is shown as mean ±SEM, n=12. Kruskal-Wallis test followed by Dunn's post hoc test were performed *p<0.05, ** p<0.01; ***p<0.001; ****p<0.0001.*

and MCP-1 were evaluated by ELISA (described in section 2.1.3) 24 hours after treatment with haemoglobin (section 2.2.5.1). Results showed that all concentrations of haemoglobin significantly increased the release of IL-6, IL-8 and MCP-1 (figure 6-5 A, B and C) cytokines into hPAECs supernatants.

6.2.2.3 Free-haemoglobin increases the release of hepcidin from hPAECs

Haemoglobin increased inflammatory responses this was especially apparent for IL-6, which is an agonist for hepcidin production as described in section 3.2.2. Therefore, hepcidin release was investigated in relation to haemoglobin treatment by real-time PCR and ELISA. Real-time PCR analysis of hPAECs mRNA after 2 hours treatment with haemoglobin showed that hepcidin transcription was increased by all 3 concentrations of free-haemoglobin reaching significance at 10 μM (figure 6-6 B). Similarly, ELISA analysis of hPAECs supernatants after 24 hours treatment with free-haemoglobin for 24 hours showed an increase in hepcidin release by the 3 concentrations of haemoglobin used, with significance demonstrated at 3 and 10 μM concentrations (figure 6-6 B).

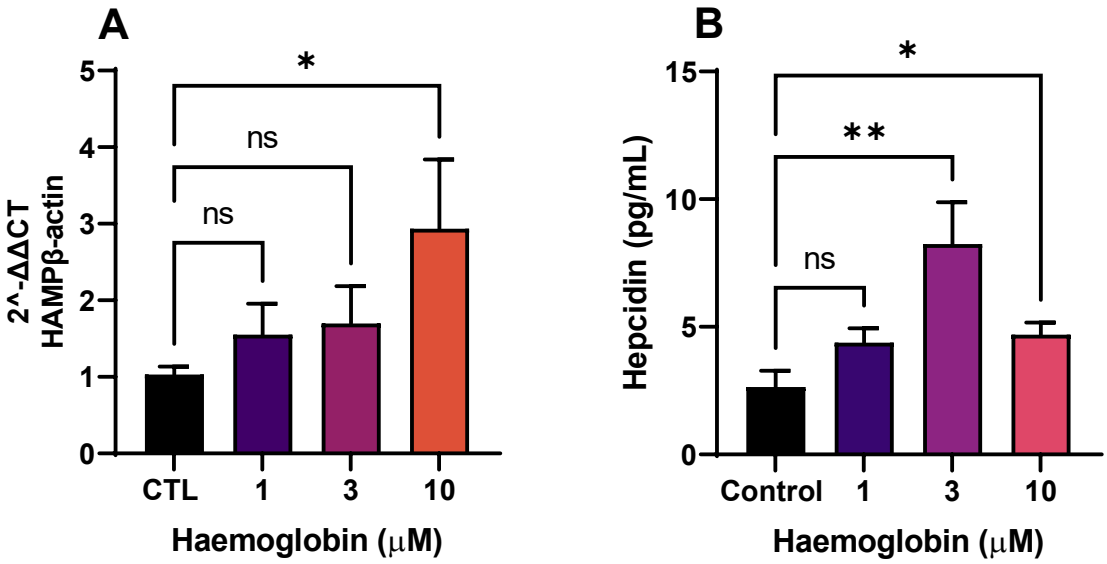

Figure 6-6 - Haemoglobin increases the release of the hormone hepcidin. *(A) hPAEC mRNA transcription after 2 hours treatment with haemoglobin. Data is shown as mean ±SEM, n=8. One-way ANOVA test followed by Dunnett's post hoc test were performed * p<0.05. (B) Hepcidin release in hPAEC supernatants 24 hours after haemoglobin treatments. Data is shown as mean ±SEM, n=12. Kruskal-Wallis test followed by Dunn's post hoc test were performed *p<0.05; ** p<0.01; ***p<0.001; ****p<0.0001.*

6.2.3 Haemoglobin causes the activation of hPAECs

Endothelial activation is an important step during inflammation, and occurs in response to pro-inflammatory cytokines and other stimuli, resulting in an increase in expression levels of leukocyte adhesion molecules such as intercellular adhesion molecule-1 (ICAM-1) and vascular cell adhesion molecule-1 (VCAM-1) (Pinte et al., 2016). To investigate if the increase in inflammatory markers shown in section 6.2.2., affected ICAM-1 and VCAM-1 expression on the surface of hPAECs, flow cytometry was utlilised (section 2.8.5). After 24 hours of haemoglobin stimulation both ICAM-1 and VCAM-1 protein expression was

increased on hPAECs membrane surface reaching significance at 10 μM (figure 6-7).

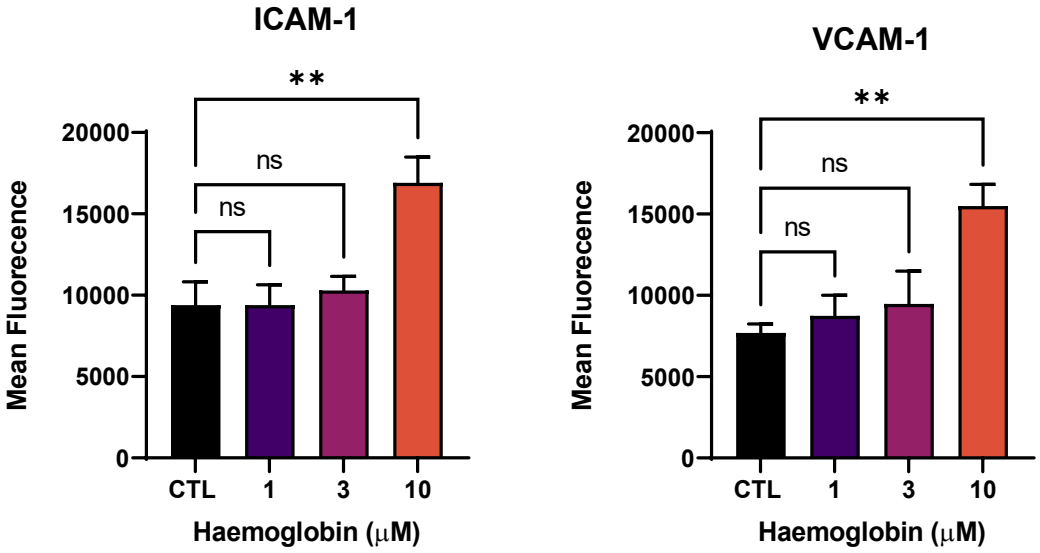

Figure 6-7 The expression of ICAM-1 and VCAM-1, markers of endothelial cell activation, are increased by haemoglobin treatments (24 hours). *ICAM-1 and VCAM-1 expression was determined by flow cytometry as described in section 2.8. Data is shown as mean ±SEM, n=4. One-way ANOVA test followed by Dunnett's post hoc test were performed ** p<0.01.*

6.2.4 Haemoglobin elevates the production of Reactive oxygen Species

To investigate whether haemoglobin cause oxidative stress, the production of reactive oxygen species (ROS) was measured in hPAECs. ROS were measured by flow cytometry using the Dihydroethium (DHE) assay as described in section 2.8.3.2, after 24 hours treatment with haemoglobin. ROS production by hPAECs

increased in a dose response manner reaching significance at the 3 and 10 μM haemoglobin concentrations (figure 6.8).

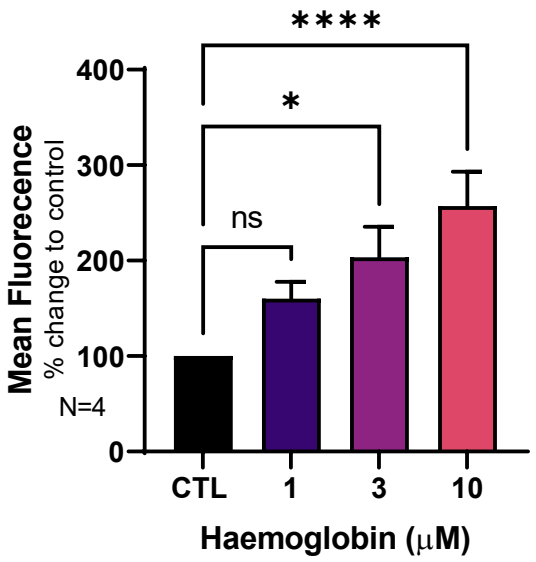

Figure 6-8 Haemoglobin elevates the production of Reactive oxygen Species (ROS). *ROS release was measured by flow cytometry as described in section 2.8. Data is shown as mean ±SEM, n=4. Kruskal-Wallis test followed by Dunn's post hoc test were performed *p<0.05; ****p<0.0001.*

The key producers of ROS in cells are the NOX family of NADPH oxidases. Pulmonary NOX2 has been implicated in vascular remodelling (Panday et al., 2015); therefore the expression of NOX2 was investigated in hPAECs after 2 hours stimulation with haemoglobin by real-time PCR (section 2.4.4) and western blot (section 2.5). NOX2 mRNA transcription was elevated by all concentrations of haemoglobin, however significance was only reached at 1 and 10 μM (figure 6-9 A). Western blot analysis of hPAECs lysates after 24 hours of haemoglobin treatment showed that gp91 phox, a subunit of NOX2, is expressed in hPAECs

and visual analysis suggested a possible increase protein in dose response manner (figure 6-9 B).

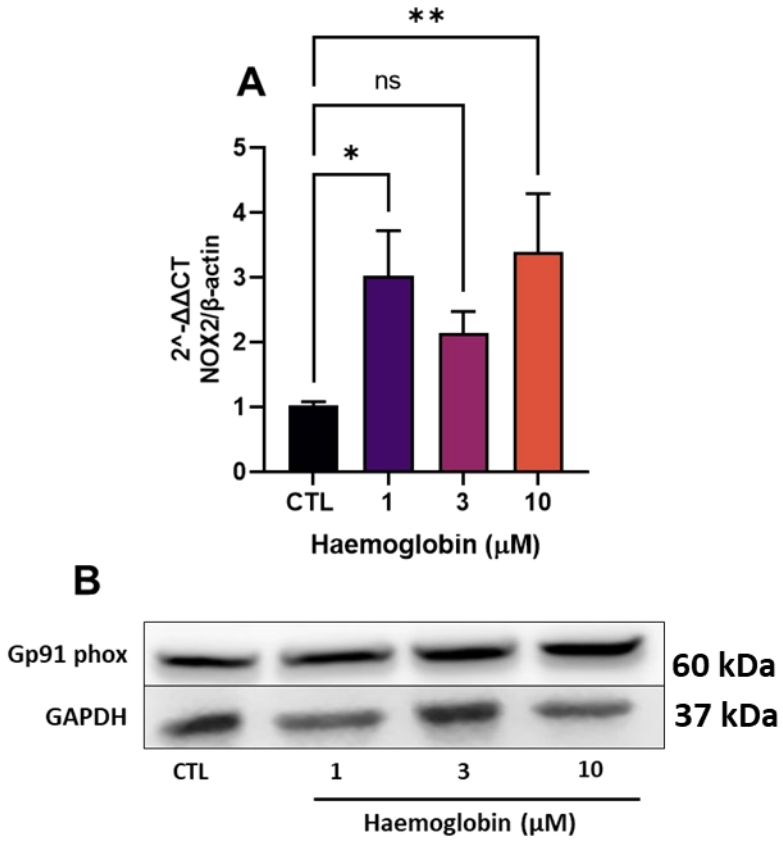

Figure 6-9 NOX2 expression in hPAECs is increased by haemoglobin exposure. ***(A)*** *NOX2 mRNA transcription after 2 hours stimulation with haemoglobin. Data is shown as mean ±SEM, n=8. One-way ANOVA test followed by Dunnett's post hoc test were performed * p<0.05; **p<0.01.* ***(B)*** *Expression of gp91phox a subunit of NOX2 in hPAECs after 24 hours treatment with haemoglobin at 3 different concentrations n=1. Western blot was performed as described in section 2.5.*

6.2.5 hPAECs proliferation is increased by haemoglobin in a time-dependent manner

Endothelial cell proliferation, and formation of plexiform lesions are a hallmark of PAH (Jonigk et al., 2011). Therefore, hPAECs proliferation was investigated following haemoglobin stimulation for 24, 48, 72, and 96 hours by the MTS assay as described in section 2.3.1. Free-haemoglobin at the three concentrations used significantly increased hPAECs proliferation in a time-dependent manner (except 10 μM at 96 hours). For 24 hours treatment the significant increase was also shown by the BrdU assay (figure 6.11 B). More interestingly it seems that this was a concentration independent effect as different concentrations exhibited similar responses (figure 6-10 and 6-11 A). However, time of exposure does seem to play a more important role as proliferation increased by around 10% at 24h, 15% at 48h, 30% at 72h and 42% at 96h (figure 6-9 and 6-11 B).

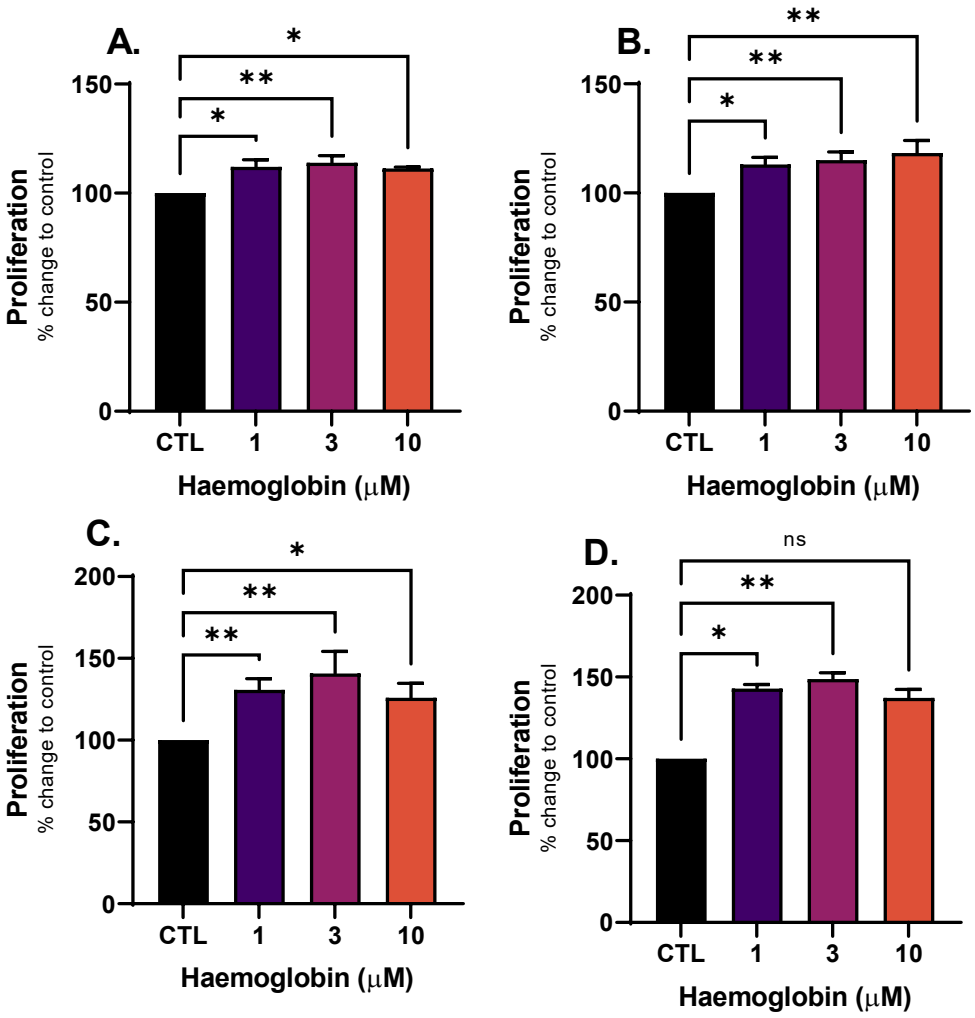

Figure 6-10 hPAECs proliferation is increased by haemoglobin in a time-dependent manner 24h (A), 48h (B), 72h (C) and 96h (D). *hPAECs proliferation was determined by the MTS assay as described in section 2.3.1. Data is shown as mean ±SEM, n=6. Statistical test were performed separately by each time point against each correspondent controls. One-way ANOVA test followed by Dunnett's post hoc test were performed * p<0.05*

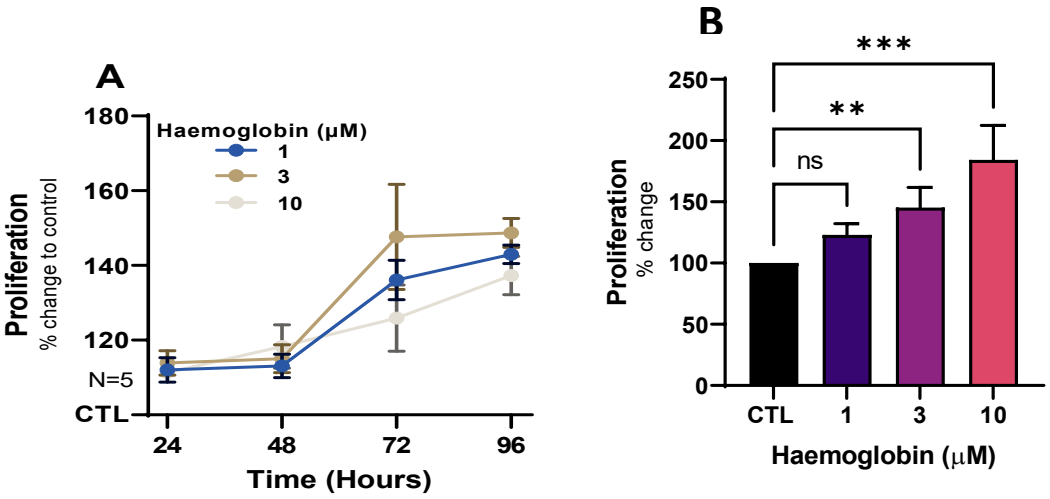

Figure 6-11 hPAECs proliferation is increased by free-haemoglobin in a time-dependent manner. (A) *Graph representing the increased proliferation of hPAECs through time. Data is shown as mean ±SEM, n=6, statistical test is shown in figure 6-10.* ***(B)*** *Graph showing the proliferation of hPAECs by the BrdU after treatment with haemoglobin for 24 hours. Data is shown as mean ±SEM, n=6. Kruskal-Wallis test followed by Dunn's post hoc test were performed; **p<0.01, ***p<0.001.*

6.2.6 Haemoglobin treatments does not affect hPAECs viability

hPAECs cell viability was determined by the alamar blue assay (section 2.2.6), after 24 hours treatment with haemoglobin. For the assay a 2-fold serial dilution was undertaken, starting at the top concentration (10 µM). Analysis determined that haemoglobin did not affect hPAEC viability at the concentrations tested (figure 6-12). Even though, Alamar Blue is describe as a viability test it also detects cell metabolic function, it can also show cell proliferation. The results shown in figure 6-12 demosntrate an dose response increase in cell proliferation after treatment with haemoglobin reaching significance at 5 µM.

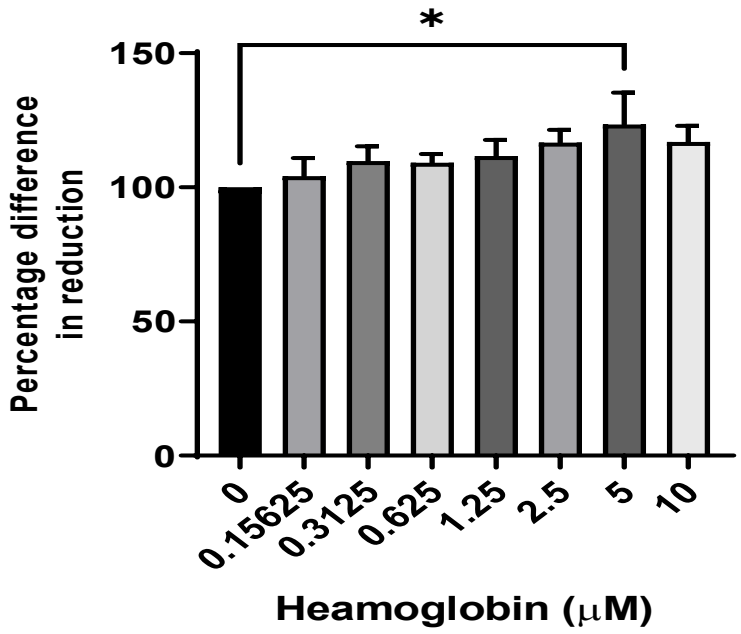

Figure 6-12 Haemoglobin treatments does not affect hPAECs viability*. Cell viability was determined by the Alamar Blue assay and the assay was performed as described in section 2.2.6. Data is shown as mean ±SEM, n=3. Kruskal-Wallis test followed by Dunn's post hoc test were performed *p<0.05*

6.3 Summary and Limitations

6.3.1 Summary

This study demonstrates for the first time that the CD163 scavenger receptor is expressed in hPAECs, and that its expression can be modulated by haemoglobin (section 6.2.1).Haemoglobin treatment increased the expression of the inflammatory cytokines IL-6, IL-8, MCP-1 (section 6.2.2.1 and 6.2.2.2) and hepcidin (section 6.2.2.3). Furthermore endothelial cells became activated by haemoglobin as demonstrated by the increased expression of ICAM-1 and VCAM-1 (section 6.2.3). ROS release was elevated by haemoglobin in hPAECs and the expression of the NADPH oxidase NOX2 was also increased by

haemoglobin (section 6.2.4). hPAEC proliferation was stimulated by haemoglobin, and it increased in a time-dependent manner (6.2.5).

Free-haemoglobin has been proposed as a contributor for the development of PAH (Brittain et al., 2014), the results described above further strengthens the indication that cell free haemoglobin could have a role in the pathophysiology of PAH. Many of the features of clinical PAH are consequences of dysregulation of endothelial cell signalling, which includes pulmonary inflammation, oxidative stress, proliferation, and accumulation of inflammatory cells (Evans et al., 2021). The results above demonstrated that haemoglobin can induce hAPECs to have these characteristics, such as increased release of inflammatory markers, elevated ROS production, increased proliferation and activation of endothelial cells that leads to recruitment of inflammatory cells. Moreover, is thought the initial trigger for the development of PAH is a combination of genetic and environmental factors that leads to endothelial cell injury (Ranchoux et al., 2018).

6.3.2 Limitations

The main limitation of this chapter is the use of western blotting (WB) to detect and identify some of the proteins of interest. To have the best accuracy possible, reagents and experimental design were carefully optimised and streamlined to ensure reproducible results. Detection of CD163 was very difficult, at the beginning the blot were completely blank, therefore 3 different antibodies were tested and only one was able to detect CD163 on a blot, however due to time constrain replication of these western blots for quantification (densitometry) was not possible. Detection of ICAM-1 and VCAM-1 was also attempted by western

blotting and with the antibodies available detection was not accomplished by western blotting. To overcome this issue flow cytometry was used to detect and quantify these protein in hPAECs.

7. Chapter 7 - General Discussion

7.1 197The biological context of the iron regulatory ferroportin/hepcidin axis

Iron is essential for all aerobic life as it required for multiple biological processes involving oxygen utilisation such as oxygen transport and mitochondrial respiration. Iron is a limited but also potentially reactive resource that therefore requires strict control and management. Excess iron in specific compartments can be toxic to tissues and cells, both directly, or as is more often the case, through the generation of damaging reactive oxygen species which can inflict damage to biomolecules including DNA, proteins and lipids; iron deficits can be similarly deleterious. Consequently, when homeostatic control of iron resources is compromised there are potential negative implications ranging from organelle and cellular dysfunction up to whole organ and body wide consequences. Therefore, tight regulation of iron homeostasis is required at both systematic and cellular levels. Cellular iron is mainly regulated by the iron regulatory proteins (IRP 1 and 2), these RNA binding proteins, integrated with iron sensing mechanisms, regulate proteins involved in iron homeostasis (Recalcati et al., 2010). Systematically iron is mainly controlled by the ferroportin/hepcidin axis. Hepcidin is a small peptide hormone that negatively regulates the iron-exporter ferroportin located on cell membranes. This axis was firstly thought to be only expressed in tissues/cells involved in iron recycling and homeostasis such as macrophages, hepatocytes and enterocytes (Sangkhae and Nemeth, 2017). However, more recently the axis has now been found in other cell types including pulmonary artery smooth muscle cells (Ramakrishnan et al., 2018b), cardiomyocytes (Lakhal-Littleton et al., 2015), retinal and brain vascular

endothelial cells (Baumann et al., 2019), demonstrating the possibility of localised control beyond classical concepts of iron turnover. Dysregulation of this axis has given rise to several disorders as described in section 1.2.4.5 demonstrating further the importance of homeostatic control.

7.2 The ferroportin/hepcidin axis is expressed in hPAECs

The main purposed theme of this thesis was to investigate the role of iron homeostasis and the hepcidin/ferroportin axis in relation to the pathogenesis of PAH. PAH is a rare disease characterised by persistent pulmonary vascular remodelling causing obliteration of the vasculature increasing mean pulmonary artery pressure and vascular resistance, leading to right heart failure and death (Quatredeniers et al., 2021). The link between iron dysregulation and PAH is well stablished (Ruiter et al., 2011, Rhodes et al., 2011b): iron deficiency in PAH patients correlated with poor outcomes, increased disease severity, lower cardiac indices, higher pulmonary artery resistance and reduced 6-minute walk test (Viethen et al., 2014, Ruiter et al., 2011, Rhodes et al., 2011a). Moreover, hepcidin has been found to be elevated in IPAH patients independently of increased IL-6, which may impair iron regulation in these patients (Rhodes et al., 2011a). A clinical trial (NCT1447628) of IPAH and HPAH patients showed that iron repletion by administration of a single infusion was well tolerated, however it did not provide any clinical benefit (Howard et al., 2021), suggesting that iron availability may not be the issue but impaired localised iron handling within the vasculature could be.

Previous studies by this laboratory have demonstrated that ferroportin and hepcidin are expressed in hPASMCs and that treatments of these cells with hepcidin caused increase in iron accumulation and cell proliferation. Proliferation of hPASMCs was abated by a ferroportin stabilising antibody (Ramakrishnan et al., 2018b) exemplifying that manipulation of the ferroportin/hepcidin axis can lead to PAH phenotype. The entirely novel studies presented in Chapter 3, sectiction 3.2.1 demonstrate that the hepcidin/ ferroportin axis is also present in hPAECs; ferroportin mRNA and protein expression are clearly demonstrated (figure 3-2), and additionally IL-6, a known positive regulator for hepcidin production and release, caused gene expression of hepcidin mRNA and also hepcidin release from these cells (figure 3-3).

Unexpectedly, hepcidin treatment of hPAECs upregulated *HAMP* (hepcidin gene) mRNA expression (figure 3-5 A and B) and ELISA analysis of hPAECs supernatants after hepcidin treatment showed a substantial increase in hepcidin release (figure 3-5 C). One important issue of measuring hepcidin release in hPAECs supernatants after hepcidin treatment, was that newly synthesised hepcidin could not be differentially detected from residual hepcidin treatments. In order to resolve this issue media containing the concentration of hepcidin used for treatments was incubated in wells without hPAECs for the same time period and under the same conditions as used for cell incubations. The hepcidin detected in these cell free control wells demonstrated at 75-fold reduced in measurable levels detected in comparison to the wells containing hepcidin treated hPAEC cells, which suggested a limited half-life for free hepcidin under these conditions and further that endogenous production and release of hepcidin

from hepcidin treated hPAECs was occurring. To investigate hepcidin half-life further additional experiments were undertaken wherein hepcidin was dissolved in water and PBS at the same concentrations as for cell treatments (results not shown, as hepcidin could not be detected by the assay kit used), however in these experiments hepcidin was not detected probably due to the short half-life of hepcidin (Ruchala and Nemeth, 2014, Xiao et al., 2010). Autocrine regulation of hepcidin has previously been demonstrated in macrophages, monocytes and cardiomyocytes (Lakhal-Littleton et al., 2016, Collins et al., 2008, Theurl et al., 2008). The results presented in these studies strongly suggest this is also the case for hPAECs. Interestingly, hepcidin treatment of hPAECs also upregulated the release of IL-6 (figure 3-4), which could also be a contributing factor in the autocrine loop observed.

Hepcidin and IL-6 treatments of hPAECs also increased the release of the cytokine interleukin-8 (IL-8) and of the chemokine monocyte chemoattractant protein-1 (MCP-1), and as mentioned above hepcidin also elevated IL-6; all potent mediators of inflammation. Inflammation has been recognised as an area of interest in PAH and the immune system has been proposed as a key contributor to the pathobiology of PAH (Frid et al., 2020). The cytokine IL-6 is found to be elevated in PAH animal models and patients and serves as a marker of right ventricular dysfunction in PAH (Prins et al., 2018). Overexpression of IL-6 in a mouse model reproduced the muscularisation and proliferative arteriopathy seen in PAH patients (Steiner et al., 2009). IL-8 has been shown to induce migration of human airway smooth muscle cells (hASMC), and this response was abolished by neutralising antibodies against IL-8 receptors CXCR1 and CXCR2

(Govindaraju et al., 2006). Proliferation and migration of human bronchial smooth muscle cells (hBSMCs) was increased after exposure to IL-8, and the effects were inhibited by neutralising IL-8 (Tang et al., 2013). Studies have indicated that MCP-1 contributes to VEGF-mediated angiogenesis and increased vascular permeability (Yamada et al., 2003), characteristics of PAH. In addition, a study demonstrated that MCP-1 mediates the angiogenic effect of TGF-β by recruiting VSMCs and mesenchymal precursors to endothelial cells and this response was attenuated by MCP-1 inhibition (Ma et al., 2006). This study has provide compelling evidence that hepcidin treatment of hPAECs cause these cells to release potent mediators of inflammation and stimulators of cell migration and proliferation, which could lead to the hyper proliferative phenotype of PAH hPASMCs. Further, experiments are necessary to determine whether the release of these mediators could influence hPASMC proliferation and migration.

7.2.1 The effects of IL-6 and hepcidin in hPAECs proliferation

Histological findings of PAH patients' lung tissues show remodelling of small pulmonary arteries and arterioles with differing degrees of endothelial cell proliferation and hypertrophy of smooth muscle cells (Jonigk et al., 2011). Proliferation analysis of hPAECs by two assays demonstrated that IL-6 significantly increased proliferation of these cells (figure 3-6), as expected. A study of human endothelial progenitor cells (HEPC) revealed that IL-6 stimulated HEPC proliferation and this increase was attenuated by a neutralizing antibody against IL-6 (Fan et al., 2007). IL-6 overexpression in mice resulted in distal muscularisation and plexogenic arteriopathy similar to pathological lesions found in PAH patients, suggesting that IL-6 stimulates proliferation of endothelial cells

and smooth muscle cells (Steiner et al., 2009, Furuya et al., 2010). In contrast to IL-6 based studies, hepcidin treatment of hPAECs did not stimulate proliferation in these cells (figure 3-7), which suggests that IL-6 proliferation is independent of the ferroportin/hepcidin axis. Steiner et al. (2009), observed that IL-6 increased the expression of vascular endothelial growth factor (VEGF) and vascular endothelial growth factor receptor 2 (VEGFR2) in PAECs of mice, which ultimately caused the increased proliferation seen. Interestingly, hepcidin has been shown to stimulate hPASMCs proliferation (Ramakrishnan et al., 2018b) contrasting with the results for hPAECs presented in chapter 3. Taken together these findings suggest that manipulation of the ferroportin/hepcidin axis generates different responses between these two cell types.

It could be postulated that the proliferative response of hPASMCs resulting from hepcidin exposure is caused by an increase of intracellular iron facilitated by loss of ferroportin mediated cellular iron export. hPAECs on the other hand may be better adapted to cope with this raised level of intracellular iron levels. This notion is supported by observations relating to mitochondrial function between cell types in response to hepcidin challenge. Whereas mitochondrial metabolism showed pronounced disturbance in hPASMCs (figure 5-2), this was not replicated in hPAECs where mitochondria metabolism remained unchanged (figure 3-9 and 3-10). Importantly, mitochondria have a critical role in cellular iron metabolism and are a major hub of iron utilisation and accumulation (Paul et al., 2017). Iron overload in cells is problematic due to the ability of iron to catalyse damaging ROS formation, which can then damage mitochondria. A study of rat cardiac myocytes exposed to high iron levels was shown to cause damage to

mitochondrial DNA (mtDNA), reducing the respiratory function (Gao et al., 2009). Previous studies by this laboratory have demonstrated that hepcidin treatment of hPASMCs significantly increased mitochondrial ROS levels; conversely there were no changes in mitochondrial ROS in hPAECs after hepcidin treatment. Furthermore, hepcidin challenge in hPASMC caused mitochondrial fragmentation, potentially linked to elevated ROS production; in contrast, hPAECs mitochondrial morphology did not change after exposure to hepcidin (figure 5-1) (Issitt et al., 2019). Mitochondrial function has been extensively studied in cancer, and overall mitochondrial fragmentation is identified in many cancers, due to the reduced oxidative metabolism in these mitochondria preserving glycolytic intermediates that can be used for cancer proliferation (Dai and Jiang, 2019). Previously, in another study from this laboratory, it was shown that conditioned media from hPAECs treated with hepcidin increased hPASMCs migration (Pedersen et al., 2018) and proliferation (Shackshaft et al., 2017). To evaluate the effect of hPAECs conditioned media in hPASMC mitochondrial metabolism, oxygen consumption rate (OCR) was measured. The results showed a shift to a more energetic phenotype chapter 5 (figure 5-3), which may explain the increase in migration and proliferation of PASMCs observed. However, further studies are needed to investigate if hPAEC conditioned media with hepcidin also causes hPASMC mitochondria fragmentation. Mitochondria functional dysregulation has been increasingly recognised as possible driver of PAH (Marshall et al., 2018); the studies presented in this thesis provide evidence that modulation of the hepcidin/ferroportin axis can cause changes in the

mitochondrial function of hPASMCs, which may be of relevance to the PAH phenotype.

7.3 Hepcidin and IL-6 both downregulates the expression of BMPR2 in hPAECs, mimicking pulmonary arterial hypertension phenotype

Alterations in the *BMPR2* gene were the first genetic variants linked to pathophysiology of PAH. Perturbed BMPR2 signalling it is also present in the lung vasculature of idiopathic PAH patients (Happé et al., 2020, Atkinson et al., 2002). The penetrance of BMPR2 mutations is incomplete, estimated to be 14% for males and 42% for females (Larkin et al., 2012), therefore BMPR2 mutations are thought to be disease permissive rather than pathogenic. This gives rise to the "second hit" hypothesis, whereby mutations in other genes, together with environmental factors, will lead to the development of PAH.

The two main pathways for the regulation of hepcidin synthesis are (1) the BMP-SMAD pathway that it is regulated by iron levels and (2) through inflammation via the activation of the JAK-STAT pathway by IL-6. The studies presented in chapter 4 demonstrate that both IL-6 and hepcidin downregulate BMPR2 mRNA expression (figure 4-1) and protein expression (figure 4-2). These results were expected for IL-6 as a study by Brock et al. (2009) showed that IL-6 downregulate BMPR2 expression via a novel STAT3-microRNA cluster 17/92 in a posttranscriptional manner. However, Differing from Brock et al. (2009), the studies presented here show downregulation of BMPR2 mRNA by IL-6, which suggests a different mechanism of regulation of BMPR2. Further studies will be required to determine the identification of these mechanisms. Downregulation

of BMPR2 protein by hepcidin was demonstrated in hPAECs (chapter 4); these entirely novel findings suggest that a negative feedback mechanism is operational, given the role of BMPR2 in the regulation of hepcidin.

Paradoxically, due to BMPR2 involvement in hepcidin regulation, hepcidin synthesis would be expected to be reduced; however, the results presented in chapter 4 demonstrated a significant increase of hepcidin from hPAECs after hepcidin treatment, implying the possibility of redundancy for BMPR2 in hepcidin synthesis. A study by Mayeur et al. (2014a) showed that mice hepatocytes that lacked either BMPPR2 or ActR2a (another BMP type II receptor) exhibited a reduction in hepcidin mRNA and hepcidin serum levels and increased tissue and serum iron levels. However, deficiency of both receptors caused a marked reduction of hepcidin gene expression and serum levels leading to severe iron overload. This demonstrated that these BMP type II receptors have redundant roles in hepcidin regulation. Activation of the canonical BMP-SMAD pathway leads to SMAD 1/5 signalling, therefore a reduction in BMPR2 protein would imply a reduction of SMAD 1/5 signalling. The results presented in this study show that hepcidin treatment of hPAECs increased phosphorylation SMAD 1/5 chapter 4 (figure 4-3); moreover, BMPR2 knockdown caused an increase in SMAD1, SMAD5 and IDs mRNA expression (figure 4-8), albeit not significantly. These results suggest that hepcidin was able to cause the activation of this signalling pathway, which would explain the increase in hepcidin synthesis.

A study by Gore et al. (2014) has demonstrated that the loss of BMP signalling leads to an increase of TGFβ-SMAD signalling; when compared to controls, iPAH

patients exhibited higher levels of TGF-β and increased levels of activin receptor-like kinase 1 (ALK-1, a type of TGFβ receptor) and endoglin (another receptor of TGFβ family of receptors), predominately in endothelial cells. TGFβ signalling is involved in the regulation of mechanobiological aspects of the cell and its signalling has been implicated in ECM (extracellular matrix) activation and stiffness (Wipff and Hinz, 2008, Buscemi et al., 2011). In another study by Hiepen et al. (2019) demonstrated that BMPR2 deficient endothelial cells, when stimulated with BMP6, which traditionally signals via the ALK2/3 with BMPR2, SMAD1/5 phosphorylation was significantly increased. Furthermore, they also showed that in BMPR2 deficient cells, the signalling occurred by the formation of heteromeres comprising BMP and TGF-β receptors. These studies provide supporting evidence that the loss of BMPR2 can be redundant and/or have a compensatory mechanism for its signalling. Indeed, Sotatercept, a novel fusion protein that acts as TGF-β ligand trap to restore the balance of TGF-β signalling have been trialled in PAH patients. The PULSAR phase 2 trial results showed that Sotatercept reduced pulmonary vascular resistance among PAH patients and improved 6-minute walk distance (Humbert et al., 2021). This new therapy provides further evidence that the loss of balanced BMP/TGF-β signalling has an important role in the development of PAH (Hiepen et al., 2019).

To better understand the effects of IL-6 and hepcidin on downstream targets of BMP-SMAD signalling, the expression of the family of inhibitor of differentiation (Id 1, 2, 3 and 4) proteins was evaluated in hPAECs after treatment. Id proteins are mainly regulated by the BMP-SMAD pathway in endothelial cells (Valdimarsdottir et al., 2002). These proteins are highly conserved with important

regulatory roles in several cellular processes (Ling et al., 2014). There is a growing interest on the involvement of Id proteins in cancer; increased expression of these proteins in cancer is associated with poor prognosis, metastasis, elevated angiogenesis and more importantly with regard to current studies, PAH (Forootan et al., 2007, Schindl et al., 2003). Id1 and Id 3 are associated with inhibition of cell differentiation, cell growth promotion and tumour metastasis and were shown to be associated with poor clinical outcome and treatment resistance in lung adenocarcinoma (Castañon et al., 2013). In the studies presented herein, chapter 4, mRNA transcription of all four Id proteins was upregulated by hepcidin (figure 4-5) and IL-6 (figure 4-6) after 3 hours treatment. Moreover Id1 protein expression was elevated after 24h treatment with both IL-6 and hepcidin (figure 4-6). To further illustrate that the upregulation of these proteins was linked to reduced signalling of BMPR2, mRNA transcription of the four Id proteins was examined after BMPR2 knockdown (figure 4.7).Results showed a significant increase of Id1 and Id2 and a trend towards increase for both Id3 and Id4 (figure 4.8). Elevated expression of Id1 protein by BMPR2 loss in hPAECs has been been described previously by Awad et al. (2016). Furthermore increased expression of Id1 by BMPR2 deficiency has been demonstrated in human lung microvascular endothelial cells (Star et al., 2013). Id3 upregulation was also seen in two BMPR2-deficent endothelial cell models, where one expressed a single copy of truncated BMPR2 and in the other where a single copy of BMPR2 was deleted, after BMP6 treatment (main agonist ligand for hepcidin synthesis) (Hiepen et al., 2019). Contrary to these studies and the one presented here in hPAECs, loss of BMPR2 in hPASMC caused reduction of Id1 and Id3 protein was

seen as shown in two different studies, moreover, loss of Id1 has been linked to increased proliferation of hPASMC (Yang et al., 2013, Li et al., 2018). This contrasting response between hPAECs and hPASMCs, relating to the loss of BMPR2, demonstrates that BMP-SMAD signalling may function differently in each cell type and this must be accounted for when studying this pathway in the context of PAH.

7.4 A role for haemolysis in PAH

Studies have indicated that sub-clinical haemolysis is present in IPAH and HPAH patients (Souza et al., 2009a, Decker et al., 2011, Fox et al., 2012) and could be a contributory component to the development of PAH. A observational study by Nakamura et al. (2017) showed decreased levels of haptoglobin in PAH patients and that haptoglobin levels were inversely correlated with pulmonary artery pressure. Decrease levels of haptoglobin suggests the existence of subclinical haemolysis, including in the pulmonary vasculature of these patients. The studies undertaken as described in chapter 6 have demonstrated for the first time the presence of CD163, a haemoglobin scavenger receptor, in hPAECs. Real-time PCR analysis demonstrated a concentration dependent increase of CD163 transcription in response to haemoglobin treatment (figure 6-1), and western blot analysis appears to support this (figure 6-2). CD163 is a scavenger receptor that has the functions to clear haemoglobin from the extracellular compartment and was previously thought to be exclusively expressed in the surface of monocytes and macrophages (Onofre et al., 2009). The presence of CD163 on hPAECs offers a means for cellular uptake of iron containing haemoglobin and potentially provides a driver for intracellular iron retention, which can be further exacerbated

by the increased release of hepcidin by hPAECs caused by haemoglobin exposure (figure 6-6). IL-6 could be involved in these processes as increased expression is also seen (figure 6-4A).

Excess intracellular iron has been linked to oxidative stress as it disrupts redox homeostasis leading to the production damaging ROS. (Galaris et al., 2019). ROS production was observed to increase in hPAECs treated by haemoglobin in a concentration dependent manner (figure 6-8). The main enzymatic sources of ROS $O_2^{\cdot -}/H_2O_2$) are the transmembrane NADPH oxidases (NOXs); haemoglobin challenge in hPAECs upregulated mRNA transcription and protein synthesis of NOX2 (figure 6-9), providing further evidence that haemoglobin indeed promotes the release of ROS in hPAECs. Increased levels of intracellular iron have been shown to promote recruitment of monocytes to the endothelium and iron chelation was shown to prevent the activation of endothelial cells after iron challenge (Kartikasari et al., 2004). Furthermore, in vivo experiments showed that iron chelation inhibited ROS mediated expression of adhesion molecules such as ICAM-1 and VCAM-1. This is most likely due to the ability of intracellular iron to regulate the activation of transcription factors involved in the expression of these adhesion molecules (Li and Frei, 2006, Galaris et al., 2019). Flow cytometry analysis of hPAECs after treatment with haemoglobin showed increased expression of ICAM-1 and VCAM-1 (figure 6-7). ICAM-1 and VCAM-1 are adhesion molecules that are expressed in the surface of endothelial cells in response to inflammation, and are responsible for the recruitment of immune cells to the endothelium (Pinte et al., 2016). A characteristic of PAH is vascular

remodelling that includes plexiform lesions, in which immune cells such as monocytes, macrophages and dendritic cells are found (Schermuly et al., 2011b).

The current study, has further shown that hPAEC proliferation was increased in a time dependent manner when exposed to haemoglobin (figure 6-10 and 6-11 A), thus suggesting a potential role for haemoglobin in proliferative responses that may have contribute to pulmonary artery remodelling. More importantly, this increase of proliferation occurred over time, suggesting chronic exposure to haemoglobin could drive the development of a PAH phenotype. In support of this notion, Irwin et al. (2015) using a rodent model of pre-clinical chronic extracellular Hb-mediated progression of pulmonary hypertension, showed that exposure to haemoglobin for 5 weeks caused pulmonary vascular inflammation, systemic IL-6 release, medial thickening of pulmonary arteries, small arterial muscularisation and right-ventricular hypertrophy.

As mentioned above, inflammation is a characteristic of PAH. In this regard, haemolysis and haemoglobin release may also have a role. For instance, animal model studies have shown that haemoglobin induced PAH increased the release of the cytokine IL-6 (Irwin et al., 2015, Loomis et al., 2017); and previous results from this laboratory have also shown an increase in IL-6 release when hPAECs were exposed to haemoglobin for 24h (Ramakrishnan et al., 2016). Here, exposure of hPAECs to haemoglobin caused mRNA upregulation of the cytokines IL-6, IL-8 and MCP-1 (figure 6-4) and significant increases of these cytokines was measurable in cell supernatants (figure 6-5). These cytokines have been shown to modulate hPAEC and hPASMC proliferation and migration as

discussed in section 7.2.1. Interestingly, haemoglobin has been shown to induce vascular cell damage that can indirectly activate the toll-like receptor 9 (TLR9) as demonstrated with a murine model (Loomis et al., 2017). Furthermore, the TLR family of 11 proteins that are expressed on many cell types, including endothelial cells, are key proteins in the innate immune response through recognition of pathogen- and danger-associated molecular patterns (PAMPs/DAMPs). DAMPs are endogenous molecules that can initiate and maintain an inflammatory response.

Loomis et al. (2017) showed that CpG DNA motifs released by membrane damage caused by oxidative stress, a consequence of haemolysis, can stimulate TRL9 and consequently increase IL-6 expression. IL-6 mRNA expression was increased in rPAEC when exposed to either haemoglobin or CpG DNA for 24h and expression was inhibited when co-treated with a TLR9 inhibitor and haptoglobin. They also showed in co-culture of rPAEC and rPASMC that haemoglobin induced TLR9 regulated IL-6 pathway activity. In addition, rPAEC treated with either CpG DNA or haemoglobin resulted in a higher metabolic activity in rPASMC compared to vehicle control. Furthermore, this increase in metabolic activity was down-regulated when rPAEC were treated with haemoglobin together with an IL-6 neutralizing antibody. These results support previous work undertaken within this laboratory in which conditioned media from hPAECs treated with haemoglobin (10 μM) increased hPASMC migration (Shackshaft et al., 2017).

7.5 Conclusion

The findings presented here provide compelling evidence that disrupted iron homeostasis has an important role in the pathophysiology of PAH. The iron-regulatory axis formed by ferroportin and hepcidin is present in both hPAECs and hPASMCs that allows for local iron homeostatic control and modulation of this axis in these cells presents a PAH like phenotype (figure 7-1) that could contribute to vascular remodelling. Interestingly, hepcidin and IL-6 caused aberrant-BMPR2 signalling, in which BMPR2 protein is downregulated; however, downstream pathways of BMPR2 remain active. Furthermore, the results presented in this thesis supports the hypothesis that subclinical haemolysis may have a critical role to the pathophysiology of the vascular remodelling found in PAH (figure 7-2).

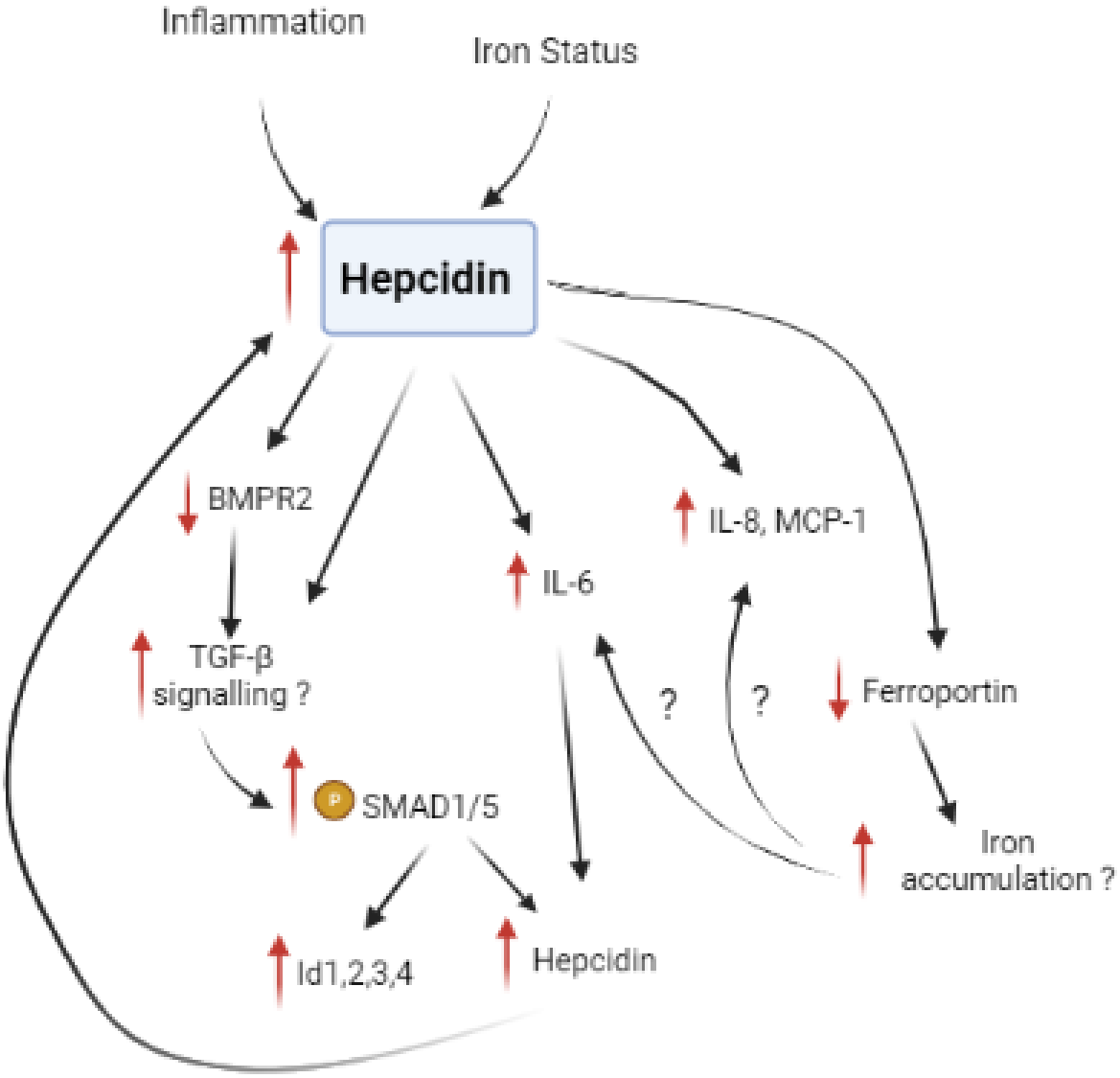

Figure 7-1 Diagram showing the effect of hepcidin in hPAECs that could contribute to the development of PAH*. Elevated levels of serum hepcidin has been identified in PAH patients. Hepcidin downregulated BMPR2, however SMAD1/5 phosphorylation was increase, which increased expression of Id 1,2,3,4 proteins and hepcidin. This signalling may occur by activation of other TGF-β receptors to compensate for the loss of BMPR2. Upregulation of hepcidin cause degradation and internalisation of ferroportin that could lead to iron accumulation. Increased iron retention has been linked to activation of transcription factors that will cause the release of inflammatory markers, in this case IL-6, IL-8 and MCP-1. IL-6 is an agonist of hepcidin, which would lead to more hepcidin synthesis. Figure created in BioRender.*

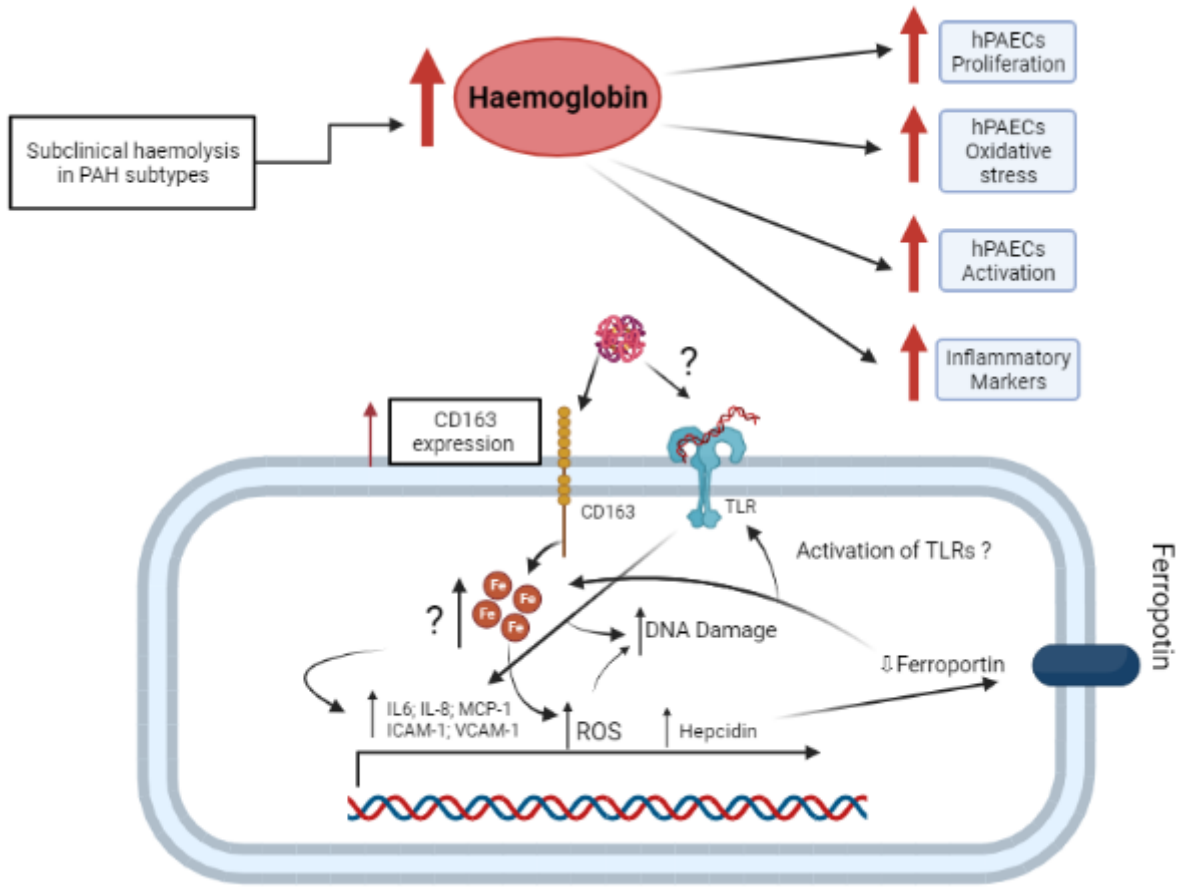

Figure 7-2 Summary of haemoglobin effects in hPAECs. *Haemoglobin treatment of hPAECs caused an increase of cell proliferation, endothelial activation, oxidative stress and inflammation markers. CD163 was found to be expressed in hPAECs that provides a route for haemoglobin uptake and increase in intracellular iron. Elevated levels of intracellular iron in turn could lead to the activation of transcription factors for the expression of the inflammatory markers IL-6, IL-8 and MCP-1 also for the adhesion molecules ICAM-1 and VCAM-1. Haemoglobin also caused and increase in reactive oxygen species (ROS), which in turn can cause DNA damage and activation of TLR signalling, which will activate transcription of inflammatory markers. It is also possible that haemoglobin itself could activate TLR signalling. Hepcidin synthesis was also increased by haemoglobin, which would lead to internalisation of ferroportin causing iron retention.*

7.6 Limitations of this study

There are many limitations to be considered in this study. Firstly, cells have a complex environment with many signalling pathways working together. Furthermore, when they are in the body cells interact with other cells, which may

influence their responses. Therefore, any conclusions need to be made with caution. The main limitation of this study is that it was not performed in low oxygen tensions; the pulmonary artery is a low oxygen environment as it conveys deoxygenated blood into the lungs; moreover hypoxia has a critical role in PAH and also iron regulation, which warrants further examination in the context of these studies. Initially hypoxia studies were part of this study, however the equipment available to induce hypoxia was not appropriate, and hypoxia state was not reached.

Another limitation was that intracellular iron could not be easily measured. Two commercially available kits from ABCAM (ab8336) and sigma (MAK025) were tested; however, they were not sensitive enough to measure intracellular iron in our models. Different cell densities were also tested with these kits, however primary cells were used for this study and expanding them to have necessary numbers for these kits was not feasible. The calcein-AM method, a widely used method to assay intracellular iron, was also tested. However it required a lot of troubleshooting to adapt to the equipment available in the lab and due to time constrains was abandoned

7.7 Future Works

This study provides an insight into the potential role of iron homeostasis, more importantly the role of the hepcidin/ferroportin axis, in pulmonary vascular cells and how disruption of iron homeostasis linked to this axis can lead to a PAH phenotype. However more work is required to strengthen our understanding of

iron regulation in PAH. Some future experiments that will be useful are discussed below.

7.7.1 Hypoxia studies

As mentioned above in the limitations section, the lack of low oxygen experiments is a shortcoming. The main issue was the unavailability of the correct equipment. Fortunately, our group has started a collaboration with a group expert in hypoxia, and now have all the required equipment to perform these experiments going forward.

7.7.2 Quantification of labile iron pool and total iron

Quantification of intracellular iron was difficult to determine with available commercial methods. However a protocol published by Abbasi et al. (2021) describes a new method to determined iron concentration, the unified-ferene assay a colorimetric method that enables a 2-in1 quantification of both labile iron and total iron from cultured cells.

7.7.3 Ferroportin knockdown experiments

A novel part of this study was the effect of hepcidin in downregulation of BMPR2 expression. In the present study it is not possible to stablish if these effects are caused degradation of ferroportin after hepcidin treatment, or if it is hepcidin acting in another, yet to determine, pathway. A simple way to deconvolute this issue would be to knockdown ferroportin in hPAECs and evaluate BMPR2 expression.

7.7.4 Perform studies with blood outgrowth endothelial cells (BOECs) and tissues samples derived from patients with PAH

To explore if these results translate to a PAH disease setting, BOECs derived from patients with known BMPR2 mutations would provide a more in-depth analysis of disrupted BMP signalling as it pertains to the hepcidin/ ferroportin axis in PAH. Additionally, a comparison with BOECs derived from patients without BMPR2 mutations would provide a more detailed understanding. The use of transplant and post-mortem lung tissue from PAH patients could be used to assess distribution of hepcidin, ferroportin, iron, mitochondrial morphology, mitochondrial iron status and other identified relevant indices that are observable by appropriate staining and confocal imaging.

8. References

ABBASI, U., ABBINA, S., GILL, A., BHAGAT, V. & KIZHAKKEDATHU, J. N. 2021. A facile colorimetric method for the quantification of labile iron pool and total iron in cells and tissue specimens. *Scientific Reports,* 11**,** 6008.

ADAN, A., ALIZADA, G., KIRAZ, Y., BARAN, Y. & NALBANT, A. 2017. Flow cytometry: basic principles and applications. *Critical Reviews in Biotechnology,* 37**,** 163-176.

ADAN, A., KIRAZ, Y. & BARAN, Y. 2016. Cell Proliferation and Cytotoxicity Assays. *Curr Pharm Biotechnol,* 17**,** 1213-1221.

AHMED, M. H., GHATGE, M. S. & SAFO, M. K. 2020. Hemoglobin: Structure, Function and Allostery. Springer International Publishing.

ANDERSON, G. J. & FRAZER, D. M. 2017. Current understanding of iron homeostasis. *The American Journal of Clinical Nutrition,* 106**,** 1559S-1566S.

ANDREWS, N. C. & SCHMIDT, P. J. 2007. Iron Homeostasis. *Annual Review of Physiology,* 69**,** 69-85.

ANDRUSKA, A. & SPIEKERKOETTER, E. 2018. Consequences of BMPR2 Deficiency in the Pulmonary Vasculature and Beyond: Contributions to Pulmonary Arterial Hypertension. *International Journal of Molecular Sciences,* 19.

ARCINIEGAS, E., FRID, M. G., DOUGLAS, I. S. & STENMARK, K. R. 2007. Perspectives on endothelial-to-mesenchymal transition: potential contribution to vascular remodeling in chronic pulmonary hypertension. *Am J Physiol Lung Cell Mol Physiol,* 293**,** L1-8.

ATKINSON, C., STEWART, S., UPTON, P. D., MACHADO, R., THOMSON, J. R., TREMBATH, R. C. & MORRELL, N. W. 2002.

Primary pulmonary hypertension is associated with reduced pulmonary vascular expression of type II bone morphogenetic protein receptor. *Circulation,* 105**,** 1672-8.

AWAD, K. S., ELINOFF, J. M., WANG, S., GAIRHE, S., FERREYRA, G. A., CAI, R., SUN, J., SOLOMON, M. A. & DANNER, R. L. 2016. Raf/ERK drives the proliferative and invasive phenotype of BMPR2-silenced pulmonary artery endothelial cells. *Am J Physiol Lung Cell Mol Physiol,* 310**,** L187-201.

BALL, M. K., WAYPA, G. B., MUNGAI, P. T., NIELSEN, J. M., CZECH, L., DUDLEY, V. J., BEUSSINK, L., DETTMAN, R. W., BERKELHAMER, S. K., STEINHORN, R. H., SHAH, S. J. & SCHUMACKER, P. T. 2013. Regulation of Hypoxia-induced Pulmonary Hypertension by Vascular Smooth Muscle Hypoxia-Inducible Factor-1α. *American Journal of Respiratory and Critical Care Medicine,* 189**,** 314-324.

BARAN, P., HANSEN, S., WAETZIG, G. H., AKBARZADEH, M., LAMERTZ, L., HUBER, H. J., AHMADIAN, M. R., MOLL, J. M. & SCHELLER, J. 2018. The balance of interleukin (IL)-6, IL-6·soluble IL-6 receptor (sIL-6R), and IL-6·sIL-6R·sgp130 complexes allows simultaneous classic and trans-signaling. *Journal of Biological Chemistry,* 293**,** 6762-6775.

BARCELLINI, W. & FATTIZZO, B. 2015. Clinical Applications of Hemolytic Markers in the Differential Diagnosis and Management of Hemolytic Anemia. *Disease Markers,* 2015**,** 7.

BARRINGTON, P., SHEETZ, M. J., CALLIES, S., WATERS, D. G., BERG, P. H., PAPPAS, D., MARBURY, T. C., DECKER, B. S. & BERG, J. K. 2016. Safety, Tolerability, Pharmacokinetics and Pharmacodynamics of an Anti-Ferroportin Antibody in Patients with Anemia Due to Chronic Renal Failure. *Blood,* 128**,** 1280.

BAUMANN, B. H., SHU, W., SONG, Y., SIMPSON, E. M., LAKHAL-LITTLETON, S. & DUNAIEF, J. L. 2019. Ferroportin-mediated iron export from vascular endothelial cells in retina and brain. *Experimental Eye Research,* 187**,** 107728.

BILLESBØLLE, C. B., AZUMAYA, C. M., KRETSCH, R. C., POWERS, A. S., GONEN, S., SCHNEIDER, S., ARVEDSON, T., DROR, R. O., CHENG, Y. & MANGLIK, A. 2020. Structure of hepcidin-bound ferroportin reveals iron homeostatic mechanisms. *Nature,* 586**,** 807-811.

BORETTI, F. S., BUEHLER, P. W., D'AGNILLO, F., KLUGE, K., GLAUS, T., BUTT, O. I., JIA, Y., GOEDE, J., PEREIRA, C. P., MAGGIORINI, M., SCHOEDON, G., ALAYASH, A. I. & SCHAER, D. J. 2009. Sequestration of extracellular hemoglobin within a haptoglobin complex decreases its hypertensive and oxidative effects in dogs and guinea pigs. *J Clin Invest,* 119**,** 2271-80.

BOUTET, K., MONTANI, D., JAÏS, X., YAÏCI, A., SITBON, O., SIMONNEAU, G. & HUMBERT, M. 2008. Review: Therapeutic advances in pulmonary arterial hypertension. *Therapeutic Advances in Respiratory Disease,* 2**,** 249-265.

BRISSOT, P., PIETRANGELO, A., ADAMS, P. C., DE GRAAFF, B., MCLAREN, C. E. & LORÉAL, O. 2018. Haemochromatosis. *Nature Reviews Disease Primers,* 4**,** 18016.

BRITTAIN, E. L., JANZ, D. R., AUSTIN, E. D., BASTARACHE, J. A., WHEELER, L. A., WARE, L. B. & HEMNES, A. R. 2014. Elevation of Plasma Cell Free Hemoglobin in Pulmonary Arterial Hypertension. *Chest*.

BROCK, M., TRENKMANN, M., GAY, R. E., MICHEL, B. A., GAY, S., FISCHLER, M., ULRICH, S., SPEICH, R. & HUBER, L. C. 2009. Interleukin-6 Modulates the Expression of the Bone Morphogenic Protein Receptor Type II Through a Novel

STAT3–microRNA Cluster 17/92 Pathway. *Circulation Research,* 104**,** 1184-1191.

BUEHLER, P. W., BAEK, J. H., LISK, C., CONNOR, I., SULLIVAN, T., KOMINSKY, D., MAJKA, S., STENMARK, K. R., NOZIK-GRAYCK, E., BONAVENTURA, J. & IRWIN, D. C. 2012. Free hemoglobin induction of pulmonary vascular disease: evidence for an inflammatory mechanism. *American journal of physiology. Lung cellular and molecular physiology,* 303**,** L312-L326.

BUSCEMI, L., RAMONET, D., KLINGBERG, F., FORMEY, A., SMITH-CLERC, J., MEISTER, J. J. & HINZ, B. 2011. The single-molecule mechanics of the latent TGF-β1 complex. *Curr Biol,* 21**,** 2046-54.

CAMASCHELLA, C., NAI, A. & SILVESTRI, L. 2020. Iron metabolism and iron disorders revisited in the hepcidin era. *Haematologica,* 105**,** 260-272.

CAMASCHELLA, C. & PAGANI, A. 2018. Advances in understanding iron metabolism and its crosstalk with erythropoiesis. *British Journal of Haematology,* 0.

CAMUS, S. M., DE MORAES, J. A., BONNIN, P., ABBYAD, P., LE JEUNE, S., LIONNET, F., LOUFRANI, L., GRIMAUD, L., LAMBRY, J. C., CHARUE, D., KIGER, L., RENARD, J. M., LARROQUE, C., LE CLESIAU, H., TEDGUI, A., BRUNEVAL, P., BARJA-FIDALGO, C., ALEXANDROU, A., THARAUX, P. L., BOULANGER, C. M. & BLANC-BRUDE, O. P. 2015. Circulating cell membrane microparticles transfer heme to endothelial cells and trigger vasoocclusions in sickle cell disease. *Blood,* 125**,** 3805-14.

CARDENAS-RODRIGUEZ, M., CHATZI, A. & TOKATLIDIS, K. 2018. Iron–sulfur clusters: from metals through mitochondria biogenesis to disease. *JBIC Journal of Biological Inorganic Chemistry,* 23**,** 509-520.

CASTAÑON, E., BOSCH-BARRERA, J., LÓPEZ, I., COLLADO, V., MORENO, M., LÓPEZ-PICAZO, J. M., ARBEA, L., LOZANO, M.

D., CALVO, A. & GIL-BAZO, I. 2013. Id1 and Id3 co-expression correlates with clinical outcome in stage III-N2 non-small cell lung cancer patients treated with definitive chemoradiotherapy. *Journal of Translational Medicine,* 11**,** 13.

CECCONI, M., JOHNSTON, E. & RHODES, A. 2006. What role does the right side of the heart play in circulation? *Critical Care,* 10**,** S5.

CHENG, R., DHORAJIA, V. V., KIM, J. & KIM, Y. 2022. Mitochondrial iron metabolism and neurodegenerative diseases. *NeuroToxicology,* 88**,** 88-101.

CLARK, D. P., PAZDERNIK, N. J. & MCGEHEE, M. R. 2019. Chapter 6 - Polymerase Chain Reaction. *In:* CLARK, D. P., PAZDERNIK, N. J. & MCGEHEE, M. R. (eds.) *Molecular Biology (Third Edition).* Academic Cell.

COLLINS, J. F., WESSLING-RESNICK, M. & KNUTSON, M. D. 2008. Hepcidin Regulation of Iron Transport. *The Journal of Nutrition,* 138**,** 2284-2288.

CONDON, D. F., NICKEL, N. P., ANDERSON, R., MIRZA, S. & DE JESUS PEREZ, V. A. 2019. The 6th World Symposium on Pulmonary Hypertension: what's old is new. *F1000Research,* 8**,** F1000 Faculty Rev-888.

COONS, J. C., POGUE, K., KOLODZIEJ, A. R., HIRSCH, G. A. & GEORGE, M. P. 2019. Pulmonary Arterial Hypertension: a Pharmacotherapeutic Update. *Curr Cardiol Rep,* 21**,** 141.

CORRADO, C. & FONTANA, S. 2020. Hypoxia and HIF Signaling: One Axis with Divergent Effects. *International journal of molecular sciences,* 21**,** 5611.

COTRONEO, E., ASHEK, A., WANG, L., WHARTON, J., DUBOIS, O., BOZORGI, S., BUSBRIDGE, M., ALAVIAN, K. N., WILKINS, M. R.

& ZHAO, L. 2015. Iron Homeostasis and Pulmonary Hypertension. *Circulation Research,* 116**,** 1680-1690.

CREED, S. & MCKENZIE, M. 2019. Measurement of Mitochondrial Membrane Potential with the Fluorescent Dye Tetramethylrhodamine Methyl Ester (TMRM). *In:* HAZNADAR, M. (ed.) *Cancer Metabolism: Methods and Protocols.* New York, NY: Springer New York.

DAI, W. & JIANG, L. 2019. Dysregulated Mitochondrial Dynamics and Metabolism in Obesity, Diabetes, and Cancer. *Frontiers in Endocrinology,* 10.

DAI, Z., LI, M., WHARTON, J., ZHU, M. M. & ZHAO, Y.-Y. 2016. Prolyl-4 hydroxylase 2 (PHD2) deficiency in endothelial cells and hematopoietic cells induces obliterative vascular remodeling and severe pulmonary arterial hypertension in mice and humans through hypoxia-inducible factor-2α. *Circulation,* 133**,** 2447-2458.

DANNEWITZ PROSSEDA, S., ALI, M. K. & SPIEKERKOETTER, E. 2020. Novel Advances in Modifying BMPR2 Signaling in PAH. *Genes,* 12**,** 8.

DASGUPTA, A., WU, D., TIAN, L., XIONG, P. Y., DUNHAM-SNARY, K. J., CHEN, K. H., ALIZADEH, E., MOTAMED, M., POTUS, F., HINDMARCH, C. C. T. & ARCHER, S. L. 2020. Mitochondria in the Pulmonary Vasculature in Health and Disease: Oxygen-Sensing, Metabolism, and Dynamics. *Comprehensive Physiology***,** 713-765.

DE CAMPOS, F. P. F. & BENVENUTI, L. A. 2017. Eisenmenger syndrome. *Autopsy & Case Reports,* 7**,** 5-7.

DECKER, I., GHOSH, S., COMHAIR, S. A., FARHA, S., TANG, W. H., PARK, M., WANG, S., LICHTIN, A. E. & ERZURUM, S. C. 2011. High levels of zinc-protoporphyrin identify iron metabolic abnormalities in pulmonary arterial hypertension. *Clin Transl Sci,* 4**,** 253-8.

DESHPANDE, C. N., RUWE, T. A., SHAWKI, A., XIN, V., VIETH, K. R., VALORE, E. V., QIAO, B., GANZ, T., NEMETH, E., MACKENZIE, B. & JORMAKKA, M. 2018. Calcium is an essential cofactor for metal efflux by the ferroportin transporter family. *Nature Communications,* 9.

DISTELMAIER, F., KOOPMAN, W. J. H., TESTA, E. R., DE JONG, A. S., SWARTS, H. G., MAYATEPEK, E., SMEITINK, J. A. M. & WILLEMS, P. H. G. M. 2008. Life cell quantification of mitochondrial membrane potential at the single organelle level. *Cytometry Part A,* 73A**,** 129-138.

DIVAKARUNI, A. S., PARADYSE, A., FERRICK, D. A., MURPHY, A. N. & JASTROCH, M. 2014. Analysis and Interpretation of Microplate-Based Oxygen Consumption and pH Data. Elsevier.

DORRONSORO, A., LANG, V., FERRIN, I., FERNÁNDEZ-RUEDA, J., ZABALETA, L., PÉREZ-RUIZ, E., SEPÚLVEDA, P. & TRIGUEROS, C. 2020. Intracellular role of IL-6 in mesenchymal stromal cell immunosuppression and proliferation. *Scientific Reports,* 10**,** 21853.

DRAKESMITH, H., NEMETH, E. & GANZ, T. 2015. Ironing out Ferroportin. *Cell Metabolism,* 22**,** 777-787.

ELSHAFAY, A., TRUONG, D. H., ABOELNAS, M. M., IDREES, H., METWALI, H. G., VUONG, N. L., SAAD, O. A., HIRAYAMA, K. & HUY, N. T. 2018. The Effect of Endothelin Receptor Antagonists in Patients with Eisenmenger Syndrome: A Systematic Review. *American Journal of Cardiovascular Drugs,* 18**,** 93-102.

EREMINIENE, E., KINDERYTE, M. & MILIAUSKAS, S. 2017. Impact of advanced medical therapy for the outcome of an adult patient with Eisenmenger syndrome. *Respir Med Case Rep,* 21**,** 16-20.

ERWIN, H. J. M. K., HAROLD, T., HANS, L. W. & DORINE, W. S. 2008. Hepcidin: from discovery to differential diagnosis. *Haematologica,* 93**,** 90-97.

ETZERODT, A. & MOESTRUP, S. K. 2013. CD163 and Inflammation: Biological, Diagnostic, and Therapeutic Aspects. *Antioxidants & Redox Signaling,* 18**,** 2352-2363.

EVANS, C. E., COBER, N. D., DAI, Z., STEWART, D. J. & ZHAO, Y.-Y. 2021. Endothelial cells in the pathogenesis of pulmonary arterial hypertension. *European Respiratory Journal,* 58**,** 2003957.

FAN, Y., YE, J., SHEN, F., ZHU, Y., YEGHIAZARIANS, Y., ZHU, W., CHEN, Y., LAWTON, M. T., YOUNG, W. L. & YANG, G.-Y. 2007. Interleukin-6 Stimulates Circulating Blood-Derived Endothelial Progenitor Cell Angiogenesis in vitro. *Journal of Cerebral Blood Flow & Metabolism,* 28**,** 90-98.

FAN, Y., YE, J., SHEN, F., ZHU, Y., YEGHIAZARIANS, Y., ZHU, W., CHEN, Y., LAWTON, M. T., YOUNG, W. L. & YANG, G.-Y. 2008. Interleukin-6 stimulates circulating blood-derived endothelial progenitor cell angiogenesis in vitro. *Journal of cerebral blood flow and metabolism : official journal of the International Society of Cerebral Blood Flow and Metabolism,* 28**,** 90-98.

FISHBANE, S., MATHEW, A. & VAZIRI, N. D. 2014. Iron toxicity: relevance for dialysis patients. *Nephrology Dialysis Transplantation,* 29**,** 255-259.

FOROOTAN, S. S., WONG, Y. C., DODSON, A., WANG, X., LIN, K., SMITH, P. H., FOSTER, C. S. & KE, Y. 2007. Increased Id-1 expression is significantly associated with poor survival of patients with prostate cancer. *Hum Pathol,* 38**,** 1321-9.

FOX, B. D., OKUMIYA, T., ATTAS-FOX, L., KASSIRER, M., RAVIV, Y. & KRAMER, M. R. 2012. Raised erythrocyte creatine in patients with pulmonary arterial hypertension--evidence for subclinical hemolysis. *Respir Med,* 106**,** 594-8.

FRID, M. G., THURMAN, J. M., HANSEN, K. C., MARON, B. A. & STENMARK, K. R. 2020. Inflammation, immunity, and vascular remodeling in pulmonary hypertension; Evidence for complement involvement? *Global Cardiology Science and Practice,* 2020.

FURUYA, Y., SATOH, T. & KUWANA, M. 2010. Interleukin-6 as a Potential Therapeutic Target for Pulmonary Arterial Hypertension. *International Journal of Rheumatology,* 2010**,** 1-8.

FUSO, L., BALDI, F. & DI PERNA, A. 2011. Therapeutic strategies in pulmonary hypertension. *Frontiers in pharmacology,* 2**,** 21-21.

GALARIS, D., BARBOUTI, A. & PANTOPOULOS, K. 2019. Iron homeostasis and oxidative stress: An intimate relationship. *Biochimica et Biophysica Acta (BBA) - Molecular Cell Research,* 1866**,** 118535.

GALIÈ, N., MANES, A. & BRANZI, A. 2003. Prostanoids for pulmonary arterial hypertension. *Am J Respir Med,* 2**,** 123-37.

GANZ, T. 2005. Hepcidin—a regulator of intestinal iron absorption and iron recycling by macrophages. *Best Practice & Research Clinical Haematology,* 18**,** 171-182.

GAO, G., LI, J., ZHANG, Y. & CHANG, Y.-Z. 2019. Cellular Iron Metabolism and Regulation. Springer Singapore.

GAO, J., ZHOU, Q., WU, D. & CHEN, L. 2021. Mitochondrial iron metabolism and its role in diseases. *Clinica Chimica Acta,* 513**,** 6-12.

GAO, X., CAMPIAN, J. L., QIAN, M., SUN, X. F. & EATON, J. W. 2009. Mitochondrial DNA damage in iron overload. *J Biol Chem,* 284**,** 4767-75.

GHIO, A. J. 2009. Disruption of iron homeostasis and lung disease. *Biochim Biophys Acta,* 1790**,** 731-9.

GHIO, S., FORTUNI, F., CAPETTINI, A. C., SCELSI, L., GRECO, A., VULLO, E., RAINERI, C., GUIDA, S., TURCO, A., GARGIULO, C. & OLTRONA VISCONTI, L. 2021. Iron deficiency in pulmonary arterial hypertension: prevalence and potential usefulness of oral supplementation. *Acta Cardiologica,* 76**,** 162-167.

GOLDENBERG, N. M., RABINOVITCH, M. & STEINBERG, B. E. 2019. Inflammatory Basis of Pulmonary Arterial Hypertension: Implications for Perioperative and Critical Care Medicine. *Anesthesiology,* 131**,** 898-907.

GOLEMBESKI, S. M., WEST, J., TADA, Y. & FAGAN, K. A. 2005. Interleukin-6 Causes Mild Pulmonary Hypertension and Augments Hypoxia-Induced Pulmonary Hypertension in Mice. *Chest,* 128**,** 572S-573S.

GONG, J.-N., ZHAI, Z.-G., YANG, Y.-H., LIU, Y., GU, S., KUANG, T.-G., XIE, W.-M., MIAO, R. & WANG, C. 2015. Serum Bilirubin and 6-min Walk Distance as Prognostic Predictors for Inoperable Chronic Thromboembolic Pulmonary Hypertension: A Prospective Cohort Study. *Chinese Medical Journal,* 128**,** 3125-3131.

GORDEUK, V. R., CASTRO, O. L. & MACHADO, R. F. 2016. Pathophysiology and treatment of pulmonary hypertension in sickle cell disease. *Blood,* 127**,** 820.

GORE, B., IZIKKI, M., MERCIER, O., DEWACHTER, L., FADEL, E., HUMBERT, M., DARTEVELLE, P., SIMONNEAU, G., NAEIJE, R., LEBRIN, F. & EDDAHIBI, S. 2014. Key role of the endothelial TGF-β/ALK1/endoglin signaling pathway in humans and rodents pulmonary hypertension. *PloS one,* 9**,** e100310-e100310.

GOVINDARAJU, V., MICHOUD, M.-C., AL-CHALABI, M., FERRARO, P., POWELL, W. S. & MARTIN, J. G. 2006. Interleukin-8: novel roles in human airway smooth muscle cell contraction and

migration. *American Journal of Physiology-Cell Physiology,* 291**,** C957-C965.

HAGAN, G., SOUTHWOOD, M., TREACY, C., ROSS, R. M., SOON, E., COULSON, J., SHEARES, K., SCREATON, N., PEPKE-ZABA, J., MORRELL, N. W. & RUDD, J. H. 2011. (18)FDG PET imaging can quantify increased cellular metabolism in pulmonary arterial hypertension: A proof-of-principle study. *Pulm Circ,* 1**,** 448-55.

HAN, H. 2018. RNA Interference to Knock Down Gene Expression. *Methods in molecular biology (Clifton, N.J.),* 1706**,** 293-302.

HAPPÉ, C., KURAKULA, K., SUN, X.-Q., DA SILVA GONCALVES BOS, D., ROL, N., GUIGNABERT, C., TU, L., SCHALIJ, I., WIESMEIJER, K. C., TURA-CEIDE, O., VONK NOORDEGRAAF, A., DE MAN, F. S., BOGAARD, H. J. & GOUMANS, M.-J. 2020. The BMP Receptor 2 in Pulmonary Arterial Hypertension: When and Where the Animal Model Matches the Patient. *Cells,* 9**,** 1422.

HELGUDOTTIR, S. S., ROUTHE, L. J., BURKHART, A., JØNSSON, K., PEDERSEN, I. S., LICHOTA, J. & MOOS, T. 2020. Epigenetic Regulation of Ferroportin in Primary Cultures of the Rat Blood-Brain Barrier. *Molecular Neurobiology,* 57**,** 3526-3539.

HIEPEN, C., JATZLAU, J., HILDEBRANDT, S., KAMPFRATH, B., GOKTAS, M., MURGAI, A., CUELLAR CAMACHO, J. L., HAAG, R., RUPPERT, C., SENGLE, G., CAVALCANTI-ADAM, E. A., BLANK, K. G. & KNAUS, P. 2019. BMPR2 acts as a gatekeeper to protect endothelial cells from increased TGFβ responses and altered cell mechanics. *PLOS Biology,* 17**,** e3000557.

HODGE, D. R., HURT, E. M. & FARRAR, W. L. 2005. The role of IL-6 and STAT3 in inflammation and cancer. *European Journal of Cancer,* 41**,** 2502-2512.

HOGG, K., THOMAS, J., ASHFORD, D., CARTWRIGHT, J., COLDWELL, R., WESTON, D. J., PILLMOOR, J., SURRY, D. & O'TOOLE, P. 2015. Quantification of proteins by flow cytometry:

Quantification of human hepatic transporter P-gp and OATP1B1 using flow cytometry and mass spectrometry. *Methods,* 82**,** 38-46.

HOODA, J., CADINU, D., ALAM, M. M., SHAH, A., CAO, T. M., SULLIVAN, L. A., BREKKEN, R. & ZHANG, L. 2013. Enhanced heme function and mitochondrial respiration promote the progression of lung cancer cells. *PloS one,* 8**,** e63402.

HOWARD, L. S. G. E., HE, J., WATSON, G. M. J., HUANG, L., WHARTON, J., LUO, Q., KIELY, D. G., CONDLIFFE, R., PEPKE-ZABA, J., MORRELL, N. W., SHEARES, K. K., ULRICH, A., QUAN, R., ZHAO, Z., JING, X., AN, C., LIU, Z., XIONG, C., ROBBINS, P. A., DAWES, T., DE MARVAO, A., RHODES, C. J., RICHTER, M. J., GALL, H., GHOFRANI, H. A., ZHAO, L., HUSON, L. & WILKINS, M. R. 2021. Supplementation with Iron in Pulmonary Arterial Hypertension. Two Randomized Crossover Trials. *Annals of the American Thoracic Society,* 18**,** 981-988.

HOWELL, K., PRESTON, R. J. & MCLOUGHLIN, P. 2003. Chronic hypoxia causes angiogenesis in addition to remodelling in the adult rat pulmonary circulation. *The Journal of physiology,* 547**,** 133-145.

HU, Y., CHI, L., KUEBLER, W. M. & GOLDENBERG, N. M. 2020. Perivascular Inflammation in Pulmonary Arterial Hypertension. *Cells,* 9**,** 2338.

HUANG, M. L.-H., BECKER, E. M., WHITNALL, M., RAHMANTO, Y. S., PONKA, P. & RICHARDSON, D. R. 2009. Elucidation of the mechanism of mitochondrial iron loading in Friedreich's ataxia by analysis of a mouse mutant. *Proceedings of the National Academy of Sciences,* 106**,** 16381-16386.

HUMBERT, M., GUIGNABERT, C., BONNET, S., DORFMÜLLER, P., KLINGER, J. R., NICOLLS, M. R., OLSCHEWSKI, A. J., PULLAMSETTI, S. S., SCHERMULY, R. T. & STENMARK, K. R. 2019. Pathology and pathobiology of pulmonary

hypertension: state of the art and research perspectives. *European Respiratory Journal,* 53.

HUMBERT, M., MCLAUGHLIN, V., GIBBS, J. S. R., GOMBERG-MAITLAND, M., HOEPER, M. M., PRESTON, I. R., SOUZA, R., WAXMAN, A., ESCRIBANO SUBIAS, P., FELDMAN, J., MEYER, G., MONTANI, D., OLSSON, K. M., MANIMARAN, S., BARNES, J., LINDE, P. G., DE OLIVEIRA PENA, J. & BADESCH, D. B. 2021. Sotatercept for the Treatment of Pulmonary Arterial Hypertension. *N Engl J Med,* 384**,** 1204-1215.

HUMBERT, M., MONTANI, D., PERROS, F., DORFMÜLLER, P., ADNOT, S. & EDDAHIBI, S. 2008. Endothelial cell dysfunction and cross talk between endothelium and smooth muscle cells in pulmonary arterial hypertension. *Vascular Pharmacology,* 49**,** 113-118.

HUMBERT, M., MONTI, G., BRENOT, F., SITBON, O., PORTIER, A., GRANGEOT-KEROS, L., DUROUX, P., GALANAUD, P., SIMONNEAU, G. & EMILIE, D. 1995. Increased interleukin-1 and interleukin-6 serum concentrations in severe primary pulmonary hypertension. *Am J Respir Crit Care Med,* 151**,** 1628-31.

HUNTER, H. N., FULTON, D. B., GANZ, T. & VOGEL, H. J. 2002. The solution structure of human hepcidin, a peptide hormone with antimicrobial activity that is involved in iron uptake and hereditary hemochromatosis. *J Biol Chem,* 277**,** 37597-603.

IRWIN, D. C., BAEK, J. H., HASSELL, K., NUSS, R., EIGENBERGER, P., LISK, C., LOOMIS, Z., MALTZAHN, J., STENMARK, K. R., NOZIK-GRAYCK, E. & BUEHLER, P. W. 2015. Hemoglobin induced lung vascular oxidation, inflammation, and remodeling contributes to the progression of hypoxic pulmonary hypertension and is attenuated in rats with repeat dose haptoglobin administration. *Free Radic Biol Med*.

ISSITT, T. & TOE, Q. 2018. *Hepcidin treatment of human pulmonary artery smooth muscle cells and mitochondrial dysfunction*.

ISSITT, T., TOE, Q., MOHD GHAZALY, M., QUINLAN, G. J. & WORT, S. J. 2019. Pulmonary vascular cell mitochondrial dysfunction in response to hepcidin. *European Respiratory Journal,* 54**,** PA1415.

JANZ, D. R., BASTARACHE, J. A., PETERSON, J. F., SILLS, G., WICKERSHAM, N., MAY, A. K., ROBERTS, L. J., 2ND & WARE, L. B. 2013a. Association between cell-free hemoglobin, acetaminophen, and mortality in patients with sepsis: an observational study. *Crit Care Med,* 41**,** 784-90.

JANZ, D. R., BASTARACHE, J. A., SILLS, G., WICKERSHAM, N., MAY, A. K., BERNARD, G. R. & WARE, L. B. 2013b. Association between haptoglobin, hemopexin and mortality in adults with sepsis. *Crit Care,* 17**,** R272.

JANZ, D. R. & WARE, L. B. 2015. The role of red blood cells and cell-free hemoglobin in the pathogenesis of ARDS. *Journal of intensive care,* 3**,** 20-20.

JONIGK, D., GOLPON, H., BOCKMEYER, C. L., MAEGEL, L., HOEPER, M. M., GOTTLIEB, J., NICKEL, N., HUSSEIN, K., MAUS, U., LEHMANN, U., JANCIAUSKIENE, S., WELTE, T., HAVERICH, A., RISCHE, J., KREIPE, H. & LAENGER, F. 2011. Plexiform lesions in pulmonary arterial hypertension composition, architecture, and microenvironment. *The American journal of pathology,* 179**,** 167-179.

KAPITSINOU, P. P., RAJENDRAN, G., ASTLEFORD, L., MICHAEL, M., SCHONFELD, M. P., FIELDS, T., SHAY, S., FRENCH, J. L., WEST, J. & HAASE, V. H. 2016. The endothelial prolyl-4-hydroxylase domain 2/hypoxia-inducible factor 2 axis regulates pulmonary artery pressure in mice. *Molecular and cellular biology,* 36**,** 1584-1594.

KARAMANIAN, V. A., HARHAY, M., GRANT, G. R., PALEVSKY, H. I., GRIZZLE, W. E., ZAMANIAN, R. T., IHIDA-STANSBURY, K., TAICHMAN, D. B., KAWUT, S. M. & JONES, P. L. 2014. Erythropoietin upregulation in pulmonary arterial hypertension. *Pulmonary circulation,* 4**,** 269-279.

KARTIKASARI, A. E. R., GEORGIOU, N. A., VISSEREN, F. L. J., VAN KATS-RENAUD, H., VAN ASBECK, B. S. & MARX, J. J. M. 2004. Intracellular Labile Iron Modulates Adhesion of Human Monocytes to Human Endothelial Cells. *Arteriosclerosis, Thrombosis, and Vascular Biology,* 24**,** 2257-2262.

KASHIV, Y., AUSTIN, J. R., LAI, B., ROSE, V., VOGT, S. & EL-MUAYED, M. 2016. Imaging trace element distributions in single organelles and subcellular features. *Scientific reports,* 6**,** 1-9.

KATO, G. J., PIEL, F. B., REID, C. D., GASTON, M. H., OHENE-FREMPONG, K., KRISHNAMURTI, L., SMITH, W. R., PANEPINTO, J. A., WEATHERALL, D. J., COSTA, F. F. & VICHINSKY, E. P. 2018. Sickle cell disease. *Nature Reviews Disease Primers,* 4**,** 18010.

KELL, D. B. 2009. Iron behaving badly: inappropriate iron chelation as a major contributor to the aetiology of vascular and other progressive inflammatory and degenerative diseases. *BMC Medical Genomics,* 2**,** 2-2.

KHERBECK, N., TAMBY, M. C., BUSSONE, G., DIB, H., PERROS, F., HUMBERT, M. & MOUTHON, L. 2013. The Role of Inflammation and Autoimmunity in the Pathophysiology of Pulmonary Arterial Hypertension. *Clinical Reviews in Allergy & Immunology,* 44**,** 31-38.

KIM, Y., PARK, J. & KIM, M. 2017. Diagnostic approaches for inherited hemolytic anemia in the genetic era. *Blood research,* 52**,** 84-94.

KOUREMBANAS, S., MARSDEN, P. A., MCQUILLAN, L. P. & FALLER, D. V. 1991. Hypoxia induces endothelin gene expression and

secretion in cultured human endothelium. *J Clin Invest,* 88**,** 1054-7.

KRAUSE, A., NEITZ, S., MÄGERT, H.-J., SCHULZ, A., FORSSMANN, W.-G., SCHULZ-KNAPPE, P. & ADERMANN, K. 2000. LEAP-1, a novel highly disulfide-bonded human peptide, exhibits antimicrobial activity11The nucleotide sequence data reported in this paper have been submitted to the GenBank/EBI Data Bank with accession number AJ277280. Scanning of this sequence against the data base resulted in the identification of related sequences with the accession numbers AD000684 and P81172. *FEBS Letters,* 480**,** 147-150.

KRUGER, N. J. The Bradford Method for Protein Quantitation. Humana Press.

KUHN, L. C. 2015. Iron regulatory proteins and their role in controlling iron metabolism. *Metallomics,* 7**,** 232-243.

LAKHAL-LITTLETON, S., WOLNA, M., CARR, C. A., MILLER, J. J. J., CHRISTIAN, H. C., BALL, V., SANTOS, A., DIAZ, R., BIGGS, D., STILLION, R., HOLDSHIP, P., LARNER, F., TYLER, D. J., CLARKE, K., DAVIES, B. & ROBBINS, P. A. 2015. Cardiac ferroportin regulates cellular iron homeostasis and is important for cardiac function. *Proceedings of the National Academy of Sciences,* 112**,** 3164.

LAKHAL-LITTLETON, S., WOLNA, M., CHUNG, Y. J., CHRISTIAN, H. C., HEATHER, L. C., BRESCIA, M., BALL, V., DIAZ, R., SANTOS, A., BIGGS, D., CLARKE, K., DAVIES, B. & ROBBINS, P. A. 2016. An essential cell-autonomous role for hepcidin in cardiac iron homeostasis. *eLife,* 5**,** e19804.

LAL, A. 2020. Iron in Health and Disease: An Update. *The Indian Journal of Pediatrics,* 87**,** 58-65.

LARKIN, E. K., NEWMAN, J. H., AUSTIN, E. D., HEMNES, A. R., WHEELER, L., ROBBINS, I. M., WEST, J. D., PHILLIPS, J. A., 3RD, HAMID, R. & LOYD, J. E. 2012. Longitudinal analysis casts

doubt on the presence of genetic anticipation in heritable pulmonary arterial hypertension. *American journal of respiratory and critical care medicine,* 186**,** 892-896.

LATHA RAMAKRISHNAN, S. L. P., QUEZIA K TOE, LAURA E WEST , SHARON MUMBY, HELEN CASBOLT, BENJAMIN GARFIELD, THEO ISSITT, ALLAN LAWRIE, S JOHN WORT , GREGORY J QUINLAN 2018. The Hepcidin / Ferroportin axis modulates proliferation of pulmonary artery smooth muscle cells. *Scientific Reports*.

LEE, C., LIM, H. K., SAKONG, J., LEE, Y. S., KIM, J. R. & BAEK, S. H. 2006. Janus kinase-signal transducer and activator of transcription mediates phosphatidic acid-induced interleukin (IL)-1beta and IL-6 production. *Mol Pharmacol,* 69**,** 1041-7.

LEE, J. W., KO, J., JU, C. & ELTZSCHIG, H. K. 2019. Hypoxia signaling in human diseases and therapeutic targets. *Experimental & Molecular Medicine,* 51**,** 1-13.

LI, F., WANG, J., ZHU, Y., LIU, L., FENG, W., SHI, W., WANG, Q., ZHANG, Q., CHAI, L. & LI, M. 2018. SphK1/S1P Mediates PDGF-Induced Pulmonary Arterial Smooth Muscle Cell Proliferation via miR-21/BMPRII/Id1 Signaling Pathway. *Cell Physiol Biochem,* 51**,** 487-500.

LI, L. & FREI, B. 2006. Iron Chelation Inhibits NF-κB–Mediated Adhesion Molecule Expression by Inhibiting p22phox Protein Expression and NADPH Oxidase Activity. *Arteriosclerosis, Thrombosis, and Vascular Biology,* 26**,** 2638-2643.

LILL, R., DUTKIEWICZ, R., ELSÄSSER, H. P., HAUSMANN, A., NETZ, D. J., PIERIK, A. J., STEHLING, O., URZICA, E. & MÜHLENHOFF, U. 2006. Mechanisms of iron-sulfur protein maturation in mitochondria, cytosol and nucleus of eukaryotes. *Biochim Biophys Acta,* 1763**,** 652-67.

LING, F., KANG, B. & SUN, X. H. 2014. Id proteins: small molecules, mighty regulators. *Curr Top Dev Biol,* 110**,** 189-216.

LOOMIS, Z., EIGENBERGER, P., REDINIUS, K., LISK, C., KAROOR, V., NOZIK-GRAYCK, E., FERGUSON, S. K., HASSELL, K., NUSS, R., STENMARK, K., BUEHLER, P. & IRWIN, D. C. 2017. Hemoglobin induced cell trauma indirectly influences endothelial TLR9 activity resulting in pulmonary vascular smooth muscle cell activation. *PLOS ONE,* 12**,** e0171219.

LUMB, A. B. 2017. Chapter 1 - Functional Anatomy of the Respiratory Tract. *In:* LUMB, A. B. (ed.) *Nunn's Applied Respiratory Physiology (Eighth Edition).* Elsevier.

MA, J., WANG, Q., FEI, T., HAN, J.-D. J. & CHEN, Y.-G. 2006. MCP-1 mediates TGF-β–induced angiogenesis by stimulating vascular smooth muscle cell migration. *Blood,* 109**,** 987-994.

MA, W., HAN, W., GREER, P. A., TUDER, R. M., TOQUE, H. A., WANG, K. K., CALDWELL, R. W. & SU, Y. 2011. Calpain mediates pulmonary vascular remodeling in rodent models of pulmonary hypertension, and its inhibition attenuates pathologic features of disease. *The Journal of clinical investigation,* 121.

MALYSZKO, J. 2009. Hemojuvelin: The Hepcidin Story Continues. *Kidney and Blood Pressure Research,* 32**,** 71-76.

MARSHALL, J. D., BAZAN, I., ZHANG, Y., FARES, W. H. & LEE, P. J. 2018. Mitochondrial dysfunction and pulmonary hypertension: cause, effect, or both. *American journal of physiology. Lung cellular and molecular physiology,* 314**,** L782-L796.

MASSAGUÉ, J. 2012. TGFβ signalling in context. *Nature Reviews Molecular Cell Biology,* 13**,** 616-630.

MATHEW, R., HUANG, J., WU, J. M., FALLON, J. T. & GEWITZ, M. H. 2016. Hematological disorders and pulmonary hypertension. *World Journal of Cardiology,* 8**,** 703-718.

MAYEUR, C., LEYTON, P. A., KOLODZIEJ, S. A., YU, B. & BLOCH, K. D. 2014a. BMP type II receptors have redundant roles in the regulation of hepatic hepcidin gene expression and iron metabolism. *Blood,* 124**,** 2116-2123.

MAYEUR, C., LOHMEYER, L. K., LEYTON, P., KAO, S. M., PAPPAS, A. E., KOLODZIEJ, S. A., SPAGNOLLI, E., YU, B., GALDOS, R. L., YU, P. B., PETERSON, R. T., BLOCH, D. B., BLOCH, K. D. & STEINBICKER, A. U. 2014b. The type I BMP receptor Alk3 is required for the induction of hepatic hepcidin gene expression by interleukin-6. *Blood,* 123**,** 2261-2268.

MENA, N. P., URRUTIA, P. J., LOURIDO, F., CARRASCO, C. M. & NÚÑEZ, M. T. 2015. Mitochondrial iron homeostasis and its dysfunctions in neurodegenerative disorders. *Mitochondrion,* 21**,** 92-105.

MEYNARD, D., KAUTZ, L., DARNAUD, V., CANONNE-HERGAUX, F., COPPIN, H. & ROTH, M.-P. 2009. Lack of the bone morphogenetic protein BMP6 induces massive iron overload. *Nature Genetics,* 41**,** 478-481.

MINNECI, P. C., DEANS, K. J., ZHI, H., YUEN, P. S., STAR, R. A., BANKS, S. M., SCHECHTER, A. N., NATANSON, C., GLADWIN, M. T. & SOLOMON, S. B. 2005. Hemolysis-associated endothelial dysfunction mediated by accelerated NO inactivation by decompartmentalized oxyhemoglobin. *J Clin Invest,* 115**,** 3409-17.

MUCKENTHALER, M. U., RIVELLA, S., HENTZE, M. W. & GALY, B. 2017. A Red Carpet for Iron Metabolism. *Cell,* 168**,** 344-361.

MUKHOPADHYAY, D., TSIOKAS, L., ZHOU, X. M., FOSTER, D., BRUGGE, J. S. & SUKHATME, V. P. 1995. Hypoxic induction of human vascular endothelial growth factor expression through c-Src activation. *Nature,* 375**,** 577-81.

MUMBY, S., RAMAKRISHNAN, L., KEMPNY, A., QUINLAN, G. & WORT, J. 2016. Dysregulation of iron homeostasis in

Eisenmenger syndrome; comparison to idiopathic pulmonary arterial hypertension and healthy controls. *European Respiratory Journal,* 48.

NAITO, Y., HOSOKAWA, M., HAO, H., SAWADA, H., HIROTANI, S., IWASAKU, T., OKUHARA, Y., EGUCHI, A., HIROTA, S., OHYANAGI, M., TSUJINO, T. & MASUYAMA, T. 2013. Impact of dietary iron restriction on the development of monocrotaline-induced pulmonary vascular remodeling and right ventricular failure in rats. *Biochem Biophys Res Commun,* 436**,** 145-51.

NAKAMURA, H., KATO, M., NAKAYA, T., KONO, M., TANIMURA, S., SATO, T., FUJIEDA, Y., OKU, K., OHIRA, H., BOHGAKI, T., YASUDA, S., TSUJINO, I., NISHIMURA, M. & ATSUMI, T. 2017. Decreased haptoglobin levels inversely correlated with pulmonary artery pressure in patients with pulmonary arterial hypertension: A cross-sectional study. *Medicine,* 96**,** e8349.

NEMETH, E. & GANZ, T. 2014. Anemia of inflammation. *Hematology/oncology clinics of North America,* 28**,** 671-vi.

NEMETH, E., PREZA, G. C., JUNG, C. L., KAPLAN, J., WARING, A. J. & GANZ, T. 2006. The N-terminus of hepcidin is essential for its interaction with ferroportin: structure-function study. *Blood,* 107**,** 328-33.

NEMETH, E., RIVERA, S., GABAYAN, V., KELLER, C., TAUDORF, S., PEDERSEN, B. K. & GANZ, T. 2004. IL-6 mediates hypoferremia of inflammation by inducing the synthesis of the iron regulatory hormone hepcidin. *The Journal of clinical investigation,* 113**,** 1271-1276.

NICKEL, J. & MUELLER, T. D. 2019. Specification of BMP Signaling. *Cells,* 8**,** 1579.

NICOLAS, G., BENNOUN, M., DEVAUX, I., BEAUMONT, C., GRANDCHAMP, B., KAHN, A. & VAULONT, S. 2001. Lack of

hepcidin gene expression and severe tissue iron overload in upstream stimulatory factor 2 (USF2) knockout mice. *Proceedings of the National Academy of Sciences,* 98**,** 8780-8785.

NIELSEN, M., MADSEN, M., MØLLER, H. & MOESTRUP, S. 2006. *The macrophage scavenger receptor CD163: Endocytic properties of cytoplasmic tail variants*.

NING, Y., MANEGOLD, P. C., HONG, Y. K., ZHANG, W., POHL, A., LURJE, G., WINDER, T., YANG, D., LABONTE, M. J., WILSON, P. M., LADNER, R. D. & LENZ, H.-J. 2011. Interleukin-8 is associated with proliferation, migration, angiogenesis and chemosensitivity in vitro and in vivo in colon cancer cell line models. *International journal of cancer,* 128**,** 2038-2049.

OH, S. P., SEKI, T., GOSS, K. A., IMAMURA, T., YI, Y., DONAHOE, P. K., LI, L., MIYAZONO, K., TEN DIJKE, P., KIM, S. & LI, E. 2000. Activin receptor-like kinase 1 modulates transforming growth factor-beta 1 signaling in the regulation of angiogenesis. *Proc Natl Acad Sci U S A,* 97**,** 2626-31.

ONOFRE, G., KOLÁCKOVÁ, M., JANKOVICOVÁ, K. & KREJSEK, J. 2009. Scavenger receptor CD163 and its biological functions. *Acta Medica (Hradec Kralove),* 52**,** 57-61.

OUSTAMANOLAKIS, P., KOUTROUBAKIS, I. E., MESSARITAKIS, I., MALLIARAKI, N., SFIRIDAKI, A. & KOUROUMALIS, E. A. 2011. Serum hepcidin and prohepcidin concentrations in inflammatory bowel disease. *European Journal of Gastroenterology & Hepatology,* 23.

PAK, O., ALDASHEV, A., WELSH, D. & PEACOCK, A. 2007. The effects of hypoxia on the cells of the pulmonary vasculature. *European Respiratory Journal,* 30**,** 364.

PANDAY, A., SAHOO, M. K., OSORIO, D. & BATRA, S. 2015. NADPH oxidases: an overview from structure to innate immunity-

associated pathologies. *Cellular & Molecular Immunology,* 12**,** 5-23.

PARK, C. H., VALORE, E. V., WARING, A. J. & GANZ, T. 2001. Hepcidin, a Urinary Antimicrobial Peptide Synthesized in the Liver*. *Journal of Biological Chemistry,* 276**,** 7806-7810.

PAUL, B. T., MANZ, D. H., TORTI, F. M. & TORTI, S. V. 2017. Mitochondria and Iron: current questions. *Expert review of hematology,* 10**,** 65-79.

PEDERSEN, S., TOE, Q., JOHN WORT, S., QUINLAN, G. & RAMAKRISHNAN, L. 2018. *Stabilised ferroportin activity affects pulmonary vascular cells responses: implications for pulmonary hypertension*.

PIETRANGELO, A. 2017. Ferroportin disease: pathogenesis, diagnosis and treatment. *Haematologica,* 102**,** 1972-1984.

PINTE, S., CAETANO, B., LE BRAS, A., HAVET, C., VILLAIN, G., DERNAYKA, R., DUEZ, C., MATTOT, V. & SONCIN, F. 2016. Endothelial Cell Activation Is Regulated by Epidermal Growth Factor-like Domain 7 (Egfl7) during Inflammation. *Journal of Biological Chemistry,* 291**,** 24017-24028.

PIPERNO, A., GALIMBERTI, S., MARIANI, R., PELUCCHI, S., RAVASI, G., LOMBARDI, C., BILO, G., REVERA, M., GIULIANO, A., FAINI, A., MAININI, V., WESTERMAN, M., GANZ, T., VALSECCHI, M. G., MANCIA, G. & PARATI, G. 2011. Modulation of hepcidin production during hypoxia-induced erythropoiesis in humans in vivo: data from the HIGHCARE project. *Blood,* 117**,** 2953.

POLI, M., GIRELLI, D., CAMPOSTRINI, N., MACCARINELLI, F., FINAZZI, D., LUSCIETI, S., NAI, A. & AROSIO, P. 2011. Heparin: a potent inhibitor of hepcidin expression in vitro and in vivo. *Blood,* 117**,** 997-1004.

PONKA, P. 1997. Tissue-specific regulation of iron metabolism and heme synthesis: distinct control mechanisms in erythroid

cells. *Blood, The Journal of the American Society of Hematology,* 89**,** 1-25.

PRICE, L. C., WORT, S. J., PERROS, F., DORFMÜLLER, P., HUERTAS, A., MONTANI, D., COHEN-KAMINSKY, S. & HUMBERT, M. 2012. Inflammation in Pulmonary Arterial Hypertension. *Chest,* 141**,** 210-221.

PRINS, K. W., ARCHER, S. L., PRITZKER, M., ROSE, L., WEIR, E. K., SHARMA, A. & THENAPPAN, T. 2018. Interleukin-6 is independently associated with right ventricular function in pulmonary arterial hypertension. *J Heart Lung Transplant,* 37**,** 376-384.

RAFIKOVA, O., WILLIAMS, E. R., MCBRIDE, M. L., ZEMSKOVA, M., SRIVASTAVA, A., NAIR, V., DESAI, A. A., LANGLAIS, P. R., ZEMSKOV, E., SIMON, M., MANDARINO, L. J. & RAFIKOV, R. 2018. Hemolysis-induced Lung Vascular Leakage Contributes to the Development of Pulmonary Hypertension. *American Journal of Respiratory Cell and Molecular Biology,* 59**,** 334-345.

RAHA, A. A., VAISHNAV, R. A., FRIEDLAND, R. P., BOMFORD, A. & RAHA-CHOWDHURY, R. 2013. The systemic iron-regulatory proteins hepcidin and ferroportin are reduced in the brain in Alzheimer's disease. *Acta Neuropathologica Communications,* 1**,** 55.

RAMAKRISHNAN, L., ANWAR, A., WORT, J. & QUINLAN, G. 2016. P244 Haemoglobin mediated proliferation and il-6 release in human pulmonary artery endothelial cells: a role for cd163 and implications for pulmonary vascular remodelling. *Thorax,* 71**,** A220-A220.

RAMAKRISHNAN, L., PEDERSEN, S. L., TOE, Q. K., QUINLAN, G. J. & WORT, S. J. 2018a. Pulmonary Arterial Hypertension: Iron Matters. *Frontiers in Physiology,* 9**,** 641.

RAMAKRISHNAN, L., PEDERSEN, S. L., TOE, Q. K., WEST, L. E., MUMBY, S., CASBOLT, H., ISSITT, T., GARFIELD, B., LAWRIE, A., WORT, S. J. & QUINLAN, G. J. 2018b. The Hepcidin/Ferroportin axis modulates proliferation of pulmonary artery smooth muscle cells. *Scientific Reports,* 8**,** 12972.

RAMPERSAD, S. N. 2012. Multiple Applications of Alamar Blue as an Indicator of Metabolic Function and Cellular Health in Cell Viability Bioassays. *Sensors,* 12**,** 12347-12360.

RANCHOUX, B., HARVEY, L. D., AYON, R. J., BABICHEVA, A., BONNET, S., CHAN, S. Y., YUAN, J. X. J. & PEREZ, V. D. J. 2018. Endothelial dysfunction in pulmonary arterial hypertension: an evolving landscape (2017 Grover Conference Series). *Pulmonary circulation,* 8**,** 2045893217752912-2045893217752912.

RECALCATI, S., GAMMELLA, E., BURATTI, P. & CAIRO, G. 2017. Molecular regulation of cellular iron balance. *IUBMB Life,* 69**,** 389-398.

RECALCATI, S., MINOTTI, G. & CAIRO, G. 2010. Iron regulatory proteins: from molecular mechanisms to drug development. *Antioxid Redox Signal,* 13**,** 1593-616.

REITER, C. D., WANG, X., TANUS-SANTOS, J. E., HOGG, N., CANNON, R. O., 3RD, SCHECHTER, A. N. & GLADWIN, M. T. 2002. Cell-free hemoglobin limits nitric oxide bioavailability in sickle-cell disease. *Nat Med,* 8**,** 1383-9.

RHODES, C. J., HOWARD, L. S., BUSBRIDGE, M., ASHBY, D., KONDILI, E., GIBBS, J. S., WHARTON, J. & WILKINS, M. R. 2011a. Iron deficiency and raised hepcidin in idiopathic pulmonary arterial hypertension: clinical prevalence, outcomes, and mechanistic insights. *J Am Coll Cardiol,* 58**,** 300-9.

RHODES, C. J., WHARTON, J., HOWARD, L., GIBBS, J. S. R., VONK-NOORDEGRAAF, A. & WILKINS, M. R. 2011b. Iron deficiency

in pulmonary arterial hypertension: a potential therapeutic target. *European Respiratory Journal,* 38**,** 1453.

RICHARDSON, D. R., LANE, D. J. R., BECKER, E. M., HUANG, M. L. H., WHITNALL, M., RAHMANTO, Y. S., SHEFTEL, A. D. & PONKA, P. 2010. Mitochondrial iron trafficking and the integration of iron metabolism between the mitochondrion and cytosol. *Proceedings of the National Academy of Sciences,* 107**,** 10775.

RISHI, G., WALLACE, D. F. & SUBRAMANIAM, V. N. 2015. Hepcidin: regulation of the master iron regulator. *Bioscience reports,* 35**,** e00192.

RISS, T. L., MORAVEC, R. A., NILES, A. L., DUELLMAN, S., BENINK, H. A., WORZELLA, T. J. & MINOR, L. 2004. Cell Viability Assays. *In:* MARKOSSIAN, S., SITTAMPALAM, G. S., GROSSMAN, A., BRIMACOMBE, K., ARKIN, M., AULD, D., AUSTIN, C. P., BAELL, J., CAAVEIRO, J. M. M., CHUNG, T. D. Y., COUSSENS, N. P., DAHLIN, J. L., DEVANARYAN, V., FOLEY, T. L., GLICKSMAN, M., HALL, M. D., HAAS, J. V., HOARE, S. R. J., INGLESE, J., IVERSEN, P. W., KAHL, S. D., KALES, S. C., KIRSHNER, S., LAL-NAG, M., LI, Z., MCGEE, J., MCMANUS, O., RISS, T., SARADJIAN, P., TRASK, O. J., JR., WEIDNER, J. R., WILDEY, M. J., XIA, M. & XU, X. (eds.) *Assay Guidance Manual.* Bethesda (MD): Eli Lilly & Company and the National Center for Advancing Translational Sciences.

RITTER, M., BUECHLER, C., LANGMANN, T., ORSO, E., KLUCKEN, J. & SCHMITZ, G. 1999. The scavenger receptor CD163: regulation, promoter structure and genomic organization. *Pathobiology,* 67**,** 257-61.

ROL, N., KURAKULA, K. B., HAPPÉ, C., BOGAARD, H. J. & GOUMANS, M.-J. 2018. TGF-β and BMPR2 Signaling in PAH: Two Black Sheep in One Family. *International journal of molecular sciences,* 19**,** 2585.

ROTHER, R. P., BELL, L., HILLMEN, P. & GLADWIN, M. T. 2005. The clinical sequelae of intravascular hemolysis and extracellular plasma hemoglobin: A novel mechanism of human disease. *JAMA,* 293**,** 1653-1662.

ROWAN, S. C., KEANE, M. P., GAINE, S. & MCLOUGHLIN, P. 2016. Hypoxic pulmonary hypertension in chronic lung diseases: novel vasoconstrictor pathways. *Lancet Respir Med,* 4**,** 225-36.

RUCHALA, P. & NEMETH, E. 2014. The pathophysiology and pharmacology of hepcidin. *Trends in pharmacological sciences,* 35**,** 155-161.

RUITER, G., LANKHORST, S., BOONSTRA, A., POSTMUS, P. E., ZWEEGMAN, S., WESTERHOF, N., VAN DER LAARSE, W. J. & VONK-NOORDEGRAAF, A. 2011. Iron deficiency is common in idiopathic pulmonary arterial hypertension. *European Respiratory Journal,* 37**,** 1386.

RUITER, G., LANSER, I. J., DE MAN, F. S., VAN DER LAARSE, W. J., WHARTON, J., WILKINS, M. R., HOWARD, L. S., VONK-NOORDEGRAAF, A. & VOSKUYL, A. E. 2014. Iron deficiency in systemic sclerosis patients with and without pulmonary hypertension. *Rheumatology (Oxford),* 53**,** 285-92.

RYAN, J., DASGUPTA, A., HUSTON, J., CHEN, K.-H. & ARCHER, S. L. 2015. Mitochondrial dynamics in pulmonary arterial hypertension. *Journal of molecular medicine (Berlin, Germany),* 93**,** 229-242.

SAIKI, R. K., SCHARF, S., FALOONA, F., MULLIS, K. B., HORN, G. T., ERLICH, H. A. & ARNHEIM, N. 1985. Enzymatic amplification of beta-globin genomic sequences and restriction site analysis for diagnosis of sickle cell anemia. *Science,* 230**,** 1350-4.

SANDERSON, M. J., SMITH, I., PARKER, I. & BOOTMAN, M. D. 2014. Fluorescence Microscopy. *Cold Spring Harbor Protocols,* 2014**,** pdb.top071795.

SANGKHAE, V. & NEMETH, E. 2017. Regulation of the Iron Homeostatic Hormone Hepcidin. *Advances in Nutrition,* 8**,** 126-136.

SAVALE, L., TU, L., RIDEAU, D., IZZIKI, M., MAITRE, B., ADNOT, S. & EDDAHIBI, S. 2009. Impact of interleukin-6 on hypoxia-induced pulmonary hypertension and lung inflammation in mice. *Respiratory Research,* 10**,** 6.

SCHAER, D. J. & BUEHLER, P. W. 2013. Cell-free hemoglobin and its scavenger proteins: new disease models leading the way to targeted therapies. *Cold Spring Harbor perspectives in medicine,* 3**,** a013433.

SCHAER, D. J., VINCHI, F., INGOGLIA, G., TOLOSANO, E. & BUEHLER, P. W. 2014. Haptoglobin, hemopexin, and related defense pathways—basic science, clinical perspectives, and drug development. *Frontiers in Physiology,* 5.

SCHERMULY, R. T., GHOFRANI, H. A., WILKINS, M. R. & GRIMMINGER, F. 2011a. Mechanisms of disease: pulmonary arterial hypertension. *Nat Rev Cardiol,* 8**,** 443-55.

SCHERMULY, R. T., GHOFRANI, H. A., WILKINS, M. R. & GRIMMINGER, F. 2011b. Mechanisms of disease: pulmonary arterial hypertension. *Nature Reviews Cardiology,* 8**,** 443-455.

SCHINDL, M., SCHOPPMANN, S. F., STRÖBEL, T., HEINZL, H., LEISSER, C., HORVAT, R. & BIRNER, P. 2003. Level of Id-1 protein expression correlates with poor differentiation, enhanced malignant potential, and more aggressive clinical behavior of epithelial ovarian tumors. *Clin Cancer Res,* 9**,** 779-85.

SEMENZA, G. L. 2007. Hypoxia-inducible factor 1 (HIF-1) pathway. *Sci STKE,* 2007**,** cm8.

SHACKSHAFT, T., WORT, S., QUINLAN, G. & RAMAKRISHNAN, L. 2017. S112 Conditioned media from human pulmonary arterial endothelial cells treated with hepcidin or haemoglobin cause proliferation and migration of human pulmonary artery smooth muscle cells. *Thorax,* 72**,** A68-A69.

SHEHAT, M. G. & TIGNO-ARANJUEZ, J. 2019. Flow Cytometric Measurement Of ROS Production In Macrophages In Response To FcγR Cross-linking. *Journal of visualized experiments : JoVE***,** 10.3791/59167.

SHEIKH, A. Q., SADDOUK, F. Z., NTOKOU, A., MAZUREK, R. & GREIF, D. M. 2018. Cell Autonomous and Non-cell Autonomous Regulation of SMC Progenitors in Pulmonary Hypertension. *Cell Reports,* 23**,** 1152-1165.

SIMPSON, R. J. & MCKIE, A. T. 2015. Iron and oxygen sensing: a tale of 2 interacting elements? *Metallomics,* 7**,** 223-31.

SLEMC, L. & KUNEJ, T. 2016. Transcription factor HIF1A: downstream targets, associated pathways, polymorphic hypoxia response element (HRE) sites, and initiative for standardization of reporting in scientific literature. *Tumour Biol,* 37**,** 14851-14861.

SOMMER, N., GHOFRANI, H. A., PAK, O., BONNET, S., PROVENCHER, S., SITBON, O., ROSENKRANZ, S., HOEPER, M. M. & KIELY, D. G. 2021. Current and future treatments of pulmonary arterial hypertension. *British Journal of Pharmacology,* 178**,** 6-30.

SONNWEBER, T., NACHBAUR, D., SCHROLL, A., NAIRZ, M., SEIFERT, M., DEMETZ, E., HASCHKA, D., MITTERSTILLER, A.-M., KLEINSASSER, A., BURTSCHER, M., TRÜBSBACH, S., MURPHY, A. T., WROBLEWSKI, V., WITCHER, D. R., MLECZKO-SANECKA, K., VECCHI, C., MUCKENTHALER, M. U., PIETRANGELO, A.,

THEURL, I. & WEISS, G. 2014. Hypoxia induced downregulation of hepcidin is mediated by platelet derived growth factor BB. *Gut,* 63**,** 1951.

SOON, E., HOLMES, A. M., TREACY, C. M., DOUGHTY, N. J., SOUTHGATE, L., MACHADO, R. D., TREMBATH, R. C., JENNINGS, S., BARKER, L., NICKLIN, P., WALKER, C., BUDD, D. C., PEPKE-ZABA, J. & MORRELL, N. W. 2010. Elevated levels of inflammatory cytokines predict survival in idiopathic and familial pulmonary arterial hypertension. *Circulation,* 122**,** 920-7.

SOUTHGATE, L., MACHADO, R. D., GRÄF, S. & MORRELL, N. W. 2020. Molecular genetic framework underlying pulmonary arterial hypertension. *Nature Reviews Cardiology,* 17**,** 85-95.

SOUZA, R., FERNANDES, C. J. & JARDIM, C. V. 2009a. Other causes of PAH (schistosomiasis, porto-pulmonary hypertension and hemolysis-associated pulmonary hypertension). *Semin Respir Crit Care Med,* 30**,** 448-57.

SOUZA, R., FERNANDES, C. J. C. D. S. & JARDIM, C. V. P. 2009b. Other Causes of PAH (Schistosomiasis, Porto-Pulmonary Hypertension and Hemolysis-Associated Pulmonary Hypertension). *Semin Respir Crit Care Med,* 30**,** 448-457.

STAR, G. P., GIOVINAZZO, M. & LANGLEBEN, D. 2013. ALK2 and BMPR2 knockdown and endothelin-1 production by pulmonary microvascular endothelial cells. *Microvascular Research,* 85**,** 46-53.

STEINER, M. K., SYRKINA, O. L., KOLLIPUTI, N., MARK, E. J., HALES, C. A. & WAXMAN, A. B. 2009. Interleukin-6 Overexpression Induces Pulmonary Hypertension. *Circulation Research,* 104**,** 236-244.

STENMARK, K. R., FRID, M. & PERROS, F. 2016. Endothelial-to-Mesenchymal Transition. *Circulation,* 133**,** 1734-1737.

SU, H., LIU, X., DU, J., DENG, X. & FAN, Y. 2020. The role of hemoglobin in nitric oxide transport in vascular system. *Medicine in Novel Technology and Devices,* 5**,** 100034.

TAHERI, N., , G. R., MOJERLOO, M., HADAD, M., MIRKARIMI, H., NEJAD, R. & JOSHAGHANI, H. 2015. Comparison of serum levels of hepcidin and pro-hepcidin in hemodialysis patients and healthy subjects. *Saudi Journal of Kidney Diseases and Transplantation,* 26**,** 34-38.

TALBOT, N. P., LAKHAL, S., SMITH, T. G., PRIVAT, C., NICKOL, A. H., RIVERA-CH, M., LEÓN-VELARDE, F., DORRINGTON, K. L., MOLE, D. R. & ROBBINS, P. A. 2012. Regulation of hepcidin expression at high altitude. *Blood,* 119**,** 857.

TAMURA, Y., PHAN, C., TU, L., LE HIRESS, M., THUILLET, R., JUTANT, E.-M., FADEL, E., SAVALE, L., HUERTAS, A., HUMBERT, M. & GUIGNABERT, C. 2018. Ectopic upregulation of membrane-bound IL6R drives vascular remodeling in pulmonary arterial hypertension. *The Journal of clinical investigation,* 128**,** 1956-1970.

TAN, A. S., BATY, J. W., DONG, L.-F., BEZAWORK-GELETA, A., ENDAYA, B., GOODWIN, J., BAJZIKOVA, M., KOVAROVA, J., PETERKA, M. & YAN, B. 2015. Mitochondrial genome acquisition restores respiratory function and tumorigenic potential of cancer cells without mitochondrial DNA. *Cell metabolism,* 21**,** 81-94.

TANG, H., SUN, Y., SHI, Z., HUANG, H., FANG, Z., CHEN, J., XIU, Q. & LI, B. 2013. YKL-40 Induces IL-8 Expression from Bronchial Epithelium via MAPK (JNK and ERK) and NF-κB Pathways, Causing Bronchial Smooth Muscle Proliferation and Migration. *The Journal of Immunology,* 190**,** 438-446.

THENAPPAN, T., CHAN, S. Y. & WEIR, E. K. 2018. Role of extracellular matrix in the pathogenesis of pulmonary arterial

hypertension. *American Journal of Physiology-Heart and Circulatory Physiology,* 315**,** H1322-H1331.

THEURL, I., SCHROLL, A., SONNWEBER, T., NAIRZ, M., THEURL, M., WILLENBACHER, W., ELLER, K., WOLF, D., SEIFERT, M., SUN, C. C., BABITT, J. L., HONG, C. C., MENHALL, T., GEARING, P., LIN, H. Y. & WEISS, G. 2011. Pharmacologic inhibition of hepcidin expression reverses anemia of chronic inflammation in rats. *Blood,* 118**,** 4977-84.

THEURL, I., THEURL, M., SEIFERT, M., MAIR, S., NAIRZ, M., RUMPOLD, H., ZOLLER, H., BELLMANN-WEILER, R., NIEDEREGGER, H., TALASZ, H. & WEISS, G. 2008. Autocrine formation of hepcidin induces iron retention in human monocytes. *Blood,* 111**,** 2392-9.

THOMPSON, J. W., SALAHUDEEN, A. A., CHOLLANGI, S., RUIZ, J. C., BRAUTIGAM, C. A., MAKRIS, T. M., LIPSCOMB, J. D., TOMCHICK, D. R. & BRUICK, R. K. 2012. Structural and Molecular Characterization of Iron-sensing Hemerythrin-like Domain within F-box and Leucine-rich Repeat Protein 5 (FBXL5)♦. *Journal of Biological Chemistry,* 287**,** 7357-7365.

THOMPSON, K. & RABINOVITCH, M. 1996. Exogenous leukocyte and endogenous elastases can mediate mitogenic activity in pulmonary artery smooth muscle cells by release of extracellular matrix-bound basic fibroblast growth factor. *Journal of Cellular Physiology,* 166**,** 495-505.

THOMSEN, J. H., ETZERODT, A., SVENDSEN, P. & MOESTRUP, S. K. 2013. The Haptoglobin-CD163-Heme Oxygenase-1 Pathway for Hemoglobin Scavenging. *Oxidative Medicine and Cellular Longevity,* 2013**,** 523652.

TUDER, R. M., ABMAN, S. H., BRAUN, T., CAPRON, F., STEVENS, T., THISTLETHWAITE, P. A. & HAWORTH, S. G. 2009. Development and pathology of pulmonary hypertension. *J Am Coll Cardiol,* 54**,** S3-s9.

TUDER, R. M., MARECKI, J. C., RICHTER, A., FIJALKOWSKA, I. & FLORES, S. 2007. Pathology of pulmonary hypertension. *Clinics in chest medicine,* 28**,** 23-vii.

TZAVLAKI, K. & MOUSTAKAS, A. 2020. TGF-β Signaling. *Biomolecules,* 10**,** 487.

ULRICH, S., SAXER, S., HASLER, E. D., SCHWARZ, E. I., SCHNEIDER, S. R., FURIAN, M., BADER, P. R., LICHTBLAU, M. & BLOCH, K. E. 2019. Effect of domiciliary oxygen therapy on exercise capacity and quality of life in patients with pulmonary arterial or chronic thromboembolic pulmonary hypertension: a randomised, placebo-controlled trial. *European Respiratory Journal,* 54.

VALDIMARSDOTTIR, G., GOUMANS, M. J., ROSENDAHL, A., BRUGMAN, M., ITOH, S., LEBRIN, F., SIDERAS, P. & TEN DIJKE, P. 2002. Stimulation of Id1 expression by bone morphogenetic protein is sufficient and necessary for bone morphogenetic protein-induced activation of endothelial cells. *Circulation,* 106**,** 2263-70.

VAN DE BRUAENE, A., DELCROIX, M., PASQUET, A., DE BACKER, J., DE PAUW, M., NAEIJE, R., VACHIERY, J. L., PAELINCK, B., MORISSENS, M. & BUDTS, W. 2011. Iron deficiency is associated with adverse outcome in Eisenmenger patients. *Eur Heart J,* 32**,** 2790-9.

VIEDT, C., VOGEL, J., ATHANASIOU, T., SHEN, W., ORTH, S. R., KÜBLER, W. & KREUZER, J. 2002. Monocyte chemoattractant protein-1 induces proliferation and interleukin-6 production in human smooth muscle cells by differential activation of nuclear factor-kappaB and activator protein-1. *Arterioscler Thromb Vasc Biol,* 22**,** 914-20.

VOELKEL, M. A., WYNNE, K. M., BADESCH, D. B., GROVES, B. M. & VOELKEL, N. F. 2000. Hyperuricemia in Severe Pulmonary Hypertension. *Chest,* 117**,** 19-24.

VYAS, S., ZAGANJOR, E. & HAIGIS, M. C. 2016. Mitochondria and cancer. *Cell,* 166**,** 555-566.

VYORAL, D. & JIRI, P. 2017. Therapeutic potential of hepcidin – the master regulator of iron metabolism. *Pharmacological Research,* 115**,** 242-254.

WANG, R.-H., LI, C., XU, X., ZHENG, Y., XIAO, C., ZERFAS, P., COOPERMAN, S., ECKHAUS, M., ROUAULT, T., MISHRA, L. & DENG, C.-X. 2005. A role of SMAD4 in iron metabolism through the positive regulation of hepcidin expression. *Cell Metabolism,* 2**,** 399-409.

WARE, L. B., FESSEL, J. P., MAY, A. K. & ROBERTS, L. J., 2ND 2011. Plasma biomarkers of oxidant stress and development of organ failure in severe sepsis. *Shock,* 36**,** 12-7.

WELSH, D. J., SCOTT, P. H. & PEACOCK, A. J. 2006. p38 MAP kinase isoform activity and cell cycle regulators in the proliferative response of pulmonary and systemic artery fibroblasts to acute hypoxia. *Pulm Pharmacol Ther,* 19**,** 128-38.

WIPFF, P. J. & HINZ, B. 2008. Integrins and the activation of latent transforming growth factor beta1 - an intimate relationship. *Eur J Cell Biol,* 87**,** 601-15.

WOJTALA, A., BONORA, M., MALINSKA, D., PINTON, P., DUSZYNSKI, J. & WIECKOWSKI, M. R. 2014. Chapter Thirteen - Methods to Monitor ROS Production by Fluorescence Microscopy and Fluorometry. *In:* GALLUZZI, L. & KROEMER, G. (eds.) *Methods in Enzymology.* Academic Press.

WU, L. J.-C., LEENDERS, A. G. M., COOPERMAN, S., MEYRON-HOLTZ, E., SMITH, S., LAND, W., TSAI, R. Y. L., BERGER, U. V., SHENG, Z.-H. & ROUAULT, T. A. 2004. Expression of the iron transporter ferroportin in synaptic vesicles and the blood–brain barrier. *Brain Research,* 1001**,** 108-117.

XIAO, J. J., KRZYZANSKI, W., WANG, Y.-M., LI, H., ROSE, M. J., MA, M., WU, Y., HINKLE, B. & PEREZ-RUIXO, J. J. 2010. Pharmacokinetics of anti-hepcidin monoclonal antibody Ab 12B9m and hepcidin in cynomolgus monkeys. *The AAPS journal,* 12**,** 646-657.

YAMADA, M., KIM, S., EGASHIRA, K., TAKEYA, M., IKEDA, T., MIMURA, O. & IWAO, H. 2003. Molecular Mechanism and Role of Endothelial Monocyte Chemoattractant Protein-1 Induction by Vascular Endothelial Growth Factor. *Arteriosclerosis, Thrombosis, and Vascular Biology,* 23**,** 1996-2001.

YANG, J., LI, X., LI, Y., SOUTHWOOD, M., YE, L., LONG, L., AL-LAMKI, R. S. & MORRELL, N. W. 2013. Id proteins are critical downstream effectors of BMP signaling in human pulmonary arterial smooth muscle cells. *American journal of physiology. Lung cellular and molecular physiology,* 305**,** L312-L321.

YANG, Q., LIU, W., ZHANG, S. & LIU, S. 2020. The cardinal roles of ferroportin and its partners in controlling cellular iron in and out. *Life Sciences,* 258**,** 118135.

YANG, X., LONG, L., REYNOLDS, P. N. & MORRELL, N. W. 2011. Expression of mutant BMPR-II in pulmonary endothelial cells promotes apoptosis and a release of factors that stimulate proliferation of pulmonary arterial smooth muscle cells. *Pulm Circ,* 1**,** 103-10.

YAO, J. S., ZHAI, W., YOUNG, W. L. & YANG, G.-Y. 2006. Interleukin-6 triggers human cerebral endothelial cells proliferation and migration: The role for KDR and MMP-9. *Biochemical and Biophysical Research Communications,* 342**,** 1396-1404.

YÉPEZ, V. A., KREMER, L. S., IUSO, A., GUSIC, M., KOPAJTICH, R., KOŇAŘÍKOVÁ, E., NADEL, A., WACHUTKA, L., PROKISCH, H. & GAGNEUR, J. 2018. OCR-Stats: Robust estimation and

statistical testing of mitochondrial respiration activities using Seahorse XF Analyzer. *PLOS ONE,* 13**,** e0199938.

YOUNG, J. M., WILLIAMS, D. R. & THOMPSON, A. A. R. 2019. Thin Air, Thick Vessels: Historical and Current Perspectives on Hypoxic Pulmonary Hypertension. *Frontiers in Medicine,* 6.